Novel insights into the molecular mechanisms of endocrine resistance in ERα positive breast cancer

Silvia-Elena Glont

Clare College

University of Cambridge

This dissertation is submitted for the degree of Doctor of Philosophy

September 2020

Declaration

This dissertation is the result of my own work and includes nothing which is the outcome of work done in collaboration except as specified in the text. It is not substantially the same as any that I have submitted, or, is being currently submitted for a degree or diploma or other qualification at the University of Cambridge or any other University or similar institution except as specified in the text. I further state that no substantial part of my dissertation has already been submitted, or is being currently submitted for any such degree, diploma, or other qualification at the University of Cambridge or any other University or similar institution except as specified in the text. In accordance with the guidelines of the Degree Committee for the Faculties of Clinical Medicine and Veterinary Medicine, this thesis does not exceed 60,000 words.

Silvia-Elena Glont

Signed_____

Date_____

Summary

Silvia-Elena Glont

Novel insights into the molecular mechanisms of endocrine resistance in ERα positive breast cancer

ERα transcriptional activity drives tumour development and metastasis in more than 70% of breast cancer cases. Tamoxifen is the most widely and successfully used endocrine treatment for pre-menopausal women with ERα positive breast cancer. However, subgroups of patients are resistant to this drug. Investigation into the mechanisms of the endocrine refractory phenotype would therefore open possibilities for novel targeted therapies. One key aspect of ERα gene regulation is its accessibility to compacted chromatin. FOXA1 is a pioneer transcription factor that has the ability to bind to 'closed' chromatin and open it up for ERα subsequent binding, thereby creating the regulatory elements that are used by ERα.

In this thesis, the dependence of the ERα hormone receptor on FOXA1 is reinforced and the latter is confirmed as a *bone fide* pioneer transcription factor and a promising drug target in hormone-dependent cancers.

Moreover, novel molecular mechanisms of Tamoxifen resistance were investigated using quantitative multiplexed rapid immunoprecipitation mass spectrometry of endogenous proteins (qPLEX-RIME) in multiple *in vitro* and *in vivo* breast cancer models. The results showed that the two key proteins ERα and FOXA1 are enriched in the resistant phenotype, together with their newly-identified interactor ETV6. The role of ETV6 in endocrine resistance was confirmed using an independent siRNA screen. In addition, the direct contribution of ETV6 to breast cancer progression was proved by the promoting effects of ETV6 overexpression on colony formation ability of endocrine sensitive cell lines.

Furthermore, chromatin immunoprecipitation followed by sequencing (ChIP-seq) analysis revealed that Tamoxifen resistance is associated with a global redistribution of FOXA1, ERα, ETV6- DNA interactions and altered genomic landscape. This

differential binding of the three transcription factors also results in compromised transcriptional programmes in endocrine resistance, as assessed by RNA-seq.

In addition, inhibition of MAPK pathway reduced breast cancer progression and modulated ETV6-chromatin interactions.

Importantly, the clinical significance of ETV6 copy number amplifications was assessed in the METABRIC cohort (Curtis et al., 2012). They correlate with significantly reduced disease-free survival in Luminal B breast cancer subtype, which is the more aggressive ERα positive subtype and is more likely to metastasise.

Moreover, by conducting a screen of 1000 FDA-approved drugs, potential candidates for the treatment of hormone-refractory breast cancer were identified. Further *in vitro* and *in vivo* validation would consolidate these findings.

Taken together, the data presented in this dissertation reinforces FOXA1 independence of hormonal signalling, it identifies ETV6 as a novel ERα and FOXA1 co-factor that drives a more proliferative phenotype and proposes alternative therapies for the endocrine refractory phenotype.

Acknowledgements

I would first like to thank my PhD supervisor, Professor Jason S Carroll for offering me the opportunity to work in such a motivating environment and for his continuous support. Jay, you shaped me as a person and as a scientist and I will always be grateful to you.

Sankari, thank you for all your supervision and for always being my friend. Your input enhanced my understanding of our research field and your guidance enabled me to ask my own scientific questions. It was a pleasure to work with you.

Rasmus, thank you for all the insightful discussions, for sharing your lab expertise and for showing me how to be an incredibly capable scientist and a kind and fair person. Your advice has been invaluable throughout my PhD.

Special thanks to colleagues in bioinformatics, especially Dr Igor Chernukhin (Carroll Group), Dr Kamal Kishore and Dr Ashley Sawle (Bioinformatics Core Facility, CRUK-CI) and Dr Oscar Rueda (Caldas Group) for their expertise and immense support.

Dearest Carroll Lab members: Rebecca Broome, Eva, Sunny, Anca, Sanjeev, Danya, Shalini, Rebecca Burrell, Al, Steve, Simon, Adam, Kelly, Caryn, Jill, Stacey thank you for all your help and for making the lab such an amazing place to work.

I wish to thank CRUK-CI core facilities: Proteomics, Genomics, Histopathology and ISH and the Research Instrumentation & Cell Services for all their support along the way.

I acknowledge Cancer Research UK for funding my PhD studies.

Thanks to all my friends from all around the world, especially to Ioana, Maria, Adelyne, Mona, Monica, Iulia, Magda, Bobi, Diana: you made my PhD adventure wonderful!

Thank you to my beloved family, my boy Theo for being understanding of my long days in the lab, my husband Mihai for being there for me every time, to my wonderful mum and dad, and mum- and dad-in-law, my grandma, Adina, Gabi, Cristina, Christopher.

I am who I am thanks to every one of you! It has been a worthwhile journey and I am very grateful to you.

Key Abbreviations and Acronyms

AD1	Activation domain 1
AD2	Activation domain 2
AF-1	Activation function 1
AF-2	Activation function 2
AI	Aromatase inhibitor
AIB1	Amplified in breast cancer 1
ALL	Acute lymphoblastic leukaemia
AMBIC	Ammonium hydrogen carbonate
AML	Acute myeloid leukaemia
AP1	Activator protein 1
AP-2γ	Activating enhancer-binding protein 2 gamma
AR	Androgen receptor
ATP	Adenosine triphosphate
bp	Base pairs
BRCA 1/2	Breast cancer gene 1/2
BRG1	Brahma-Related Gene 1
°C	Degrees Celsius
CARM1	Coactivator-associated arginine methyltransferase 1
CBP	CREB-binding protein
cDNA	Complementary deoxyribonucleic acid
ChIA-PET	Chromatin interaction analysis by pared-end tag sequencing
ChIP	Chromatin immunoprecipitation
ChIP-seq	Chromatin immunoprecipitation followed by high-throughput sequencing
CRISPR	Clustered regularly interspaced short palindromic repeats
CRUK-CI	Cancer Research UK Cambridge Institute
Da	Daltons
DBD	DNA binding domain
DFS	Disease free survival
DMEM	Dulbecco's Modified Eagle's Medium
DMSO	Dimethyl sulphoxide

DNA	Deoxyribonucleic acid
dNTP	Deoxynucleoside triphosphates
DSG	Disuccinimidyl glutarate
DTT	Dithiothreitol
E2	17β-oestradiol
EDTA	Ethylene diamine tetraacetic acid
EGTA	Ethylene glycol tetraacetic acid
ERα	Estrogen Receptor alpha
ERβ	Estrogen Receptor beta
ERE	Estrogen response element
ETS	E26 transformation-specific
ETV6	ETS variant transcription factor 6
FBS	Foetal bovine serum
FDR	False discovery rate
FOXA1	Forkhead box A1
GATA3	GATA binding protein 3
GR	Glucocorticoid receptor
GREAT	Genomic Regions Enrichment of Annotations Tool
GREB1	Growth regulation by estrogen in breast cancer 1
HAT	Histone acetyltransferase
HDAC	Histone deacetylase
HER2	Human epidermal growth factor receptor 2
Hi-C	High-throughput chromosome conformation capture
HMT	Histone methyltransferase
IgG	Immunoglobulin G
kg	Kilobase
kDa	Kilodaltons
LB	Luria Broth buffer
LBD	Ligand binding domain
M	Molar
MACS	Model-based analysis for ChIP-sequencing
MAPK	Mitogen-activated protein kinase
METABRIC	Molecular Taxonomy of Breast Cancer International Consortium

mRNA	Messenger ribonucleic acid
MS	Mass spectrometry
mTOR	Mammalian target of rapamycin
NCOA	Nuclear receptor co-activator
NCOR	Nuclear receptor co-repressor
NSG	NOD scid gamma mouse
NTRK3	Neurotrophic tyrosine kinase, receptor, type 3
P	Promoter
PAX1	Paired box protein PAX-1
PBS	Phosphate-buffered saline
PBX1	Pre-B-cell leukaemia transcription factor 1
PCR	Polymerase chain reaction
PDX	Patient-derived xenograft
PGR/PR	Progesterone receptor
PIK3CA	Phosphatidylinositol-4,5-Bisphosphate 3-Kinase Catalytic Subunit Alpha
PRMT	Protein arginine methyltransferase
PTEN	Phosphatase and tensin homolog
q-PCR	Quantitative polymerase chain reaction
qPLEX-RIME	Quantitative multiplexed rapid immunoprecipitation mass spectrometry of endogenous proteins
qRT-PCR	Quantitative reverse transcription polymerase chain reaction
RARα	Retinoic acid receptor alpha
RIME	Rapid immunoprecipitation mass spectrometry of endogenous proteins
RIP140	Receptor-interacting protein 140
RIPA	Radioimmunoprecipitation assay buffer
RPMI	Roswell Park Memorial Institute
RUNX	Runt-related transcription factor 1
RXRα	Retinoic acid receptor RXR-alpha
SD	Standard deviation
SDS	Sodium dodecyl sulphate
SERD	Selective estrogen receptor degrader
SERM	Selective estrogen receptor modulator
SP1	Specificity protein 1

TBS	Tris-buffered saline
TE	Tris ethylene diamine tetraacetic acid
TF	Transcription factor
TFF1	Trefoil factor 1
TLE3	Transducin-like enhancer protein 3
TMPRSS2	Transmembrane Serine Protease 2
TMT	Tandem mass tag
TP53	Tumour protein p53
TSS	Transcription start site
U	Units
UBC	Ubiquitin C
V	Volt
XBP1	X-box binding protein 1
3C	Chromosome conformation capture

Contents

List of Figures

List of Tables

Chapter 1. Introduction

1.1 Breast cancer

Breast cancer is the second most common form of cancer world-wide, just after lung cancer. There were over 2 million cases diagnosed in 2018 alone (International Agency for Research on Cancer, 2019). A large proportion of these patients have good outcomes, with survival rates increased by new treatments, but there are still 626,000 world-wide annual deaths resulting from this disease. These statistics place breast cancer as the fifth cancer-related cause of death globally.

In particular, in the UK, there are 55,000 new cases reported annually and 11,400 deaths per year (Cancer Research UK, 2020).

Therefore, there is a clinical need to improve breast cancer's early detection and treatment.

1.1.1 Risk factors

There are numerous risk factors that predispose women to breast cancer development, such as hormone levels, family history, gene mutations or unhealthy lifestyle.

It is known that more than three quarters of breast cancer cases are driven by estrogen receptor α (ERα). Its ligand, the hormone estrogen (E2), promotes cell growth and changes in its levels can trigger oncogenesis. Such perturbations have been associated with the age at which women have their first full-term pregnancy, the number of pregnancies, as well as the use of hormone replacement therapy (Key et al., 2001).

The most prevalent hereditary risks are mutations in tumour suppressors BRCA1 and BRCA2, which have been linked with dysregulation of cell cycle checkpoint, genetic instability and apoptosis (Dine and Deng, 2013). These cases account for approximately 5-10% of all breast cancers (Ford et al., 1998, Miki et al., 1994, Ripperger et al., 2009, Wooster et al., 1995).

Other prevailing cancer-predisposing alterations are the ones in *TP53, ERBB2 (HER2)* and *PIK3CA (Koboldt et al., 2012)*. In addition, there are a plethora of other mutations and deregulations that are not yet fully understood (Curtis et al., 2012, Koboldt et al., 2012, Pereira et al., 2016). These factors underscore the importance of identifying those deregulation events that drive breast cancer development and progression in order to better diagnose and treat this disease.

1.1.2 Breast cancer classification

The first step towards better management of breast cancer is to correctly classify it.

This heterogeneous disease can be stratified based on the cell type of origin into ductal and lobular cancer, with ductal carcinomas accounting for 90% of the cases (Li et al., 2003).

In addition, gene expression analysis led to the most common classification of breast tumours. They can be divided into five distinct categories. The subtypes, normal breast-like, luminal A and luminal B tumours, ERBB2 (HER2) positive and basal-like are used to predict disease course and response to different therapies (Sørlie et al., 2001).

Yet, resistance to currently-available treatments occurs as a consequence of breast cancer's cellular and molecular heterogeneity and even within subtypes, treatment response is variable.

The need to gain better insight into somatic drivers of breast cancer motivated the Molecular Taxonomy of Breast Cancer International Consortium (METABRIC) project, which addressed this issue. A combination of copy number and gene expression analyses on a cohort of approximately 2,000 patients identified 11 subgroups of breast cancer based on their molecular drivers (Curtis et al., 2012, Rueda et al., 2019). The discovery of their molecular drivers opened the possibility to tailor treatments for each cancer genotype.

1.2 Estrogen receptor alpha (ERα)

It is known that the steroid hormone estrogen (17β-estradiol) plays an important role in the female reproductive system (Zwart et al., 2011). Estrogens are involved in the development and function of numerous tissues and physiological processes including the development and maintenance of the female sexual organs, the reproductive cycle and various neuroendocrine functions (Zhao et al., 2003).

Estrogen's actions are mediated by ERα and ERβ nuclear hormone receptors (Gburcik and Picard, 2006), which, together with androgen receptor (AR), progesterone receptor (PR) and glucocorticoid receptor (GR), are part of the nuclear receptor super-family (Rastinejad et al., 2013). ERα and ERβ also have crucial roles in certain disease states, particularly in mammary and endometrial carcinomas (Brueggemeier et al., 2005). The role of ERβ in breast cancer remains unclear, with the current paradigm suggesting that it can function as a cell growth repressor (Ström et al., 2004).

On the other hand, ERα has been intensely studied due to its causal role in breast tumorigenesis where it functions as a transcription factor to initiate gene expression changes that promote cell cycle progression.

1.2.1 ERα structure

ERα encompasses several functional domains that serve specific roles (Kumar et al., 2011) (Fig.1.1). The N-terminal Domain contains an activation function domain (AF1) that acts in a hormone independent manner and facilitates ERα dimerisation prior to DNA binding (Berry et al., 1990).

The DNA-binding domain (DBD) enables ERα interactions with specific genomic regions and its subsequent transcriptional programme (Klinge, 2001). ERα-DNA interactions also modulate the recruitment of co-regulatory proteins (Glass and Rosenfeld, 2000). In Addition, the Hinge region contains a nuclear localisation signalling domain, which gets unmasked upon ligand binding and serves as a flexible region connecting the DNA-binding domain and the ligand binding domain (Kuiper et al., 1996). Moreover, the ligand binding domain (LBD) contains an activation function domain (AF2), which requires estrogen presence (Berry et al., 1990) and is responsible for most of the functions activated by the hormone (Beato et al., 1995). In

addition, the AF2 is responsible for the recruitment of co-activators and co-repressors and is also involved in ERα homo- and heterodimerisation (Danielian et al., 1992).

The C-terminal domain was also found to modulate gene transcription in a ligand-specific manner (Koide et al., 2007, Montano et al., 1995). It is also known to impact receptor dimerisation (Yang et al., 2008).

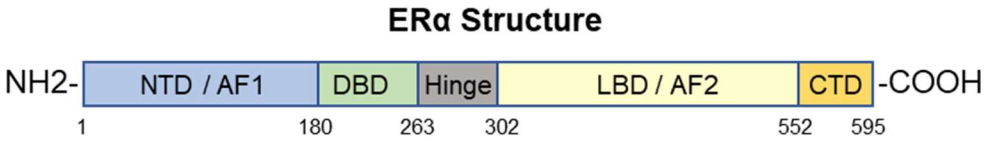

Figure 1.1. ERα protein structure; N-terminus to C-terminus: N-terminus containing the activation function domain AF1; DNA binding domain (DBD); Hinge Region; Ligand binding domain (LBD) that contains the activation function domain AF2; C-terminal domain (CTD).

1.2.2 ERα-chromatin direct interactions

ERα-chromatin interactions have been extensively studied due to their determinant role in the ERα transcriptional programme. ERα can directly interact with DNA through its DNA-binding domain that specifically associates with a palindromic hexanucleotide 5′ AGGTCAnnnTGACCT 3′ within the chromatin (Klein-Hitpass et al., 1989). These motifs have been termed Estrogen Receptor Elements (ERE).

Using genomic technologies in breast cancer models, it was shown that ERα is rarely associated with promoter regions of target genes. Only ~3-5% of ERα binding events occur within 1-5 kb of the TSS (Carroll et al.,2005, Carroll et al., 2006). Instead, it binds to enhancer elements at significant distances from the transcription start sites (10-100kb). Then, DNA-looping occurs and brings enhancers in spatial proximity to promoter regions of target genes (Fig.1.2). Thus, transcription is initiated (Fullwood et al., 2009, Pan et al., 2008).

ERα-regulated enhancer-promoter interactions dictate gene activation and their deregulations can trigger tumourigenesis. Therefore, there is significant interest in understanding their interaction.

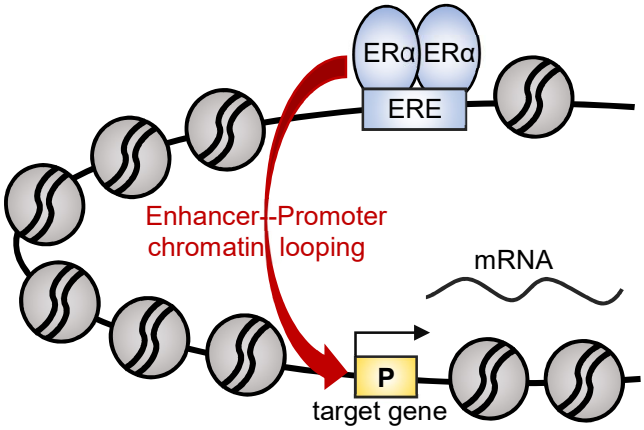

Figure 1.2. Model of ERα direct binding to chromatin: ERα binds to enhancers; enhancer-promoter (P) looping brings ERα in close proximity to its target genes to initiate their transcription.

Chromosome conformation capture (3C) is a technique used to study the frequency of interaction between two genomic loci and to detect their relative spatial disposition (Dekker et al., 2002). The physical association between ERα enhancers and promoter regions of target genes such as PGR, GREB1 and TFF1 was proved using 3C (Bonéy-Montoya et al., 2010, Jia et al., 2017).

In addition, *Fullwood et al* studied ERα chromatin loops in MCF-7 cells in a genome-wide manner, using chromatin interaction analysis by paired-end tag sequencing (ChIA-PET). They concluded that more than 80% of the ERα-chromatin interactions occur at enhancers and that loops tend to connect more than one enhancer to one promoter, impacting on ERα transcription regulation (Fullwood et al., 2009).

More recently, genome-wide mapping of chromatin interactions (Hi-C) was conducted in breast cancer cells. Hi-C showed that the transcriptional regulatory machinery assembled at enhancers is brought in close proximity to promoters of target genes upon estrogen stimulation (Mourad et al., 2014). This was clear evidence of the regulatory role of estrogen on the ERα-chromatin interactions and subsequent gene regulation in cancer.

1.3 ERα complex

In addition to ERα-chromatin direct interactions, there are also numerous associated proteins that contribute to ERα activity. These co-factors can either enable ERα to

access its target genes through different mechanisms, or can mediate gene activation and repression. ERα cooperative factors are of particular importance as their deregulations can contribute to breast cancer development and progression and can influence endocrine response.

1.3.1 Pioneer transcription factors

A special class of ERα-associated proteins are the pioneer transcription factors. They are able to access highly compacted chromatin and subsequently assist in chromatin opening and binding of other nuclear receptors, such as ERα. This ability motivated the use of the term 'Pioneer Transcription Factor' (Cirillo et al., 1998). Examples of such proteins are FOXA1, GATA3, PBX1 or AP2γ. Importantly, these transcription factors seem to be interconnected.

Pre-B-cell leukaemia transcription factor 1 (PBX1) was shown to enhance ERα signalling by promoting chromatin accessibility at specific genomic loci and subsequently guiding ERα to them. Half of the ERα binding sites are co-occupied by XBP1 and the regions demarcated by PBX1 are associated with a more aggressive tumour phenotype in breast cancer (Magnani et al., 2011).

Furthermore, ERα binding sites are enriched for activating enhancer-binding protein 2 gamma (AP2γ) DNA consensus motifs and a significant number of ERα bound genomic sites are co-occupied by AP-2γ and FOXA1 transcription factors. Inhibition of AP-2γ repressed ERα-DNA binding and gene transcription (Tan et al., 2011).

In addition, it was suggested that GATA binding protein 3 (GATA3), one of the key markers of ERα positive tumours (Perou et al., 2000) possessed pioneer transcription factor activity (Cirillo et al., 2002). Further investigations revealed that loss of GATA3 in MCF-7 cells impacts on ERα binding sites resulting in both stronger and weaker ERα-chromatin interactions. It appeared that GATA3 mediated enhancer accessibility at these regions, therefore affecting ERα-driven transcription (Theodorou et al., 2013). Other studies defined GATA3's key role in cell growth. Its silencing in T47D ERα positive cells significantly reduced proliferation upon estrogen stimulation (Eeckhoute et al., 2007).

Whilst all of the above factors contribute to some degree to the maintenance of the ERα-chromatin interactions, FOXA1 was shown to be the critical factor that determines

ERα initial binding to chromatin (Carroll et al., 2005, Hurtado et al., 2011). Subsequently, FOXA1 defines the particular locations where ERα can bind to the genome (Glont et al., 2019, Hurtado et al., 2011).

1.3.1.1 FOXA1 pioneer transcription factor

FOXA1 is a key characteristic of ERα positive breast cancer (Perou et al., 2000, Sørlie et al., 2001). It is also known as hepatic nuclear factor 3 HNF3 and it belongs to the Forkhead box (FOX) family of transcription factors.

FOXA and GATA factors have been linked to liver development. Their pioneer activity was first uncovered using *in vivo* footprinting in mouse liver. FOXA and GATA occupancy at the albumin (Alb1) enhancer site proceeded all other factors. Importantly, their expression was required for the induction of the liver program, but FOXA was more active in this process than GATA (Liu et al., 1991).

Subsequently, it was shown that FOXA1 is required for the normal development of a number of organs, including prostate, liver, kidney, pancreas, lung and breast (Behr et al., 2004, Bernardo et al., 2010, Gao et al., 2008). In particular, FOXA1 is involved in the hormonal induced branching of the breast ducts during puberty and pregnancy (Bernardo et al., 2010).

More recently, FOXA1 has been identified as a determinant factor in ERα positive breast cancer. The initial finding that ERα binding sites are enriched for forkhead motifs (Carroll et al., 2005), was later consolidated by several studies that have established their co-occupancy (Lupien et al., 2008) and, most importantly, that FOXA1 acts upstream of ERα, therefore dictating the ERα transcriptional programme (Glont et al., 2019, Hurtado et al., 2011).

1.3.1.1.1 FOXA1 structure

FOXA1 pioneer activity is conferred by its structure (Fig.1.3). Its winged helix DNA binding domain (DBD) resembles that of the linker histone H1 (Clark et al., 1993). FOXA1 uses one of the ‘faces’ of its DBD to displace H1 histones and bind to highly compacted chromatin. It uses the other ‘face’ of its DBD to recruit other proteins to DNA (Cirillo et al., 1998, Cirillo and Zaret, 1999). In addition, its high-affinity for DNA also results from the binding of its C-terminus to histones H3 and H4 (Cirillo et al., 1998, Cirillo and Zaret, 1999, Taube et al., 2010). Moreover, FOXA1 has a N-terminal

trans-activation domain (TA) that assists in the recruitment of other co-regulatory proteins (Pani et al., 1992) (Figure 1.3.).

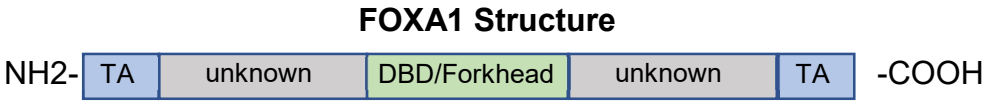

Figure 1.3. FOXA1 protein structure: FOXA1 encompasses two transactivation domains (TA) and a winged helix DNA binding domain.

1.3.1.1.2 FOXA1 binds to forkhead motifs within the chromatin

FOXA1 binds to the consensus element A(A/T)TRTT(G/T)RYTY (Overdier et al., 1994). It acts as a pioneer transcription factor that can actively facilitate the assembly of the ERα transcriptional machinery by opening the chromatin locally (Cirillo et al., 2002) (Figure 1.4.). It can also enhance transcription by recruiting chromatin modifiers and co-regulators that contribute to gene activation (Boyer et al., 2005).

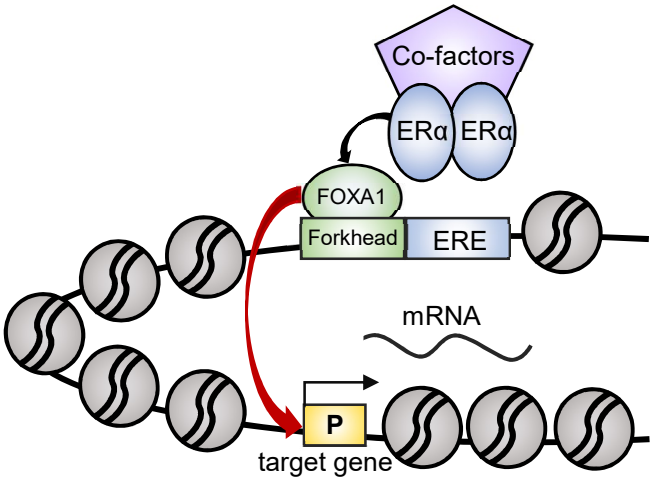

Figure 1.4. Model of FOXA1 opening silent chromatin for ERα and its cofactors.

1.3.1.1.3 FOXA1-ERα interaction in breast cancer

FOXA1 is a marker for good prognosis in ERα positive breast carcinomas (Hisamatsu et al., 2012). The functional interaction between ERα and FOXA1 has been extensively studied. Coupling chromatin immunoprecipitation with global analytical methods (ChIP-on-chip or ChIP–seq) permitted the unbiased mapping of transcription factor binding. The first global mappings of ERα-chromatin binding sites showed they are enriched both for ERE motifs (either full or half motif) and for forkhead motifs (Carroll et al., 2005, Carroll et al., 2006). The co-occupancy of FOXA1 and ERα was then

validated by genome-wide mapping of their binding sites in several cell lines. For all the cell lines assessed, more than 50% of all ERα-DNA binding sites were co-occupied by FOXA1 (Hurtado et al., 2011).

The importance of FOXA1 in mediating ERα association with chromatin is shown when FOXA1 is specifically silenced using RNAi. In the absence of FOXA1, the majority of ERα-DNA binding events were reduced. In addition, gene expression microarray analysis revealed that FOXA1 inhibition abolishes the expression of both upregulated and downregulated ERα target genes (Hurtado et al., 2011). More recently, it was shown that FOXA1–chromatin interactions were not influenced by estrogen treatment, implying that FOXA1 acts upstream of ERα (Glont et al., 2019). Thus, there is a general requirement of FOXA1 for ERα induced transcription and perturbations in either FOXA1 or ERα can trigger tumourigenesis.

1.3.2 Tethering proteins

One class of ERα cooperative factors that enable its binding to DNA are the tethering proteins. For example, activator protein 1 (AP1) and specificity protein 1 (SP1) were shown to modulate ERα-chromatin interactions and subsequent activation of target genes (Jakacka et al., 2001, Porter et al., 1997). In addition, runt-related transcription factor 1 (RUNX1) plays a role in tethering ERα to the DNA in the context of mutated ERα DNA binding domain (Stender et al., 2010). An illustration of ERα-DNA tethering is shown in Figure 1.5.

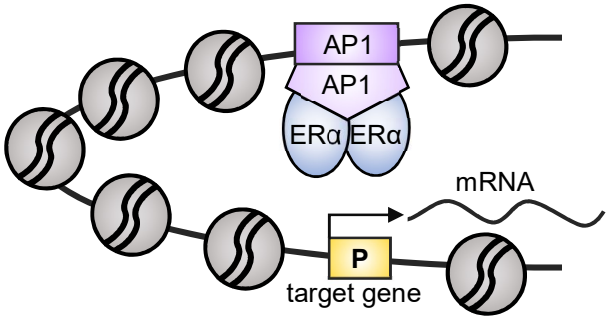

Figure 1.5. ERα tethering to DNA by its co-factors: as example, AP1 tethering is illustrated; other tethering proteins enable ERα-mediated transcription in a similar manner.

1.3.3 Histone modifiers

Histone modifiers possess chromatin remodelling properties that can influence ERα-DNA interactions. They can be either co-activators or co-repressors and they can work in a cooperative or competitive manner, thus influencing ERα mediated transcription.

1.3.3.1 Co-activators

Examples of histone modifiers that act as co-activators are the p160 family members NCOA1 (SRC1), NCOA2 (SRC2) and NCOA3 (AIB1) (Anzick et al., 1997, Hong et al., 1997, Oñate et al., 1995). P160 factors are recruited to the ERα complex by interacting with the AF2 domain of ERα (Heery et al., 1997). Consequently, p160 members act by recruiting acetyltransferases (HATs) such as CREB-binding protein (CBP) and p300. HATs interact with the activation domain 1 (AD1) of p160. HATs modify histone N-terminal domains though addition of acetyl groups (Rollins et al., 2015). Histone acetylation decondenses chromatin and facilitates the recruitment of further factors.

The importance of this process is underscored by the fact that histone acetylation, in particular at lysine 27 of histone H3 (H3K27Ac), is a key mark associated with active enhancers (Zhou et al., 2011). It increases at many ERα-regulated enhancers in response to estrogen treatment (Lupien et al., 2009).

In addition, HATs CBP and p300 mediate interactions with active RNA polymerase II, thus contributing to the transcriptional machinery (Neish et al., 1998).

Other co-activators recruited by p160 to the ERα complex are histone methyltransferases (HMTs) such as protein arginine methyltransferases 1 (PRMT1) and 4 (PRMT4 or CARM1). HMTs interact with p160 activation domain 2 (AD2). CARM1 recruitment triggers demethylation of arginine residues of histone 3, resulting in the activation mark H3R17me2 (Chen et al., 2000). PRMT1 methylates histone H4 at arginine, resulting in the histone mark H4R3Me2. Histone methylation, together with acetylation, contributed to chromatin decondensation and enhanced ERα-mediated transcription (Chen et al., 2000, Wagner et al., 2006).

1.3.3.2 Co-repressors

In addition to ERα co-activators, there are also co-repressors. Their interaction contributes to the ERα-mediated gene repression that occurs after estrogen treatment (Zubairy and Oesterreich, 2005). The nuclear receptor co-repressor (NCOR), receptor-interacting protein 140 (RIP140) and repressor of estrogen receptor activity (REA) interact with the AF2 domain of ERα (Watson et al., 2012). In turn, they recruit deacetylases (HDACs) to the ERα complex (Castet et al., 2004, Delage-Mourroux et al., 2000, Lazar, 2003, Varlakhanova et al., 2010). HDACs mediated co-repression is achieved by removing the activating histone acetylation marks and subsequently contributing to chromatin condensation.

1.3.4 ATP-dependent remodellers

Estrogen-activated gene expression is also influenced by ATP-dependent chromatin remodellers. These complexes alter the nucleosomal organisation, making chromatin more or less accessible for transcription factors such as ERα (Wang et al., 2007). Examples include members of the SWItch/Sucrose Non-Fermentable (SWI/SNF) complex such as Brahma-related gene 1 (BRG1) and BRG1- associated factor 57 (BAF57). They interact with AF2 of ERα and modulate ERα-transcriptional activity (DiRenzo et al., 2000, García-Pedrero et al., 2006).

A model of the ERα-associated proteins in breast cancer is provided in Figure 1.6.

All these factors interact with ERα through its AF2 domain. This implies they work either cooperatively or competitively and the balance between all partners in the ERα complex dictates its transcriptome. In fact, it has already been shown that NCOA1 and REA compete for the ERα AF2 domain (Delage-Mourroux et al., 2000).

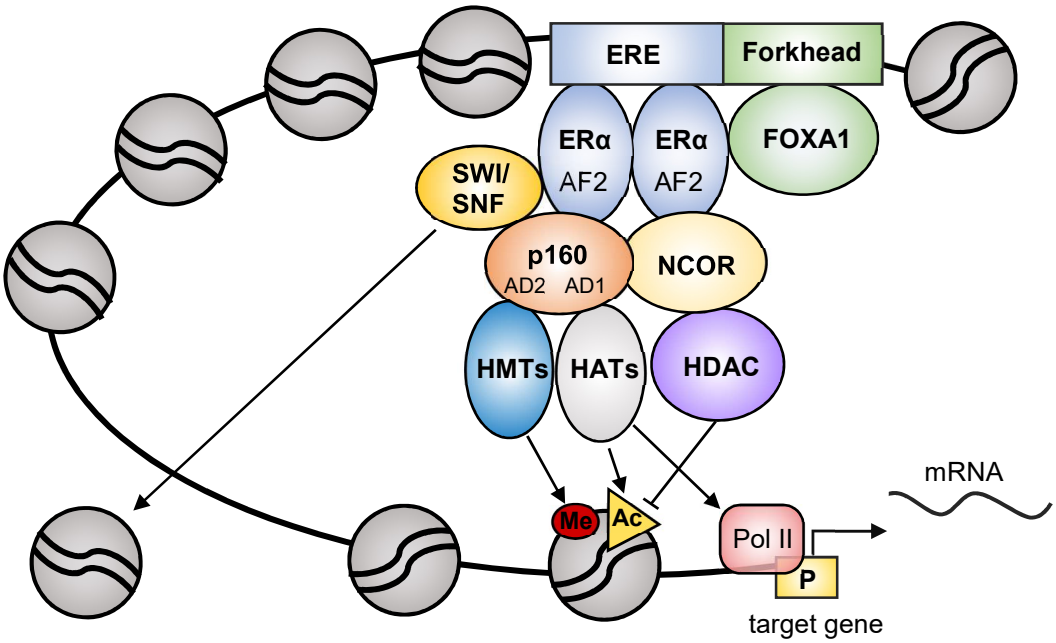

Figure 1.6. Model of ERα-associated proteins in breast cancer: Pioneer transcription factors such as FOXA1 open up compacted chromatin for the ERα complex. ERα recruits p160 co-activators (NCOA1, NCOA2, NCOA3) which in turn can recruit acetyltransferases (HATs) (e.g. CBP, p300) or histone methyltransferases HMTs (e.g. PRMT1, CARM1). Histone acetylation, in particular H3K27Ac and histone methylation (H3R17me) result in chromatin decondensation and facilitate transcription activation by RNA polymerase II (Pol II). ERα can also recruit co-repressors (e.g. NCOR, REA, RIP140) that in turn recruit deacetylases (HDACs). The latter remove the acetylation marks, resulting in chromatin condensation; SWI/SNF complex is also recruited and can alter nucleosomal organisation.

1.4 Targeted therapies for ERα positive breast cancer

More than 75% of breast cancers are driven by ERα. Therefore, decades of research have been invested in generating therapeutic strategies against ERα and its ligand, estrogen. There are three main classes of such drugs: selective estrogen-receptor modulators [SERMs] such as Tamoxifen; selective estrogen-receptor degraders [SERDs] such as Fulvestrant; aromatase inhibitors [AIs] such as Letrozole.

1.4.1 Selective estrogen-receptor modulators

Tamoxifen is the first selective estrogen-receptor response modulator [SERM] and it was developed in the early 1970s. Ever since, it has been successfully used in both pre- and post-menopausal ERα positive breast carcinomas (Brown, 2002). Several clinical trials proved its effectiveness for patients that were progressing after surgery or radiation (Cole et al., 1971). In addition, 5 years of Tamoxifen preventative treatment in healthy women at a high risk for this disease, reduces the annual death rate by 31% (Nazarali and Narod, 2014).

Within breast cancer cells, Tamoxifen is converted to its active metabolite, 4-hydroxytamoxifen (4OHT) that mimics endogenous E2. Their structural resemblance confers 4OHT high affinity for ERα ligand binding domain, therefore competing with E2 to bind to ERα. Tamoxifen-ERα interaction stops the binding of E2 and thus prevents the ERα-induced activation of genes involved in proliferation (Jordan, 1994).

Whilst in breast tissue Tamoxifen acts as an estrogen antagonist, it has agonist effects in other types of tissues, notably in uterus tissue. Its estrogenic abilities in the uterus have been associated with risk of endometrial cancer (Fisher et al., 1994). Other side effects reported for Tamoxifen are hot flushes, vein thrombosis and pulmonary embolism (Lin et al., 2018).

The need for drugs that would successfully treat breast cancer with decreased associated risks, motivated the development of second SERMS, such as Raloxifene (Black et al., 1983). Significant interest was shown in it initially, as it did not have the endometrial hyperplasia stimulating side effect, but more recent trials have shown it is less effective in treating breast cancer compared to Tamoxifen. The rate of invasive breast cancer was approximately 24% higher in patients taking Raloxifene than in those taking Tamoxifen (Vogel et al., 2010).

1.4.2 Selective estrogen-receptor degraders

Selective estrogen-receptor degraders [SERDS], such as Fulvestrant, are second generation drugs. They have pure anti-estrogen activity in all tissue types. Fulvestrant has very high affinity for ERα. Its binding to ERα induces an ERα conformational change that stops ERα- ERα dimerisation and nuclear translocation. Fulvestrant also

triggers ERα degradation, resulting in depletion of its total levels (Dauvois et al., 1993, Fawell et al., 1990). Subsequently, ERα transcriptional activity is abolished. Fulvestrant is indicated for the treatment of ERα positive, HER2 negative advanced breast cancer in pre- or postmenopausal women (Deeks, 2018).

1.4.3 Aromatase inhibitors

Estrogen results from the conversion of androgen by aromatase, a member of the cytochrome P450 class of enzymes (Cole and Robinson, 1990). In pre-menopausal women, high levels of estrogen are produced predominantly by the ovary, although a small proportion is also secreted by peripheral tissues. By contrast, in post-menopausal setting, the latter are the sole source of E2.

Aromatase inhibitors, such as Letrozole or Anastrozole inhibit ERα-dependent cell growth by suppressing estrogen production (Miller, 2003).

They are typically used as first line of therapy in post-menopausal setting, where ERα is only produced by peripheral tissues. In contrast, their effect is counteracted in pre-menopausal patients by the high ovarian estrogen production.

Trials using modern AIs showed they reduce the risk of relapse in post-menopausal patients with endocrine-responsive early breast cancer. AIs had better results in these patients compared with Tamoxifen (Coates et al., 2007).

However, resistance to these therapies occurs in approximately 30% of cases, within 1.5 years of treatment (Sporn and Lippman, 2003). Therefore, there is a need to better understand breast cancer's aetiology and the mechanisms of drug resistance.

1.5 Mechanisms of resistance to endocrine therapy

Tamoxifen has significantly improved the outcome of ERα positive breast cancer patients. However, there are cases with intrinsic resistance to endocrine therapy. In addition, 30% of patients treated with Tamoxifen acquire resistance after approximately 15 months of treatment (EBCTCG, 2005). Interestingly, in the endocrine refractory context Tamoxifen seems to promote cell growth.

There is significant interest in understanding the mechanisms of resistance, with the purpose of developing new therapeutic strategies to bypass Tamoxifen resistance.

1.5.1 Intrinsic resistance

The main mechanism for *de novo* endocrine resistance is the lack of ERα expression. For those breast cancer cases that are positive for ERα, cytochrome P450 2D6 (*CYP2D6*) enzyme is responsible for the conversation of Tamoxifen to its active metabolite, Endoxifen. Consequently, those patients that carry inactive alleles of CYP2D6 are resistant to endocrine therapy (Hoskins et al., 2009, Musgrove and Sutherland, 2009).

1.5.2 Acquired Tamoxifen resistance

Several mechanisms have been postulated to account for acquired resistance following prolonged exposure to Tamoxifen. These include changes in genomic landscape, changes in FOXA1 and ERα structure and function, alterations in FOXA1 and ERα protein interactors, increased expression or signalling of growth factor receptor pathways, dysregulations in cell cycle related pathways and dysregulations in microRNA (Osborne and Schiff, 2011).

1.5.2.1 ERα alterations in Tamoxifen resistance

It is now known that ERα-DNA interaction occurs for patients with both early and advanced, tamoxifen non-responsive disease (Ross-Innes et al., 2012a). ERα ChIP-seq was conducted in primary ERα-positive breast tumours from patients with different clinical outcomes and in metastases; differential binding analysis identified a number of genomic regions bound by ERα in patients with good prognosis that are absent in the poor prognosis group. There were also many ERα binding events unique to the poor prognosis subgroup. Therefore, Tamoxifen resistance does not imply loss of ERα-DNA interactions, but a redistribution of its binding events resulting in aberrant gene expression.

Several ERα alterations have been reported, each potentially contributing to Tamoxifen resistance. Large studies have reported *ESR1* amplifications in up to 30% of primary and metastatic ERα positive breast cancers (Basudan et al., 2019, Brown et al., 2008, Holst et al., 2007, Nembrot et al., 1990). Using approaches such as next-generation sequencing, FISH or NanoString sequencing, it has been shown that the patients harbouring copy number aberrations of *ESR1* also expressed high levels of

ERα proteins (Jeselsohn et al., 2014). ERα overexpression may contribute to reduced sensitivity to endocrine therapies. Contradictory reports presented *ESR1* amplification as an indicator of longer disease-free survival and increased sensitivity to Tamoxifen treatment (Holst and Singer, 2016, Tomita et al., 2009). These conflicting results reflect the need for more dedicated studies to fully understand the clinical implications of *ESR1* amplifications. Taken together, it seems that at least in certain subsets of patients, *ESR1* amplification plays a role in resistance to endocrine therapy and metastatic disease progression.

Advances in sequencing technologies have also enabled the identification of *ESR1* mutations in breast cancer. Three point-mutations, Y537S, Y537N, and D538G were identified as most frequent in the *ESR1* Ligand-Binding Domain. They trigger a change in ERα receptor conformation, making it constitutively active in a ligand-independent manner (Jeselsohn et al., 2018). Consequently, patients that harbour these mutations are unlikely to respond to estrogen production inhibitors [AIs] (Toy et al., 2013). It is worth mentioning that *ESR1*-Y537S and *ESR1*-D538G mutants were partially sensitive to high doses of Fulvestrant and Tamoxifen (Toy et al., 2017). Importantly, *ESR1* mutations are rarely detected in the treatment of naïve cases; they are predominant in endocrine-refractory metastatic breast cancer (Robinson et al., 2013). This strongly suggests a role of *ESR1* point mutations in acquired endocrine resistance.

Furthermore, genomic structural rearrangements (RES) involving *ESR1* gene have been identified in a small percentage of recurrent metastatic ERα positive breast cancer. The *ESR1* fusions identified are ESR1-YAP1 and ESR1-PCDH11X (Lei et al., 2018). In order to gain fusion partners, *ESR1* commonly loses its ligand binding domain (LBD). As the majority of endocrine therapies are designed against ERα LBD, cases harbouring *ESR1* fusions are usually resistant to endocrine therapies. As such, Tamoxifen and Fulvestrant are completely ineffective against ERα fusion proteins (Veeraraghavan et al., 2014).

In breast cancer, post-translational modifications (PTMs) mediate the coupling between the extranuclear signalling cascades initiated by estrogen-ERα interaction and the ERα-mediated genomic actions (Kastrati et al., 2019). PTMs include phosphorylation, acetylation, methylation, sumoylation, ubiquitination, and thiol

oxidation (Le Romancer et al., 2011). By far, phosphorylation is the most common and functionally explored ERα PTM, also being implicated in endocrine therapy response.

ERα phosphorylation emerges through overexpression of various receptor tyrosine kinases such as HER2, Epithelial Growth Factor Receptor (EGFR), and Insulin like growth factor receptor (IGF1R) (Knowlden et al., 2005, Nicholson et al., 2005); In turn, the overexpression of these receptors activates MAPK and PI3K/Akt signalling pathways (Hasson et al., 2013). This results in ligand-independent ERα activation.

Phosphorylation affects ERα conformation, dimerisation, ability to recruit co-regulators and DNA binding. *Bostner et al* observed that in primary tumours from postmenopausal patients, an overactive PI3K/Akt/mTOR pathway together with nuclear phosphorylated ERα at S167 and S305 sites, was associated with significantly reduced response to tamoxifen (Bostner et al., 2013).

1.5.2.2 FOXA1 alterations in Tamoxifen resistance

FOXA1 was found to play a critical role for ERα function in both tamoxifen-sensitive and resistant context (Ross-Innes et al., 2012a). *Ross-Innes et al* conducted *in vitro* validation of the ERα binding reprograming seen in advanced breast cancer patients. This work has shown that FOXA1 and ERα co-localise in both Tamoxifen sensitive and resistant cell lines, implying that FOXA1 may redirect ERα to its novel target regions (Fig.1.7).

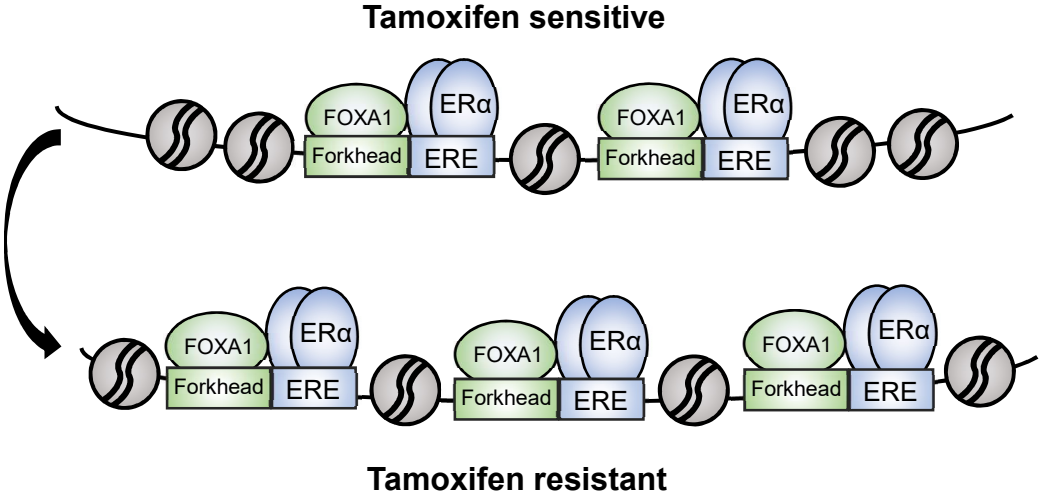

Figure 1.7. ERα and FOXA1 binding redistribution in Tamoxifen resistant compared to sensitive cell lines: FOXA1 redirects ERα to its novel binding sites.

Several studies reported that FOXA1 alterations can contribute to the novel transcriptional programme associated with endocrine resistance.

For example, FOXA1 overexpression was shown to mediate endocrine resistance by altering the ERα transcriptome and IL-8 expression in ERα-positive breast cancer (Fu et al., 2016).

The Cancer Genome Atlas (TCGA) study identified novel oncogenic alterations in breast cancer, including in FOXA1 (Koboldt et al., 2012).They have reported that 1% of the 773 breast cancer tumours tested had a focal amplification of the genomic region that encompassing *FOXA1 (*14q21.1). Most of these tumours were ERα positive and two of them were HER2 positive (Koboldt et al., 2012). However, there was no evidence of amplification of this region in the larger study published by *Curtis et al.* which categorised 1992 breast cancers on the basis of copy number changes and mRNA profiles (Curtis et al., 2012). Therefore, these amplifications are rare and their role in endocrine response is yet to be determined.

In addition, FOXA1 mutations have been observed in 1.8% of the TCGA cases (Koboldt et al., 2012), as well as in invasive lobular carcinomas (Ciriello et al., 2015). They may increase FOXA1 expression and activity, therefore they potentially contribute to enhanced ERα activity and subsequent endocrine therapy resistance. These mutations are A153V (missense mutation), S194fs (frame shift mutations), H247Y (missense); D226N (missense), S250F (missense;); I176M (missense) (Koboldt et al., 2012). Experimental modelling of these mutations within the DNA binding domain is yet to be conducted therefore it is not known whether they increase or perturb FOXA1 function.

FOXA proteins can also gain post-translational modifications in certain malignancies. For example, FOXA1 can undergo SUMOylation in prostate cell lines. This is a post-translational modification of proteins by small ubiquitin-like modifier (SUMO) proteins. FOXA1 is modified at lysines K6 and K389 and these changes influence its transcriptional activity (Sutinen et al., 2014). In addition, acetylation of FOXA1 has also been observed in liver. Specific acetylation inhibits FOXA1-chromatin binding and attenuates the ability of FOXA1 to remodel DNA (Kohler and Cirillo, 2010).

In human liver carcinoma cell lines, FOXA2 is phosphorylated in response to insulin, by Akt, a key mediator of the phosphatidylinositol 3-kinase pathway (Wolfrum et al.,

2003). Its phosphorylation inhibits FOXA2-mediated transcription as a consequence of its nuclear exclusion and cytoplasmic re-localisation. Importantly, Akt did not phosphorylate or regulate FOXA1, suggesting that there are distinct regulatory mechanisms associated with related FOXA proteins.

All these events raise the possibility that similar post-translational modifications occur for FOXA1 in breast cancer and therefore it is relevant to detect them and assess their role in breast cancer and potentially exploit them therapeutically.

1.5.2.3 Alterations in ERα and FOXA1 co-factor levels

ERα and FOXA1 are part of a dynamic complex in which other co-regulatory proteins play pivotal roles in breast cancer and drug response.

It has been demonstrated that overexpression of co-activator proteins can contribute to the Tamoxifen refractory phenotype. For example, high levels of AIB1 *in vitro* enhance Tamoxifen agonistic activity (Kressler et al., 2007, Webb et al., 1998). Moreover, patients receiving Tamoxifen treatment and that exhibit high levels of AIB1 either alone or in combination with high levels of HER2 have poorer prognosis (Fuqua et al., 2003).

Moreover, low levels of co-repressor protein NCOR also predict poor response to Tamoxifen (Lavinsky et al., 1998), supporting the hypothesis that reduction in co-repressor activity may also contribute to tamoxifen resistance.

In addition, enhanced interactions between the pioneer transcription factor PBX1 and target genomic regions are associated with a more aggressive tumour phenotype in breast cancer (Magnani et al., 2011).

More recently, Rapid Immunoprecipitation Mass spectrometry of Endogenous proteins (RIME) was developed (Mohammed et al., 2013). It has enabled the study of protein-protein interactions. RIME was applied for the identification of ERα interactome and known co-factors such as FOXA1, GATA3, NCOA3, CBP, NCOR, TLE3, RXRα were found as part of the its complex. Importantly, novel interactors were also discovered, with GREB1 being the top enriched ERα interactor both *in vitro* and *in vivo* (Mohammed et al., 2013).

The need to understand the changes in protein-protein interactions in different biological contexts motivated the development of a quantitative multiplexed workflow

that couples RIME with isobaric labelling (quantitative Multiplexed Rapid Immunoprecipitation Mass spectrometry of Endogenous proteins or qPLEX-RIME) (Papachristou et al., 2018). Using this technique, *Papachristou et al* described the dynamic changes in ERα interactome in breast cancer cells treated with Tamoxifen and also successfully applied qPLEX-RIME to PDX and clinical samples for the identification of ERα-associated proteins.

This powerful proteomics tool opens the possibility to identify novel ERα and FOXA1 protein interactors and to study their quantitative changes between Tamoxifen resistant and sensitive context. Such studies may elucidate novel mechanisms of Tamoxifen resistance, as these changes may trigger a more aggressive phenotype.

1.5.2.4 Overexpression of growth factors and kinase signalling pathways

The cross-talk between ERα and tyrosine kinase signalling is evidenced by the reciprocal expression of ERα and growth factors such as EGFR or ERBB2 (deGraffenried et al., 2004, Faridi et al., 2003). The overexpression of these growth factors triggers aberrant activation of MAPK and PI3K/Akt/mTOR kinase signalling pathways, resulting in abnormal cell growth (Creighton et al., 2010, Hutcheson et al., 2003, McClelland et al., 2001). Therefore, they can affect cell growth and endocrine response (Mills et al., 2018). Importantly, overexpression of ERBB2 is one of the best-characterised mechanisms of endocrine resistance (Arpino et al., 2008).

Activation of the kinase signalling pathways can also occur independently of ERα, can stimulate cell growth and contribute to cancer development and progression.

1.5.2.5 Cell cycle regulators

In breast epithelium, cell cycle is tightly regulated by the cyclin D/cyclin-dependent kinases 4 and 6 (CDK4/6)–retinoblastoma protein (RB) pathway. Therefore, dysregulations of CDH4/6 are tumourigenic. Such alterations involve overexpression of Cyclin D1 (CCND1), gene copy gains of CDK4, loss of negative regulators such as p16 tumour suppressor gene or dysfunctional retinoblastoma tumour suppressor protein (RB) (Cancer Genome Atlas, 2012). These dysfunctions are maintained independently of ERα, thus compromising the efficacy of ERα inhibition (Cariou et al., 2000).

1.6 ETS family of transcription factors

The E26 transformation-specific (ETS) family of transcription factors were discovered approximately 30 years ago. The family is composed of 28 members, divided into 12 subfamilies. Ever since their discovery, evidence has emerged that ETS factors can mediate differentiation and lineage specification during normal development. They are involved in maintaining cell homeostasis, by regulating cell cycle, differentiation, proliferation, apoptosis, tissue remodelling and angiogenesis (Findlay et al., 2013). Therefore, perturbations in ETS family members render them crucial onco-drivers in various cancer types.

1.6.1 ETS factors in cancer

Several alterations of the ETS factors have been linked to carcinogenesis. Among these perturbations, there are their copy number amplifications, mutations and chromosomal rearrangements. ETS-dependent gene activation is also influenced by post-translational modifications. Notably, ETS phosphorylation can influence their binding to DNA as well as increase their interactions with co-activator or co-repressor proteins, thus impacting on their transcriptional activity (Charlot et al., 2010). Therefore, phosphorylation may be a key mechanism for ETS aberrant signalling in cancer cells.

In addition, it has been shown that in gastrointestinal stromal tumour (GIST), mutated and constitutively active tyrosine kinase receptor KIT stabilises ETV1 (member of the ETS family) through MEK-ERK pathway. This results in ETV1 overexpression and an oncogenic ETS transcriptional programme (Chi et al., 2010).

Importantly, chromosomal rearrangements involving the ETS genes have been reported in various cancer types. For example, it was shown that approximately half of prostate tumours contain the TMPRSS2–ETS fusions (Mehra et al., 2007). The fusion on its own can drive prostatic intraepithelial neoplasia (PIN) and its combination with loss of tumour suppressor PTEN was shown to induce prostate adeno-carcinomas in mouse models (Squire, 2009).

In particular, in breast cancer, a number of abnormalities involving members of the ETS family have been reported. For example, copy number amplifications of the

genomic regions encompassing for ETV3 and ELF3 were identified in breast carcinoma samples and ELF3 amplification was linked to carcinogenesis (Mesquita et al., 2013). In addition, overexpression of ETS1 and ETS2 were also identified in breast cancer and linked to repression of BRCA1 expression (Baker et al., 2003, Ibrahim et al., 2012). Furthermore, prostate derived ETS factor (PDEF) was identified as an oncogenic driver in ERα positive breast cancer (Sood et al., 2017).

1.6.2 ETV6 (TEL-1, TEL) in cancer

ETV6 (also known as *TEL*) is one of the ETS factors and was originally discovered in a leukaemia-associated chromosomal translocation (Golub et al., 1994). It has subsequently been identified as a fusion partner in more than 30 chromosomal translocation oncogenes (de Braekeleer et al., 2013).

1.6.2.1 ETV6 structure

ETV6 contains an ETS DNA-binding domain on its C-terminal (Fig.1.8). The DNA binding domain has a winged helix-turn-helix structure that recognises and binds to a 4-nucleotide (GGAA) DNA motif (Karim et al., 1990).

ETV6 also contains an N-terminal pointed (PNT) domain, known as the helix loop helix (HLH) domain (Klämbt, 1993) that is responsible for the homo- and hetero-dimerisation of ETV6 (Lacronique et al., 1997) (Fig.1.8).

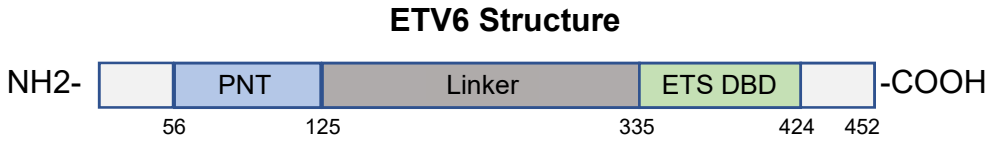

Figure 1.8. ETV6 protein structure: from the N terminus to the C terminus, ETV6 contains the pointed domain, the linker and the ETS-DNA binding domain.

Both the DBD and the PNT domains of ETV6 are highly conserved within the ETS family. In the past, these high similarities created difficulties in distinguishing between the effects of individual ETS factors on gene expression and biological processes (Hollenhorst et al., 2011). As our research tools such as proteomics, genomics and genetics gain higher resolution, we have begun to unravel these redundancies.

1.6.2.2 ETV6 deregulations in cancer

ETV6 was found to be involved in translocations involving other genes such as RUNX, PAX5 and NTRK3 (Kralik et al., 2011, Odero et al., 2001). Consequently, the ETV6 DNA binding domain becomes part of oncogenic fusion proteins, resulting in altered expression of ETV6 target genes. In particular, ETV6- NTRK3 gene fusion is the driving oncogenic event in 92% of the secretory breast carcinoma clinical samples assessed by *Tognon et al* (Tognon et al., 2002).

Importantly, copy-number aberrations of ETV6 are associated with significantly worse prognosis of breast cancer patients within the METABRIC cohort (Curtis et al., 2012).

Germline mutations of ETV6 have also been detected in families with predisposition to develop haematological disease, such as AML and childhood ALL (Moriyama et al., 2015). Their occurrence is indicative of their potential contribution to leukemogenesis, though more studies need to be conducted to understand how ETV6 mutations influence its function.

In contrast, certain studies describe ETV6 as a tumour suppressor gene. For example, ETV6 expression levels were significantly lower in colorectal cancer tissues compared to paired normal tissues (Wang et al., 2016). Another previous study has shown that upregulation of *ETV6* attenuates proliferation and suppresses Ras-induced transformation (Van Rompaey et al., 2000).

These conflicting results suggest a complex role of ETV6 that can act as an oncogene or can have anti-oncogenic effects in a context-dependent manner.

1.7 Current alternative therapies for endocrine resistant breast cancer

HER2 positive breast cancer is a more aggressive subtype, associated with poor prognosis and high mortality, but the development of targeted therapies against HER2 has significantly improved patient survival. Trastuzumab (Herceptin®) is a monoclonal antibody against HER2 that inhibits its homodimerisation, thus preventing the HER2-mediated aberrant cell growth (Namboodiri and Pandey, 2011). Herceptin is FDA-approved for the adjuvant treatment of HER2-positive early and metastatic breast

cancer (Gianni et al., 2012). HER2 targeted therapy is also used in combination with tyrosine-kinase inhibitors such as Lapatinib or aromatase inhibitors such as Anastrozole (de Azambuja et al., 2014, Kaufman et al., 2009)

In addition, a novel therapeutic strategy for ERα positive, HER2 positive breast cancer patients has recently been developed. It combines the monoclonal antibody Trastuzumab (T) with the potent cytotoxic maytansine derivative (DM1) and it is termed T-DM1 (Okines, 2017).

Moreover, in recent years, combination therapies targeting both the ERα and the PI3K/AKT/mTOR pathways have proved successful. Clinical trials have assessed the combination between aromatase inhibitors and Everolimus, a selective inhibitor of mTOR. This combinatorial therapeutic strategy has significantly prolonged patient disease-free survival (Yardley et al., 2013). As a result, Everolimus was FDA-approved for postmenopausal patients with ERα positive breast cancer. However, due to the heterogeneity of breast cancer, a subset of patients did not respond to this drug (Martelotto et al., 2014). Therefore, it is crucial to find biomarkers that predict the efficacy of Everolimus in clinical settings.

CDK4/6 inhibitors prevent the phosphorylation of the RB tumour suppressor, resulting in cancer cell cycle arrest in G1. Such inhibitors (e.g. Palbociclib, Ribociclib) were shown to substantially improve the progression-free survival and are now FDA-approved for use in combination with endocrine therapy to treat advanced stage ERα positive disease (Finn et al., 2015).

Tamoxifen resistance is therefore a major challenge in breast cancer. Understanding some of the mechanisms behind resistance has facilitated the development of novel targeted therapies that have substantially improved patient outcome. Yet subsets of patients do not respond to any of the available therapeutic strategies, indicating there still are alternative escape routes for breast cancer progression. As such, further understanding of the determinant factors for endocrine resistance, is critical to improving breast cancer treatment.

1.8 Aims

The ERα transcription factor is a master regulator in mediating the breast cancer phenotype. Therefore, several therapies against ERα or its ligand estrogen have been developed and successfully improved patient survival. In addition, extensive work has determined that FOXA1 acts upstream of ERα, thus dictating its transcriptional programme. As such, FOXA1 is an attractive therapeutic target that may benefit ERα breast cancer patients, including those with endocrine resistance. Moreover, in recent years, targeted agents against several other pathways have been developed and successfully prolonged disease-free survival. Yet, certain patients do not respond to any of these therapies and therefore it is vital to further understand the molecular mechanisms of endocrine resistance in ERα positive breast cancer with the goal of identifying alternative determinant factors that may be therapeutically targeted.

In this context, the aims of this thesis are:

1. to reinforce the concept of FOXA1 being a pioneer transcription factor in ERα positive breast cancer;

2. to further characterise ERα and FOXA1 role in endocrine resistant compared to sensitive context;

3. to shed light on the role of the newly identified ERα/FOXA1 interactor called ETV6 in breast cancer progression and endocrine-resistant phenotype;

4. to identify potential new candidates for the treatment of hormone-refractory breast cancer.

Chapter 2. Materials and Methods

2.1 Materials

2.1.1 Cell lines and media

All cell lines were maintained at 37°C and 5% CO2 in a humidified atmosphere.
MCF-7, ZR-75-1, MDA-MB-231, HEK293FT and MCF-10A cell lines were obtained from ATCC (Middlesex, UK).
MCF-7 and HEK293FT cells were cultured in Dulbecco's Modified Eagle Medium DMEM (Gibco, Thermo Scientific, Leicestershire, UK, ref. 41966). ZR-75-1 and MDA-MB-231 cells were grown in RPMI-1640 medium (Gibco, Thermo Scientific, Leicestershire, UK, ref. 21875-034). Both media were supplemented with foetal bovine serum (FBS), 50 U/ml penicillin, 50 µg/ml streptomycin and 2 mM L-glutamine.
MCF-10A cells were cultured in Mammary Epithelial Cell Growth Basal Medium MEBM (Lonza, Basel, Switzerland ref. CC-3151), supplemented with MEGM Mammary Epithelial Cell Growth Medium Kit (Lonza, ref. CC-4136).
Tamoxifen resistant MCF-7-TRF and ZR-75-1-TamR cell lines were derived from MCF-7 and ZR-75-1, respectively, by continuous exposure to 4-hydroxy-Tamoxifen (Sigma-Aldrich, H7904) until they have become resistant to the compound. The concentration of Tamoxifen was progressively increased to 1µM for MCF-7-TRF and 100nM for ZR-75-1-TamR.
Cells were genotyped periodically by short-tandem repeat (STR) profiling using the PowerPlex 16HS Cell Line panel and analysed using Applied Biosystems Gene Mapper ID v3.2.1 software by external provider Genetica DNA Laboratories (LabCorp Specialty Testing Group). Cells were also tested periodically for mycoplasma using the MycoProbe Mycoplasma detection kit (R&D).

2.1.2 PDX material

PDX material was kindly provided by Prof Carlos Caldas and Dr Alejandra Bruna *(CRUK-Cambridge Institute, UK)* and by Prof Elgene Lim *(Garvan Institute, Sydney, Australia).* The PDXs have been propagated in immune-compromised mice. Briefly,

tumour pieces (1mm^3) were implanted into the mammary pad of NSG mice. All mice were treated with estrogen pellets. Tumours were measured twice a week. When tumours reached ~1000 mm^3, mice were sacrificed and tumours resected. They were either snap-frozen in liquid nitrogen, fixed in 10% neutral buffered formalin solution for subsequent paraffin embedding or embedded in Optimal Cutting Temperature compounds (OCT). The PDXs have been provided as frozen material and access to the paraffin embedded tissue was granted. Description of PDX models used is provided in Table 2.1 below:

PDX ID	tissue type	tamoxifen status	IHC assessment	other comments
AB555	primary tumour	Tamoxifen resistant	ER positive; FOXA1 positive; HER2 negative	
STG143	primary tumour	Tamoxifen resistant	ER positive; FOXA1 positive; HER2 negative	
STG195	Pleural effusion	Tamoxifen and AI resistant	ER positive; FOXA1 positive; HER2 negative	Y537S ESR1 mutation
HCI005	pleural effusion	Tamoxifen resistant	ER positive; FOXA1 positive; HER2 negative; PR positive	
HCI006	pleural effusion	Tamoxifen resistant	ER positive; FOXA1 positive; HER2 negative; PR positive	same patient sample as HCI005, passaged in sister mouse
HCI011	pleural effusion	Tamoxifen resistant	ER positive; FOXA1 positive	
HCI013	pleural effusion	Tamoxifen resistant	ER positive; FOXA1 positive	

Table 2.1. Patient derived xenograft models used and their characterisation.

2.1.3 Clinical samples

Clinical samples were kindly provided by Dr Wilbert Zwart and his colleagues *(NKI, Amsterdam, The Netherlands).* They consisted of six primary breast cancer tumour samples and four pleural effusions (Table 2.2). All samples were collected under

project “Analyses on pleural effusions breast cancer patients”, registration number CFMPB411 at the biobank from the *Cancer Institute (NKI). T*he samples were provided frozen. In addition, frozen sections were cut for IHC staining.

Clinical sample ID	Tissue type	IHC assessment	Other comments
T15-09974	primary breast cancer	ER positive; FOXA1 positive; HER2 negative; PR positive	
T15-09974	primary breast cancer	ER positive; FOXA1 positive; HER2 negative; PR positive	Technical rep; smaller than 1.
T13-02381	primary breast cancer	ER positive; FOXA1 positive; HER2 negative; PR positive	
T11-12448	primary breast cancer	ER positive; FOXA1 positive; HER2 negative; PR positive	
T-1112441	primary breast cancer	ER positive; FOXA1 positive; HER2 negative; PR positive	
T12-01538	primary breast cancer	ER positive; FOXA1 positive	
M6	pleural effusion	ER positive; FOXA1 positive	
M28	pleural effusion	ER positive; FOXA1 positive; HER2 negative; PR positive	
M31	pleural effusion	ER positive; FOXA1 positive	
M32	pleural effusion	ER positive; FOXA1 positive	

Table 2.2. Clinical samples used and their characterisation.

2.1.4 Antibodies

Antibodies used for western blot are listed in Table 2.3:

Primary Antibodies				
Protein Target	**Antibody reference**	**Antibody source and clonality**	**Antibody dilution/**	**Protein molecular weight**
ERα	Novocastra, Leica NCL-L-ER-6F11	mouse monoclonal	1 in 50	66 kDa
FOXA1	Abcam, ab23738	rabbit polyclonal	1 in 1000	50-37 kDa
β-Actin	Cell Signalling, 4970S	Rabbit monoclonal	1 in 1000	42 kDa
ETV6	Sigma Aldrich, WH0002120M1	mouse monoclonal	1 in 500	55 kDa
pERK	Cell Signalling, 9106S	mouse monoclonal	1 in 2000	42 and 44 kDa
GAPDH	Cell Signalling, 97166S	mouse monoclonal	1 in 1000	37 kDa
	Cell Signalling, 2118S	rabbit monoclonal	1 in 1000	
Histone 3	Cell Signalling, 9715S	rabbit polyclonal	1 in 2000	17 kDa
Secondary Antibodies				
Antibody reference		**Antibody source and clonality**		**Antibody dilution**
IRDye® 800 CW, Li-Cor Biosciences 926-32210		Goat anti-Mouse IgG		1 in 5,000
IRDye® 680LT Li-Cor Biosciences 926-68020		Goat anti-Mouse IgG		1 in 20,000
IRDye 680LT Li-Cor Biosciences 926-68071		Goat anti-Rabbit IgG		1 in 15,000
IRDye® 800CW Li-Cor Biosciences 926-32211		Goat anti-Rabbit IgG		1 in 15,000

Table 2.3. List of antibodies used for western blot and their targets.

Antibodies used for immunohistochemistry are listed in Table 2.4:

Protein Target	Antibody reference	Antibody source and clonality	Application	Concentration	Retrieval
ERα	Novocastra, Leica NCL-L-ER-6F11	mouse monoclonal	IHC paraffin tissue	1.071 µg/ml	Sodium Citrate, 30', 100°C
			IHC frozen tisue	0.75 µg/ml	None
FOXA1	Abcam 23738	rabbit polyclonal	IHC paraffin tissue	0.8 µg/ml	Sodium citrate, 20', 100°C
			IHC frozen tissue	1.25 µg/ml	None
ETV6	Sigma, WH0002120M1	mouse monoclonal	IHC paraffin tissue	1.25 µg/ml	Tris EDTA, 20'
			IHC frozen tissue	1.25 µg/ml	none

Table 2.4. **Antibodies and conditions used for immunohistochemistry (IHC)**.

Antibodies used for ChIP and RIME are listed in Table 2.5:

Protein Target	Antibody reference	Antibody source and clonality	Concentration	Application
ERa	Santa Cruz, sc-543	rabbit polyclonal	10 µg/µl	ChIP, RIME
	Abcam, ab3575	rabbit polyclonal	10 µg/µl	ChIP, RIME
	EMD Milipore, 06-935	rabbit polyclonal	10 µg/µl	ChIP, RIME
	Abcam, ab80922	rabbit polyclonal	10 µg/µl	ChIP
	Santa Cruz, sc-514857 (C-3)	mouse monoclonal	10 µg/µl	ChIP
	Diagenode, C15100066	mouse monoclonal	10 µg/µl	ChIP
FOXA1	Abcam, ab5089	goat polyclonal	10 µg/µl	ChIP, RIME
	Abcam, ab23738	rabbit polyclonal	10 µg/µl	ChIP, RIME
HRK27Ac	Abcam, ab4729	rabbit polyclonal	10 µg/µl	ChIP
ETV6	Bethyl Lab, A303-674A-M	rabbit polyclonal	10 µg/µl	ChIP, RIME

Table 2.5. Antibodies used for ChIP and RIME.

2.1.5 Primers

Primers for ChIP-qPCR are listed in Table 2.6:

Name	Forward primer (5'- 3')	Reverse primer (5'- 3')
XBP1 enh 1	ATACTTGGCAGCCTGTGACC	GGTCCACAAAGCAGGAAAAA
GREB1 enh 3	GAAGGGCAGAGCTGATAACG	GACCCAGTTGCCACACTTTT
RARα intron	GCTGGGTCCTCTGGCTGTTC	CCGGGATAAAGCCACTCCAA
MYC enh	GCTCTGGGCACACACATTGG	GGCTCACCCTTGCTGATGCT
ESR1 Enh 3	GAAACAGCCCCAAATCTCAA	TTGTAGCCAGCAAGCAAATG
ER3 negative site	GCCACCAGCCTGCTTTCTGT	CGTGGATGGGTCCGAGAAAC
XBP1 negative site	ACCCTCCAAAATTCTTCTGC	ATGAGCATCTGAGAGCAAGC

Table 2.6. Primer sequences for ChIP-qPCR.

Primers for qRT-PCR are listed in Table 2.7:

Name	Forward primer (5'-3')	Reverse primer (5'- 3')
ESR1	TGATTGGTCTCGTCTGGCG	CATGCCCTCTACACATTTTCCC
FOXA1	GGGGGTTTGTCTGGCATAGC	GCACTGGGGGAAAGGTTGTG
GATA3	CGGCTTCGGATGCAAGTCCAGGC	TTGTGATAGAGCCCGCAGGCGTT
ETV6	AGGTGGAAGACATTGAGGGG	CCAAGGGCACAGGTAAGAGA
UBC control	ATTTGGGTCGCGGTTCTTG	TGCCTTGACATTCTCGATGGT

Table 2.7. Primer sequences for qRT-PCR.

2.1.6 siRNA library and siRNA

The LP_34662 RNAi Cherry-pick Library used was purchased from Dharmacon, Horizon Discovery (ref. *G-CUSTOM-294730).* Information about all target genes and siRNA sequences from the library are provided in Annexe 1:

Targets from the siRNA library were then validated using the siRNA reagents listed in Table 2.8. All siRNA transfections were achieved using the Lipofectamine RNAiMAX transfection reagent, as per manufacturer's guidance (Invitrogen, ref. 13778).

siRNA and target gene	reference no	siRNA sequence 5'-3'
SMARTpool: ON-TARGETplus FOXA1 siRNA	L-010319-00	GCACUGCAAUACUCGCCUU
		CCUCGGAGCAGCAGCAUAA
		GAACAGCUACUACGCAGAC
		CCUAAACACUUCCUAGCUC
SMARTpool: ON-TARGETplus non-targeting siRNA	D-001810-10	UGGUUUACAUGUCGACUAA
		UGGUUUACAUGUUGUGUGA
		UGGUUUACAUGUUUUCUGA
		UGGUUUACAUGUUUUCCUA
Individual: ON-TARGETplus ETV6 siRNA	J-010510-10	GGGAUUACGUCUAUCAGUU
Individual: ON-TARGETplus ETV6 siRNA	J-010510-11	CAGGUGAUGUGCUCUAUGA

Table 2.8. Sequences of siRNAs.

2.1.7 Compounds and compound library

The compound library L1300-Selleck-FDA-Approved-Drug-Library-978cpds (Stratech, Selleckchem) was used. A list of all 978 compounds and their description is provided in the Annexe 2: The individual drugs used to treat cells are listed in the Table 2.9:

Compound	Mechanism of action	Company and reference number
17β-estradiol	hormone	Sigma-Aldrich, E2758
4-hydroxy-Tamoxifen	SERM	Sigma-Aldrich, H7904
Fulvestrant	SERD	Selleckchem, S1191
Trametinib	MEK 1/ 2 inhibitor	Selleckchem, GSK1120212
Everolimus	mTOR inhibitor	ApexBio, 159351-69-6

Table 2.9. List of compounds used and their mechanism of action.

2.1.8 Purified plasmids

The vector used to overexpress ETV6 was purchased from Genecopoeia (ref. EX-F0874-Lv181). The matched empty control vector pReceiver-Lv181 (Genecopoeia, ref. EX-NEG-Lv181) was used and the map for the plasmid is provided in Figure 2.1:

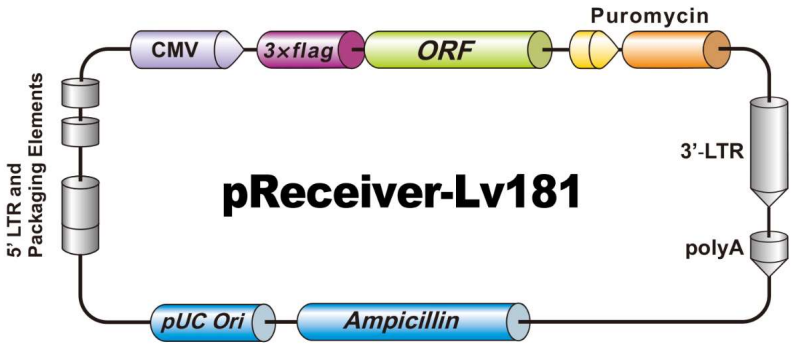

Figure 2.1 pReceiver-Lv181 vector map.

2.2 Methods

2.2.1 Cell culture

Cell stocks were thawed at 37°C, centrifuged at 1300 rpm for 3 minutes, resuspended in their corresponding growth medium and plated. They were cultured until 80-90% confluent. Then, they were rinsed twice using sterile phosphate-buffered saline (PBS), trypsinised, neutralised with growth media containing 10% FBS, and pelleted by centrifugation for 3 minutes at 1300 rpm. Cells were resuspended in medium. For continuous culture, they were replated at a dilution between 1:3 and 1:6. To conduct experiments, cells were counted using LUNA™ Automated Cell Counter (Logos Biosystems, ref. L10001) and seeded at the appropriate density. In order to create frozen stocks, cells were resuspended in 10%DMSO and 90% FBS and slowly frozen to -80°C using the Nalgene® Freezing container (Sigma Aldrich, ref.C1562-1EA).

2.2.2 siRNA transfections

To assess the effect of target gene knock-down on cell growth and viability, an siRNA library screen was conducted and then validated using single siRNA transfections. All

siRNA transfections were achieved using the RNAiMax reagent. Briefly, cells were plated in full media at the appropriate density and grown for 24 hours. They were then transfected using the Lipofectamine RNAiMax reagent as per manufacturer's guidance. The transfection reagent was diluted in Opti-MEM (Gibco, ref. 31985-047). At the same time, the siRNA was separately diluted in Opti-MEM. They were incubated separately for 5 minutes, after which they were mixed and incubated for a further 20 minutes at room temperature. The mixture was then added to the cells in full growth media. After 24 hours, the media was changed with fresh normal media and cells were further grown for the relevant amount of time.

2.2.3 Hormone and compound treatments

MCF-7 and ZR-75-1 cells were plated at 30% confluency to assess the effects of 17β-estradiol on FOXA1-chromatin binding. The following morning, media was changes and replaced with phenol red-free DMEM supplemented with 5% charcoal/dextran stripped FBS. The cells were maintained in hormone-depleted media for 72 hours, and media was changed daily. Then, cells were treated either with ethanol or with 10nM of 17β-estradiol (Sigma) for 45 minutes, as previously described (Schmidt et al., 2009). The drug effects on cells were tested through treatment with the appropriate concentration of the compounds, diluted in Opti-MEM.

2.2.4 FDA-approved compound screen

The drug screen was conducted in three biological replicates for each screened cell line. There was one technical replicate for each of the 978 compounds in every biological replicate.

First, cells were counted and resuspended in their corresponding full media, at 30% confluency. They were seeded in 384-well plates with opaque walls using the Multidrop™ Combi Reagent Dispenser (Thermo, ref. 5840300) and incubated for 24 hours. Cells were then treated with 1 μM of each of the 978 compounds. The appropriate volume of the drug diluted in DMSO was dispensed using the Echo®555 liquid handler (Labcyte, ref. 001-5234). Treatment was allowed for 96 hours after which cell viability was assessed using *CellTiter-Glo® Luminescent Cell Viability Assay, (Promega, ref.G7571).* Percentage viability over control DMSO was calculated.

Only drugs that inhibited growth with 50% in all three biological replicates were considered for further analysis.

2.2.5 pLenti overexpression of target genes

MCF-7 and ZR-75-1 cells that overexpress ETV6, as well as their matched controls, were generated as follows:

2.2.5.1 Transformation of competent cells

DH5α Library Efficiency cells (Invitrogen, cat. no. 18262-014) were transformed either *with* empty control vector pReceiver-Lv181 (Genecopoeia, ref. EX-NEG-Lv181) or with the p-ETV6-Lv181 (Genecopoeia ref. EX-F0874-Lv181).
Briefly, competent cells were gently thawed on ice. For each reaction, 50 µl of E. Coli competent cells were mixed gently with 10 ng of plasmid DNA and incubated on ice for 30 minutes. The cells were then heat-shocked for 45 seconds in a 42°C water bath and then placed on ice for 2 minutes. 950 µl of luria broth (LB) (10g/l tryptone powder, 5g/l yeast extract powder, 85.5 mM NaCl) was added to the cells and then they were incubated at 37°C for 1 hour, at 225 rpm. Then, 100 µl of the transformed bacteria mix were spread on agar plates (LB containing 14 g/l agar) treated with 100 ug/ml Ampicillin. Plates were incubated overnight at 37°C. The following morning, colonies containing the transformed plasmid were picked, added to 200 mls of LB media containing 100 µg/ml ampicillin and grown again overnight.

2.2.5.2 Purification of Plasmid DNA

In order to isolate the plasmid DNA from the transformed bacteria, the QIAfilter Plamid Maxi Kit (cat. no. 122345) was used. The protocol was followed as described by the manufacturer. The DNA concentration was quantified using a NanoDrop® ND-1000 Spectrophotometer (Thermo Scientific, Leicestershire, UK). The plasmids were subjected to Sanger Sequencing to validate they contained the correct insert.

2.2.5.3 Viral production

In order to generate the cDNA lentiviral particles, 4 million HEK293FT cells were plated in complete DMEM, in 10cm plates. The following morning, they were transfected with the following mix, diluted in 1 ml Opti-MEM medium:

- 5ug pCMV-gag-pol-tat-rev
- 2.5ug pMD2-VSV-G
- 37.5 ul Lipofectamine 2000 transfection reagent.
- 5ug of transfer plasmid (either p-ETV6-Lv181 or empty p-Lv181)

The transfection medium was left onto HEK293FT cells overnight. The following morning, the medium was changed with 8 mls of fresh complete DMEM medium. Cells were grown for 48 more hours, after which the supernatant containing cDNA lentiviral particles was collected and filtered through 0.45μm filters.

2.2.5.4 Viral infection

MCF-7 and ZR-75-1 cells were counted and 300,000 cells were plated per well in a 6-well plate, in their corresponding media. The following morning, they were infected with 2ml of the viral supernatant supplemented with 10μg/ml Polybrene for 24 hours.

The following morning, infection media was changed to fresh complete media. Cells were allowed to recover for 72 hrs, after which cells containing the plasmid were selected with 1μg/ml puromycin.

2.2.6 Assessment of cell growth and viability

2.2.6.1 Cell growth

Colony Formation Assays were conducted to validate Tamoxifen resistance in MCF-7-TRF and ZR-75-1-TamR, as well as to assess cell response to various drugs. Cells were plated in 6 or 12 well plates. The following day, they were treated appropriately and incubated for 10-15 days. Treatments were refreshed periodically. At the end of the assay, cells were fixed for 5 minutes using 4% formaldehyde and stained using crystal violet. They were washed, air dried and visualised on GelCount Optronix (Scintica Instrumantation). Colony mask area total density was assessed using the GelCount software.

Cell confluency as a measure of cell growth was assessed using the IncuCyte Zoom Live Cell Analysis System (Essen Bioscience). Cells were seeded in the appropriate plates (6-96 well plates) and growth was monitored for at least 120 hours via phase

contrast images taken at 3-hour intervals. Confluence was assessed using the default settings of the IncuCyte ZOOM software.

2.2.6.2 Cell viability

Cell viability in response to drugs, knock-downs or overexpressions was assessed using CellTiter-Glo® Luminescent Cell Viability Assay, (Promega, ref. G7571), as described by the manufacturer. Briefly, cells were grown and treated appropriately in 96 or 384 opaque-walled plates. CellTiter-Glo® Reagent was prepared by mixing the substrate with the buffer. Then, the reagent was added at a 1:1 ratio to the media from the plates. Contents were mixed for 2 minutes on an orbital shaker. Plates were incubated for 10 minutes at room temperature and luminescence was recorded using the PheraStar FS microplate reader (BMG LABTECH).

2.2.7 Assessment of gene expression

2.2.7.1 RNA isolation and quantification

Cells were washed twice in ice-cold PBS and harvested in PBS. Total RNA was extracted using the RNeasy kit (Qiagen), according to manufacturer's instructions. The extracted RNA was quantified by measuring the absorbance using a NanoDrop ND-1000 Spectrophotometer (Thermo Scientific).

2.2.7.2 cDNA synthesis

Total RNA was used for cDNA synthesis, using the Super Script III Reverse Transcriptase kit (Invitrogen, ref. 18080085). Briefly, 1 µg of total RNA, 100 ng of random primers, 1 µl 10 mM dNTP Mix (10 mM each dATP, dGTP, dCTP and dTTP at neutral pH) were diluted to a final volume of 13 µl using nuclease-free water.
The mix was incubated at 65°C for 5 minutes and then placed on ice for one minute.
Then, the following reagents were added: 4 µl 5X First-Strand Buffer, 1 µl 0.1 M DTT (1,4-dithiothreitol), 1 µl RNaseOUT™ Recombinant RNase Inhibitor (Cat. no. 10777-019, 40 units/µl) and 1 µl of SuperScript™ III RT (200 units/µl).
Reactions were incubated at 25°C for 5 minutes to allow primers to anneal and then heated at 50°C for 30 minutes.
The enzymatic reaction was inactivated at 70°C for 15 minutes.

The newly synthetized cDNA was diluted 1:10 and subsequently used for quantitative reverse transcriptase PCR (qRT-PCR) analysis.

2.2.7.3 Quantitative RT-PCR

Reactions were performed in triplicate and analysed using the Stratagene Mx3005P Real Time machine. Each reaction mix contained 1X Power SYBR Green PCR Master Mix (Applied Biosystems, ref. 4367659), forward and reverse primers (final concentration of 10 μM) and 2 ul of diluted cDNA. The mix was diluted to 15 μl using nuclease-free water. The hot-start Taq polymerase from the Master Mix was heat-activated at 95°C, followed by 40 cycles of 15 seconds at 95°C and 30 seconds at 60°C. Fluorescence was read in each cycle. For the final step, the temperature was slowly increased from 65 to 95°C and a melting curve was generated by continuously reading the fluorescence. Gene expression relative to a house keeping gene UBC was determined using the delta-delta Ct method (Livak and Schmittgen, 2001)

2.2.7.4 RNA sequencing (RNA-seq)

Library preparation was performed using the TruSeq stranded mRNA library prep kit (Illumina) and sequencing was conducted by the Genomics Core Facility from CRUK-Cambridge Institute) using NovaSeq 50bp single-end reads. Approximately 30 million reads per sample were generated.

2.2.7.4.1 RNA-seq bioinformatics analysis

Data processing and bioinformatic analysis was performed by Dr Igor Chernukhin (CRUK-CI, Cambridge). The RNA-seq reads were aligned to the Human Reference Genome (hg 38) using STAR tool (Dobin and Gingeras, 2015). Normalised read counts were interrogated for differential gene expression using DESeq2 (Love et al., 2014).

2.2.8 Assessment of protein levels

2.2.8.1 Western blot

2.2.8.1.1 Whole cell lysate preparation for western blot

Cells were washed twice in ice-cold PBS and then scraped in 100 μl Pierce RIPA Buffer (Thermo Scientific, ref. 89901) supplemented with protease inhibitors (Roche,

Mannheim, Germany). Protein lysates were sonicated at high speed for two cycles of 30 seconds on, 30 seconds off and then the cellular debris was removed by centrifugation at 20,000 rpm for 10 minutes, at 4°C. The whole cell lysate was transferred to clean eppendorfs for quantification.

2.2.8.1.2 Chromatin and cytoplasmic protein extractions

One 15 cm plate per sample used. Cells were washed twice with PBS and scraped in PBS containing Protease inhibitors. Following centrifugation at 8,000rpm, 3 minutes, 4ºC, pellets were subjected to a chromatin isolation protocol adapted after (Méndez and Stillman, 2000).

Pellets were resuspended in 500 Buffer A (10mM Hepes (pH 7.9),10mM KCl, 1.5mM MgCl2, 0.34M Sucrose, 10% glycerol) to which 1mM DTT, 0.1% Triton X-100 and protease inhibitors were added. Samples were incubated on ice for 10 minutes. Samples were centrifuged at 3,500 rpm for 5 minutes, at 4°C. Supernatant containing the cytosolic fraction was retained in separate eppendorfs and stored at -20°C. Nuclei were further washed in buffer A containing 1 mM DTT, but no detergent. Nuclei were pelleted and resuspended in 500 µl Buffer B (3mM EDTA, 0.2mM EGTA) containing 1mM DTT and protease inhibitors. Samples were incubated on ice for 30 minutes, with occasional vortexing.

Samples were centrifuged at 4,000 rpm for 5 minutes, at 4°C and then washed 5 times in 500 µl Buffer B containing 1mM DTT and protease inhibitors. After the last spin, pellets were resuspended in 50 µl Pierce RIPA buffer, sonicated for two cycles of 30 seconds on, 30 seconds off, centrifuged at maximum speed for 10 minutes. Supernatant containing the chromatin fraction was taken to clean tubes for quantification.

2.2.8.1.3 Western blot analysis

Protein quantification for whole cell lysate, chromatin and cytoplasmic extracts was achieved using the infrared (IR)-based biomolecular quantitation system Direct Detect® (Millipore, Massachusetts USA).

Twenty-five µg proteins per whole lysate or 15 µg proteins for the chromatin and cytoplasmic fractions were used for western blot analysis.

Precision Plus, ProteinTM dual color Standards Protein molecular weight marker (Bio-Rad, #161-0974) was used for the determination of protein sizes.

Following electrophoresis, the resolved proteins were transferred onto a nitrocellulose membrane using the iBlot® 2 Dry Blotting System (Invitrogen, California, USA). The membrane containing the irreversibly bound proteins was then blocked for unspecific binding of the antibodies to the membrane using the Odyssey Blocking Buffer (Li-Cor, 927-40000). The membranes were immunoblotted overnight with the appropriate primary antibodies diluted in Odyssey blocking buffer: TBS plus 0.1% Tween 20. Detection of the primary antibodies was achieved using the appropriate secondary antibodies. The proteins were visualised using the Odyssey CLx Infrared Technology (Li-Cor) and images were taken with the automated capture option from Image studio Version 4.0 software.

2.2.8.2 Immunohistochemistry (IHC)

Immunohistochemistry (IHC) assays were conducted by the Histopathology Core Facility (CRUK-CI).

The 3 µm paraffin sections were dewaxed in xylene and rehydrated through graded ethanol concentrations on a Leica ST5020 system. IHC staining for paraffin embedded sections was then conducted on the BOND-III platform (Leica Biosystems), while frozen sections were stained on Bond RX (Leica Biosystems). All IHC was run using a modified version of the BOND polymer refine detection kit (Leica Microsystems, ref. DS9800).

The tissue pre-treatment conditions and concentration were optimised for each primary antibody (Table 2.4): The rabbit polyclonal anti-FOXA1 antibody was detected with the kit's polymer conjugated secondary antibody (anti-rabbit Poly-HRP-IgG). The mouse monoclonal anti ERα and anti ETV6 antibodies were detected by the post primary (rabbit anti-mouse IgG) first, followed by the anti-rabbit polymer. The polymer was finally detected with the 3-3'-diaminobenzidine (DAB) enhancer (Leica Microsystems, ref AR9432).

Stained sections were de-hydrated and cleared on the Leica ST5020 system and mounted using the Leica cover slipper (ref. CV5030).

Staining was viewed following digitisation using the Aperio platform (Leica Biosystems).

2.2.9 Chromatin Immunoprecipitation for ChIP-qPCR and ChIP-seq

2.2.9.1 Bead preparation

The type of Protein A or G Dynabeads® (Invitrogen) was chosen depending on the antibody species used. Aliquots of 50 µl beads were made for each sample. They were washed 3 times with PBS + 5mg/ml BSA and resuspended in 1 ml PBS/BSA. Five µg of the appropriate antibody was added for each sample and the mix was rotated at 12 rpm, overnight, at 4°C.

The following day, beads were washed three times with PBS/PBA, in order to remove the unbound antibody. They were then resuspended in LB3+1%Triton X-100 (enough for 200µl of beads for each supernatant).

2.2.9.2 Sample preparation for chromatin immunoprecipitation

Sample preparation was conducted as follows: Frozen clinical samples and PDX material were embedded in Optimal Cutting Temperature compound (OTC) and cryosectioned at 30 microns. Samples were cross-linked for 25 minutes at room temperature using 2mM disuccinimidyl glutarate (DSG), while rotating at 15prm. Then, a final concentration of 1% methanol-free formaldehyde was added straight to the DSG solution and samples were cross-linked with the mixture for 20 more minutes, maintaining the rotation. Afterwards, the cross-linking was quenched with 2.5M glycine (pH7.5) 1:10, for 10 minutes. In order to remove the supernatant, samples were centrifuges at 2,000 g for five minutes at 4ºC and sections were pelleted. Pellets were washed twice in ice-cold PBS, samples were spun down and PBS removed. Finally, the material was resuspended in 3 ml of Lysis buffer 3 (LB3) (10mM Tris–HCl, pH 8, 100mM NaCl, 1mM EDTA, 0.5mM EGTA, 0.1% Na–Deoxycholate) containing protease inhibitors (Roche).

Samples were then sonicated in 5 ml eppendorfs, using the tip sonicator (details) in cycles of 30 seconds on, 60 seconds off, at an amplitude of 40 watts, until chromatin fragment size was approximately 200-700bp. 50µl aliquots of sonicated chromatin were reverse cross-linking (95C, 10min); purified using the PCR purification kit and eluted in 30 ul milliQ. They were run on an E-gel to confirm sufficient sonication.

Triton X-100 was added to the samples, to reach a final concentration of 1% in LB3+ protease inhibitors (PI) and centrifuged at 20,000g for 10 min at 4ºC. A small aliquot of supernatant was kept as input for ChIP-seq**.** After centrifuging the clinical/PDX samples, the clean supernatant was added to the bead-bound antibody and the mix was rotated overnight.

For cell line samples, cells were seeded in 15cm^2 plates, treated accordingly and collected at 80-90% confluency. Two plates were used per sample. Cells were cross-linked by adding 2mM DSG solution directly to the plates and incubated for 20 minutes at room temperature. The solution was then removed and replaced with 1% formaldehyde ((Thermo, #28908) for 10 minutes. The cross-linker was quenched with 0.1M glycine. Then, cells were washed and harvested in ice-cold PBS containing protease inhibitors (Roche). In order to enrich for the nuclear fraction, pellets were resuspended in Lysis Buffer 1 (50mM Hepes–KOH, pH 7.5, 140mM NaCl, 1mM EDTA, 10% Glycerol, 0.5% NP-40/Igepal CA-630, 0.25% Triton X-100) and rotated for 10 minutes at 4ºC. Cells were then pelleted, resuspended in Lysis buffer 2 (10mM Tris–HCL, pH8.0, 200mM NaCl, 1mM EDTA, 0.5mM EGTA) and incubated for 5 minutes at 4ºC with rotation. Cells were then pelleted, resuspended in 300 µl Lysis buffer 3 (10mM Tris–HCl, pH 8, 100mM NaCl, 1mM EDTA, 0.5mM EGTA, 0.1% Na–Deoxycholate) and sonicated using the Bioruptor PLUS sonicator (Diagenode, Liege, Belgium, ref. B01020001) for 15 cycles (30 seconds on, 30 seconds off) or until chromatin fragment size were between 200 and 700 bp. After sonication the samples were centrifuged at maximum speed for 10 minutes at 4ºC and a small aliquot of supernatant was kept as input for ChIP-seq**.** The rest of the supernatant was added to the bead-bound antibody and rotated overnight.

After overnight incubation of the samples, the beads-antibody-chromatin complex were washed six times with RIPA buffer (50mM HEPES pH 7.6, 1mM EDTA, 0.7% Na deoxycholate, 1% NP-40, 0.5M LiCL) followed by one wash with TE (pH 7.4). Both ChIP samples and inputs were then de-crosslinked by adding 200 µl elution buffer (1% SDS, 0.1 M NaHCO3) for 16 hours at 65ºC. After reverse crosslinking, DNA was isolated and purified using the phenol-chloroform-isoamyl DNA extraction method. ChIP-seq and the input libraries were prepared using the ThruPlexChIP Sample Prep Kit (Illumina).

2.2.9.3 ChIP-qPCR

Quantitative RT-PCR Reactions were performed in triplicate and analysed using the Stratagene Mx3005P RealTime machine. Every reaction mix contained Power SYBR® Green PCR Master Mix (Applied Biosystems, California, USA), 10 µM of each primer, 2 µl of ChIP samples or 2 µl of 1:10 diluted inputs. nuclease-free H_2O was added to a final volume of 15 µl. First, the hot-start Taq polymerase was heat-activated at 95°C for 10 minutes, followed by 40 cycles of 15 seconds at 95°C and 30 seconds at 60°C. The fluorescence from each well was read in each cycle. For the final step, the temperature was slowly increased from 65 to 95°C and a melting curve was generated by continuously reading the fluorescence. The results were analysed using the delta-delta Ct method (Livak and Schmittgen, 2001).

2.2.9.4 ChIP Sequencing

ChIP-seq reads were mapped to hg38 genome using bowtie2 2.2.6 (Langmead and Salzberg, 2012). Aligned reads with the mapping quality less than 5 were filtered out. A Minimum of three independent biological replicates were conducted, unless otherwise specified. The read alignments from the three replicates were combined into a single library and peaks were called using MACS2 version 2.0.10.20131216 (Zhang et al., 2008). Matched input controls were used as background. The peaks yielded with MACS2 q value ≤ $1e^{-3}$ were selected for downstream analysis.

2.2.9.4.1 Motif Analysis

MEME tool FIMO version 4.9.1 (Bailey et al., 2009) was used for searching all known transcription factor motifs from JASPAR database (JASPAR CORE 2016 vertebrates) in the tag-enriched sequences. As a background control, peak size - matching sequences corresponding to known open chromatin regions in MCF-7 cells were randomly selected from hg38. Motif frequency for both tag-enriched and control sequences calculated as sum of motif occurrences adjusted with MEM q-value. Motif enrichment analysis was performed by calculating the odds of finding an overrepresented motif among MACS2-defined peaks by fitting Student's t-cumulative distribution to the ratios of motif frequencies between tag-enriched and background sequences. Yielded p-values were further adjusted using Benjamini-Hochberg correction.

2.2.9.4.2 Differential analysis and heatmaps

For visualizing tag density and signal distribution, heatmaps were generated with the read coverage in a window of +/- 2.5 or 5 kb region flanking the tag midpoint using the bin size of 1/100 of the window length. Differential binding analysis (Diffbind) was performed as described previously (Stark and Brown).

2.2.9.4.3 Integration of RNA-seq and ChIP-seq data

Genes located around +/- 50kb from the peak regions were selected. –log10 transformed p-values from DESeq2 analyses of the RNA-Seq data were subsequently used for ranking and weighting of genes. GSEA pre-ranked analysis tool from Gene Set Enrichment Analysis (GSEA) software, version 2.2.3, was used for the evaluation of statistically significant genes.

2.2.10 Rapid Immunoprecipitation Mass-spectrometry of Endogenous Proteins (RIME)

2.2.10.1 Chromatin immunoprecipitation for RIME

Chromatin immunoprecipitation was performed as described in section 2.2.9.2 until the RIPA washing step after the overnight incubation of bead-bound antibody and chromatin. For RIME experiments, beads were washes 10 times with RIPA, followed by 2 AMBIC washes (10 nM ammonium hydrogen carbonate). Supernatant was removed from the beads and they were frozen at -80°C.

2.2.10.2 Sample preparation and LC-MS/MS analysis

RIME sample preparation was performed by the Proteomics Core Facility (CRUK-CI) (Glont et al., 2019, Papachristou et al., 2018).

Briefly, tryptic digestion of bead-bound proteins was conducted overnight at 37°C, using 10µL trypsin solution (15ng/ul) (Pierce) prepared in 100mM AMBIC. The following morning, a second digestion was achieved by adding fresh trypsin solution to the samples for 4 extra hours, at 37°C. At the end of the second step, the tubes were placed on a magnet and the supernatant solution was collected and acidified by the addition of 2µl 5% formic acid.

The peptides were cleaned with the Ultra-Micro C18 Spin Columns (Harvard Apparatus) according to manufacturer's protocol.

For non-quantitative RIME, digested peptide mixtures were reconstituted in 15µl loading buffer (2% acetonitrile, 0.1% formic acid, water) and analysed on LTQ Velos-Orbitrap MS (Thermo Scientific) coupled with the Ultimate RSLCnano-LC system (Dionex).

For quantitative RIME**,** the samples were dried using speedvac, resuspended in 100µl 0.1M Triethylammonium bicarbonate buffer (TEAB) and labelled using TMT 10-plex reagents (Thermo Fisher). The peptide mixture was fractionated with Reverse-Phase cartridges at high pH (Pierce). Nine fractions were collected using different elution solutions in the range of 5-50% acetonitrile. Peptide fractions were analysed on nano-ESI Fusion Lumos (Thermo Scientific) coupled with Dionex Ultimate 3000 UHPLC.

2.2.10.3 RIME data processing and bioinformatics analysis

Data processing was conducted by the Proteomics Core Facility and bioinformatics analysis by Dr Kamal Kishore (Bioinformatics Core facility, CRUK-CI).

2.2.10.3.1 Non-quantitative RIME

In order to identify specific peptides and proteins from non-quantitative RIME experiments, the raw mass-spectrometry files were processed using the SequestHT search engine from Proteome Discoverer 2.1 software. The filtering parameters included: precursor mass tolerance 20ppm, maximum missed cleavages sites 2, fragment mass tolerance 0.02Da.

The protein intensities were normalised by the summed intensity separately for the IgG control pulldowns and for the target protein pull downs.

The plots for bait protein coverage were created using the qPLEXanalyzer tool (Papachristou et al, 2018)**.**

2.2.10.3.2 Quantitative RIME

The raw MS files were processed with the Sequest HT search engine on the Proteome Discoverer 2.1 software for peptide and protein identification.

Pre-processed quantitative data (peptide or protein-level intensities) generated by Proteome Discoverer were imported into R and data was analysed using the

qPLEXanalyser tool (Papachristou et al., 2018) to identify differentially abundant proteins.

2.2.11 Survival analysis

For analysis of disease-free survival, Kaplan-Meier plots were generated. The METABRIC cohort (Curtis et al., 2012, Rueda et al., 2019) was stratified based on the copy number of the genomic region encompassing for ETV6. The effect of ETV6 gains/amplifications were assessed in ERα positive compared to ERα negative subtypes. In addition, ETV6 copy numbers were assessed separately in Luminal A, Luminal B, HER2 positive, triple negative groups.

2.2.12 Additional statistical analysis

Additional statistical analysis was performed in GraphPad Prism Software Inc., version 7. Either one-way or two -way analysis of variance (ANOVA) were employed to assess significant difference between the means of the groups compared. Results are represented as mean value with standard deviation. P values less than 0.05 were considered as statistically significant.

Chapter 3. FOXA1 function is independent of ERα signalling

The work in this chapter is the basis of the paper: Silvia-E. Glont, Igor Chernukhin and Jason S. Carroll: Comprehensive Genomic Analysis Reveals that the Pioneering Function of FOXA1 Is Independent of Hormonal Signaling, Cell Reports, 2019; 26(10): 2558–2565.e3, DOI: 10.1016/j.celrep.2019.02.036 Sequencing was performed by the Genomics Core Facility and ChIP-seq analysis was conducted by Dr Igor Chernukhin.*

3.1 Introduction

The development and differentiation in eukaryotic systems are dictated by gene expression events. ERα is a master regulator of breast cancer phenotype. The ERα transcriptional program culminates in cell division, defining its critical role in normal mammary gland development and in malignancy (Carroll, 2016).

The ERα-chromatin interactions have first been described once genome-wide mapping of transcription factors methodologies were developed (Carroll et al., 2005, Carroll et al., 2006). Interestingly, it was revealed that ERα-binding events occur at enhancer regions located at significant distances from promoters (Carroll et al., 2005, Carroll et al., 2006, Lin et al., 2007). As a consequence, transcription initiation requires long-distance interaction between the cis-regulatory elements and the promoter regions of target genes (Fullwood et al., 2009). *Carroll et al* has also linked ERα and FOXA1 for the first time. ERα binding sites were enriched for forkhead motifs (Carroll et al., 2005). Subsequent studies have shown that approximately half of ERα chromatin binding sites are co-occupied by FOXA1 (Hurtado et al., 2011).

One key aspect of ERα gene regulation is its accessibility to the estrogen response elements (ERE) from compacted chromatin. The concept of pioneer transcription factors (PTFs) developed over decades of research. They have the unique ability to bind to ‘closed’ chromatin. Forkhead box protein (FOXA) family members have been shown to bind to silent chromatin and initiate gene activation. FOXA1 pioneer activity is given by its ability to bind to nucleosomal embedded DNA through its winged-helix

domain that is similar to the H1 linker histone. It dislodges H1 and can induce nucleosome rearrangements via an ATP-independent mechanism (Zaret and Carroll, 2011). Subsequently, they remodel the adjacent chromatin landscape, assist in chromatin opening and binding of secondary transcription factors such as steroid receptors, specifically ERα in breast cancer and AR in prostate cancer (Bernardo and Keri, 2012, Cirillo et al., 2002, Cirillo et al., 1998).

Several studies indicate a transcription factor hierarchy in breast cancer, with FOXA1 being the initiator and ERα the secondary protein. On the one hand, FOXA1 knockdown with RNAi results in impaired ERα binding to chromatin (Hurtado et al., 2011). On the other hand, inhibiting ERα does not impact on FOXA1-chromatin interactions (Lupien et al., 2008). Importantly, FOXA1 is required for growth of drug-resistant cancer models and it has been shown to directly contribute to endocrine resistance (Fu et al., 2016).

All these findings support the dependence of hormone receptor signalling on FOXA1 pioneer transcription factor (Nakshatri and Badve, 2007, Jozwik and Carroll, 2012). As such, FOXA1 is an attractive therapeutic target. Its inhibition would act upstream of ERα and benefit ERα positive breast cancer patients, including those resistant to endocrine therapy. FOXA1 inhibition would bypass the mechanisms of endocrine resistance.

Contrary to the pioneer transcription factor model, another mechanism of transcription regulation has been described, namely dynamic assisted loading. In this model, transcription factors can modulate each other. One factor can recruit ATP-dependent remodelling complexes, which in turn open up chromatin for the other (Biddie et al., 2011, Grøntved et al., 2013, Miranda et al., 2013). This process allows the second factor to bind to chromatin. This model is different from the pioneer transcription concept in three fundamental aspects. First, there is a reciprocal modulation of the transcription factors and which one comes first is dependent on the local chromatin environment. Secondly, residence time of the proteins on chromatin is in the region of seconds. Lastly, the chromatin remodelling in the dynamic assisted loading is an ATP-dependent process (Voss and Hager, 2014). Certain studies have implied that ERα and FOXA1 undergo dynamic assisted loading, therefore being able to modulate each other. Upon ERα knock down, *Caizzi et al* observed the loss of a number of FOXA1-chromatin binding sites (Caizzi et al., 2014). In addition, *Swinstead et al* suggested

there is a subset of FOXA1 genomic binding sites induced by steroid activation (Swinstead et al., 2016). These new studies challenge the importance of FOXA1 targeted therapy upstream of ERα.

3.2 Aims

Given the recent studies that challenged the paradigm of FOXA1 pioneer activity in ERα positive breast cancer, the aim of this chapter was to investigate the hierarchy of these transcription factors. This study aims to shed light on whether FOXA1 binding events are regulated by hormone stimuli or whether FOXA1 is indeed a *bone fide* pioneer factor that acts upstream of ERα.

3.3 Results

ERα and FOXA1 play pivotal roles in breast cancer. There are two distinct models for their transcription regulation. On the one hand, the pioneer transcription model places FOXA1 first to open up chromatin for ERα. On the other hand, the dynamic assisted loading postulates that the two transcription factors can modulate each other. Shedding light into which of the two transcriptional regulation models is applicable for FOXA1 and ERα is crucial, as this can influence therapeutic strategies.

In this context, we sought to assess if hormone steroid treatment can modulate FOXA1 in ERα positive breast cancer cell lines. For this purpose, MCF-7 and ZR-75-1 cells were first deprived of hormones for three days. Then, they were treated either with vehicle or with 10nM of estrogen for 45 minutes. This time point has previously shown to induce maximal ERα binding and enhancer activity (Shang et al., 2000). ERα induction after hormone treatment was tested using ERα ChIP-qPCR at known binding loci. ChIP-qPCR was conducted in three biological replicates from independent passages (Fig.3.1).

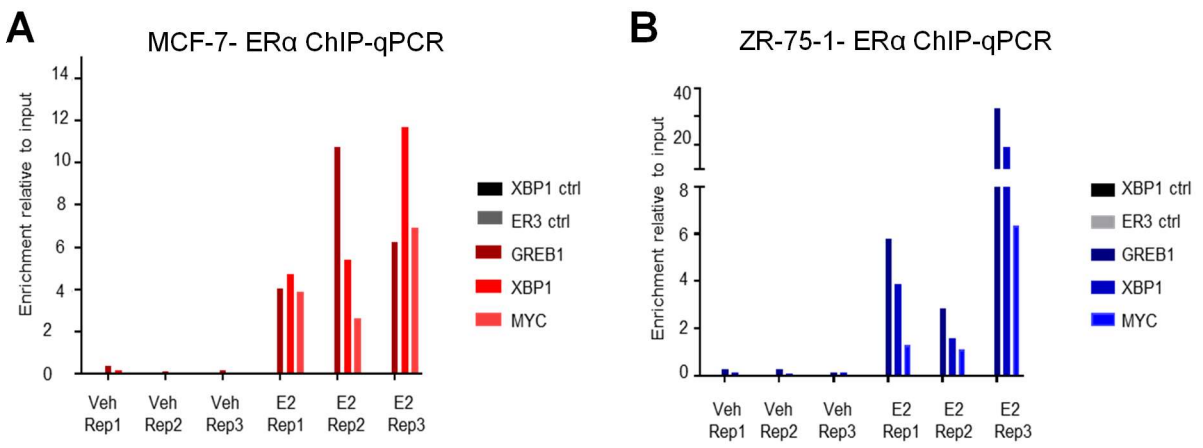

Figure 3.1. Validation of estrogen activity in MCF-7 (A) and ZR-75-1 (B) cells: ERα ChIP-qPCR was conducted in biological triplicates, at known ERα binding loci; these samples were matched with the FOXA1 ChIP-seq used for the study.

The next step was to perform FOXA1 ChIP-seq on both cell lines, to elucidate if estrogen treatment affects FOXA1-chromatin binding. The samples used for this experiment matched the ones used to confirm estrogen induction. Matched Input samples were also included.

Importantly, while our study included three independent biological replicates, the work conducted by *Swinstead et al* only had two replicates. In addition, PCA analysis revealed that the three biological replicates used in our study clustered very closely, while the ones used by *Swinstead et al* did not cluster (Glont et al., 2019).

To ensure peaks are biologically relevant and not artefacts given by the antibody, two different FOXA1 antibodies were used for ChIP-seq: ab23738 and ab5089. Peaks were called using MACS2 (Stark and Brown, Ross-Innes et al., 2012).

In MCF-7 cells, the ab23738 antibody generated 64,823 FOXA1 peaks in vehicle-treated and 62,000 peaks in estrogen-treated condition. ChIP-seq using ab5089 antibody resulted in 37,318 FOXA1 binding sites in vehicle and 35,925 in estrogen treated samples (Table 3.1).

In ZR-75-1 cells, FOXA1 ChIP-seq using ab23738 antibody resulted in 70,602 FOXA1 peaks in vehicle and 66,604 peaks in estrogen conditions. ab5089 generated 35,763 FOXA1 peaks in vehicle conditions and 31,361 peaks in E2 conditions (Table 3.1).

Therefore, the global numbers of FOXA1 binding sites did not suffer major changes in estrogen stimulated compared to vehicle conditions in neither of the cell lines and with neither of the two antibodies used.

Cell line	Antibody	Condition	Total no. of peaks
MCF7	ab23738	Vehicle	64823
		Estrogen	62000
	ab5089	Vehicle	37318
		Estrogen	35925
ZR751	ab23738	Vehicle	70602
		Estrogen	66604
	ab5089	Vehicle	35763
		Estrogen	31361

Table 3.1. Total number of FOXA1 ChIP-seq peaks obtained using ab237338 and ab5089 antibodies, in MCF-7 and ZR-75-1.

To exclude the possibility that FOXA1 binding is redistributed after hormone treatment, resulting in similar numbers of binding events, but in fact at different genomic loci, DiffBind analysis was conducted (Ross-Innes et al., 2012) (Table 3.2).

Cell line	Antibody	Conditions	Differential binding comparison		
			gained	lost	common
MCF7	ab23738	Estrogen vs Vehicle	14	2	72627
	ab5089	Estrogen vs Vehicle	357	5	41948
ZR751	ab23738	Estrogen vs Vehicle	23	2	76830
	ab5089	Estrogen vs Vehicle	109	1	38205

Table 3.2. Differential binding comparison between vehicle and estrogen treatment.

In MCF-7 cells, ChIP-seq experiments using the ab23738 antibody gave 14 peaks gained and 2 peaks lost after estrogen stimulation. These differentially bound regions represent less than 0.02% of the total number of FOXA1 peaks (Fig.3.2.A and C). The ab5089 FOXA1 antibody gave the biggest change observed in our study (Fig.3.2.A-C): a total of 357 FOXA1 peaks enriched in estrogen conditions (representing less than 1% of all peaks called) and 5 peaks enriched in vehicle conditions (Fig.3.2.B).

In ZR-75-1 cells, ChIP-seq experiments using ab23738 antibody revealed 23 estrogen-enriched and 2 vehicle-enriched FOXA1 binding sites (Fig.3.2. D and F). The ab5089 antibody gave 109 estrogen-induced FOXA1 binding sites and 1 vehicle-enriched site (Fig.3.2. E). all these changes are less than 0.03% of the total number of peaks in ZR-75-1.

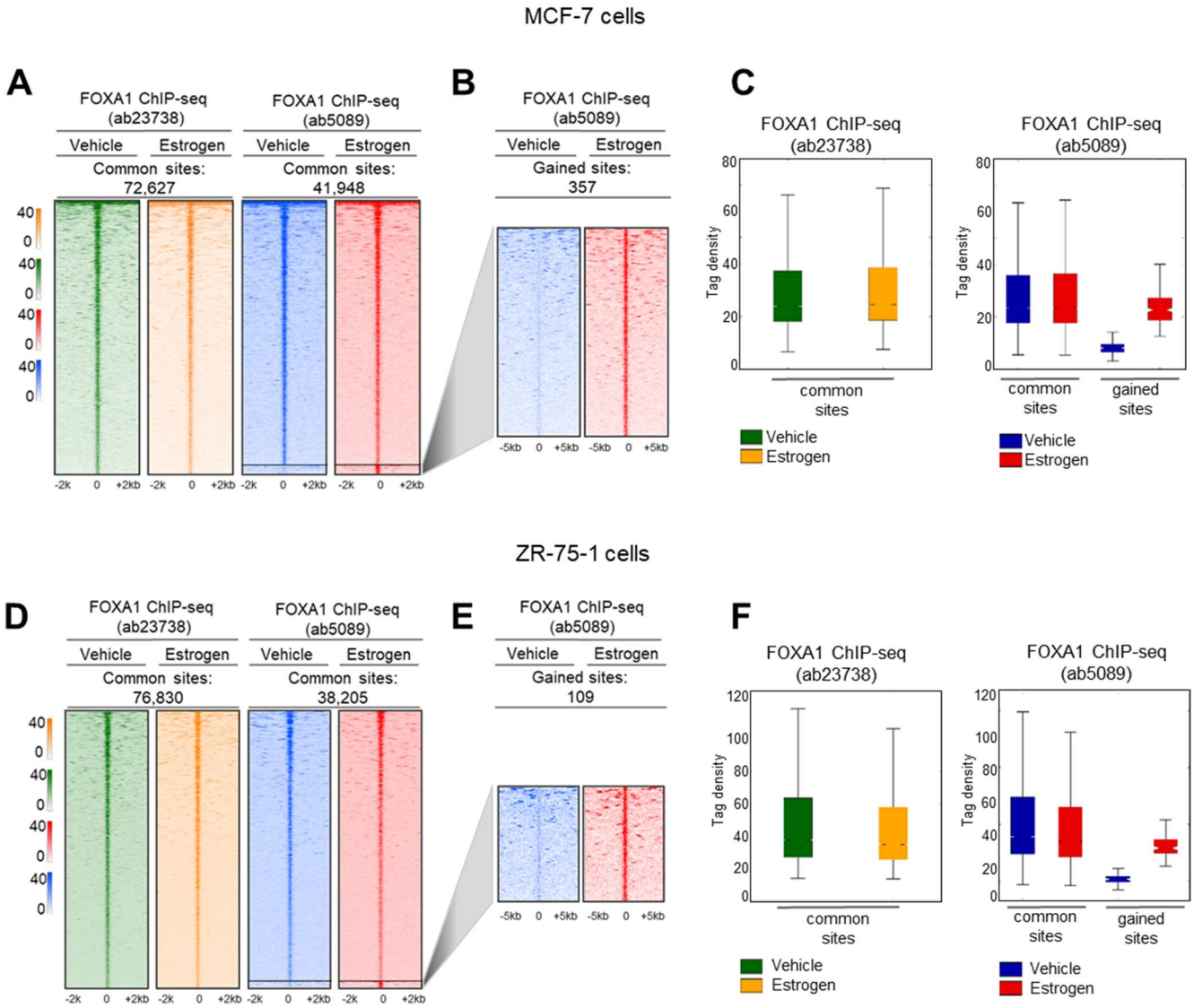

Figure 3.2. Analysis of FOXA1 ChIP-seq binding with two separate antibodies in response to estrogen treatment in MCF-7 and ZR-75-1 cells: ChIP-seq tag densities visualised at FOXA1-occupied genomic locations in control and estrogen-treated MCF-7 (A and C) and ZR-751 cells. ChIP-seq tag densities visualised at FOXA1-occupied genomic locations in control and estrogen-treated MCF-7 (**A** and **C**) and ZR-75-1 (**D** and **F**) cells, using antibodies ab23738 and ab5089. Zoomed heatmaps show differential binding of FOXA1 specific to ab5089 in MCF-7 cells (**B**) and ZR-75-1 (**E**), respectively.

Overall, the ChIP-seq data obtained using two different anti-FOXA1 antibodies and conducted in two independent cell line models, showed that only 0.02-1% of the FOXA1 binding sites are induced by estrogen. This is just a very small fraction of the total FOXA1-chromatin interactions that seem to be hormonally regulated.

The ab5089 antibody produced a small number of estrogen-induced FOXA1 binding sites (357 sites), although it is important to note that these differential binding events constitute less than 1% of total FOXA1 binding events in the ChIP-seq dataset. Only 28 common FOXA1 binding events were identified in both MCF-7 and ZR-75-1 cell lines, implying that these differential sites are not reproducible between different cancer models (Fig.3.3.A).

Motif analysis for the estrogen-induced FOXA1 binding sites in MCF-7 and ZR-75-1 revealed the Estrogen Responsive Element (EREs) motif ($p=1x10^{-42}$), but no Forkhead motifs (Fig.3.3.B). This finding suggests that FOXA1 is not directly interacting with the chromatin at these regions. The small number of estrogen-induced FOXA1 binding sites might be indirect FOXA1 binding events mediated via chromatin loops connecting estrogen-induced genes and their enhancers.

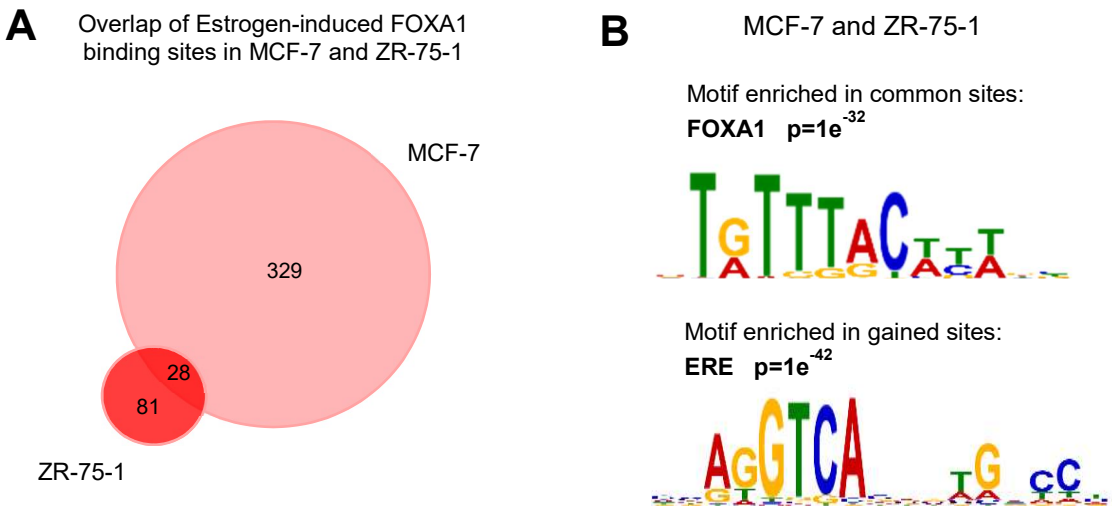

Figure 3.3. Analysis of FOXA1 binding sites using ab5089 antibody in MCF-7 and ZR-75-1: (A) Overlap of estrogen-enriched FOXA1 binding sites between MCF-7 and ZR-75-1 cells; **(B)** Transcription factor motifs found overrepresented in the common and estrogen induced FOXA1 sites.

This hypothesis was explored on the highest difference detected in the ChIP-seq experiments: the 357 estrogen-induced FOXA1 binding sites from MCF-7 cell line seen with the ab5089 antibody. To understand the underlying properties of these binding sites, the ChIP-seq data was integrated with previously published RNA-seq performed in estrogen-stimulated MCF-7 compared to vehicle (Fig.3.4.A) (Hurtado et al, 2011). Almost all the 357 E2-induced binding sites were significantly biased towards the most estrogen-regulated genes from the RNA-seq data investigated (Fig. 3.4.B).

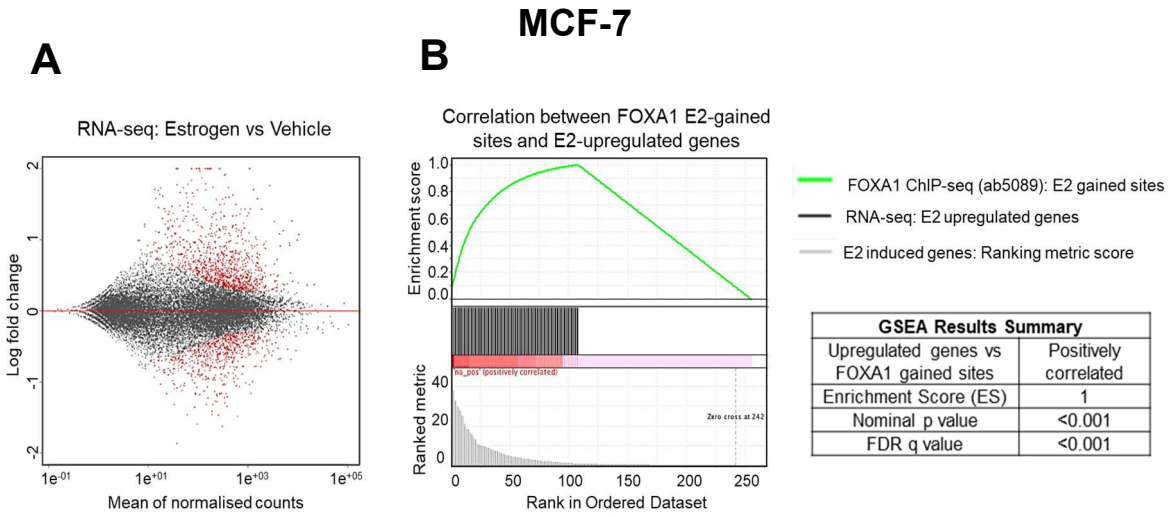

Figure 3.4. Integration of the estrogen-enriched FOXA1 binding events with estrogen-mediated gene expression events: (A) RNA-seq expression profile following short-term (3hr) estrogen treatment of MCF-7, shown as a dispersion plot. **(B)** GSEA Pre-ranked test correlating estrogen-induced genes with the 357 estrogen-induced FOXA1 binding sites.

It has previously been established that the estrogen-induced genes, especially those with the greatest estrogen response, are regulated by clusters of closely associated cis-regulatory domains (Carroll et al., 2006).

Examples of well-characterised ERα target genes are shown in Figure 3.5.A. They are either co-bound by FOXA1 and ERα, or unique to each of the two transcription factors, as shown in Figure 3.5.A. Of great relevance, the 357 sites are all in close proximity (within 2kb) from an independent ERα binding event, and within 8kb from another FOXA1 binding site (Fig.3.5.B and C). On the one hand, this indicates they are present in regions of enriched transcriptional activity and on the other hand it shows they are closer to an ERα binding event rather than to another FOXA1 site.

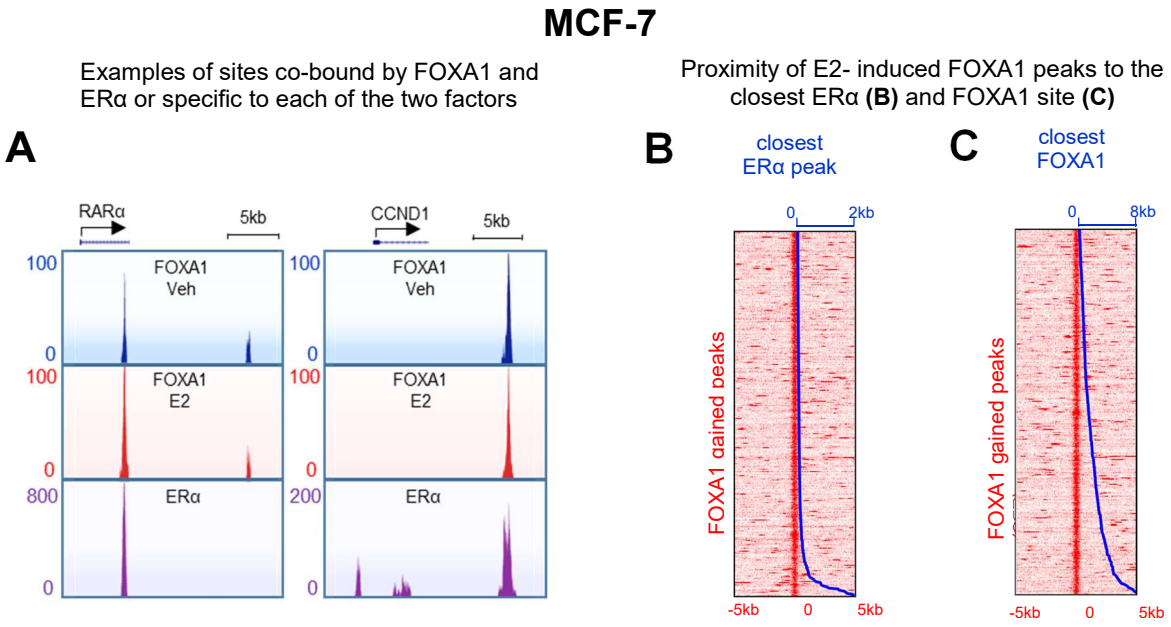

Figure 3.5. Estrogen-induced genes are regulated by clusters of closely associated *cis*-regulatory domains: (A) Examples of sites co-bound by FOXA1 and ERα, as well as sites unique to each of the two transcription factors; Proximity of estrogen-induced FOXA1 peaks and the closest ERα **(B)** or FOXA1 **(C)** site. Heatmaps represent FOXA1-gained sites in red.

This raises the possibility that the 357 sites are in fact the result of chromatin interactions between ERα binding sites and adjacent FOXA1 binding sites.

Moreover, it is known that *cis*-regulatory elements physically associate with each other after estrogen stimulation (Pan et al., 2008, Fullwood et al., 2009). Therefore, the hypothesis that FOXA1 could associate with adjacent ERα binding sites through chromatin looping has emerged. The cross-linking in the ChIP-seq protocol fixes these indirect chromatin loops and creates FOXA1 binding sites that are not direct *cis*-regulatory elements and thus represent “shadow peaks”. At these regions, FOXA1 does not function as a pioneer factor and new regulatory elements are not created.

Therefore, there is the possibility that the small fraction (<1%) of the FOXA1 binding sites that appear to be induced by estrogen stimulation are in fact just indirect peaks mediated via ERα at those genomic regions. Chromatin interaction analysis by paired-end tag sequencing (ChIA-PET) is a novel methodology for unbiassed mapping of ERα-mediated chromatin interactions that occur in the presence of estrogen, in MCF-7 cells (Fullwood et al., 2009).

To assess whether the 357 estrogen induced FOXA1 peaks are indeed novel binding sites or simply 'shadow peaks', correlation analysis between ChIA-PET and the hormone-mediated sites was conducted. Remarkably, 319 of the 357 estrogen induced FOXA1 peaks were detected in experimentally identified ERα ChIA-PET chromatin loops (Fig.3.6). This represents the vast majority of 89% of the E2 specific sites (Fig.3.6.A). Examples of estrogen-induced FOXA1 binding sites existing within ChIA-PET chromatin loops, are shown in Figure 3.6.B.

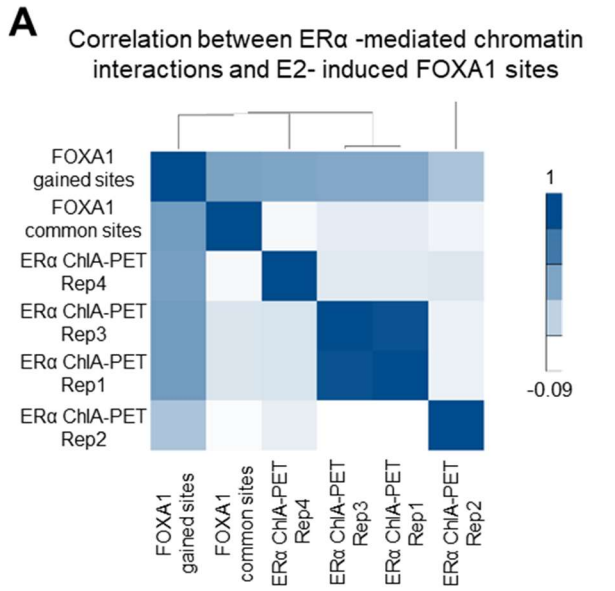

ChIA-PET Results Summary		
sample	no. sites	no. of sites overlapped with FOXA1 gained peaks
ERα ChIA-PET Rep1	14393	319
ERα ChIA-PET Rep2 (technical rep)	14393	319
ERα ChIA-PET Rep3	2710	200
ERα ChIA-PET Rep4	6671	257

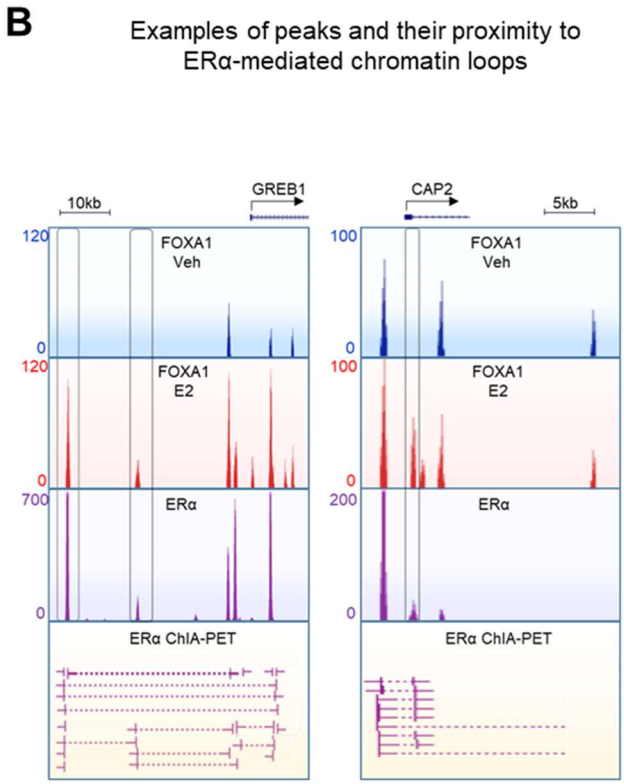

Figure 3.6. ERα binding mediates indirect FOXA1 binding via chromatin looping at *cis*-regulatory elements: (A) Correlation between ERα-mediated chromatin interactions (ChIA-PET) and the 357 estrogen-induced FOXA1 binding sites (ab5089). The table shows the correlation values between ChIA-PET interactions and the 357 estrogen-induced FOXA1 binding sites. **(B)** Examples of ERα and FOXA1 peaks at regions that are involved in chromatin loops, as detected by ChIA-PET. The images of the ChIA-PET loops are taken from (Fullwood et al., 2009).

This finding confirms that the limited number of estrogen-induced FOXA1 binding events are in fact created by clusters of *cis*-regulatory elements brought into proximity

by chromatin looping. Therefore, FOXA1 is not influenced by steroid hormones, it remains a *bone fide* pioneer factor that binds upstream of nuclear receptors.

3.4 Discussion

In breast cancer, gene regulation is dictated by ERα, which regulates its target genes from enhancer regions (Carroll et al., 2005, Lin et al., 2007). However, additional factors are required for ERα activity (Shang et al., 2000, Glass and Rosenfeld, 2000).

Resistance to ERα targeted drugs develops through different mechanisms, including but not limited to changes in genomic landscape, mutations in ERα or its co-factors or changes in co-activators and co-repressors levels. These abnormalities result in ligand-independent ERα activity. Therefore, there is significant interest in developing novel targeted therapies that may bypass endocrine resistance in ERα breast cancer.

One determinant component of the ERα complex is FOXA1, which has previously been described as a pioneer transcription factor. FOXA1 is able to open silent chromatin for the nuclear receptor and hence influences its transcriptional programme. Therefore, inhibition of FOXA1 upstream of ERα represents a therapeutic opportunity to overcome ERα-associated mechanisms of resistance (Nakshatri and Badve, 2007, Nakshatri and Badve, 2009, Jozwik and Carroll, 2012). This is of particular relevance, as FOXA1 has been shown to be required for ERα binding and activity in both endocrine sensitive and resistant context (Ross-Innes et al., 2012).

FOXA1 activity upstream of ERα was recently challenged with claims that it can be modulated by E2 (Swinstead et al., 2016), in an ATP-dependent manner. The implications are that FOXA1 may be inhibited by drugs targeting the ERα pathway and therefore the benefits of direct inhibition of FOXA1 are abolished.

The genomic analysis conducted in this chapter reveals that less than 1% of FOXA1 binding sites emerge after hormonal stimulation in MCF-7 cells. This percentage is even smaller when other antibodies are used or in different cell lines. As such, more the 99% of FOXA1 binding sites are not affected by the hormonal status.

Importantly, the changes in FOXA1 binding that appear to be linked with estrogen-stimulation are peaks that form within clusters of ERα/FOXA1 binding sites at genes that are regulated. They lack the hallmarks of genuine FOXA1 binding sites, as they do not result in the creation of new regulatory elements and they do not result in new gene expression events. The lack of robust, reproducible FOXA1 binding sites confirms that FOXA1 binding is not estrogen regulated and that it functions upstream of ERα. In support of this conclusion, previous experimental data showed that the breast cancer treatment with the ERα degrader Fulvestrant does not alter FOXA1 binding (Hurtado et al., 2011).

In addition, it is worth mentioning that the conclusion of *Swinstead et al* that steroid treatment can modulate FOXA1 was mainly based on their ChIP-seq analyses. Yet, only 1000 new FOXA1 binding sites appeared after estrogen stimulation, representing just a minor fraction of the total number of FOXA1 peaks found in their study. Notably, *Swinstead et al* only included two biological replicates which did not cluster according to conditions, as evidenced by PCA analysis (Glont et al., 2019). Our study included three biological replicates, collected from independent passages. Therefore, the apparent estrogen-mediated FOXA1 binding events seen in the *Swinstead et al* study are likely an artefact resulting from inadequate number of robust replicates.

In addition, *Swinstead et al* also assessed FOXA1 chromatin interaction time using an exogenous tagged-FOXA1 approach. The caveat of this approach is that exogenous FOXA1 alters the levels and potentially function of endogenous FOXA1 and the tagged protein might not faithfully recapitulate endogenous FOXA1. Nonetheless, there was a minimal change in FOXA1 dwell time between presence or absence of E2. Thus, this non-ChIP-based method does not offer grounds to conclude that FOXA1 is hormonally modulated.

In conclusion, our study shows that the vast majority of more than 99% of FOXA1 binding is not regulated by estrogen and the small fraction of altered FOXA1 binding events are created via chromatin loops during the course of estrogen-receptor mediated gene expression. FOXA1 therefore acts upstream of ERα, its chromatin interactions are not influenced by estrogen signalling and it remains a promising drug target in hormone-dependent cancers.

Chapter 4. Characterising novel mechanisms of endocrine resistance in ERα positive breast cancer

4.1 Introduction

ERα is the driving transcription factor in approximately three quarters of all breast cancers. This nuclear receptor mediates most of estrogen-induced effects on cell proliferation, survival and development (Musgrove and Sutherland, 2009) and therefore deregulations in ERα activity results in aberrant cell growth and tumourigenesis.

Due to ERα's causal role in breast cancer, extensive efforts have been invested into the development of efficient endocrine treatments for ERα positive breast cancer. The selective estrogen receptor modulator (SERM) Tamoxifen was the first endocrine therapy developed (Jensen and Jordan, 2003). It remains the most widely used agent in pre-menopausal women and continues to be used for post-menopausal patients (Davies et al., 2011).

However, 20-30% of breast cancer cases present with endocrine resistance (Davies et al., 2011, Hoskins et al., 2009). Several molecular mechanisms for the refractory phenotype have been identified, including changes in ERα levels and activity, changes in its protein interactors, overexpression of growth factors and kinase signalling pathways, or dysregulation of cellular proliferation. These insights have triggered the development of promising new targeted therapies that are now FDA-approved for endocrine resistant breast cancer.

A new strategy that significantly improved the outcome of ERα-positive, HER2 positive breast cancer patients is the inhibition of HER2-mediated aberrant cell growth using an antibody-drug conjugate. This compound combines the monoclonal antibody against HER2 Trastuzumab (T) with the potent cytotoxic maytansine derivative (DM1) (Okines, 2017) and it is termed T-DM1.

In addition, inhibitors of cyclin D–CDK4/6-Retinoblastoma pathway such as Palbociclib (Finn et al., 2015) or inhibitors of the AKT/mTOR signalling pathway such as the mTOR

inhibitor Everolimus have significantly improved disease-free survival in subsets of breast cancer patients (Yardley et al., 2013).

Nonetheless, there are still cases that do not respond to any of the currently-available therapies (Martelotto et al., 2014). This is a consequence of breast cancer heterogeneity and it implies that there are alternative molecular mechanisms for endocrine resistance that need to be identified and targeted for the overall improvement of breast cancer survival rates.

While ERα gene activation can be dictated by its direct interactions with the estrogen response elements (ERE) within the chromatin (Klein-Hitpass et al., 1989), there are also numerous ERα associated proteins that mediate its transcriptional activity.

Comprehensive genomic studies have identified FOXA1 as the critical pioneer transcription factor in ERα positive breast cancer. Due to its structure, it is able to access highly compacted chromatin and subsequently assist in chromatin opening and binding of the nuclear receptor. FOXA1 acts upstream of ERα and influences its transcriptional programme (Glont et al., 2019, Hurtado et al., 2011). FOXA1 plays a critical role in both Tamoxifen-sensitive and resistant context (Ross-Innes et al., 2012a). *Ross-Innes et al* conducted *in vitro* validation of the ERα binding reprograming seen in advanced breast cancer patients. This work has shown that FOXA1 and ERα co-localise in both Tamoxifen sensitive and resistant cell lines, implying that FOXA1 may redirect ERα to its novel target regions associated with endocrine resistance.

There is also a plethora of known ERα interactors that mediate gene activation or repression by promoting histone modifications or chromatin remodelling. Examples of known co-activators are members of the p160 family of transcription factors such as SRC1, SRC2 and AIB1 (Anzick et al., 1997, Hong et al., 1997, Oñate et al., 1995). They are recruited to the ERα complex and in turn recruit acetyltransferases (HATs) and histone methyltransferases (HMTs) that decondense chromatin and enhance ERα-mediated transcriptional programme (Chen et al., 2000, Rollins et al., 2015).

Moreover, co-repressors such as NCOR, RIP140 or REA mediate ERα-induced gene down-regulation by recruit deacetylases (HDACs) (Castet et al., 2004, Delage-Mourroux et al., 2000, Lazar, 2003, Varlakhanova et al., 2010). HDACs remove the acetylation marks resulting in chromatin condensation and gene inactivation.

ERα co-factors are of particular importance. They work in a cooperative or competitive manner and disbalances in their levels can contribute to breast cancer progression and influence endocrine response.

Another recent study of the molecular mechanisms underpinning endocrine resistance has found a differential interaction between ERα, GATA3 and AP1 transcription factors in therapy refractory breast cancer (Bi et al., 2020). The differential binding of GATA3 and AP1 was associated with a global enhancer reprogramming that profoundly impacted on ERα transcriptional function in treatment-resistant breast cancer. It is worth mentioning this study was only conducted in one endocrine resistant model.

Moreover, quantitative Multiplexed Rapid Immunoprecipitation Mass spectrometry of Endogenous proteins (qPLEX-RIME) (Papachristou et al., 2018) is a recently developed proteomic tool for the study of quantitative changes in protein-protein interactions between different biological contexts. This powerful proteomic tool opens the possibility to identify novel ERα and FOXA1 protein interactors and to investigate their quantitative changes between Tamoxifen resistant and sensitive context. Such studies may elucidate novel mechanisms of endocrine resistance.

ETV6 (TEL-1, TEL) is one of the ETS factors that can mediate differentiation and lineage specification during normal development. They regulate cell cycle, cell differentiation, proliferation and apoptosis (Findlay et al., 2013). Therefore, perturbations in ETS proteins render them crucial onco-drivers in various cancer types.

ETV6- NTRK3 gene fusion is the driving oncogenic event in 92% of the secretory breast carcinoma clinical samples (Tognon et al., 2002).

Importantly, copy-number amplifications of ETV6 are associated with significantly worse prognosis in ERα positive, Luminal B breast cancer cases from the METABRIC cohort (Curtis et al., 2012), suggesting ETV6 possible contribution to poor outcome in these patients.

In addition, it has been shown that in gastrointestinal stromal tumours, mutated and constitutively active tyrosine kinase receptor KIT stabilises ETV1 (member of the ETS family) through MEK-ERK pathway. This results in ETV1 overexpression and an oncogenic ETS transcriptional programme (Chi et al., 2010). This knowledge raises the possibility that other ETS family members, such as ETV6, may also be regulated by MEK/ERK pathway in breast cancer.

4.2 Aims of the chapter

In this context, the first aim of this chapter was to identify novel ERα and FOXA1 protein interactors that may contribute to the development of endocrine resistance, by conducting qPLEX-RIME. The second aim was to characterise and validate the role of the newly-identified interactor called ETV6 in breast cancer progression and endocrine refractory phenotype. This would pave the way for improved personalised treatments.

4.3 Results

4.3.1 Optimisation steps

4.3.1.1 ERα antibody validation

The work in this chapter was published in the paper: Silvia-E. Glont[#], Evangelia K. Papachristou[#], Ashley Sawle, Kelly A. Holmes, Jason S. Carroll, Rasmus Siersbaek*: Identification of ChIP-seq and RIME grade antibodies for Estrogen Receptor alpha, PLOS ONE, 2019: e0215340, DOI: https://doi.org/10.1371/journal.pone.0215340. Sequencing was performed by the Genomics Core Facility (CRUK-Cambridge Institute), ChIP-seq analysis was conducted by Dr Ashley Sawle (Bioinformatics Core, CRUK-CI) and proteomics experiments were done by Evangelia K Papachristou.*

ChIP-seq studies of ERα-chromatin interactions in different biological contexts is essential for the identification of those changes associated with aggressive breast cancer and endocrine refractory phenotype. ERα transcriptional activity can also be modulated by its association with co-regulatory proteins which can be identified using RIME. In addition, qPLEX RIME enables the study of quantitative protein changes between Tamoxifen resistant and sensitive context. Such studies may elucidate novel mechanisms of Tamoxifen resistance.

However, these techniques rely on the specificity and sensitivity of the ERα antibody used for the immunoprecipitation. To date, most ERα ChIP-seq and RIME experiments have been conducted using the sc-543 ERα antibody from Santa Cruz Biotechnology. This antibody has recently been discontinued, impacting on the ability to further study

ERα function in different contexts. Therefore, it has become paramount to identify antibodies that can replace the previously-established one.

As a result, alternative antibodies for ChIP-seq and RIME experiments were tested. The initial ChIP-qPCR comparison of sc-543 with several other ERα antibodies demonstrated that 06-935 (Millipore) and ab3575 (Abcam) can successfully enrich ERα-bound chromatin at the selected loci similarly to sc-543 (Glont et al., 2019).

ChIP-seq was then performed on MCF-7 cells to compare ERα genome-wide binding profiles obtained with sc-543, 06-935 and ab3575. IgG was used as negative control (Fig 4.1). ERα and IgG ChIP-seq were performed in at least technical duplicates using the same batch of chromatin to ensure that antibodies could be directly compared. In addition, the ERα negative cell line MDA-MB-231 was included in order to assess the non-specific enrichment of chromatin by these antibodies. For MDA-MB-231, ChIP-seq was performed in biological triplicates.

ChIP-seq analysis resulted in 6,031 ERα binding sites for sc-543 antibody, 6,192 peaks for ab3575 and 6,552 for 06-935. Importantly, none of these binding sites were observed in the IgG negative control. The vast majority of sites identified in MCF-7 cells by sc-543 overlapped with those detected by ab3575 and 06-935 (Fig.4.1.A and B). Importantly, none of the antibodies showed any significant enrichment in the ERα negative cell line MDA-MB-231 (Fig.4.1. B and D). There was only one peak detected in MDA-MB-231 using ab3575, two peaks for 06-935 and 124 peaks for sc-543. This confirms the specificity of the newly tested antibodies. In addition, motif analysis identified the ERα response element (ERE) as significantly enriched at the sites bound by ERα in MCF-7 cells for all three antibodies assessed (Fig. 4.1.C). Examples of peaks at previously described ERα binding sites are illustrated in Figure 4.1.D.

Overall, the genome-wide analyses of ERα-chromatin binding sites suggest that ab3575 and 06-935 perform similarly to sc-543 in ChIP-seq experiments, in terms of sensitivity and specificity and are valid alternatives.

The genomic data was corroborated with ERα RIME experiments (Glont et al., 2019). Proteomic analysis revealed that all three antibodies specifically identified the bait protein ERα with similar coverage, as well as its known interactors such a FOXA1, GATA3 and members of the p160 family for all three antibodies.

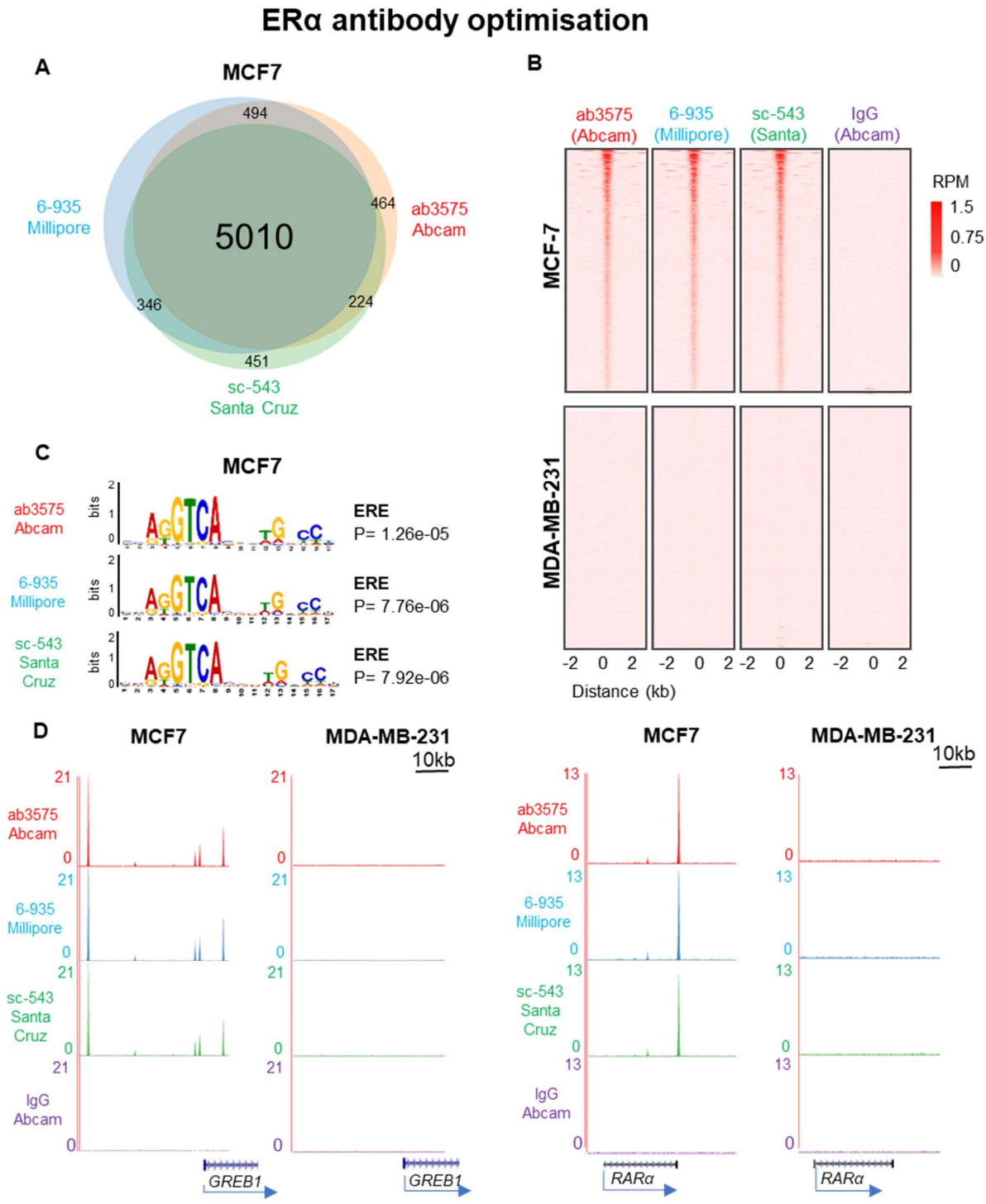

Figure 4.1. ERα antibody optimisation: ChIP-seq Comparison between sc-543 (Santa Cruz), 6-935 (Millipore) and ab3575 (Abcam); **(A)** Venn diagram showing the overlap between ERα binding sites for sc-543, 6-935 and ab3575 in MCF-7 cells. **(B)** Heatmap of total number of ERα binding sites seen in both technical replicates of MCF-7, and all three biological replicates for MDA-MB-231, respectively. **(C)** De novo motif analysis of ERα binding sites using MEME. **(D)** Examples of ERα-bound regions using sc-543, 6-935 and ab3575; tag densities are shown as reads per million.

Taken together, the genomic and proteomic data indicate that both newly tested antibodies 06-935 (EMD Millipore) and ab3575 (Abcam) perform similarly to sc-543 (Santa Cruz) for immunoprecipitation-based experiments (Glont et al., 2019).

Further assessment of the combination of 06-935 and ab3575 in equal concentrations improved the quality of the genomic and proteomic results. Therefore, the two-antibody mix was the standard used throughout all further experiments.

4.3.1.2 ETV6 antibody optimisation

As part of this chapter, the role of ETV6 in endocrine resistant ERα positive breast cancer models was investigated. Therefore, the validation of sensitive and specific antibodies for its detection was required.

To this end, western blot analysis was performed for the detection of ETV6 protein levels in the chromatin fraction of ZR-75-1 and ZR-75-1-TamR (Fig.4.2.A). The two cell lines were transfected either with non-targeting siRNA (siNT) or subjected to ETV6 silencing (siETV6). The WH0002129M1 antibody (Sigma Aldrich) accurately detected two isoforms of ETV6 in the siNT condition of the two cell lines. Importantly, there was a robust inhibition of the target protein in the siETV6 condition, confirming both the antibody specificity and the efficiency of the knockdown. The cytoplasmic marker GAPDH was not detected, while the chromatin fraction mark Histone 3 was identified, attesting the accurate chromatin purification.

Moreover, immunohistochemistry (IHC) using the WH0002129M1 antibody accurately detected ETV6 total protein levels in ZR-75-1 transfected with non-targeting siRNA, while ETV6 knockdown almost completely depleted its levels (Fig. 4.2.B).

Furthermore, RIME comparison of ETV6 WH0002120M1 (Sigma Aldrich) and A303-674 (Bethyl Laboratories) antibodies was conducted (Fig.4.2.C). Both of them detected the bait protein with a coverage of 25.44%, confirming their specificity. In addition, WH0002120M1 identified 84 ETV6 specific interactors, while A303-674 identified 631 specific interactors of the bait protein, among which there was ERα with a coverage of 4.54%. This indicates that A303-674 may be more sensitive.

Moreover, genome-wide analysis of ETV6-chromatin interactions using ChIP-seq was performed (Fig.4.2.D). While WH0002120M1 failed to generate ETV6 peaks, A303-674 successfully identified a total number of 19,298 ETV6 DNA binding events. Motif

analysis of these sites identified ETS specific motifs with high confidence (e=9.2249E-10). Examples of ETV6, ERα and FOXA1 co-bound regions are provided in Fig.4.2.D.

Taken together, whilst WH0002120M1 (Sigma Aldrich) can accurately detect ETV6 by western blot and IHC, A303-674 (Bethyl Laboratories) proved most specific and sensitive for immunoprecipitation-based experiments such as ChIP-seq and RIME.

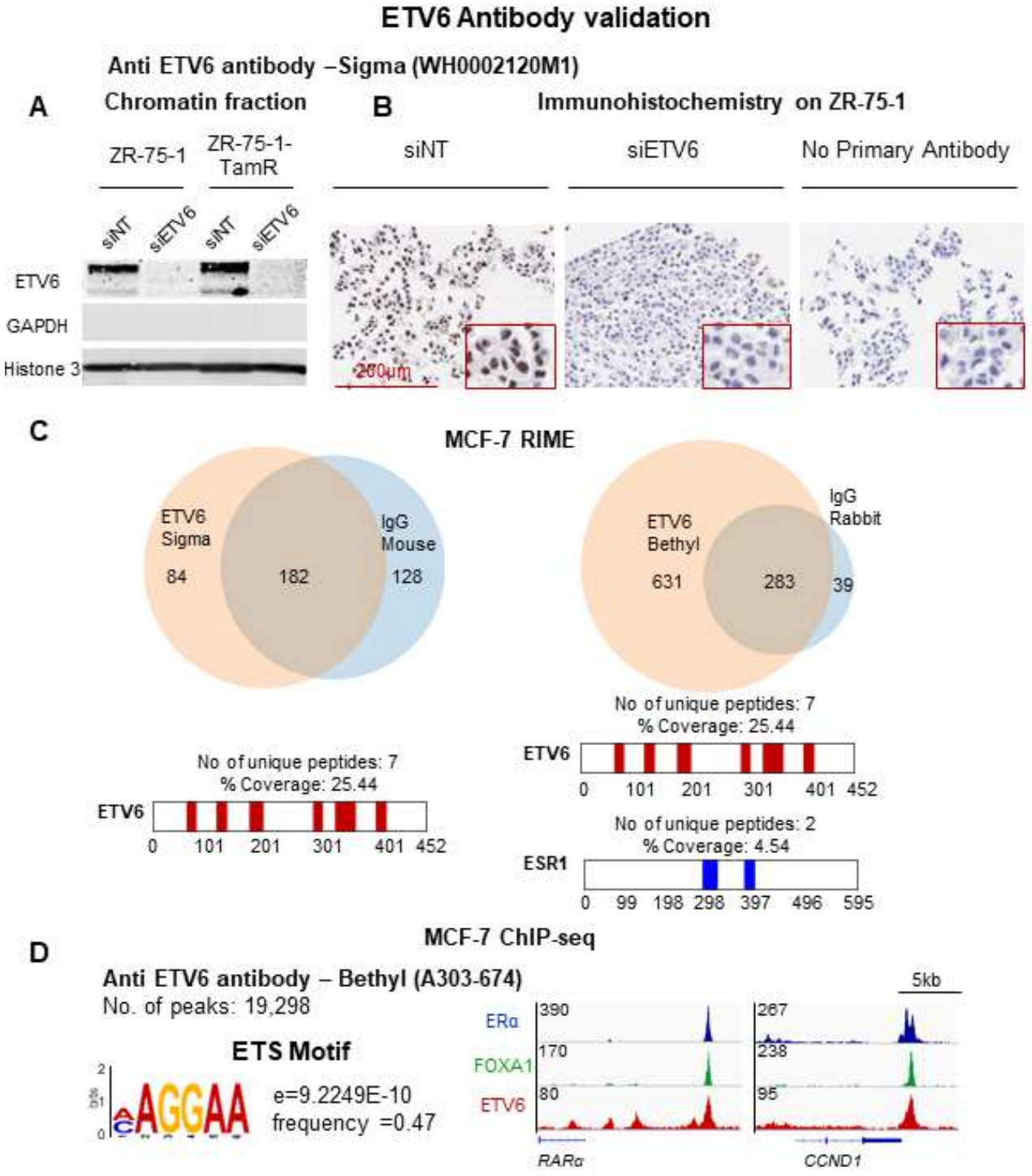

Figure 4.2. ETV6 antibody optimisation:

ZR-75-1 and ZR-75-1-TamR were transfected with 15nM of either siGENOME Non-Targeting siRNA pool (Dharmacon, D-001206-13-05) or siGENOME siRNA pool targeting ETV6 (Dharmacon, M-010510-03); after 48 hours of knockdown, samples were collected for chromatin fractionation followed by western blot protein detection **(A)** and for IHC **(B); (C)** RIME comparison of ETV6 WH0002120M1 (Sigma) and A303-674 (Bethyl) antibodies; Venn diagrams show protein interactors specific to ETV6 compared to the IgG controls; ETV6 and ERα protein coverage are illustrated;**(D)** ETV6 ChIP-seq in MCF-7 using A303-674;Motif analysis of ETV6 binding sites using MEME; examples of regions co-bound by ETV6, ERα and FOXA1.

4.3.1.3 Generation of Tamoxifen resistant breast cancer models

In order to study the molecular changes associated with acquired endocrine resistance, two *in vitro* resistant models were generated. MCF-7-TRF and ZR-75-1-TamR cell lines were derived from MCF-7 and ZR-75-1, respectively, by continuous exposure to 4-hydroxy-Tamoxifen (Sigma-Aldrich, H7904) until they became resistant to the drug. The concentration of Tamoxifen was progressively increased to 1μM for MCF-7-TRF and 100nM for ZR-75-1-TamR. This work was conducted by *Dr Aisling Redmond.*

The effect of Tamoxifen on the growth of the endocrine-resistant derivatives along with their parental cell lines was assessed (Fig.4.3.A and B). After six days of treatment, MCF-7 cell growth was significantly inhibited by 1μm of Tamoxifen (p value of 0.0005), whereas the same concentration of the compound enhanced growth of MCF-7-TRF (p value of 0.03) (Fig.4.3.A). These results attest that MCF-7-TRF are Tamoxifen resistant. Moreover, MCF-7-TRF present a more proliferative phenotype compared to their parental cells, as evidenced by the significantly higher growth rate of untreated MCF-7-TRF versus untreated MCF-7 (p value of <0.0001).

Similarly, Tamoxifen effect was assessed on ZR-75-1 and ZR-75-1-TamR (Fig.4.3.B). While ZR-75-1 cell growth was significantly reduced by 100nM of Tamoxifen (p value of <0.0001), the compound had no effect on ZR-75-1-TamR.

Moreover, the ability of the four cell lines to form colonies was investigated (Fig.4.3.C and D). The more proliferative phenotype of MCF-7-TRF compared to MCF-7 as well as ZR-75-1-TamR compared to ZR-75-1 was reinforced by the enhanced colony formation ability of the resistant cells compared to their parental cells. Furthermore, the inhibitory effects of the selective estrogen-receptor modulator [SERM] Tamoxifen and the estrogen-receptor degrader [SERD] Fulvestrant (ICI) (Fig.4.3.C and D) were

tested on the cell lines. Both compounds almost completely stopped colony formation of MCF-7 and ZR-75-1 cells, but had little or no effect on MCF-7-TRF and ZR-75-1-TamR. Thus, the derived cells seem cross-resistant to multiple endocrine therapies.

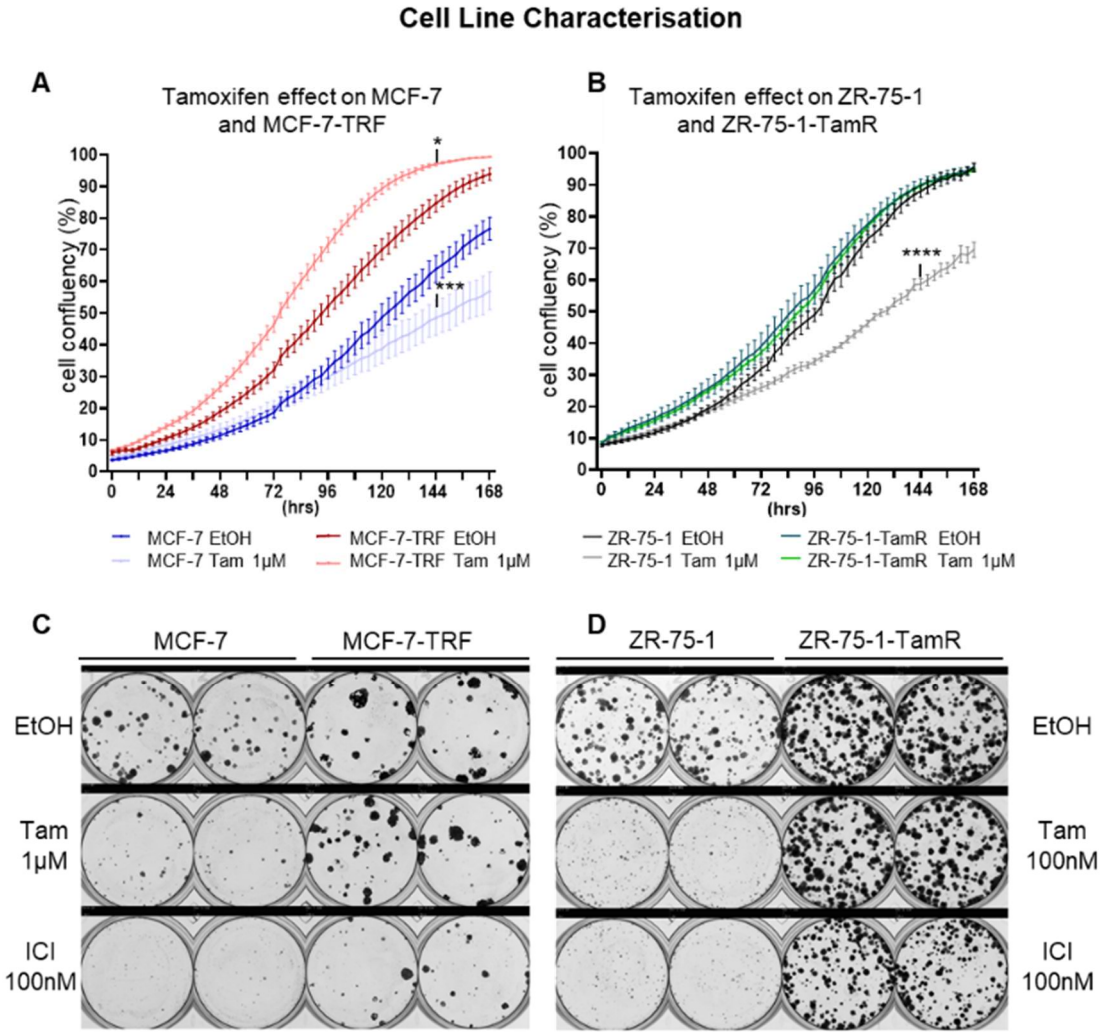

Figure 4.3. Characterisation of Tamoxifen sensitive and resistant in vitro models:

MCF-7 and MCF-7-TRF **(A)** and ZR-75-1 and ZR-75-1-TamR **(B)** cell growth in response to Tamoxifen was assessed using cell confluency as parameter on IncuCyte ZOOM™ system; cells were seeded and after 12 hours MCF-7 and MCF-7-TRF were treated with 1μM Tamoxifen, while ZR-75-1 and ZR-75-1-TamR received 100 nM of the compound; results are shown as mean ±SD of six technical replicates; Two-way-ANOVA statistical analyses were conducted in GraphPad Prism Software Inc; * = p=0.03; *** = p=0.0005; **** = p ≤ 0.0001 **(C)** Colony formation assay for MCF-7 and MCF-7-TRF in response to 1μM Tamoxifen and 100nM Fulvestrant (ICI); **(D)** Colony formation assay for ZR-75-1 and ZR-75-1-TamR in response to 100nM of either Tamoxifen or ICI; cells were seeded at a density of 300 cells per well in a six well plate. Technical duplicates were used and compound treatment duration was 14 days.

4.3.2 ETV6 is a novel interactor from the FOXA1/ERα complex that is enriched in endocrine resistance

Having established the antibodies and breast cancer models required, the following step was to investigate the quantitative differences in the ERα-FOXA1 protein complex between Tamoxifen resistant and sensitive breast cancer.

4.3.2.1 ETV6 is identified in the FOXA1 complex *in vivo*

FOXA1 interactome was studied *in vivo* using qPLEX-RIME. To achieve this, four patient derived tumour xenografts known to be ERα and FOXA1 positive, endocrine resistant were assessed (Fig.4.4).

In order to identify specific interactors of FOXA1, each sample was equally divided between FOXA1 and IgG immunoprecipitation (Fig.4.4.A). The bait protein was successfully identified with a coverage of 18.85% in the FOXA1 vs IgG qPLEX RIME (Fig.4.4.B). In addition, several specific protein interactors were also detected as enriched in the FOXA1 complex compared to IgG (Fig.4.4.C). ETV6 was one of the factors detected with a coverage of 1.55% (Fig.4.4.C).

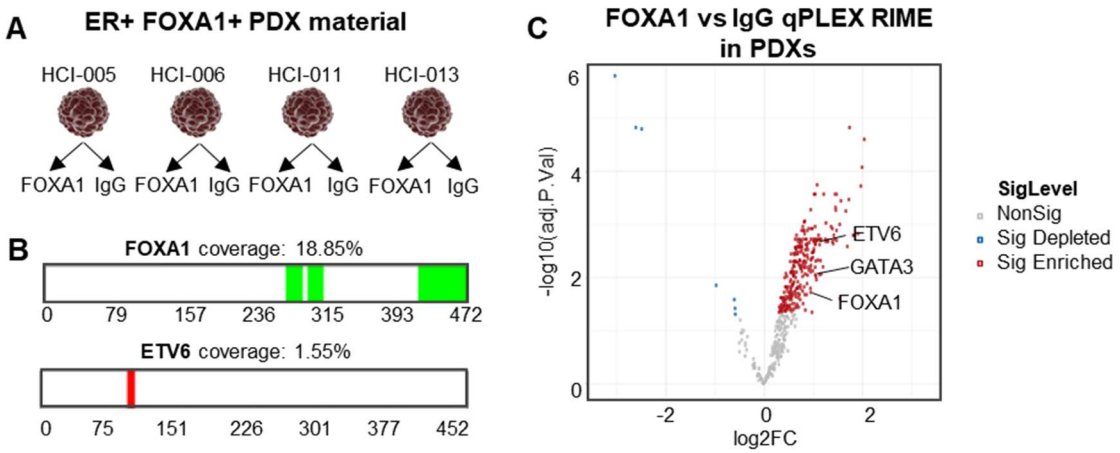

Figure 4.4. ETV6 is identified in the FOXA1 interactome in PDXs: (A) Experimental design; four PDXs were considered biological replicates; each sample was equally divided between FOXA1 and IgG control immunoprecipitation; **(B)** protein coverage plots for FOXA1 and ETV6 show the unique peptides identified with high confidence across each protein sequence; the corresponding percentage coverage is provided above each coverage plot; **(C)** Volcano plot illustrates significant changes between FOXA1 and IgG, as identified by qPLEX-RIME in the four models; proteins significantly enriched - as assessed by adjusted p value ≤0.05 - are illustrated in red and those that are significantly depleted are shown in blue.

Furthermore, FOXA1 interactome was investigated in clinical samples. For this purpose, four pleural effusions and six non-matched primary breast tumours were included (Fig 4.5). FOXA1 was successfully detected with a coverage of 11.65% across all samples (Fig.4.5.B). In addition, several interactors were identified, including ETV6 with a coverage of 3.32% (Fig.4.5.B). ETV6 presence in the FOXA1 complex in the clinical samples is highlighted in Figure 4.5.C.

Therefore, ETV6 is a novel FOXA1 interactor identified across multiple endocrine resistant breast cancer models.

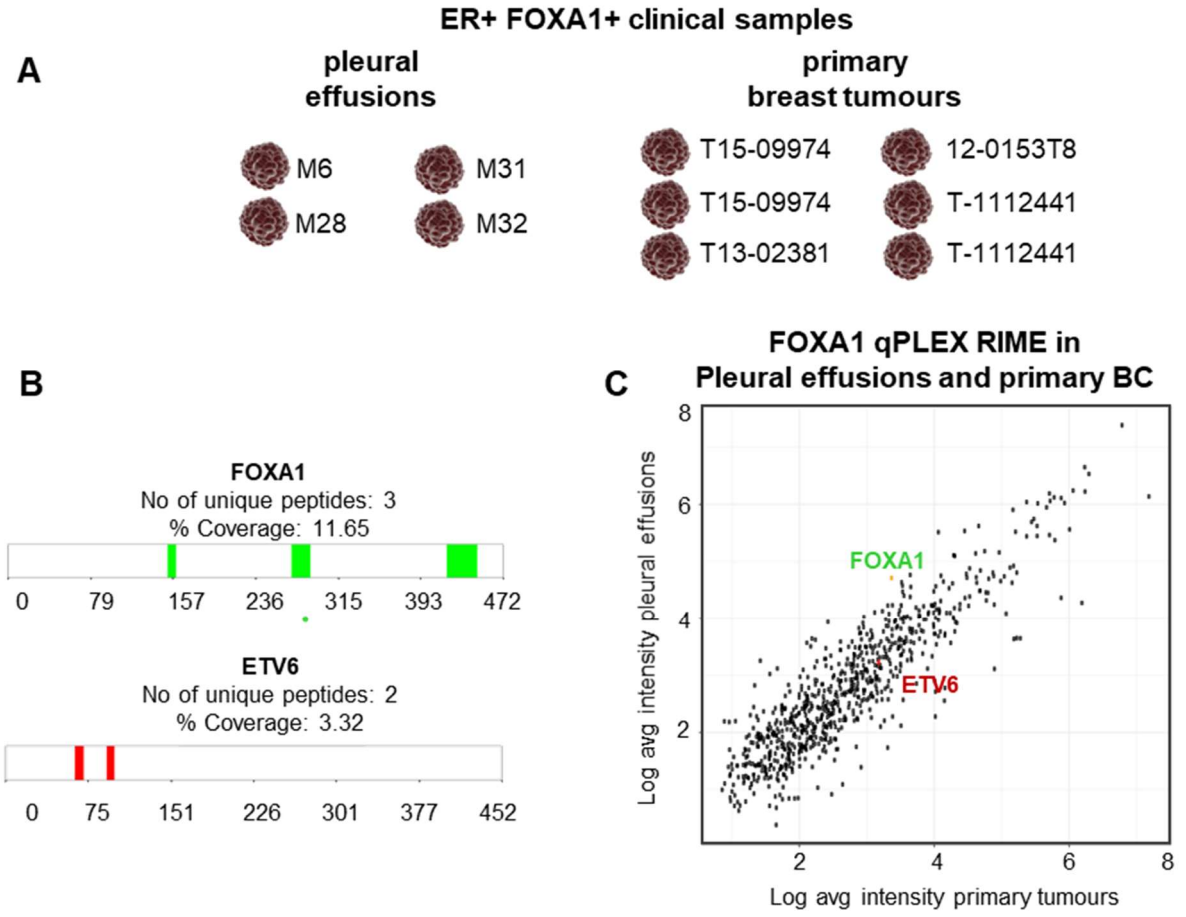

Figure 4.5. ETV6 is identified in the FOXA1 interactome in clinical samples: (A) Experimental design: FOXA1 qPLEX RIME was conducted in four pleural effusions and six primary breast cancer clinical samples, all assessed as ERα, FOXA1 positive; **(B)** protein coverage plots for FOXA1 and ETV6 show the unique peptides identified with high confidence across each protein sequence; the corresponding percentage coverage is provided above each coverage plot; **(C)** Average peptide intensity plot highlighting ETV6 in the FOXA1 interactome in clinical samples.

4.3.2.2 ETV6 interactor of ERα and FOXA1 is specifically enriched in endocrine resistant compared to sensitive breast cancer models

In order to study changes in the ERα-FOXA1 complex associated with endocrine resistance, qPLEX-RIME was conducted in MCF-7-TRF compared to MCF-7 and ZR-75-1-TamR compared to ZR-75-1 cell lines. The experimental design is illustrated in Figure 4.6. A minimum of four biological replicates of every cell line and for each factor were assessed. In order to identify specific interactors of ERα and FOXA1, IgG controls were included in every qPLEX-RIME experiment.

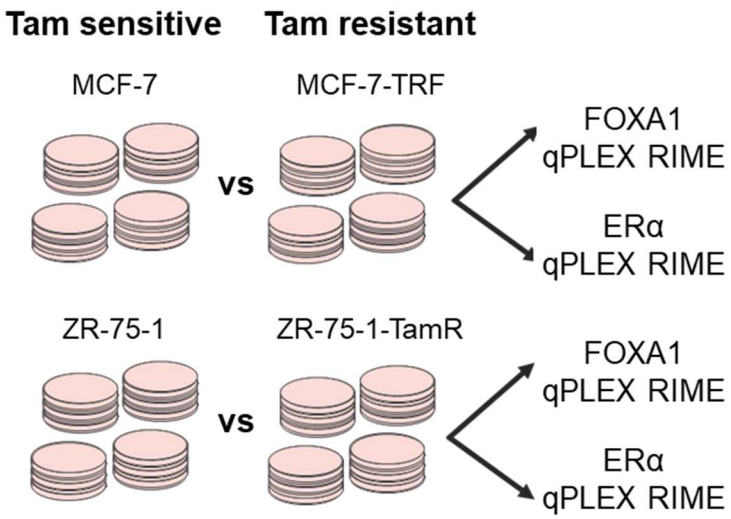

Figure 4.6. Experimental design for ERα and FOXA1 qPLEX RIME in MCF-7-TRF versus MCF-7 and ZR-75-1-TamR versus ZR-75-1.

Both ERα and FOXA1 were consistently enriched in Tamoxifen resistant cell lines compared to their sensitive counterparts across the four qPLEX-RIME experiments conducted (Fig. 4.7.A-D). Importantly, ERα pulldown validated FOXA1 presence in its complex and vice-versa.

In addition, the development of endocrine refractory phenotype triggered the significant depletion or enrichment of several specific interactors from the ERα and FOXA1 complex, as illustrated in the volcano plots (Fig.4.7.A-D). Importantly, the newly identified ERα and FOXA1 interactor ETV6 was consistently detected as significantly enriched in endocrine resistant compared to sensitive context.

ERα, FOXA1 and ETV6 percentage protein coverages confirm their detection with high confidence across all experiments (Fig.4.7.A-D).

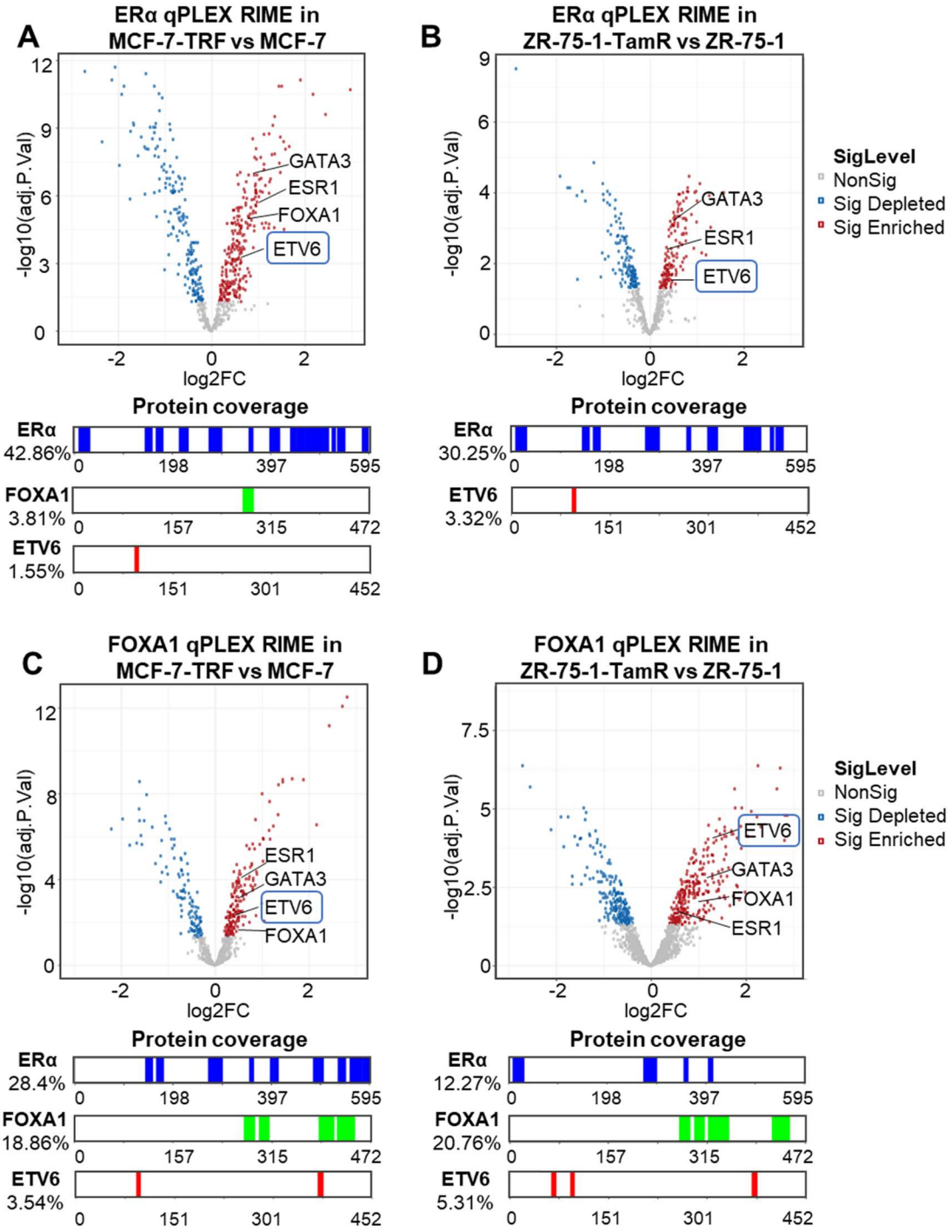

Figure 4.7. Endocrine resistance is associated with ERα and FOXA1α enrichment on the chromatin, as well as significant changes in the levels of their interactors: A-D volcano plots for ERα and FOXA1 qPLEX RIME in MCF-7-TRF versus MCF-7 and ZR-75-1-TamR versus ZR-75-1; interactors that significantly change according to adjusted p value (p adj ≤0.05 after multiple testing correction using the Benjamini-Hochberg procedure) are represented in red (enriched) and blue (depleted); protein coverage for ERα, FOXA1 and ETV6 show unique peptides identified with high confidence across each protein sequence; the corresponding percentage coverage is provided on the left side of each coverage plot.

Several proteins were significantly enriched or depleted in all four comparisons (Fig.4.8.A).

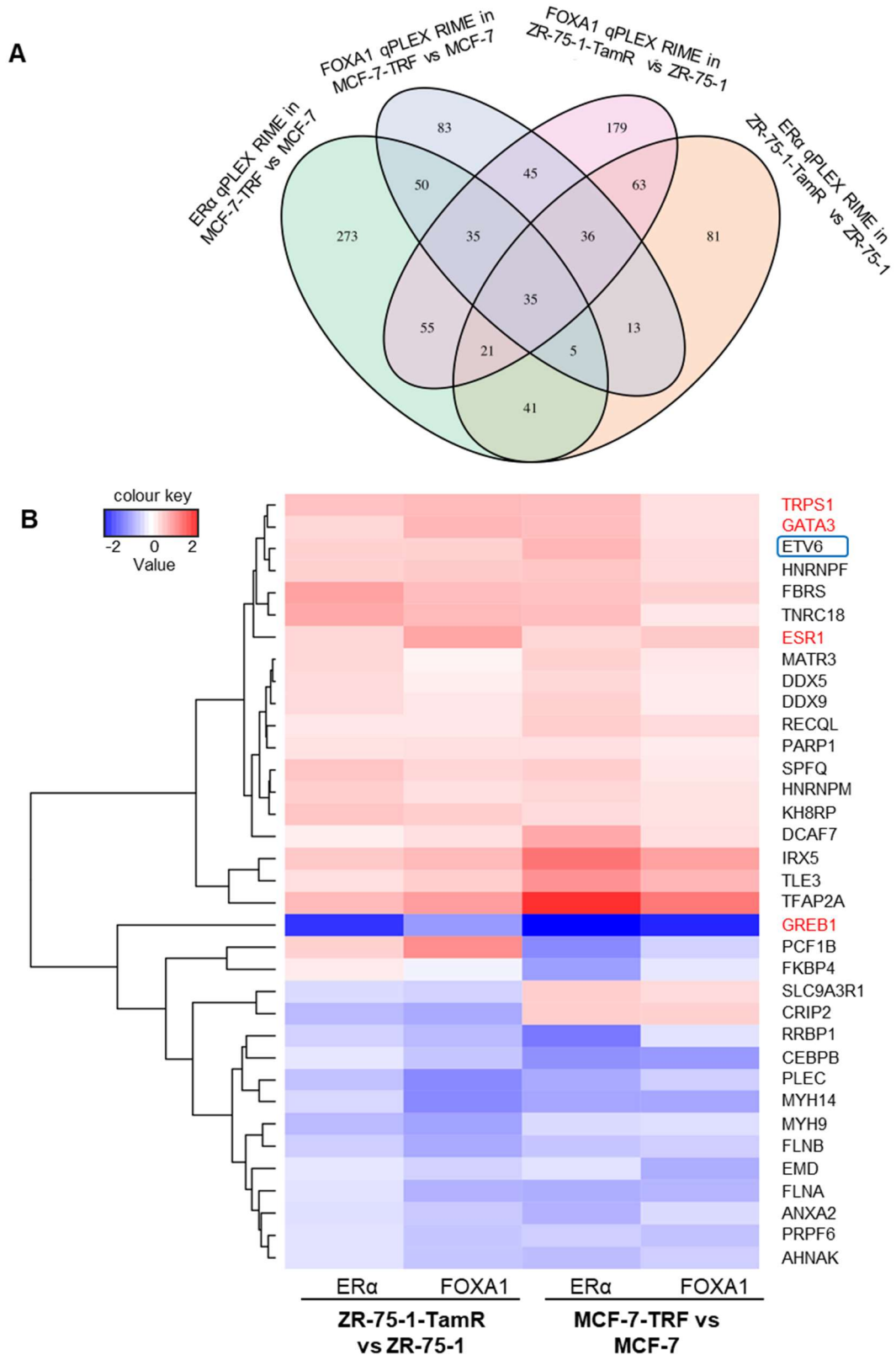

Figure 4.8. Interactors that change significantly in ERα and FOXA1 complex in MCF-7-TRF versus MCF-7 and ZR-75-1 TamR versus ZR-75-1:

(A) Venn diagram showing the overlap between proteins that commonly change significantly in the four qPLEX-RIME experiments conducted; **(B)** heatmap showing log2 fold change for the 35 interactors that are significantly enriched or depleted in ERα and FOXA1 in MCF-7-TRF vs MCF-7 and ZR-75-1-TamR vs ZR-75-1.

There were 35 proteins that significantly changed in ERα and FOXA1 complex in both MCF-7-TRF compared to MCF-7 and ZR-75-1-TamR compared to ZR-75-1 (Fig.4.8.B). Among them, there were known co-factors of ERα and FOXA1, such as TRPS1, GATA3, GREB1, TLE3 and TFAP2A.

GATA3 is one of the most well-established interactors of ERα and FOXA1 (Carroll et al., 2005, Lin et al., 2007, Theodorou et al., 2013). Notably, the ERα-induced growth in breast cancer models seems to be dependent on GATA3 (Eeckhoute et al., 2007).

TRPS1 has been described as a context-dependent regulator of epithelial cell growth and differentiation in breast cancer (Cornelissen et al., 2020, Serandour et al., 2018).

GREB1 was previously identified as a key estrogen receptor co-factor that is part of the ERα interactome (Mohammed et al., 2013, Rae et al., 2005).

The ERα transcriptional co-repressor TLE3 impairs ERα-mediated gene expression at a subset of target genes (Jangal et al., 2014).

AP-2α transcription factor (TFAP2A) is implicated in the differentiation and proliferation of the mammary gland. Its isoforms have also been linked with different activities in breast cancer (Berlato et al., 2011).

The presence of these known treatment resistance-related co-factors of ERα in the four qPLEX-RIME experiments conducted validates the quality of the data generated.

Importantly, several novel interactors were identified as changing significantly in ERα and FOXA1 interactome once Tamoxifen resistance developed, among which ETV6 was significantly enriched in endocrine resistant context. ETV6 is a member of the ETS family of transcription factors that mediate differentiation and lineage specification during normal development. Perturbations in ETS factors have previously been linked with various cancer types (Findlay et al., 2013, Tognon et al., 2002).

Furthermore, qRT-PCR was conducted to examine gene expression levels of ERα, FOXA1, GATA3 and ETV6 in the Tamoxifen resistant cell lines compared to sensitive counterparts (Fig.4.9.A). FOXA1 and GATA3 were significantly upregulated in both MCF-7-TRF compared to MCF-7 and ZR-75-1-TamR versus ZR-75-1. In addition,

ETV6 expression level was significantly higher in MCF-7-TRF versus MCF-7, though its levels remained similar in ZR-75-1-TamR compared to ZR-75-1. These findings confirm that the enrichment of these transcription factors on the chromatin assessed by qPLEX-RIME are largely associated with their gene expression upregulation. In contrast, ERα mRNA levels seemed to be depleted in endocrine resistant context, with significantly lower expression in ZR-75-1-TamR vs ZR-75-1 (p value of 0.01).

Western blot was then conducted to evaluate total protein levels of ERα, FOXA1, GATA3 and ETV6 Fig.4.9.B). All four proteins had higher levels in both MCF-7-TRF and ZR-75-1-TamR compared to their sensitive counterparts.

The results suggest that post-translational modifications may further stabilise these transcription factors, resulting in their chromatin enrichment detected by qPLEX-RIME in Tamoxifen resistant compared to sensitive cells.

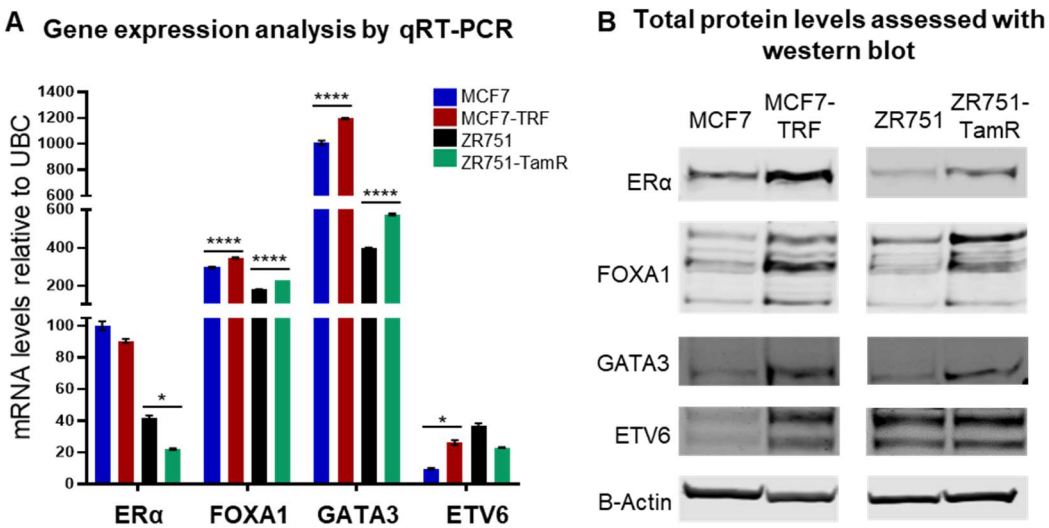

Figure 4.9. Assessment of ERα, FOXA1, GATA3 and ETV6 gene expression levels (A) and total protein levels (B) for MCF-7, MCF-7-TRF, ZR-75-1, ZR-75-1-TamR: (A) mRNA levels were assessed with qRT-PCR; results represent mean ±SD of enrichment relative to the housekeeping gene UBC. Two-way-ANOVA statistical analyses were conducted; * = p = 0.01; **** = p ≤ 0.0001; **(B)** ERα, FOXA1, GATA3 and ETV6 Western blot analysis on whole protein lysate from the four cell lines investigated. β-Actin was included as loading control.

Taken together, ERα, FOXA1 and their newly identified interactor ETV6 are enriched in endocrine resistance across multiple breast cancer models. This suggests ETV6 may play a role in cancer progression and drug-refractory phenotype and is a worthy candidate to pursue.

4.3.3 Independent validation of ETV6 relevance in endocrine resistant context

To ensure further studies would focus on the most relevant ERα and FOXA1 interactors for endocrine resistance, an siRNA screen was conducted to target the top most enriched proteins depicted in the ERα and FOXA1 qPLEX RIME in MCF-7-TRF compared to MCF-7 and ZR-75-1-TamR compared to ZR-75-1 (Fig.4.10). As expected, FOXA1 knock-down had a pronounced inhibitory effect on cell viability. Notably, ETV6 silencing also strongly affected cell viability of both Tamoxifen sensitive and resistant cell lines, confirming its relevance in the endocrine refractory phenotype.

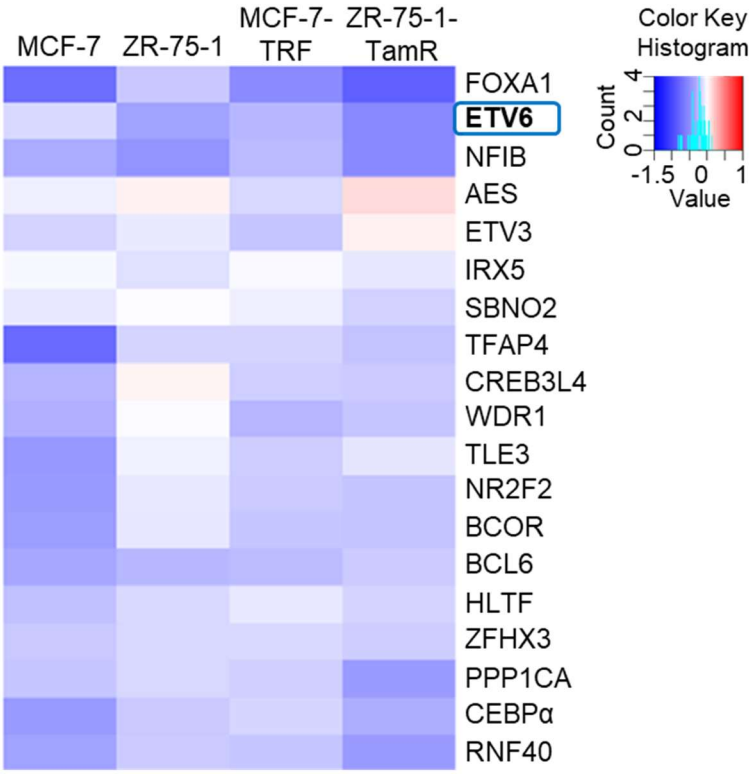

Figure 4.10. Independent siRNA screen validates ETV6 relevance in endocrine resistant context: the LP_34662 siGenome library of siRNA pools (Dharmacon, G-CUSTOM-294730) was used; non-targeting siRNA pool was also included in the library; four independent biological replicates were conducted for MCF-7, MCF-7-TRF, ZR-75-1 and ZR-75-1-TamR, each containing 6 technical replicates; cells were transfected with 15nM of either siNT or siRNA pool targeting each selected interactor; knockdown was conducted for 72 hours, after which cell viability was assessed using CellTiter-Glo® Luminescent Assay. Heatmap illustrates log2fold change compared to non-targeting siRNA for every knockdown in each cell line as an average of the four biological replicates; cell viability inhibition is illustrated in blue, while red represents cell viability promotion.

To ensure the effects of ETV6 silencing on cell viability are not specific to the pool of siRNAs used as part of the library screen, further validation was conducted.

ETV6 was inhibited using single siETV6 On-TARGET plus (Dharmacon, j-010510-10 or j-010510-11) compared to matched ON-TARGET-plus non-targeting siRNA (Dharmacon, D-001810-10). The knockdown efficiency was assessed (Fig.4.11.A). ETV6 silencing using any of the siRNAs resulted in a significant anti-proliferative effect in all four cell lines (Fig.4.11.B).

These results show that targeting ETV6 inhibit the growth of the cells that no longer respond to endocrine therapy and suggest that targeting ETV6 may be beneficial for the endocrine refractory breast cancer patients.

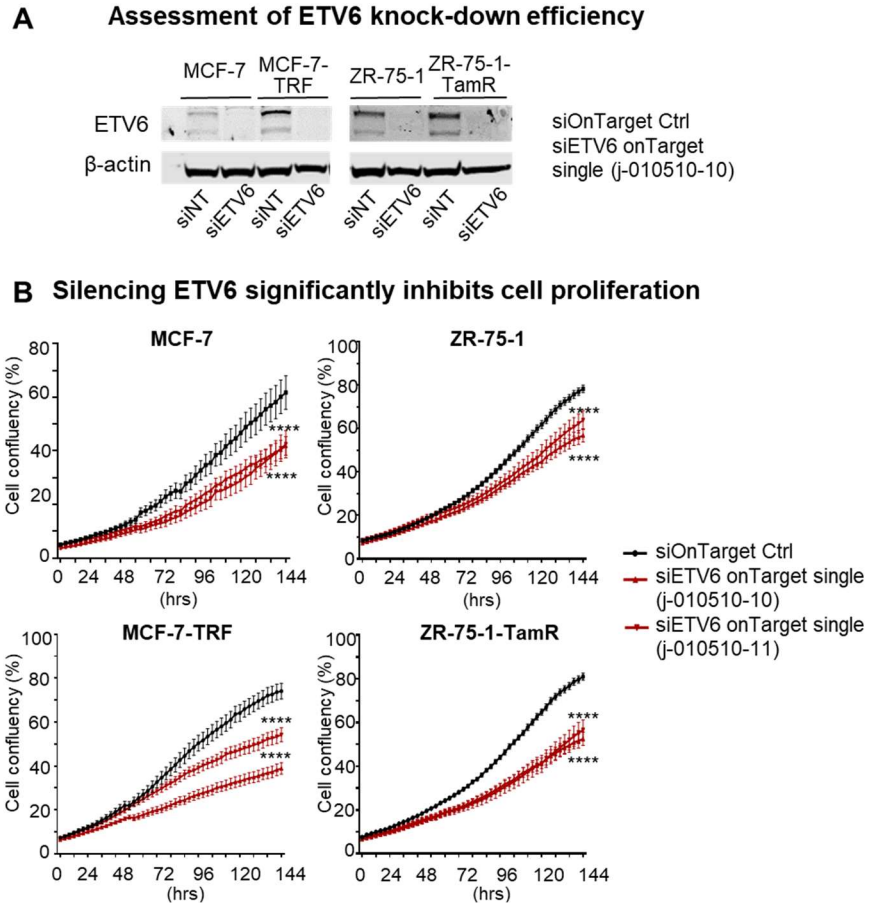

Figure 4.11. Validation of the effects of ETV6 inhibition using single siRNA: knock-down was achieved using 15nM of single siETV6 (Dharmacon, j-010510-10 or j-010510-11) and was compared to non-targeting siRNA (Dharmacon, D-001810-10); **(A)** western blot confirming robust ETV6 silencing in all four cell lines after 48 hours of knockdown **(B)** cell growth in response to ETV6 inhibition; cells were seeded and transfected the following day. T0 is the time of transfection; experiments were performed in biological triplicates; one of the replicates is illustrated; data points represent mean ±SD of six technical replicates; Two-way-ANOVA statistical analysis was conducted; **** = $p \leq 0.0001$.

4.3.4 ETV6 directly contributes to breast cancer progression associated with endocrine resistance

Furthermore, it was assessed if the more proliferative phenotype seen in MCF-7-TRF compared to MCF-7 and ZR-75-1-TamR compared to ZR-75-1 could be recapitulated by ETV6 overexpression in the sensitive cell lines (Fig.4.12).

The successful generation of pLenti overexpressing MCF-7 and ZR-75-1 cells using the p-ETV6-Lv181 (Genecopoeia ref. EX-F0874-Lv181) (*ETV6 V)* compared to the matched empty control vector (pReceiver-Lv181 (Genecopoeia, ref. EX-NEG-Lv181) *(Ctrl V)* was validated using western blot (Fig.4.12.A).

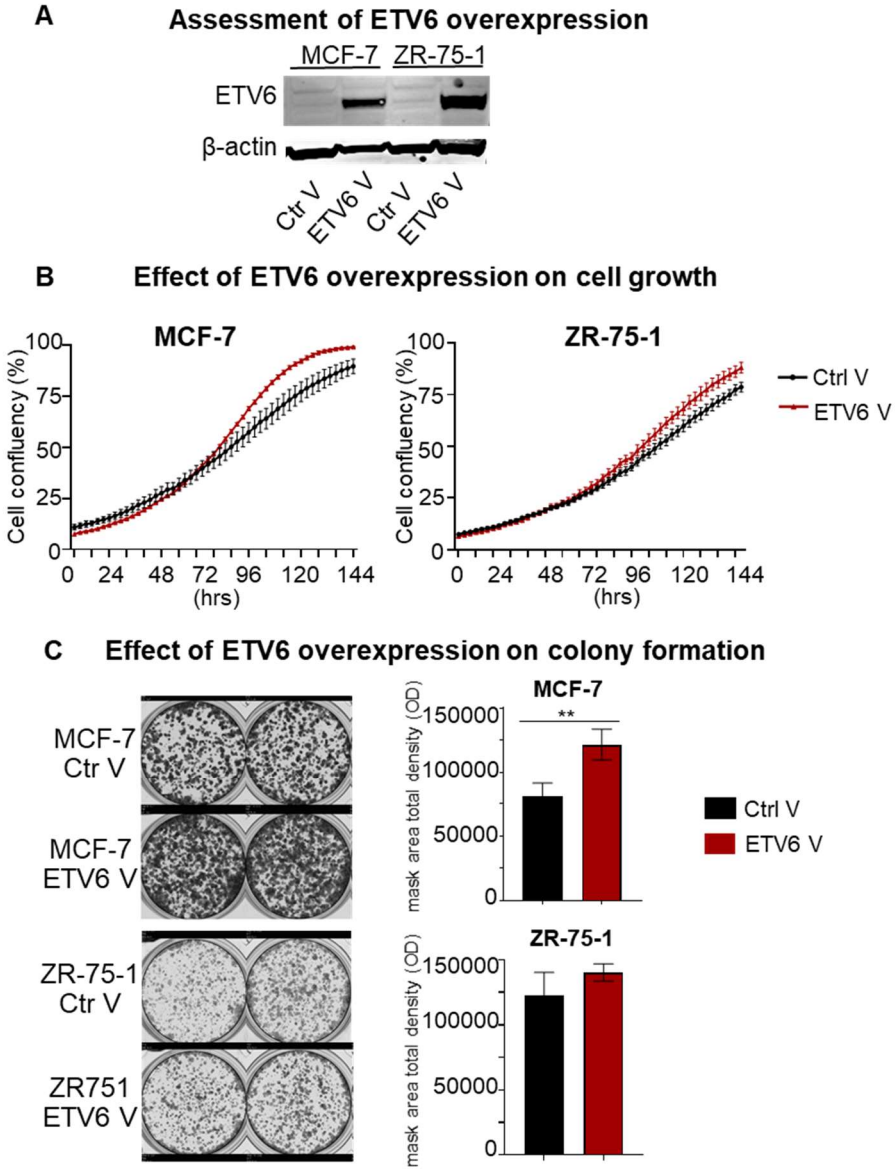

Figure 4.12. ETV6 overexpression in Tamoxifen sensitive MCF-7 and ZR-75-1 results in a more proliferative phenotype:

(A) Western blot assessment of pLenti ETV6 overexpressing MCF-7 and ZR-75-1 cells using the p-ETV6-Lv181 (Genecopoeia ref. EX-F0874-Lv181) *(ETV6 V)* compared to the matched empty control vector pReceiver-Lv181 (Genecopoeia, ref. EX-NEG-Lv181) *(Ctrl V)*; **(B)** MCF-7 and ZR-75-1 cell growth is promoted in response to ETV6 overexpression, as assessed by cell confluency using IncuCyte ZOOM^{TM} system; experiments were conducted in biological triplicates; the graphs represent one replicate and results are shown as mean ±SD of 6 technical replicates; **(C)** Colony formation assay for MCF-7 and ZR-75-1 *ETV6 V* vs *Ctrl V*; one biological replicate out of three is illustrated; cells were seeded at a density of 300 cells per well in a six well plate and were grown for 14 days; mask area total density was assessed using GelCount Optronix software; results are presented as mean ±SD and t-test analyses were conducted in GraphPad Prism; ** = p = 0.01; *ETV6 V* promotes colon formation compared to *Ctrl V*.

Cell growth was investigated for MCF-7 and ZR-75-1 that carried either Ctrl V or ETV6 V (Fig.4.12.B). ETV6 overexpression seemed to promote growth of both cell lines in multiple biological replicates, though the difference did not reach statistical significance.

An alternative assessment was therefore conducted, namely colony formation assays. It presents the major advantage of spanning over a longer time frame compared to proliferation assays and therefore the trend of ETV6 overexpression resulting in a more proliferative phenotype may become significant.

Thus, colony formation assays were conducted for ETV6 V compared to Ctrl V in MCF-7 and ZR-75-1 (Fig.4.12.C). Mask area total density was assessed as a parameter of all pixels within the mask boundary. This parameter allows quantitative comparisons between different conditions. As such, MCF-7 cells overexpressing ETV6 showed a significant increase in the colony formation assay, as assessed by mask area total density (p value of 0.01). In addition, there was also a slight enrichment in ZR-75-1 ability to form colonies upon ETV6 overexpression.

Taken together, the role of ETV6 in cancer progression which is associated with endocrine resistance was validated by the promoting effects of ETV6 overexpression on MCF-7 colony formation.

4.3.5 ERα, FOXA1, ETV6-chromatin interactions are redistributed to the same genomic regions in endocrine resistant compared to sensitive breast cancer models

Genome-wide mapping of ERα-binding events using ChIP-seq in clinical samples has previously revealed that endocrine-resistant metastatic breast cancers recruit ERα to novel regulatory regions that are associated with poor clinical outcome (Ross-Innes et al., 2012). *In vitro* validation of this work has shown that FOXA1 and ERα co-localise in Tamoxifen-sensitive and resistant models, implying FOXA1 may be the critical factor that redirects ERα to its novel target regions.

In this context, ETV6, FOXA1 and ERα chromatin interactions were assessed in endocrine resistant compared to sensitive models, in order to interrogate ETV6 role in the reprograming of ERα. In addition, the enhancer landscape at these novel binding sites was also assessed.

ChIP-seq was conducted to study ETV6, FOXA1 and ERα chromatin interactions in MCF-7, MCF-7-TRF, ZR-75-1 and ZR-75-1-TamR. To assess whether enhancers are active at these binding sites, histone H3 acetylation at Lysine K27 (H3K27Ac) marker was included (Zhou et al., 2011). The experimental design is illustrated in Figure 4.13.

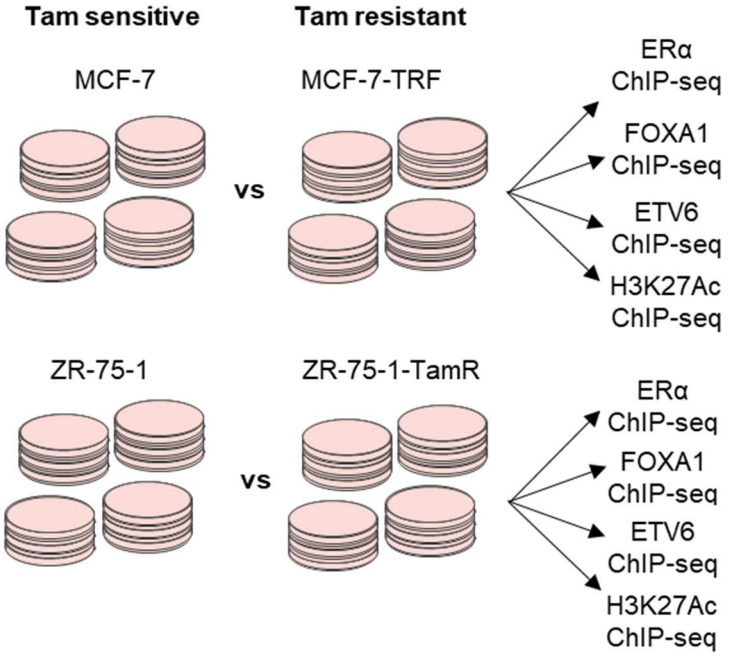

Figure 4.13. Experimental design for ERα, FOXA1, ETV6 and H3K27Ac ChIP-seq in MCF-7, MCF-7-TRF, ZR-75-1 and ZR-75-1-TamR.

ChIP-seq experiments were conducted in at least three biological triplicates. Input samples were also included and significant peaks were called using MACS2 for each group of samples against their marched inputs. For every group of samples, only peaks present in all biological replicates were considered. The total number of peaks for each factor is provided in Table 4.1:

In MCF-7 cells, ChIP-seq analysis generated 39,260 peaks for ERα, 45,622 binding sites for FOXA1, 27,967 for ETV6 and 85,413 for H2K27Ac. In MCF-7-TRF cells, there were 59,552 sites for ERα, 50,020 for FOXA1, 31,197 for ETV6 and 59,479 for H3K27Ac.

In ZR-75-1 cells, ChIP-seq generated 7,204 peaks for ERα, 50,172 binding regions for FOXA1, there were 21,729 sites for ETV6 and 76,223 for H3K27Ac. In ZR-75-1-TamR, there were 6,362 peaks for ERα, 29,630 for FOXA1, 6,347 for ETV6 and 58,421 for H3K27Ac. These results confirm the efficiency of the ChIP-seq experiments performed.

Cell line	Antibody	Total no of peaks
MCF-7	ERα (Abcam ab3575 and Millipore 06-935)	39,260
	FOXA1 (Abcam ab5089)	45,622
	ETV6 (Bethyl,A303-674A)	27,967
	H3K27Ac (Abcam ab4729)	85,413
MCF-7-TRF	ERα (Abcam ab3575 and Millipore 06-935)	59,552
	FOXA1 (Abcam ab5089)	50,020
	ETV6 (Bethyl A303-674A)	31,197
	H3K27Ac (Abcam ab4729)	59,479
ZR-75-1	ERα (Abcam ab3575 and Millipore 06-935)	7,204
	FOXA1 (Abcam ab5089)	50,172
	ETV6 (Bethyl, A303-674A)	21,729
	H3K27Ac (Abcam ab4729)	76,223
ZR-75-1-TamR	ERα (Abcam ab3575 and Millipore 06-935)	6,362
	FOXA1 (Abcam ab5089)	29,630
	ETV6 (Bethyl A303-674A)	6,347
	H3K27Ac (Abcam ab4729)	58,421

Table 4.1. Total number of peaks called in for ERα, FOXA1 and ETV6 and H3K27Ac ChIP-seq in MCF-7, MCF-7-TRF, ZR-75-1 and ZR-75-1-TamR: All ChIP-seq experiments were conducted in at least biological triplicates; Peaks were called using MACS in narrow mode for transcription factors and H3K27ac in broad mode. The numbers shown are the number of peaks/regions found to be significantly enriched at a q-value of 0.05 across all replicates for each experimental group compared to their matched inputs.

Importantly, in both the Tamoxifen sensitive and resistant models, there was a high number of sites co-bound by all three transcription factors (Fig.4.14). There were 9,905 binding events common among ERα, FOXA1 and ETV6 for MCF-7 cells, 10,697 common sites for MCF-7-TRF, 2,240 for ZR-75-1 and 1,268 for ZR-75-1-TamR. These numbers represent between 17.96% and 31.09% of the total numbers of ERα binding sites. This high overlap of the three transcription factors reinforces the association between ERα, FOXA1 and ETV6, suggesting they function together to dictate gene transcription in both Tamoxifen sensitive and resistant context.

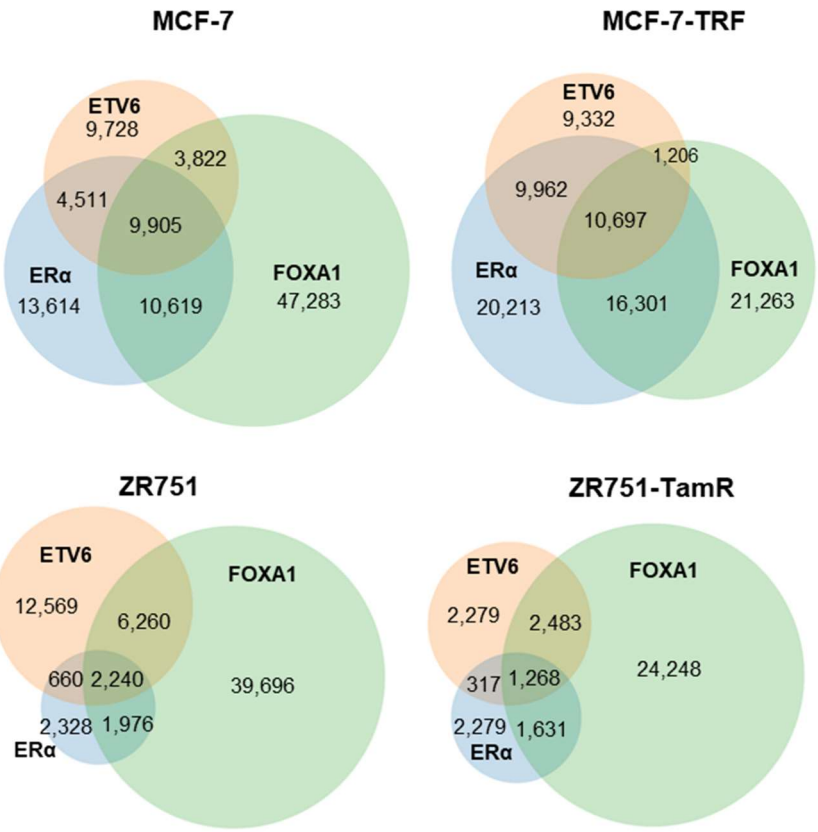

Figure 4.14. Overlap of ERα, FOXA1 and ETV6 binding sites in each cell line investigated.

Examples of two key ERα target genes (RARα and CCND1) that are co-bound by FOXA1 and ETV6 in all four cells lines are illustrated in Figure 4.15. In addition, the presence of H3K27Ac marker on the chromatin at these sites proves those regions are active for transcription.

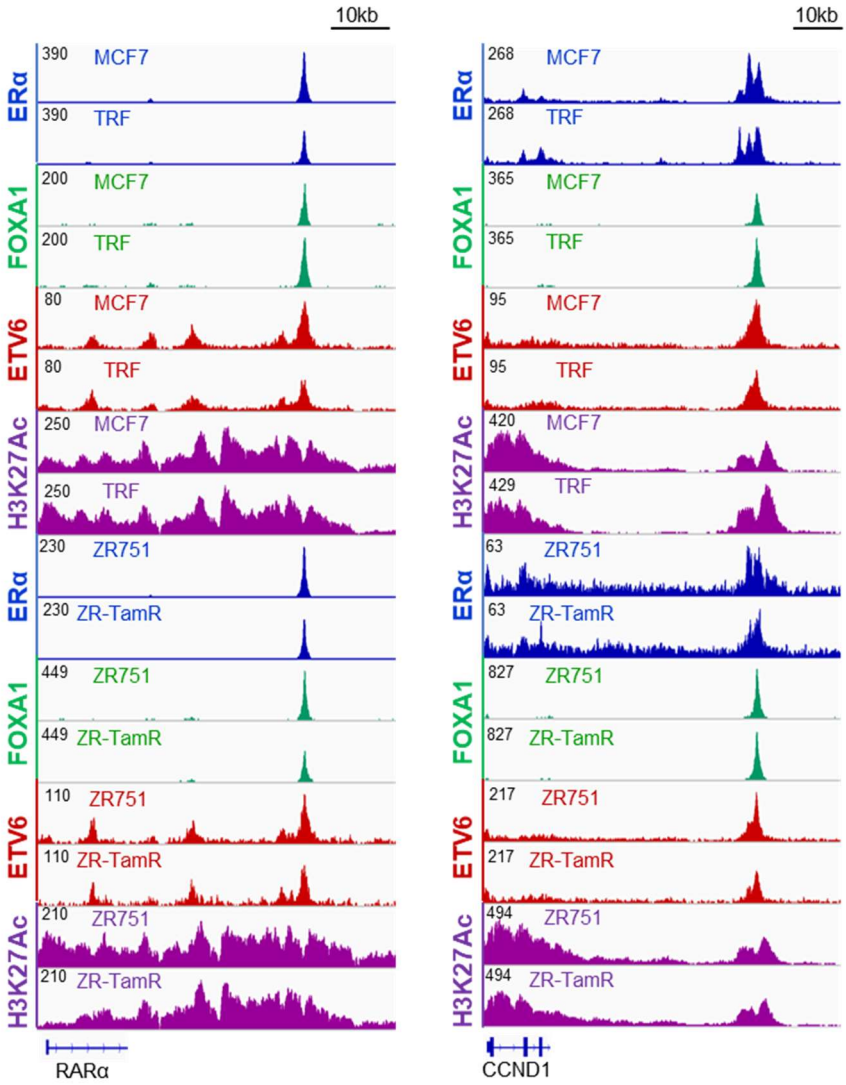

Figure 4.15. Examples of regions bound by ERα, FOXA1, ETV6 and H3K27Ac in both endocrine sensitive and resistant cell lines: IGV genome browser tracks of ChIP-seq signal for the four factors in MCF-7, MCF-7-TRF, ZR-75-1 and ZR-75-1-TamR.

To further investigate the differences in chromatin binding between Tamoxifen resistant and sensitive cell lines, DiffBind analysis was conducted for MCF-7-TRF compared to MCF-7 and ZR-75-1-TamR compared to ZR-75-1. The summary of the results is provided in Table 4.2. For MCF-7-TRF compared to MCF-7, ChIP-seq experiments for ERα gave 33,282 gained peaks and 9,363 peaks lost peaks; there were 38,976 gained and 16,604 lost FOXA1 sites and 5,685 gained and 2,658 lost ETV6 binding sites.

For ZR-75-1-TamR compared to ZR-75-1, ChIP-seq experiments showed there were 2,443 gained and 2,515 lost ERα binding sites, 7,254 gained and 11,009 lost FOXA1 peaks and 1,276 gained and 3,134 lost ETV6 chromatin interactions.

Comparison	Factor	Differential binding comparison		
		gained	lost	common
MCF7-TRF vs MCF-7	ERα	33,282	9,363	6,265
	FOXA1	38,976	16,604	11,009
	ETV6	5,685	2,658	12,858
ZR-75-1-TamR vs ZR-75-1	ERα	2,443	2,515	1.415
	FOXA1	7,254	11,009	10,873
	ETV6	1,276	3,134	6,962

Table 4.2. Differential binding analysis for MCF-7-TRF compared to MCF-7 an ZR-75-1-TamR compared to ZR-75-1.

A representation of the differentially bound ERα, FOXA1 and ETV6 binding sites in the two pairs of cell lines is illustrated in Figure 4.16.

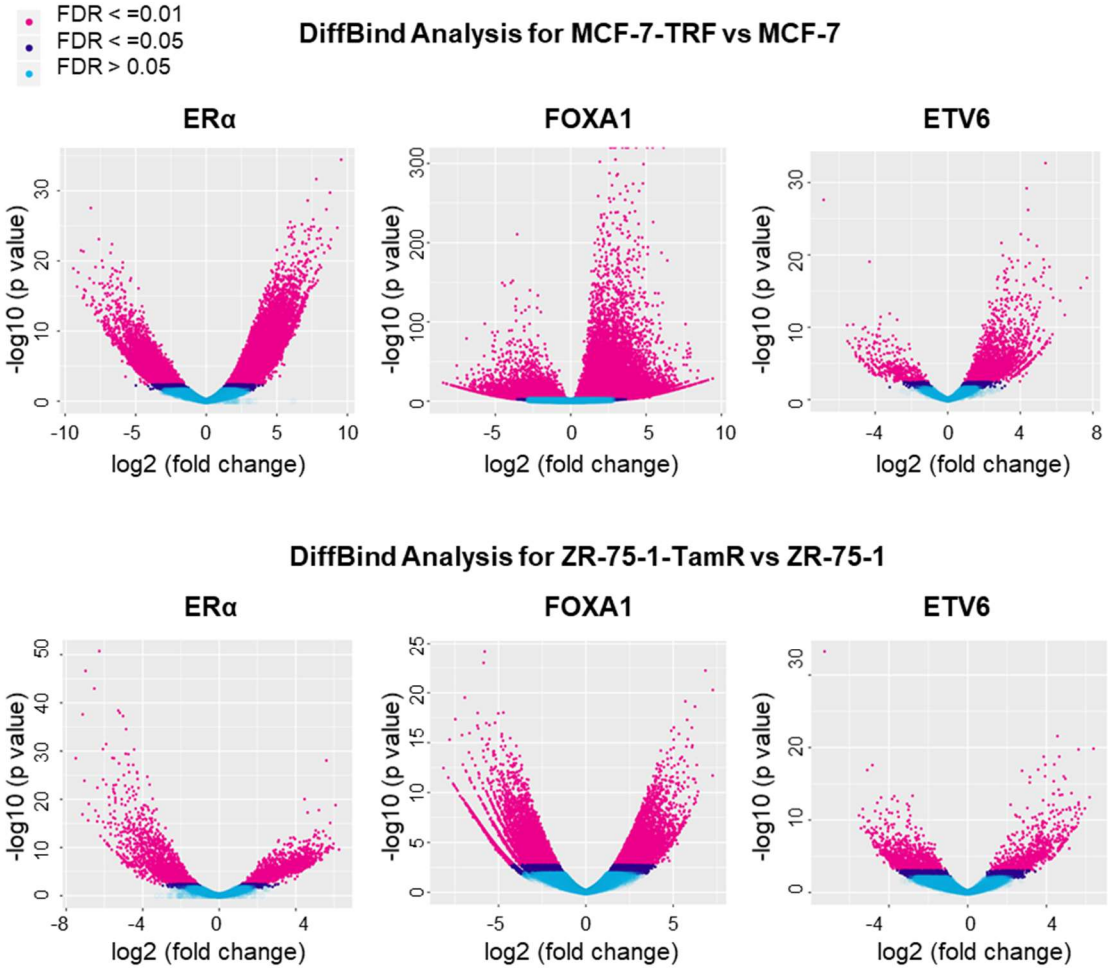

Figure 4.16. Tamoxifen resistance triggers ERα, FOXA1 and ETV6- DNA binding redistribution: Volcano plots show log2 fold change for each transcription factor in MCF-7-TRF versus MCF-7 and ZR-75-1-TamR versus ZR-75-1, respectively. Pink dots represent significant peaks with FDR <=0.01.

The DiffBind analyses conducted in the present study confirm the ERα, FOXA1 and ETV6 chromatin binding redistribution associated with endocrine resistance.

As described in Chapter 4.3., ETV6 together with ERα and FOXA1 were significantly enriched on the chromatin in Tamoxifen resistant breast cancer models compared to the sensitive ones according to qPLEX RIME assessments.

In addition, previous studies have described a global redistribution of ERα binding sites associated with endocrine-resistant metastatic breast cancer (Ross-Innes et al., 2012a). More recently, enhancer reprogramming during hormone resistance acquisition was reported (Bi et al., 2020). *Bi et al* saw an enrichment of GATA3 and AP2γ motifs on the lost sites and RUNX and JUN motifs on the gained sites when comparing endocrine resistant MCF-7 with parental MCF-7. In addition, whilst FOXA1 motif was present in all groups, ERα was only detected at the common enhancers.

In order to further understand the molecular mechanisms underlying endocrine resistance in the models used for this study, motif analysis was performed for ERα and FOXA1 differentially bound sites in MCF-7-TRF compared to MCF-7 and ZR-75-1-TamR compared to ZR-75-1 (Fig.4.15 and Fig.4.16).

Notably, ETS motifs corresponding to the ETV6 transcription factor were identified in ERα and FOXA1α gained sites but not in the lost sites for both resistant cell lines compared to their matched parental cells. These results strongly reinforce the finding that ERα, FOXA1 and ETV6 work collaboratively at the gained sites to promote cancer progression and endocrine refractory phenotype.

In addition, Forkhead motif was present in gained and lost ERα and FOXA1 sites in both MCF-7-TRF compared to MCF-7 and ZR-75-1-TamR compared to ZR-75-1. Importantly, Forkhead motifs were detected with higher confidence in the gained sites across all comparisons, according to the e value (Fig. 4.17 and Fig. 4.18). These results are in accordance with FOXA1 total protein levels being higher in Tamoxifen resistant cells (Fig.4.7), with FOXA1 enrichment in the proteomics experiments conducted in Chapter 4.3.2 (Fig.4.6), and its significantly higher gene expression in the endocrine refractory models.

Moreover, ERE motif was also present with higher confidence in the gained compared to lost ERα sites in both MCF-TRF versus MCF-7 and ZR-75-1-TamR versus ZR-75-1. ERE were also detected in the FOXA1 differentially bound regions in MCF-7-TRF compared to MCF-7. The presence of ERE and Forkhead motifs at the reprogrammed sites indicates that in the multiple models used in this study, ERα and FOXA1 directly bind to their novel cis-regulatory elements.

Furthermore, GATA3, one of the two motifs described by *Bi et al* as specific to lost sites in resistance was investigated. GATA motif was found in ERα and FOXA1 gained and lost sites for both Tamoxifen resistant cell lines compared to their matched parental cells. Importantly, GATA was found with higher confidence in the gained sites, according to the e value. These results suggest that the *Bi et al* finding that GATA is lost in treatment resistance is model-specific and not a general feature of drug resistance.

In addition, JUN and FOS proteins are known to form the AP1 transcription factor network. *Bi et al* identified JUN motifs specifically in the gained sites associated with treatment resistance. In contrast, the investigation conducted in MCF-7-TRF compared to MCF-7 and ZR-75-1-TamR compared to ZR-75-1 identified FOS and JUN in both ERα and FOXA1 gained and lost sites.

Therefore, it seems that neither loss of GATA3 nor the gain of JUN are the hallmarks of endocrine resistance.

Taken together, motif analysis reinforced the finding that ERα, FOXA1 undergo a global redistribution biased towards novel gained chromatin interactions in endocrine resistance. Importantly, ETV6 motifs are enriched at the gained sites in both Tamoxifen resistant models compared to their sensitive counterparts. These results suggest the three transcription factors work collaboratively in endocrine refractory phenotype in multiple breast cancer models.

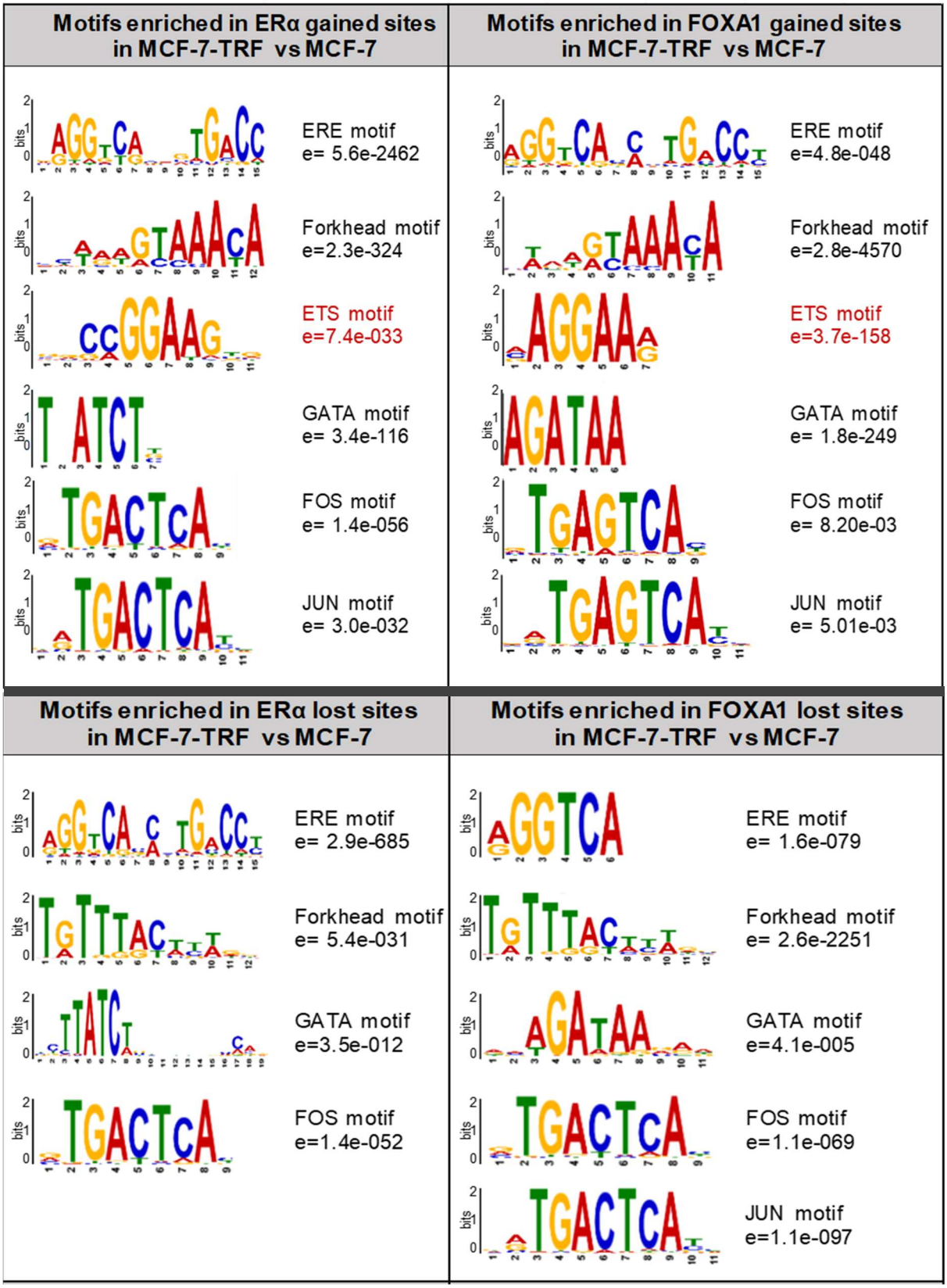

Figure 4.17. Motif analysis of ERα and FOXA1 gained and lost sites in MCF-7-TRF compared to MCF-7: enrichment analysis was performed using MEME Suite tools; e value is determined by the significance of the motif according to the discovery program reporting the motif.

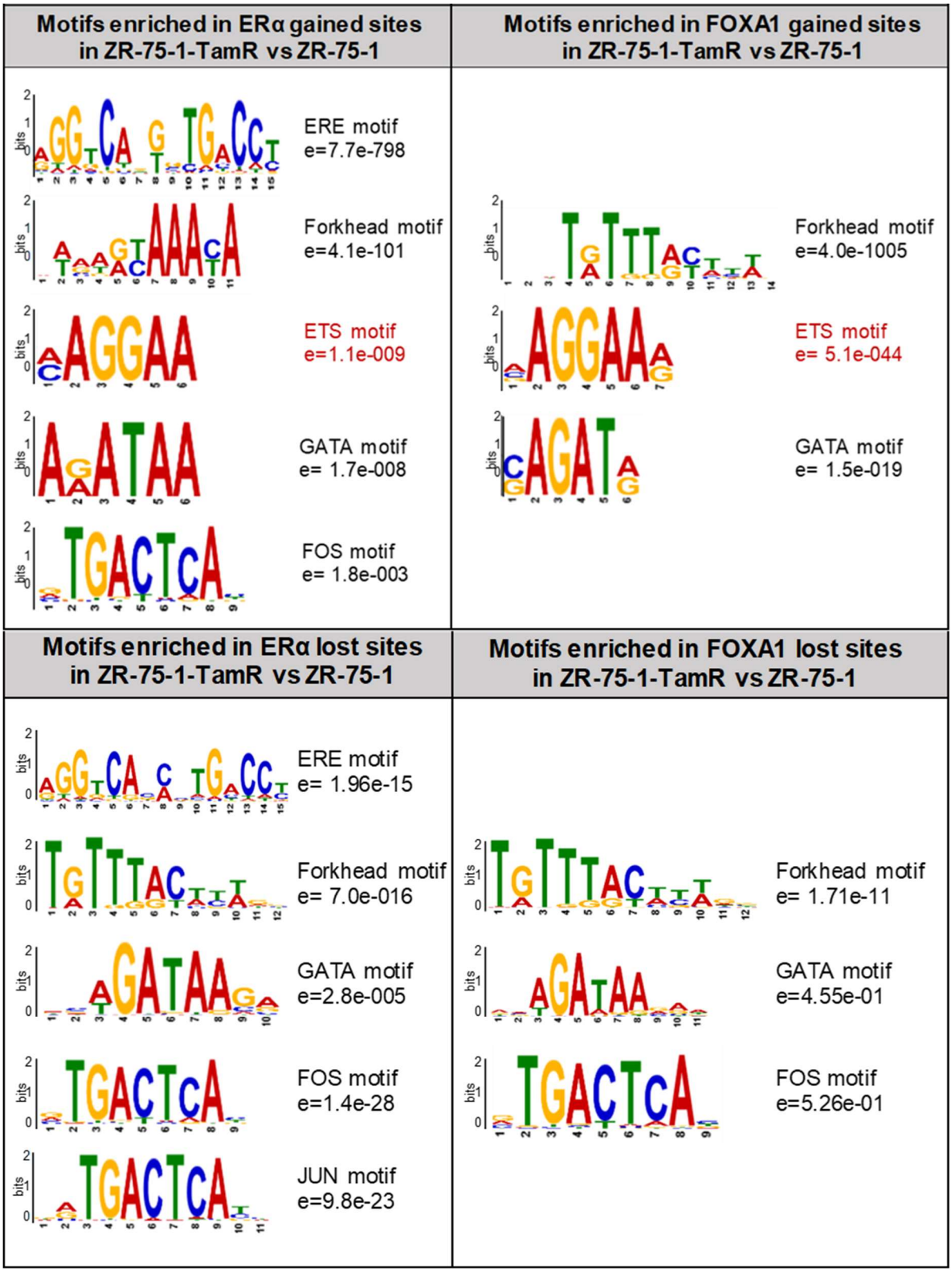

Figure 4.18. Motif analysis of ERα and FOXA1 gained and lost sites in ZR-75-1-TamR versus ZR-75-1; Enrichment analysis was performed using MEME tools; e value represents significance of the motif according to the discovery program reporting it.

Examples of ERα, FOXA1 and ETV6 co-bound regions that are gained in both MCF-7-TRF compared to MCF-7 and ZR-75-1-TamR compared to ZR-75-1 are illustrated in Figure 4.19.

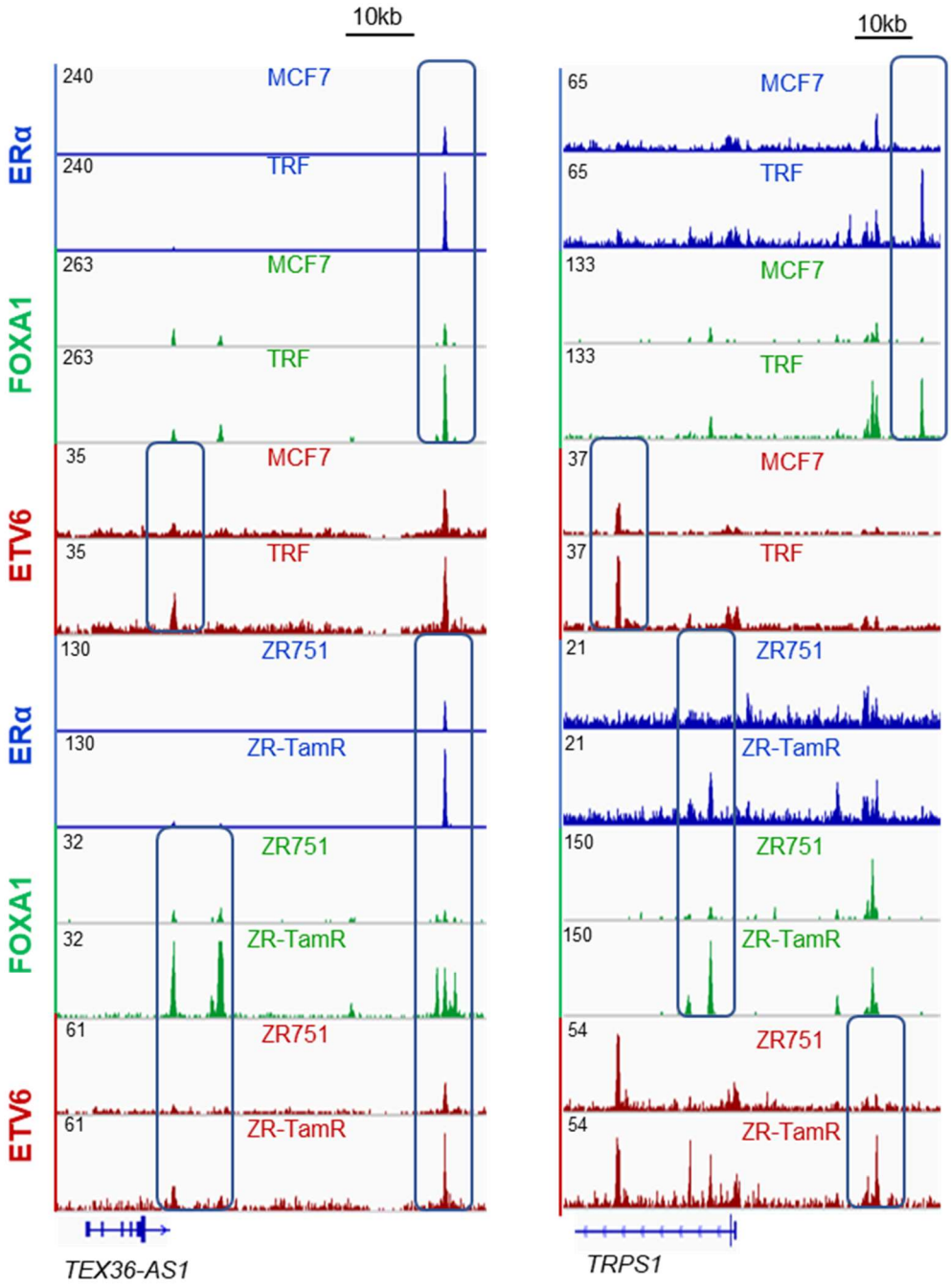

Figure 4.19. Examples of ERα, FOXA1 and ETV6 commonly gained sites in MCF-7-TRF compared to MCF-7 and ZR-75-1-TamR compared to ZR-75-1.

Further genome-wide analysis of the ETV6, ERα and FOXA1 differentially bound genomic regions associated with endocrine resistance revealed that the three transcription factors are re-distributed to the same novel sites in both MCF-7-TRF compared to MCF-7 and ZR-75-1-TamR compared to ZR-75-1 (Fig.4.20 and Fig.4.21). Importantly, there is enhancer reprogramming at the novel binding sites, as assessed by H3K27Ac (Fig.4.20.A and B and Fig.4.21.A and B).

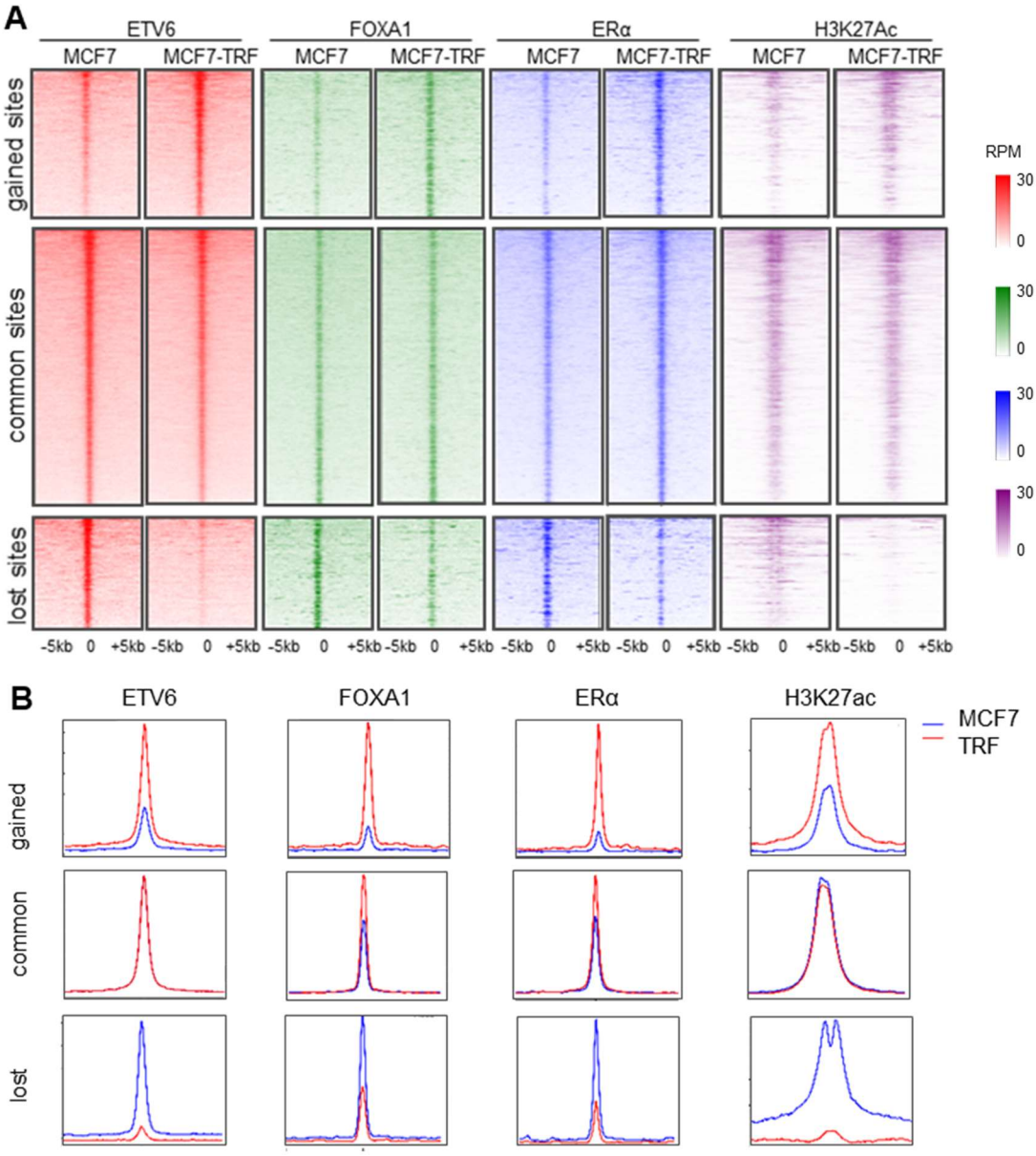

Figure 4.20. Endocrine resistance accompanies global ERα, FOXA1 and ETV6 reprogramming associated with enhancer redistribution in MCF-7-TRF versus MCF-7: (A) ChIP-seq tag densities visualised at ETV6, ERα, FOXA1 and H3K27Ac genomic locations in MCF-7-TRF vs MCF-7; heatmaps are scaled on ETV6 differentially bound sites; **(B)** Aggregate plots showing normalised signal enrichment of the four factors at gained, common and lost sites.

The regions with stronger H3K27Ac peaks in the Tamoxifen resistance cell lines compared to their sensitive counterparts corresponded to the ETV6, FOXA1 and ERα gained regions. Conversely, the genomic sites with weaker H3K27Ac peaks corresponded to regions where the three transcription factors had lost binding according to DiffBind analysis.

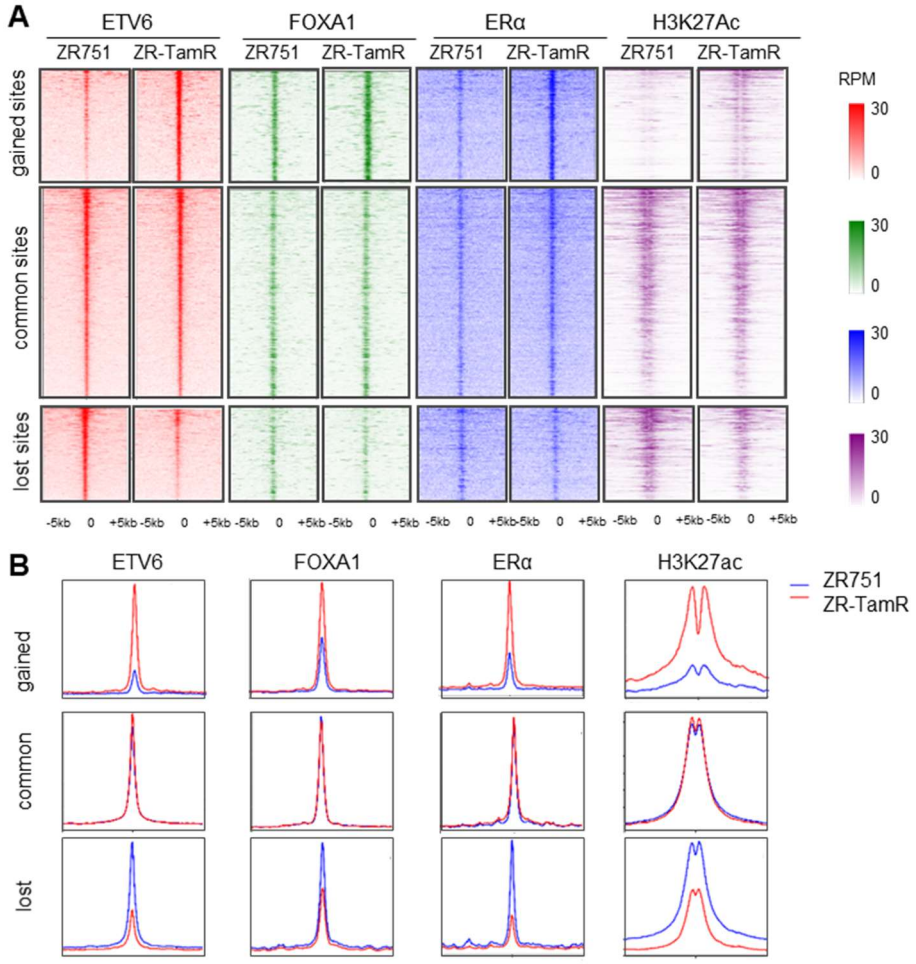

Figure 4.21. Endocrine resistance accompanies global ERα, FOXA1 and ETV6 reprogramming associated with enhancer redistribution in ZR-75-1-TamR versus ZR-75-1: (A) ChIP-seq tag densities visualised at ETV6, ERα, FOXA1 and H3K27Ac genomic locations in ZR-75-1-TamR versus ZR-75-1; heatmaps are scaled on ETV6 differentially bound sites; **(B)** Aggregate plots showing normalised signal enrichment of the four factors at gained, common and lost sites.

These results confirm that ERα positive breast cancer progression and endocrine resistance are driven by ERα, FOXA1 and ETV6 global reprogramming across multiple models which is accompanied by altered enhancer landscape.

4.3.6 ETV6-chromatin binding redistribution affects gene expression and correlates with Tamoxifen resistance signatures

RNA-seq was conducted to compare gene expression in MCF-7-TRF with MCF-7 and ZR-75-1-TamR with ZR-75-1 (Fig.4.22).

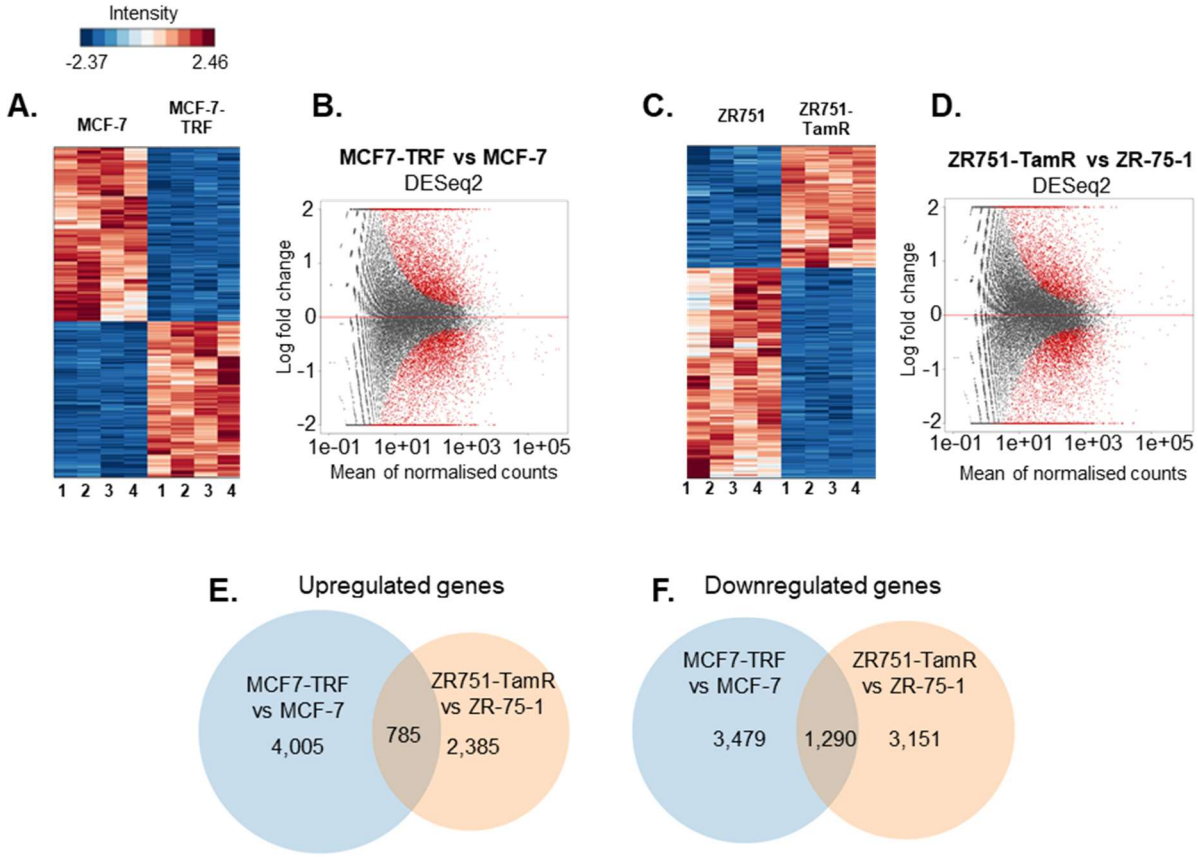

Figure 4.22. RNA-seq analysis for MCF-7-TRF compared to MCF-7 and ZR-75-1-TamR compared to ZR-75-1: four biological replicates were included for each cell line; **(A)** and **(C)** heatmaps illustrate genes that are up or downregulated in the resistant cell lines compared to their matched parental cells; relative expression (row Z scores) are plotted; **(B)** and **(D)** MA plots showing log2 fold change gene expression for MCF-7-TRF vs MCF-7 and ZR-75-1-TamR vs ZR-75-1, respectively; gene that are significantly repressed or activated in endocrine resistant compared to matched sensitive cell lines are represented in red (p value ≤ 0.05); **(E)** overlap between upregulated genes in MCF-7-TRF compared to MCF-7 and ZR-75-1-TamR compared to ZR-75-1 and downregulated genes **(F)**, respectively.

RNA-seq revealed there was a high number of repressed or activated genes in the endocrine resistant cell lines compared to the parental counterparts (Fig.4.22.A-D).

Specifically, differential expression analysis using DESeq2 resulted in 4,790 significantly upregulated genes in MCF-7-TRF compared to MCF-7 and 3,170 induced genes in ZR-75-1-TamR compared to ZR-75-1. Importantly, 785 genes were commonly activated in both pairs of cell lines (Fig.4.22.E). In addition, there were 4,769 and 4,441 repressed genes in MCF-7-TRF compared to MCF-7 and ZR-75-1-TamR compared to ZR-75-1, respectively, of which 1290 were commonly downregulated (Fig.4.22.F).

Further integrative ChIP-seq and RNA-seq analysis was conducted (Fig.4.23 and Fig. 4.24), focusing on the ETV6 differentially bound genomic regions as assessed using DiffBind (Chapter 4.3.5.). It was revealed that genes in close proximity to ETV6 ChIP-seq gained sites tend to be upregulated in both MCF-7-TRF versus MCF-7 and ZR-75-1-TamR versus ZR-75-1 (Fig.4.23.A and Fig.4.24.A). Conversely, genes in close proximity to ETV6 ChIP-seq lost sites tend to be repressed in endocrine resistant compared to sensitive context (Fig.4.23.B and Fig.4.24.B).

Moreover, higher percentage of ETV6 gained chromatin interactions in MCF-7-TRF compared to MCF-7 and ZR-75-1-TamR compared to ZR-75-1 were located closer to the upregulated genes rather than downregulated genes (Fig.4.23.C and Fig.4.24.C). In addition, a higher percentage of ETV6 gained sites were situated at significant distances from the transcription start sites of upregulated genes. These findings imply that ETV6 reprogrammed binding sites upregulate target genes from distal enhancer regions in endocrine resistance.

Furthermore, the ETV6 lost sites in MCF-7-TRF compared to MCF-7 and ZR-75-1-TamR compared to ZR-75-1 were located closer to the repressed genes rather than activated genes (Fig.4.23.D and Fig.4.24.D).

Taken together, the data suggests that ETV6 differential chromatin interactions between endocrine resistant and sensitive breast cancer models affect the transcriptome and therefore may contribute to the more aggressive phenotype associated with resistance.

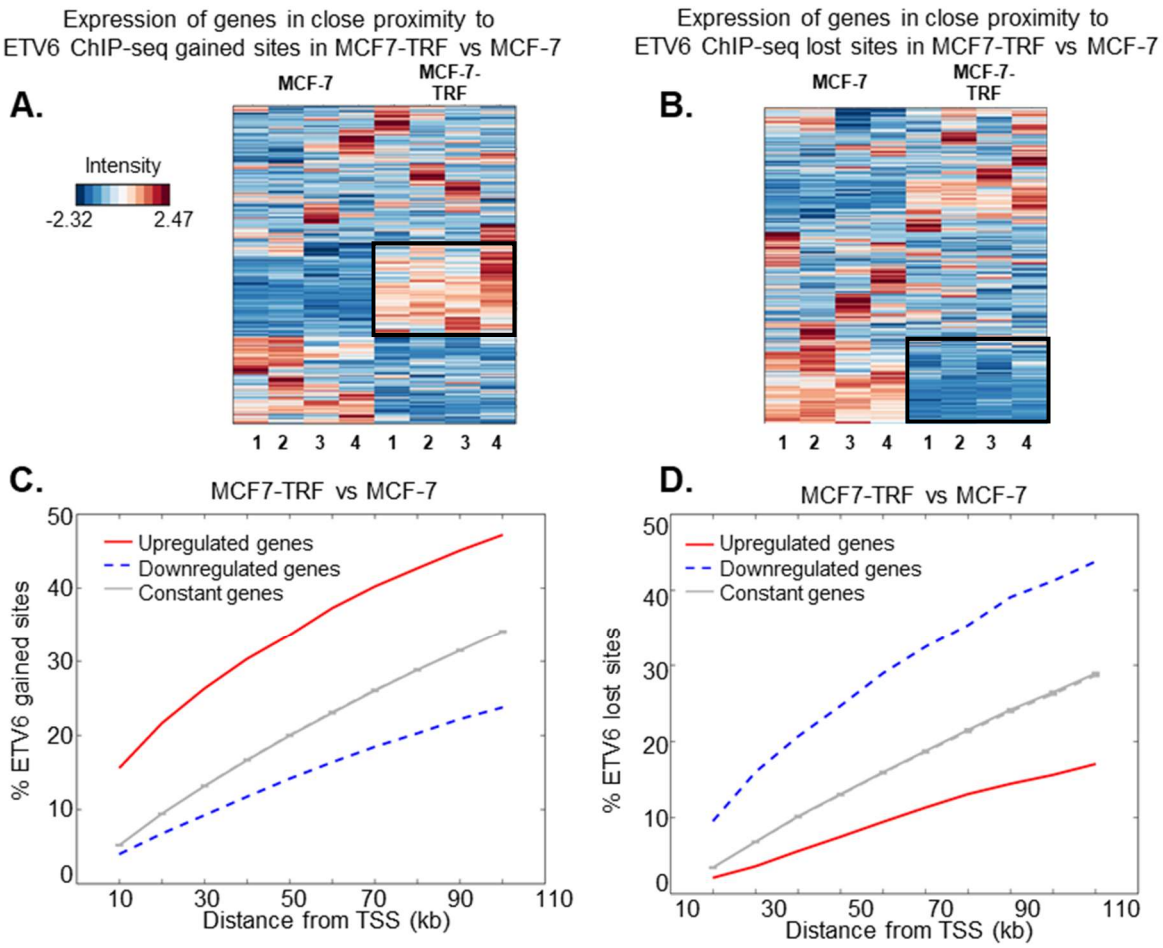

Figure 4.23. Integrative ChIP-seq and RNA-seq analysis of the expression of genes in close proximity to ETV6 differentially bound genomic regions in MCF-7-TRF compared to MCF-7: RNA-seq heatmaps illustrate expression of genes in close proximity to ETV6 ChIP-seq gained **(A)** and lost sites **(B)**, as assessed by DiffBind in Table 4.2; **(C)** and **(D)** graphs show cumulative fraction of ETV6 gained **(C)** or lost **(D)** sites within up to 100 kb of the TSS of three groups of genes: significantly upregulated genes with p value ≤ 0.05, (red line), significantly downregulated genes with p value ≤ 0.05 (blue) and genes that do not change significantly in MCF-7-TRF vs MCF-7 according to RNA-seq, called constant genes (grey).

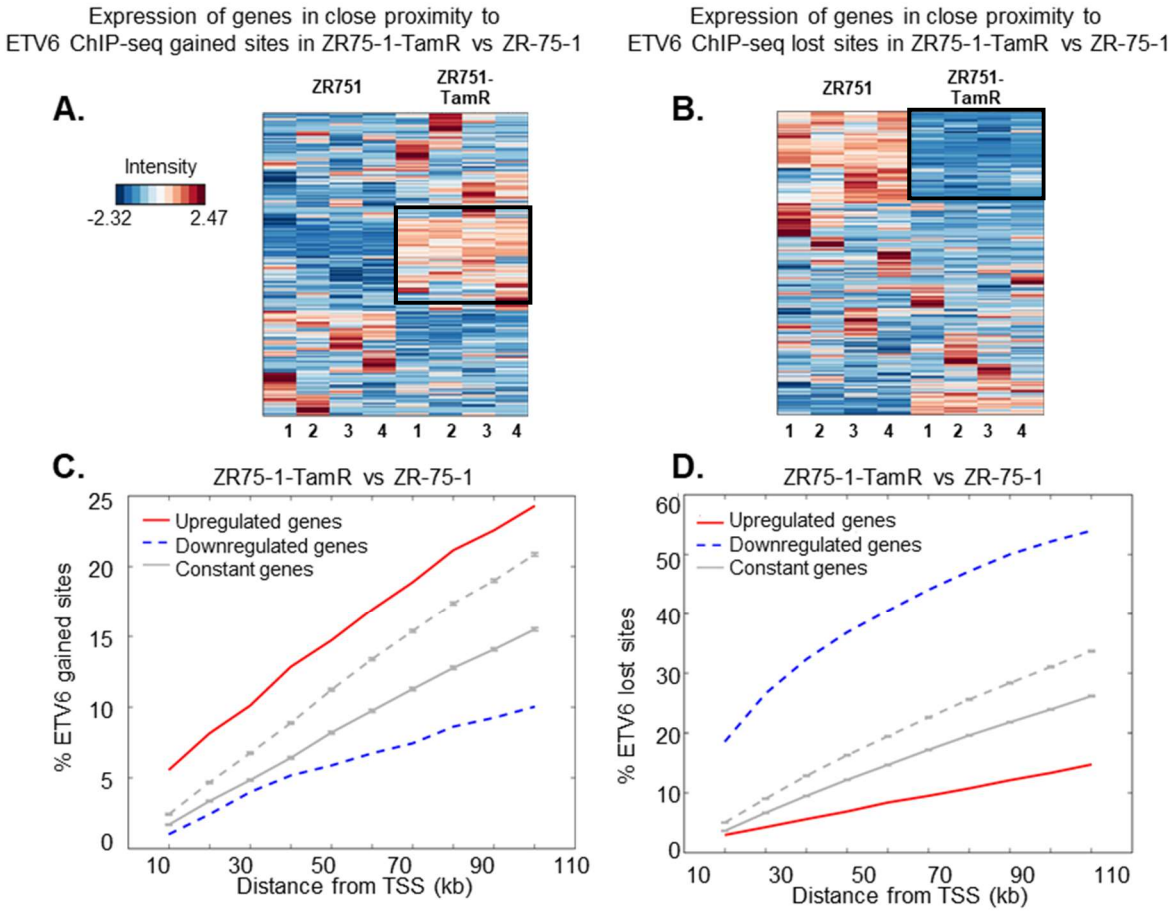

Figure 4.24. Integrative ChIP-seq and RNA-seq analysis focused on the expression of genes in close proximity to ETV6 differentially bound genomic regions in ZR-75-1-TamR compared to ZR-75-1: RNA-seq heatmaps illustrate expression of genes in close proximity to ETV6 ChIP-seq gained **(A.)** and lost sites **(B.)**, as assessed by DiffBind; **C.** and **D.** graphs show cumulative fraction of ETV6 gained **(C.)** or lost **(D.)** sites within up to 100 kb of the TSS of three groups of genes: significantly upregulated genes with p value ≤ 0.05, (red line), significantly downregulated genes with p value ≤ 0.05 (blue) and genes that do not change significantly in MCF-7-TRF vs MCF-7 according to RNA-seq, called constant genes (grey). The dotted lines indicate analysis performed on matched number of downregulated and constant genes, while the solid lines indicate analysis conducted for matched upregulated and constant genes.

Genomic Regions Enrichment of Annotations Tool (GREAT) (McLean et al., 2010) was then used to interpret the functions of genes in close proximity to ETV6 gained sites in the two pairs of cell lines (Fig.4.25.) As demonstrated in Figures 4.20 and 4.21, the ETV6 gained regions are also gained by ERα, FOXA1 and H3K27Ac, making the assessment of ETV6 reprogrammed regions relevant for the global transcription factor redistribution associated with endocrine resistance.

ETV6 gained sites in both MCF-7-TRF compared to MCF-7 and ZR-75-1-TamR compared to ZR-75-1 were highly enriched for the signatures of the genes upregulated in Tamoxifen resistance as assessed by *Massarweh et al* (Massarweh et al., 2008). In addition, in MCF-7-TRF versus to MCF-7, the ETV6 gained sites were also enriched for the Creighton endocrine resistance group 3 signature, which corresponds to upregulated genes in Tamoxifen resistant PDXs (Creighton et al., 2008).

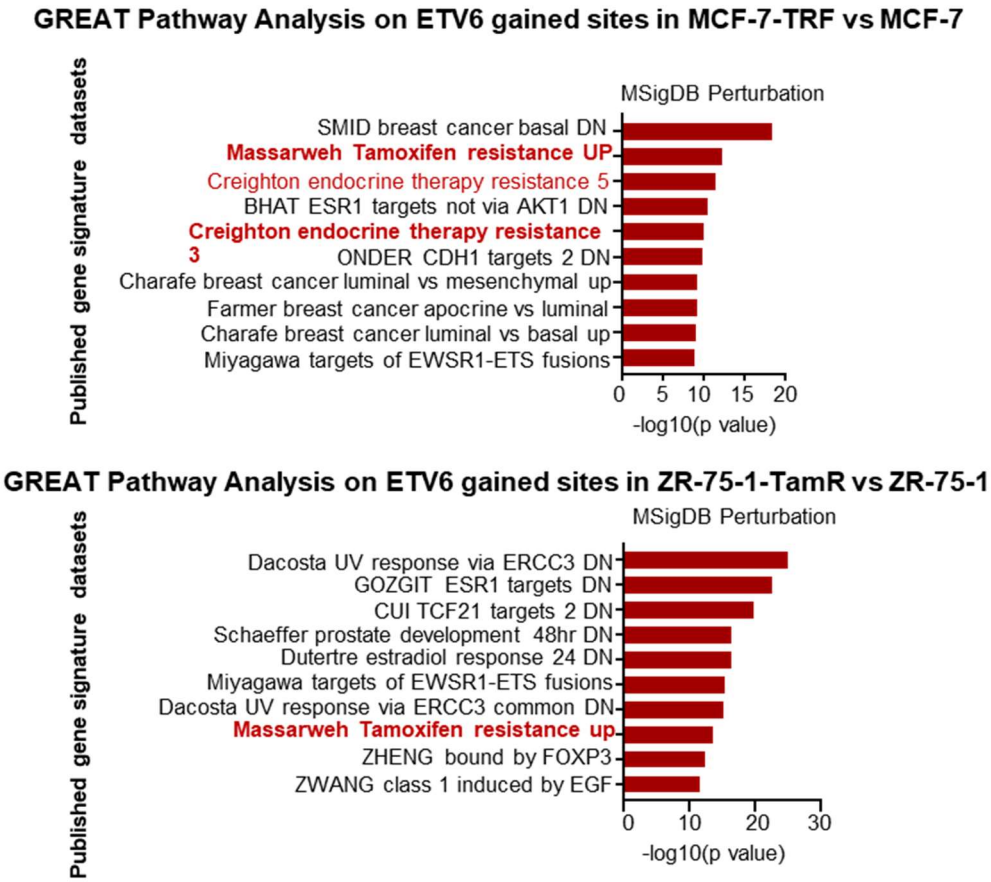

Figure 4.25. GREAT analyses of the annotations of nearby genes of gained ETV6 sites in MCF-7-TRF vs MCF-7 and ZR-75-1-TamR vs ZR-75-1: the top ten enriched Gene Ontology (GO) annotations are shown.

These results demonstrate that ETV6 gained sites tend to regulate genes associated with Tamoxifen resistance, basal cell determination and EMT/metastatic phenotype.

4.3.7 Inhibition of MAPK pathway reduces breast cancer progression and modulates ETV6-chromatin interactions

The results obtained indicate that ETV6 contributes to cancer progression and endocrine resistance and that ETV6 silencing results in a significant inhibitory effect of cell viability and growth (Fig.4.10 and Fig.4.11).

In addition, it is known that constitutively activated MAPK stabilises other ETS family members (e.g. ETV1) in gastrointestinal stromal tumours (Chi et al., 2010). This raises the possibility that ETV6 may also be regulated by MEK/ERK pathway in breast cancer and that inhibition of MAPK pathway may therefore be beneficial for endocrine resistant breast cancer.

To test this hypothesis, the MEK inhibitor Trametinib was used on MCF-7-TRF and ZR-75-1-TamR. Cells were treated with either with 500nM of the compound *(Tram)* or with vehicle *(Veh)* (Fig.4.26).

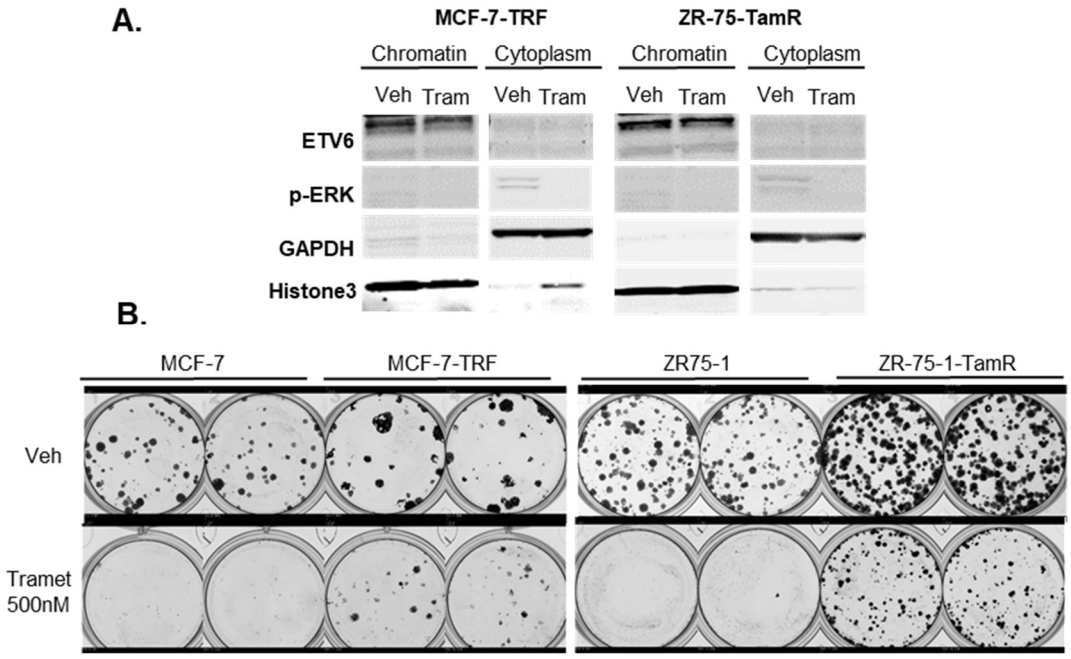

Figure 4.26. Trametinib effects on ETV6 total chromatin levels (A) and on colony formation ability for MCF-7, MCF-7-TRF, ZR-75-1 and ZR-75-1-TamR (B).

Samples were collected after 24 hours of treatment for chromatin and cytoplasmic fractionation and subjected to western blot analysis. The compound efficiency was validated by the depletion of phospho-ERK from the cytoplasm in Trametinib treated samples compared to vehicle (Fig.4.26.A). In addition, MAPK inhibition seemed to

reduce ETV6 global chromatin levels in both MCF-7-TRF and ZR-75-1-TamR (Fig.4.26.A).

Furthermore, colony formation assays were conducted in the four cell lines, over a time frame of 14 days. It was seen that Trametinib reduced the colony formation ability even for MCF-7-TRF and ZR-75-1-TamR cell lines that no longer respond to endocrine therapies (Fig.4.26.B).

Taking these results into account, the effects of Trametinib on ETV6-chormatin interactions were assessed (Fig.4.27 and Table 4.3). Cells were treated for six hours either with the MEK inhibitor *(Tramet)* or wih vehicle *(Veh).*

In MCF-7-TRF, differential binding analysis identified a general trend towards lost ETV6 binding after Trametinib treatment, with 112 sites being significantly lost (Figure 4.27.A and B and Table 4.3).

Importantly, there were 5513 lost regions in ZR-75-1-TamR treated with Trametinib compared to vehicle and just 1 gained region (Fig.4.27.C and D and Table 4.3).

ETV6 differential binding comparison			
Contrast	**lost**	**gained**	**common**
MCF-7-TRF Tramet vs Veh	112	0	8677
ZR-75-1-TamR Tramet vs Veh	5513	1	10806

Table 4.3. ETV6 Differential binding analysis for MCF-7-TRF and ZR-75-1-TamR cell lines treated with Trametinib (*Tramet*) compared to Vehicle (*Veh*).

Examples of ETV6 lost sites in both MCF-7-TRF Trametinib compared to vehicle and ZR-75-1-TamR Trametinib treated compared to vehicle are provided in Fig.4.27.E).

Taken together, these results show that MAPK pathway inhibition reduces colony formation ability of ERα breast cancer models, including those that are resistant to endocrine targeted therapies. Trametinib also modulates ETV6-chromatin binding events.

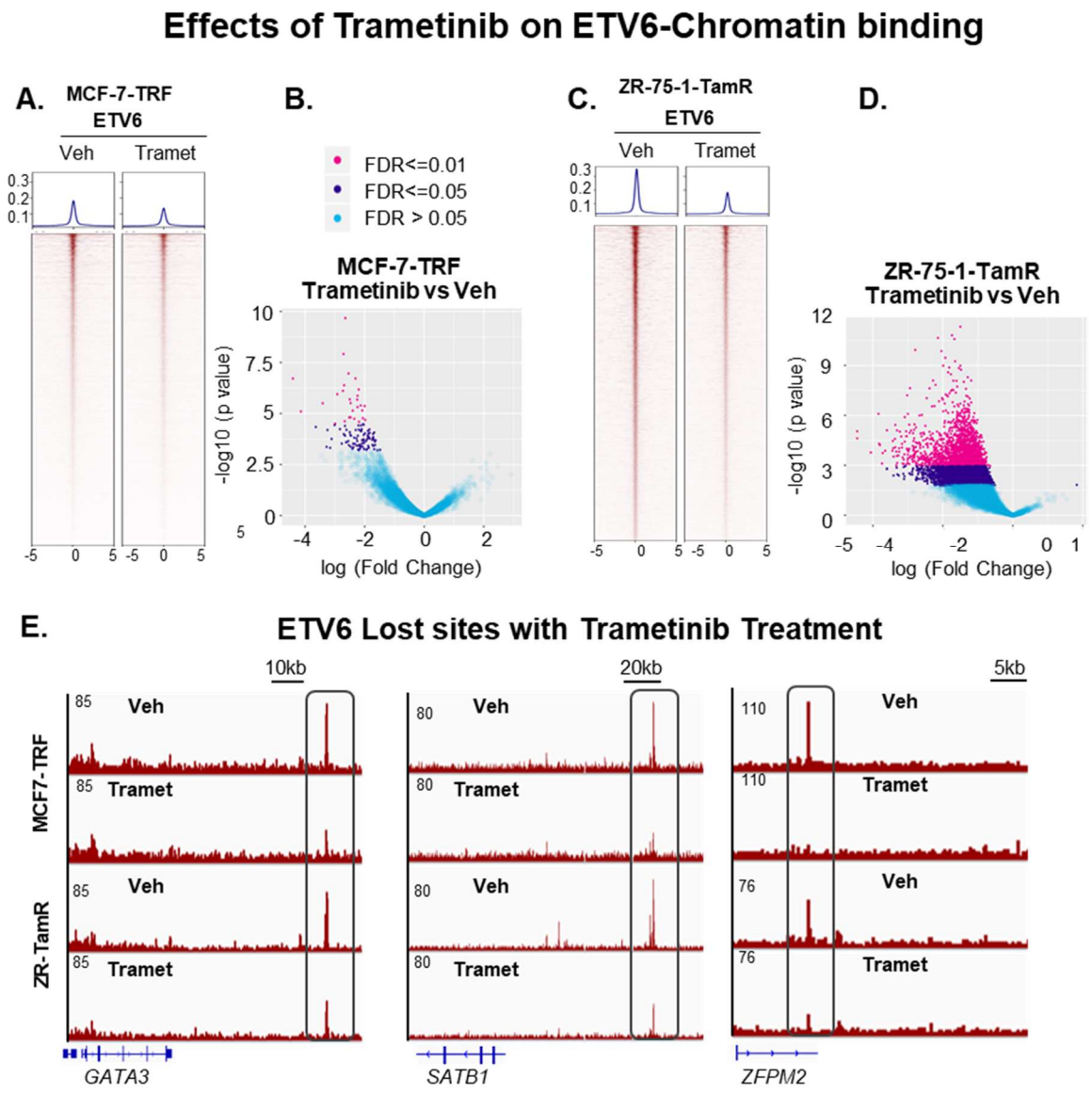

Figure 4.27. Trametinib effects on ETV6-chromatin interactions: all ChIP-seq experiments were performed in biological triplicates; ChIP-seq tag densities visualised at ETV6 binding sites for MCF-7-TRF **(A.)** or ZR-75-1-TamR **(C.)** treated with Trametinib for six hours or with vehicle (Ctrl); heatmaps are scaled on ETV6 binding in vehicle condition for each cell line investigated; Volcano plots show log2 fold change for ETV6 binding sites in MCF-7-TRF **(B.)** or ZR-75-1-TamR **(D.)** for Trametinib treatment compared to vehicle; **(E.)** Examples of ETV6 peaks that are lost with Trametinib treatment in both MCF-7-TRF and ZR-75-1.

4.3.8 ERα, FOXA1 and ETV6 cooperate to drive endocrine resistance *in vivo*

To further examine whether ERα, FOXA1 and ETV6 cooperate to drive endocrine resistance *in vivo*, ERα Luminal B endocrine resistant patient-derived xenograft samples (PDXs) were used for ChIP-seq experiments. First, immunohistochemistry was conducted to determine the positivity for the three investigated proteins (Fig.4.28).

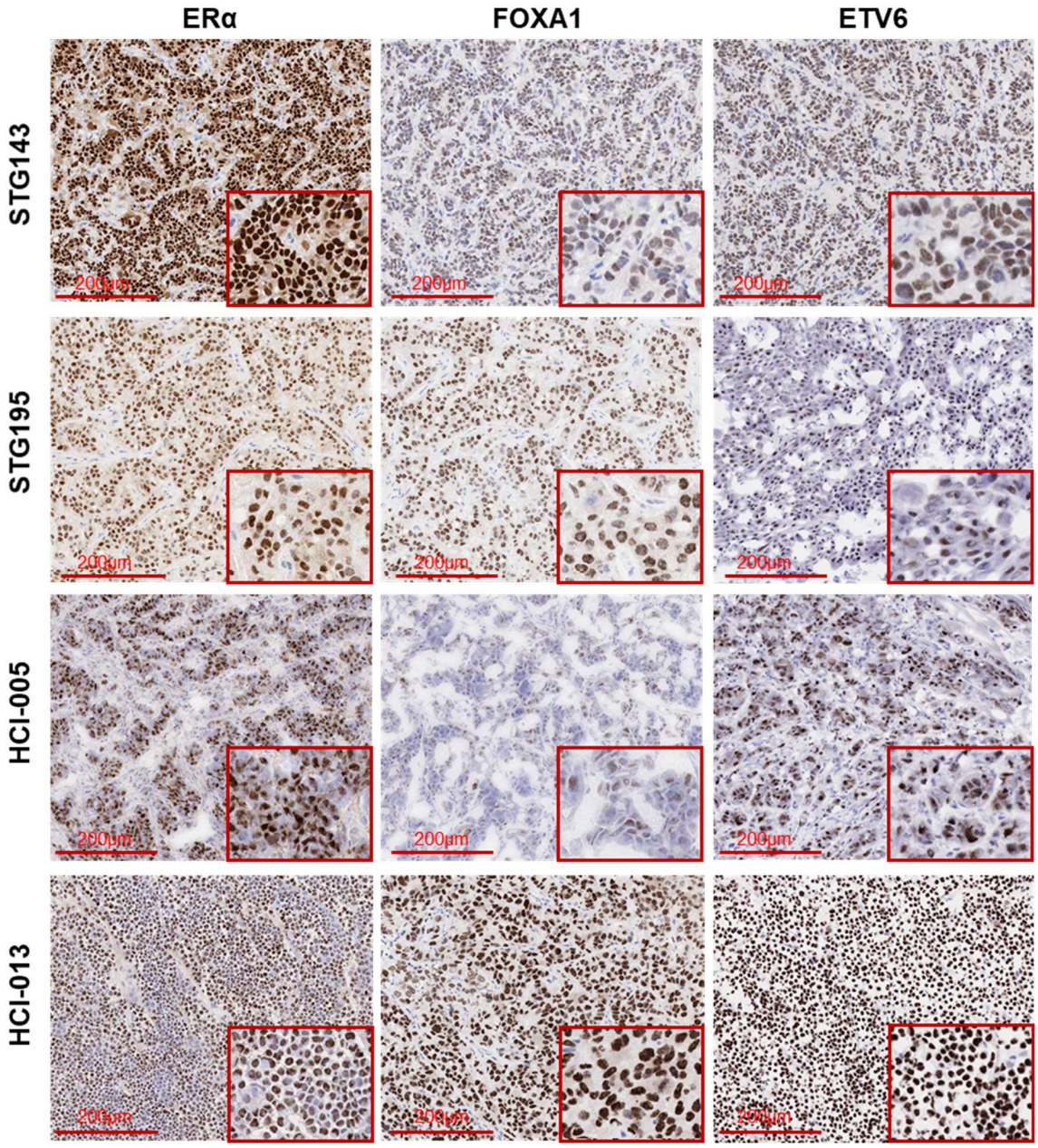

Figure 4.28. IHC assessment of ERα, FOXA1 and ETV6 protein levels in Luminal B endocrine resistant PDX models.

ERα, FOXA1 and ETV6 immunohistochemistry has identified STG143, STG195, HC-005 and HCI-013 PDXs to express different levels of the three proteins.

Therefore, these models were used for ChIP-seq experiments. The total number of peaks identified for each factor in every PDX model is provided in Table 4.4.

For HCI-013, there were 51,704 FOXA1 binding sites, 68,172 peaks for ERα and 129,673 peaks for ETV6. In addition, ChIP-seq for STG143 resulted in 59,136 binding FOXA1 binding sites, 28,500 peaks for ERα and 14,092 ETV6 sites. For STG195, 103,926 FOXA1 peaks were identified, 22,773 ERα peaks and 2,837 ETV6 peaks, respectively. For HCI-005 PDX model, 16,901 FOXA1-chromatin interactions were found, as well as 7,687 ERα and 7,969 ETV6 peaks.

The variability between number of peaks for the same factor in different PDXs may be caused by the biological difference in protein levels, as visualised with IHC. Nonetheless, all ChIP-seq experiments conducted resulted in high peak numbers and the results were further assessed to gain insight into the molecular mechanisms of endocrine resistance *in vivo*.

PDX	Factor	total no of peaks
HCI-013	FOXA1	51,704
	ERα	68,172
	ETV6	129,673
STG143	FOXA1	59,136
	ERα	28,500
	ETV6	14,092
STG195	FOXA1	103,926
	ERα	22,773
	ETV6	2,837
HCI-005	FOXA1	16,901
	ERα	7,687
	ETV6	7,969

Table 4.4. Total number of peaks called for ERα, FOXA1 and ETV6 in PDX models: peaks were called using MACS in narrow mode; the numbers shown represent peaks found to be significantly enriched at a q-value of 0.05 for each sample against their matched input.

ETV6, FOXA1 and ERα binding sites were overlapped for each PDX model (Fig.4.29). There were 11,490 regions co-bound by the three factors in HCI-013, 5,091 co-bound regions in STG143 and 885 and 340 co-bound sites in STG195 and HCI-005 respectively.

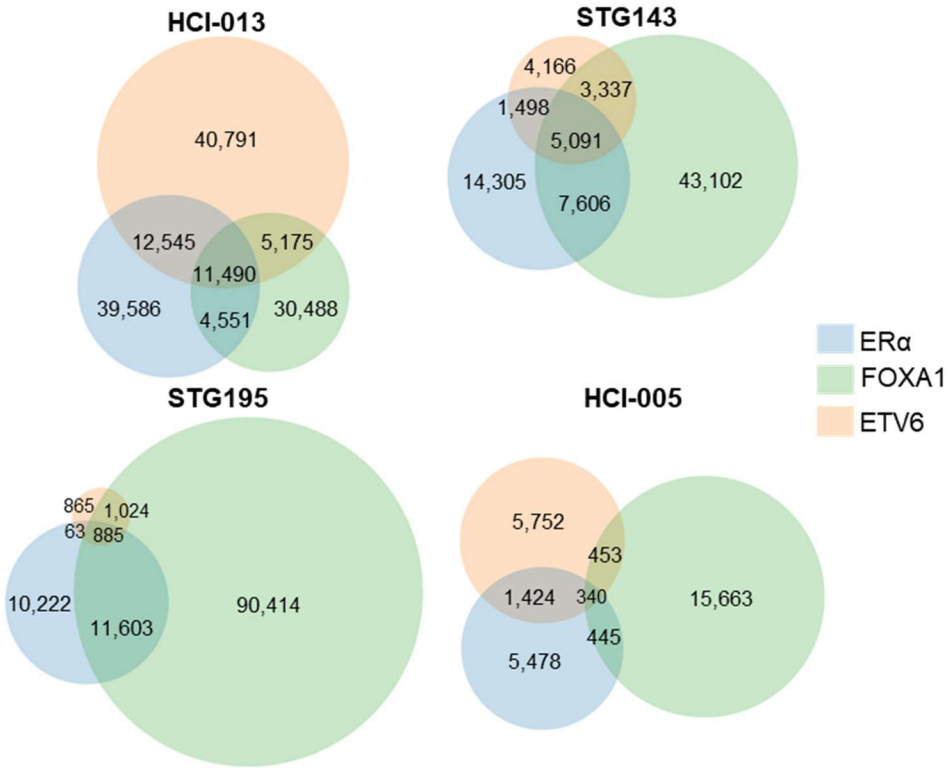

Figure 4.29. Overlap of ETV6, FOXA1 and ERα binding sites in endocrine resistant PDX models.

Furthermore, it was assessed whether the ERα gained chromatin interactions identified in both MCF-7-TRF compared to MCF-7 and ZR-75-1-TamR compared to ZR-75-1 were also present in the endocrine resistant PDX models (Fig 4.30).

For all four HCI-013, STG143, STG195 and HCI-005 PDX models, there was a high overlap between the binding of the three transcription factors and the gained sites associated with endocrine resistance in the *in vitro* models (Fig.4.30.A). *RARα* is provided as an example of a common genomic region bound across all models, while *TRPS1* and *TEX36-ASI* are examples of genes in close proximity to peaks that are gained in the two resistant cell lines compared to their sensitive counterpart (Fig.4.19) and also present in the endocrine resistant models PDX models (Fig.4.30).

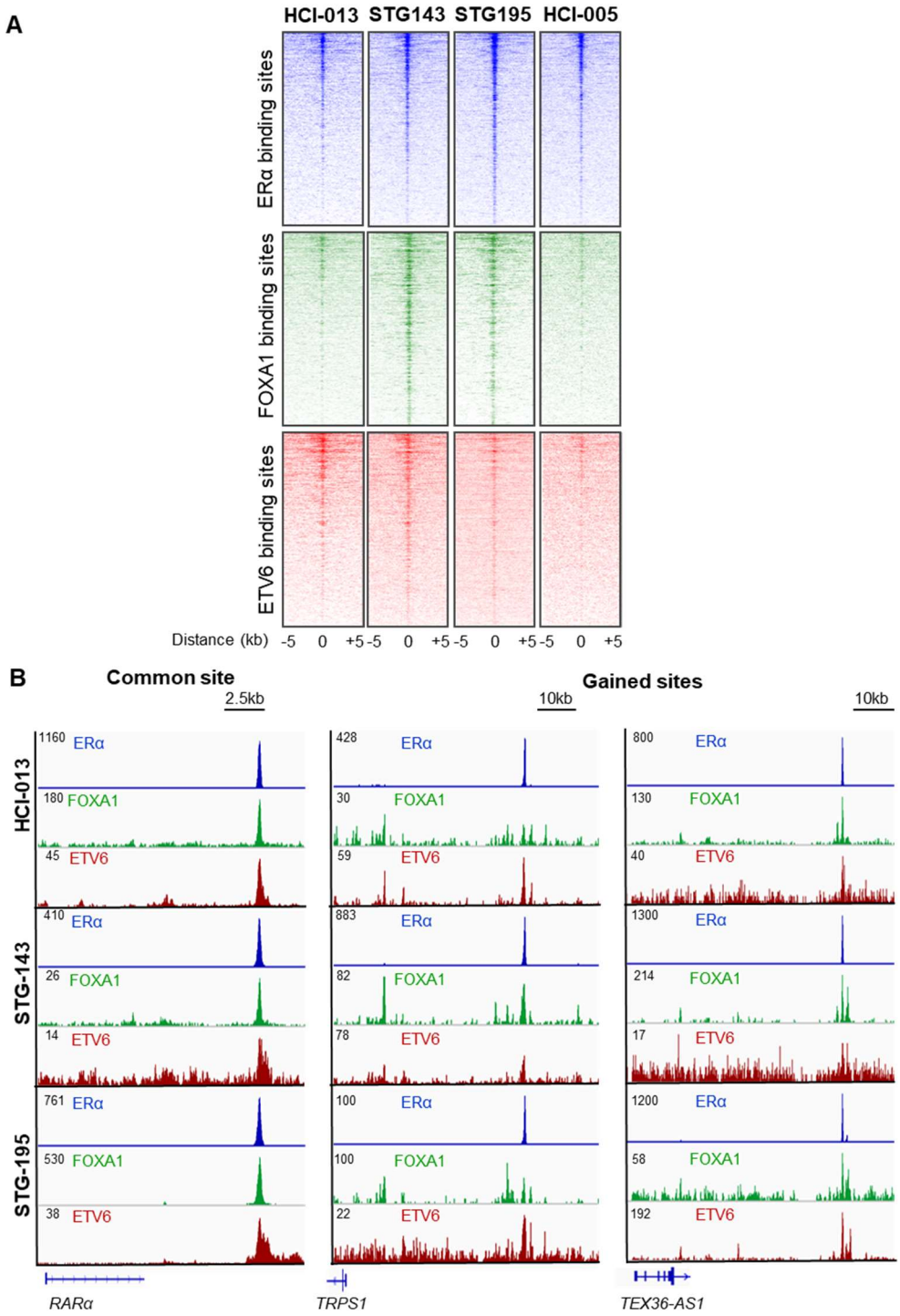

Figure 4.30. Assessment of ETV6, ERα and FOXA1-chromatin interactions in endocrine resistant PDX models: (A) ChIP-seq tag densities visualised at ETV6, ERα and FOXA1 genomic locations in HCI-013, STG143, STG195 and HCI-005; heatmaps are scaled on the ERα gained sites from both MCF-7-TRF versus MCF-7 and ZR-75-1-TamR versus ZR-75-1; **(B)** Examples of ERα, FOXA1 and ETV6 peaks present in the endocrine resistant PDXs and either common across all cell lines (*RARα*) or gained in both Tamoxifen resistant cell lines compared to the parental counterparts (*TRPS1* and *TEX36-ASI)*.

Taken together, one can conclude that there is a cooperative redistribution of ERα, FOXA1 and ETV6 associated with breast cancer progression and endocrine resistance both *in vitro* and *in vivo* models.

4.3.9 ETV6 copy number amplifications are associated with significantly reduced disease-free survival in ERα positive Luminal B breast cancer

The amplification of the genomic region encompassing ETV6 was assessed in the METABRIC cohort (Curtis et al., 2012). This analysis revealed that ETV6 copy number amplifications are specifically associated with significantly reduced disease-free survival in ERα positive Luminal B breast cancer (p value < 0.001) (Fig.4.31). Luminal B subtype is a more aggressive form of breast cancer, more likely to metastasise.

This observation confirms ETV6's role in the development of a more aggressive phenotype in ERα breast cancer. Further validation of this finding would require assessment of ETV6 copy number amplifications and gene expression levels in matched metastatic and primary breast cancer samples.

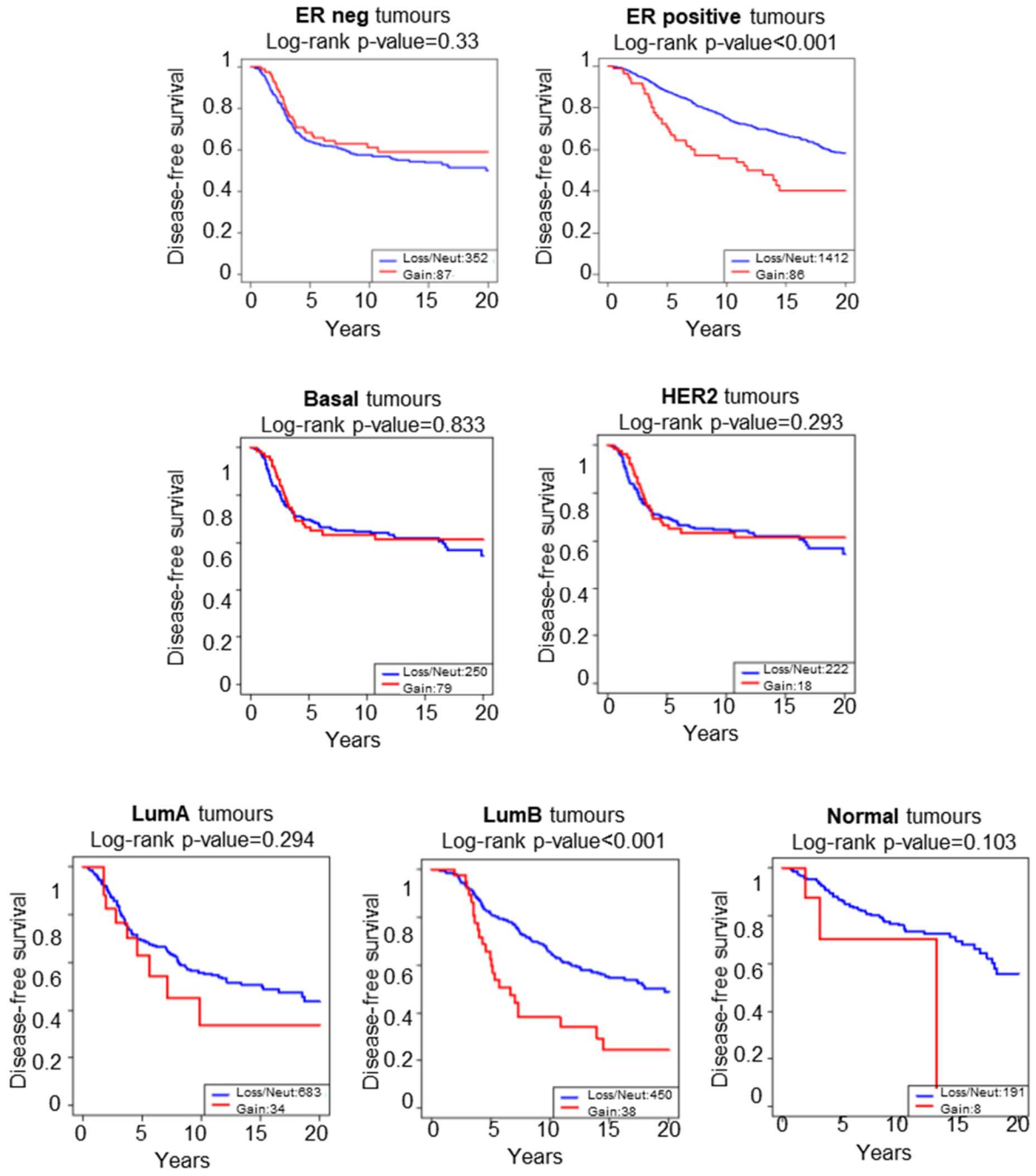

Figure 4.31. Assessment of ETV6 copy number amplifications (CNA) in the METABRIC cohort: Kaplan Meier plots were generated to assess disease-free survival (DSF); ETV6 CNA are associated with significantly reduced DSF in ERα positive breast cancer (p value < 0.001), in particular in Luminal B subtype (p value < 0.001).

4.4 Discussion

ERα is the driving transcription factor in more than three quarters of all breast cancer cases. Its transcriptional activity promotes cell growth and proliferation (Musgrove and Sutherland, 2009). Therefore, endocrine therapies such as selective estrogen receptor modulators (e.g. Tamoxifen) or estrogen-receptor degraders (e.g. Fulvestrant - ICI) have significantly prolonged patients' disease-free survival (Jensen and Jordan, 2003).

More recently developed targeted therapies - inhibitors of cyclin D–CDK4/6-Retinoblastoma pathway such as Palbociclib (Finn et al., 2015), or inhibitors of the AKT/mTOR signalling pathway such as the mTOR inhibitor Everolimus (Yardley et al., 2013) - have further improved patient outcome.

However, there are subsets of patients that do not respond to any of the currently available therapeutic strategies, which suggests there are alternative endocrine resistance mechanisms that still need to be discovered and targeted for the overall improvement of breast cancer survival rates.

FOXA1 is another key protein in ERα positive breast cancer. It acts as a transcription factor, binds to compacted chromatin and opens it up for ERα subsequent binding (Glont et al., 2019, Hurtado et al., 2011). Moreover, endocrine resistance is associated with ERα –chromatin binding reprogramming dictated by FOXA1, that results in altered transcriptional program (Ross-Innes et al., 2012).

ERα and FOXA1 co-factors are of particular importance. They work in a cooperative or competitive manner and alterations in their levels can contribute to breast cancer progression and can influence endocrine response.

In this context, the work presented in this chapter explored novel molecular mechanisms of endocrine resistance in ERα positive breast cancer. ETV6 was identified as a novel FOXA1/ERα interactor enriched in endocrine resistant compared to sensitive breast cancer models. As ETV6 mediates cell differentiation and growth (Findlay et al., 2013), its enrichment renders it as an onco-driver in breast cancer. The direct role of ETV6 in breast cancer progression associated with endocrine resistance was further validated. ETV6 overexpression in MCF-7 and ZR-75-1 promoted their

growth and colony formation ability compared to control cells (Fig.4.12). Further work to investigate the effects of ETV6 overexpression *in vivo* would reinforce this finding.

In addition, silencing ETV6 had an inhibitory effect on cell growth and viability in Tamoxifen sensitive, as well as resistant cells. This suggests that targeting ETV6 may be beneficial even for the endocrine refractory breast cancer patients (Fig. 4.10 and Fig. 4.11).

Genome-wide analysis of ETV6, ERα and FOXA1 chromatin interactions revealed that all three transcription factors are re-distributed to the same novel regions in endocrine resistance (Fig.4.20 and Fig.4.21). These results suggest the three transcription factors work collaboratively in endocrine refractory phenotype in multiple breast cancer models.

Importantly, the gained ETV6, ERα and FOXA1 regions also presented stronger H3K27Ac signal, implying these novel binding sites are active for transcription. Conversely, the ETV6, ERα and FOXA1 lost sites in endocrine resistant compared to sensitive models presented weaker H3K27Ac peaks, implying these enhancer regions are no longer active for transcription. This suggests that ETV6, ERα and FOXA1 may cooperatively associate with acetyltransferases (HATs) (e.g. CBP, p300) which in turn acetylate histone H3 at lysine 27. Further genome-wide analyses of p300 and CBP would consolidate this hypothesis.

Indeed, RNA-seq analysis confirmed that ETV6 gained sites in MCF-7-TRF compared to MCF-7 and in ZR-75-1-TamR compared to ZR-75-1 tended to upregulate target genes, while the ETV6 lost sites repressed genes in both Tamoxifen resistant cell lines compared to their matched parental cells (Fig. 4.23 and Fig.4.24).

Furthermore, GREAT analysis of the ETV6 gained sites revealed that they tend to be enriched for the signatures of upregulated genes in Tamoxifen resistance as assessed by *Massarweh et al* (Massarweh et al., 2008) and by *Creighton et al* (Creighton et al., 2008) (Fig.4.25).

In addition, previous studies have identified that ETS transcription factors are regulated by MAPK pathway (Chi et al., 2010). Therefore, the effects of MEK inhibitor Trametinib on endocrine sensitive and resistant models were assessed. It was found that inhibition of MAPK pathway reduced colony formation ability of endocrine resistant models (Fig.4.26) and modulated ETV6-chromatin interactions (Fig.4.27). This effect

might be a consequence of ETV6 translocation from the nucleus to the cytoplasm when MAPK pathway is inhibited, resulting in ETV6 loss of binding to its target genomic regions.

Further assessment of the enhancer landscape, as well as gene expression analysis of Trametinib effects on MCF-7-TRF and ZR-75-1-TamR would shed more light on these matters.

Of importance, ETV6 copy number amplifications were assessed in the METABRIC cohort (Curtis et al., 2012) (Fig.4.31). They were found to be associated with significantly reduced disease-free survival in ERα positive Luminal B breast cancer, which is the more aggressive subtype of cancer, more likely to metastasise.

Taken together, the work in this chapter describes ETV6 as a novel interactor of ERα and FOXA1 that contributes to breast cancer progression and endocrine refractory phenotype.

For the work in this chapter, proteomics analysis was performed by the Proteomics Core Facility (CRUK-CI) with further bioinformatic analysis conducted by Dr Kamal Kishore (CRUK-CI). Sequencing was performed by the Genomics Core Facility and further bioinformatics analysis was conducted by Dr Sankari Nagarajan, Dr Igor Chernukhin and Dr Ashley Sawle (CRUK-CI).

Chapter 5. Repurposing of FDA-Approved Drugs for Endocrine Resistant ERα Breast Cancer

5.1 Introduction

To date, it is known that steroid hormone estrogen is pivotal to the normal development of the female reproductive system, through its effects on cell proliferation and cell survival (Musgrove and Sutherland, 2009). Most of estrogen-induced effects are mediated by the nuclear receptor ERα and deregulations of ERα trigger abnormal cell growth. Consequently, ERα is the driving factor in approximately 70% of all breast cancers. Extensive efforts have been invested into the development of efficient endocrine treatments for these patients. The selective estrogen receptor modulator (SERM) Tamoxifen was the first endocrine therapy developed (Jensen and Jordan, 2003). It remains the most widely used agent in pre-menopausal women and continues to be used for post-menopausal patients too (Davies et al., 2011).

However, subtypes of breast cancer cases have intrinsic resistance to Tamoxifen. Some patients lack ERα expression, while others carry inactive alleles of cytochrome p450 2d6 (CYP2D6) therefore being unable to convert tamoxifen to its active metabolites (Hoskins et al., 2009).

In addition, a third of the patients treated with Tamoxifen for 5 years acquire resistance and relapse within 15 years (Davies et al., 2011). Acquired resistance happens through multiple mechanisms including, but not limited to changes in ERα levels and activity, changes in its protein interactors, cross-talk with Receptor tyrosine kinase signalling pathways or dysregulation of cellular proliferation.

The main ERα alterations linked to endocrine resistance are loss of its expression that occurs in 15–20% of cases and *ESR1* mutations that occur in 1% of cases (Clarke et al., 2003, Gutierrez et al., 2005). Post-translational modifications of ERα, also affect its function. In particular, its phosphorylation results in ligand-independent ERα activation and increased interaction with its co-factors (Bostner et al., 2013)

ERα transcriptional activity is also influenced by its interaction with other proteins. As such, enhanced interaction between ERα and PBX1 pioneer transcription factor is associated with a more aggressive tumour phenotype (Magnani et al., 2011). In addition, increased levels of co-activator proteins such as AIB1 (Kressler et al., 2007, Webb et al., 1998) and decreased expression of co-repressors such as NCOR1 also predict poor response to Tamoxifen (Lavinsky et al., 1998).

The crosstalk between ERα and tyrosine kinase signalling pathways is evidenced by the reciprocal expression of ERα and epidermal growth factors (e.g. ERBB2, EGFR) (deGraffenried et al., 2004, Faridi et al., 2003). In turn, the overexpression of the epidermal growth factors activated the MAPK and PI3K/Akt/mTOR signalling pathways (Knowlden et al., 2005). On the one hand, this process leads to ERα activation through phosphorylation. On the other hand, these tyrosine-kinase signalling pathways can promote cell growth independently of ERα thus potentiating cancer progression and endocrine-refractory phenotype.

All these events contribute to breast cancer progression and to Tamoxifen resistance, though other mechanisms may also be involved. The complexity of these processes makes it crucial to identify reliable biomarkers for response to available targeted therapies and also to identify new therapeutic strategies.

In recent years, several targeted therapies against the molecular pathways associated with Tamoxifen resistance have been proposed, either on their own or in combination with endocrine agents. Examples of such compounds are Herceptin (Trastuzumab) that is a monoclonal antibody against HER2. It inhibits its homodimerisation and prevents HER2-mediated aberrant cell growth (Namboodiri and Pandey 2011). Herceptin is FDA-approved for the treatment of HER2-positive early and metastatic breast cancer (Gianni et al., 2012) either on its own of in combination with tyrosine-kinase inhibitors such as Lapatinib or aromatase inhibitors such as Anastrozole (Kaufman, Mackey et al. 2009, de Azambuja, Holmes et al. 2014).

In addition, clinical trials have assessed the combination between aromatase inhibitors and Everolimus, a selective inhibitor of mTOR. This combinatorial therapeutic strategy has significantly prolonged patient disease-free survival (Yardley et al., 2013). Everolimus was recently FDA-approved for postmenopausal patients with ERα positive breast cancer.

However, due to the heterogeneity of breast cancer, subsets of patients do not respond to any of the available therapies (Martelotto et al., 2014) or develop resistance to them. This implies there are other undiscovered mechanisms that contribute to cancer progression and resistance to therapies.

5.2 Aims of this chapter

Using existing drugs originally developed for one disease to treat endocrine-resistant breast cancer is a very appealing approach. FDA-approved drug repurposing can speed up the process of bringing new treatments to patients, as well as reduce the costs. These drugs have well-documented mechanisms of action toxicity, pharmacology and drug-drug interaction parameters (Nowak-Sliwinska et al., 2019).

In this context, the main aim of this chapter was to identify novel therapeutic opportunities for endocrine resistant breast cancer by re-purposing FDA-approved drugs.

5.3 Results

In recent years, several mechanisms of Tamoxifen resistance in breast cancer have been identified, which led to the development of targeted therapies directed against epidermal growth factor HER2 (Namboodiri and Pandey, 2011) or against pathways such as PI3K/Akt/mTOR (Knowlden et al., 2005) and cyclin D/cyclin-dependent kinases 4 and 6 (CDK4/6)–retinoblastoma protein (RB) pathway (Finn, Crown et al. 2015). Though all these novel targeted therapies have significantly improved patient survival, there are still subsets of patients that do not respond to any of the currently-available therapeutic strategies. This is indicative of alternative pathways involved in endocrine resistance that are yet to be identified and targeted for the overall improvement of breast cancer therapy.

One way to accelerate drug development is by repurposing FDA-approved drugs. In this context, we sought to test the compound library L1300-Selleck-FDA-Approved-Drug-Library-978cpds (Stratech, Selleckchem) on ERα positive Tamoxifen sensitive

cells MCF-7 and ZR-75-1 and the endocrine resistant MCF-7-TRF and ZR-75-1-TamR cells. The normal breast epithelial MCF-10-A cells and the triple-negative MDA-MB-231 cells were also included as controls. The experimental design is illustrated in Figure 5.1:

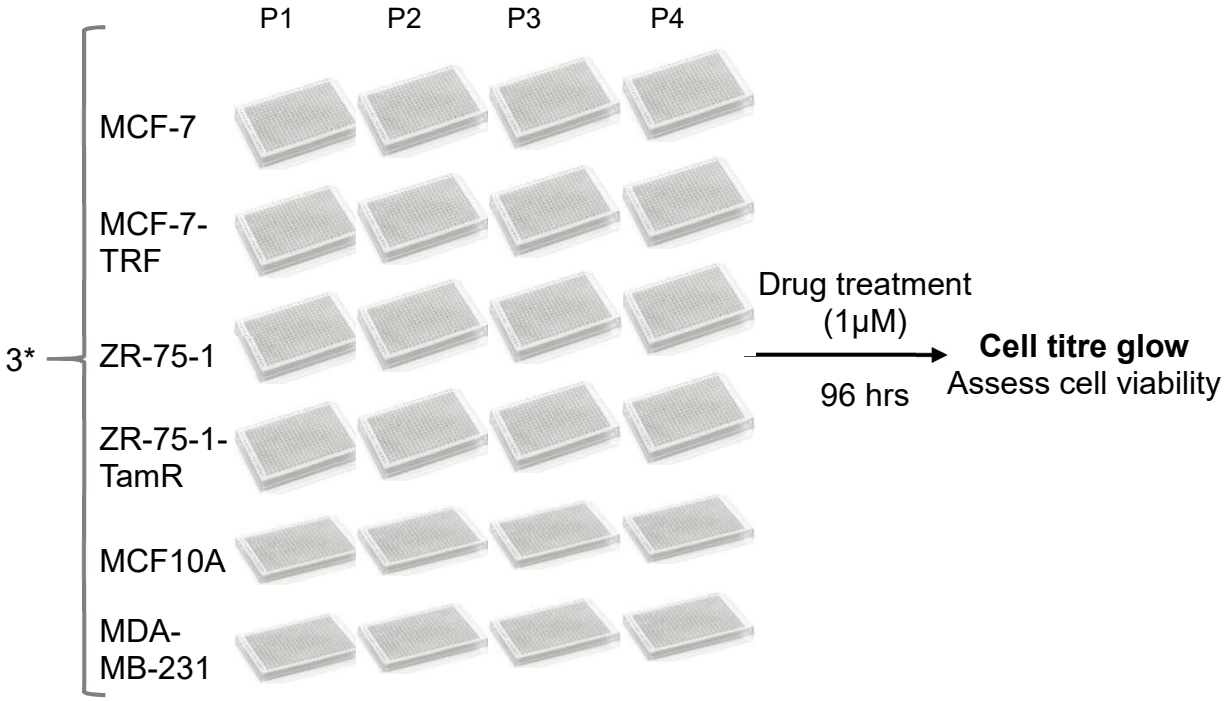

Figure 5.1. Experimental design for the compound library screen: L1300-Selleck-FDA-Approved-Drug-Library-978cpds (Stratech, Selleckchem) library was tested in biological triplicates for each of MCF-7, MCF-7-TRF, ZR-75-1, ZR-75-1-TamR, MCF-10-A and MDA-MB-231 cell lines. For each biological replicate, cells were seeded in four 384 plates using the Multidrop™ Combi Reagent Dispenser. After 24 hours of incubation, drugs were dispensed in technical singlets using the Echo®555 liquid handler. All drug treatments were performed at 1μM, for 96 hours. At the end of the four-day treatment, cell viability was assessed using CellTiter-Glo® Luminescent Assay.

The screen was performed in biological triplicates, for all cell lines except MCF-7-TRF which had 2 biological replicates. All compounds were tested at a concentration of 1μM for 96 hours. At the end of the four-day treatment, cell viability was assessed using CellTiter-Glo® Luminescent Assay and luminescence was recorded using the PheraStar FS microplate reader (BMG LABTECH). The PCA plot in Figure 5.2 illustrates the reproducibility between biological replicates for each individual cell line:

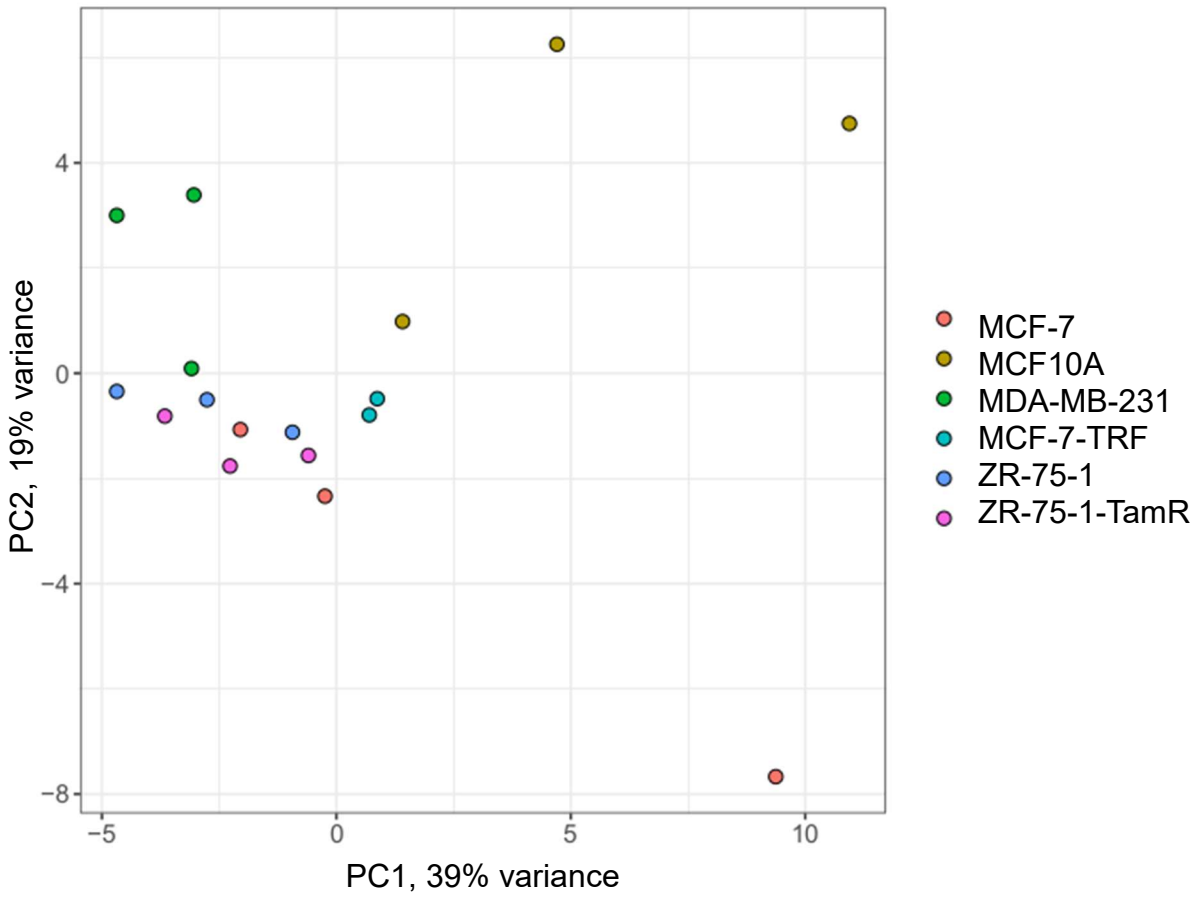

Figure 5.2. Principal component analysis (PCA) for the biological replicates of the compound screen for each cell line: the first two principal components are displayed.

For further analysis, percentage viability over control DMSO was calculated for each compound in each cell line. The average of the three biological replicates was calculated and used for further analyses.

The full list of compounds tested, as well as their percentage inhibition over control in each cell line is provided in Annexe 2, while a broad overview of the results is shown in Figure 5.3:

Most drugs had minimal inhibitory effects on the cell models used. Therefore, only drugs that reduced viability with 50% in the Tamoxifen resistant cell lines MCF-7-TRF and ZR-75-1-TamR were considered for further analysis. There were 62 such drugs. Percentage viability of all the cell lines for these filtered compounds is illustrated in Figure 5.4, as well as their main FDA-approved indications.

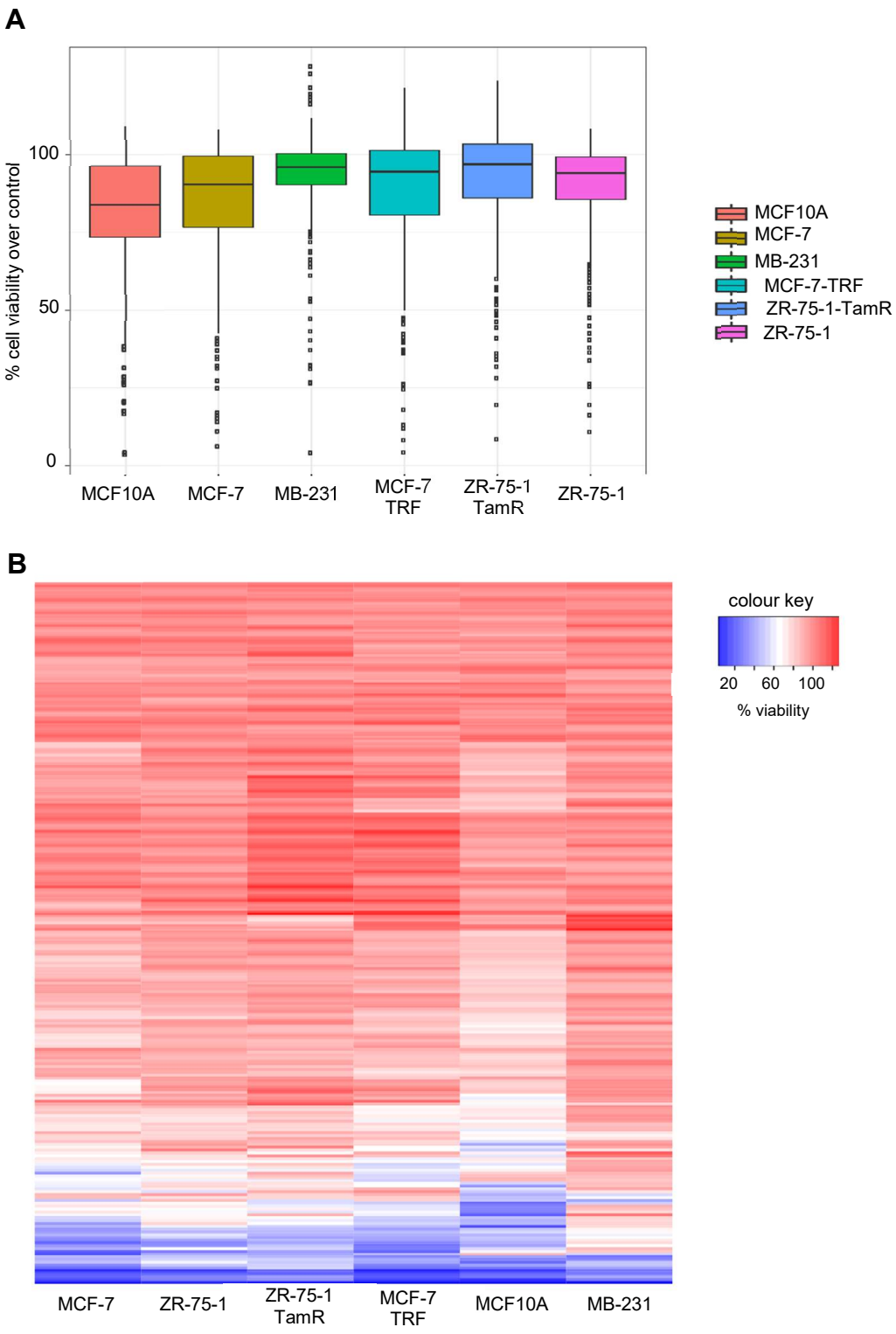

Figure 5.3. Overall results of the compound screen: (A) Box plots representing % cell viability over DMSO control for each drug in each cell line; **(B)** Heatmap representing % viability over DMSO for each compound in each cell line.

Figure 5.4. Heatmap of the compounds that affected cell viability with at least 50% in MCF-7-TRF and ZR-75-1-TamR: the effect of these compounds on MCF-7, ZR-75-1, MCF10A and MDA-MB-231 is also illustrated and the drug class and main therapeutic indication is mentioned for each of the 62 filtered drugs.

The 62 compounds that affect cell viability with at least 50% in the endocrine resistant cell lines belong to different compound classes. These classes include therapies for neurological, cardiovascular and metabolic disease, antibiotics, antivirals and vermifuges, endocrinology disease and cancer.

Interestingly, several compounds targeting mTOR pathway emerged as top inhibitors of cell viability in ERα positive cell lines. These are Everolimus, Temsirolimus, Rapamycin. In fact, such inhibitors, in combination with aromatase inhibitors, have been FDA-approved for the treatment of post-menopausal patients with ERα positive breast cancer (Yardley et al., 2013). Therefore, the presence of Everolimus, Temsirolimus and Rapamycin as top inhibitors can be considered a validation of the screen. The percentage cell viability over control for these drugs is illustrated in Table 5.1:

	% viability over control (DMSO)					
Compound	MCF-7	ZR-75-1	MCF-7-TRF	ZR-75-1-TamR	MDA-MB-231	MCF-10A
Everolimus	36.949	44.789	45.414	46.221	68.301	55.062
Temsirolimus	31.963	40.306	39.511	45.943	71.743	47.714
Rapamycin	27.166	36.250	36.149	44.255	75.447	45.990

Table 5.1. Effects of mTOR inhibitors on cell viability; % cell viability compared to vehicle is illustrated for the compounds on each cell line.

In order to measure the potency of Everolimus in reducing cell viability of Tamoxifen sensitive cells compared to resistant cells, the drug concentration was titrated and IC50 values were generated in ZR-75-1 and ZR-75-1-TamR (Fig.5.5.A). The IC50 for ZR-75-1 was 125 nM and 500nM for ZR-75-1-TamR.

Furthermore, using the Everolimus IC50 for ZR-75-1-TamR of 500nM, cell confluency of MCF-7, MCF-7-TRF, ZR-75-1 and ZR-75-1-TamR was assessed over a course of 5-day treatment (Fig.5.5.B). The compound significantly inhibited cell growth in all four cell lines, confirming its efficacy.

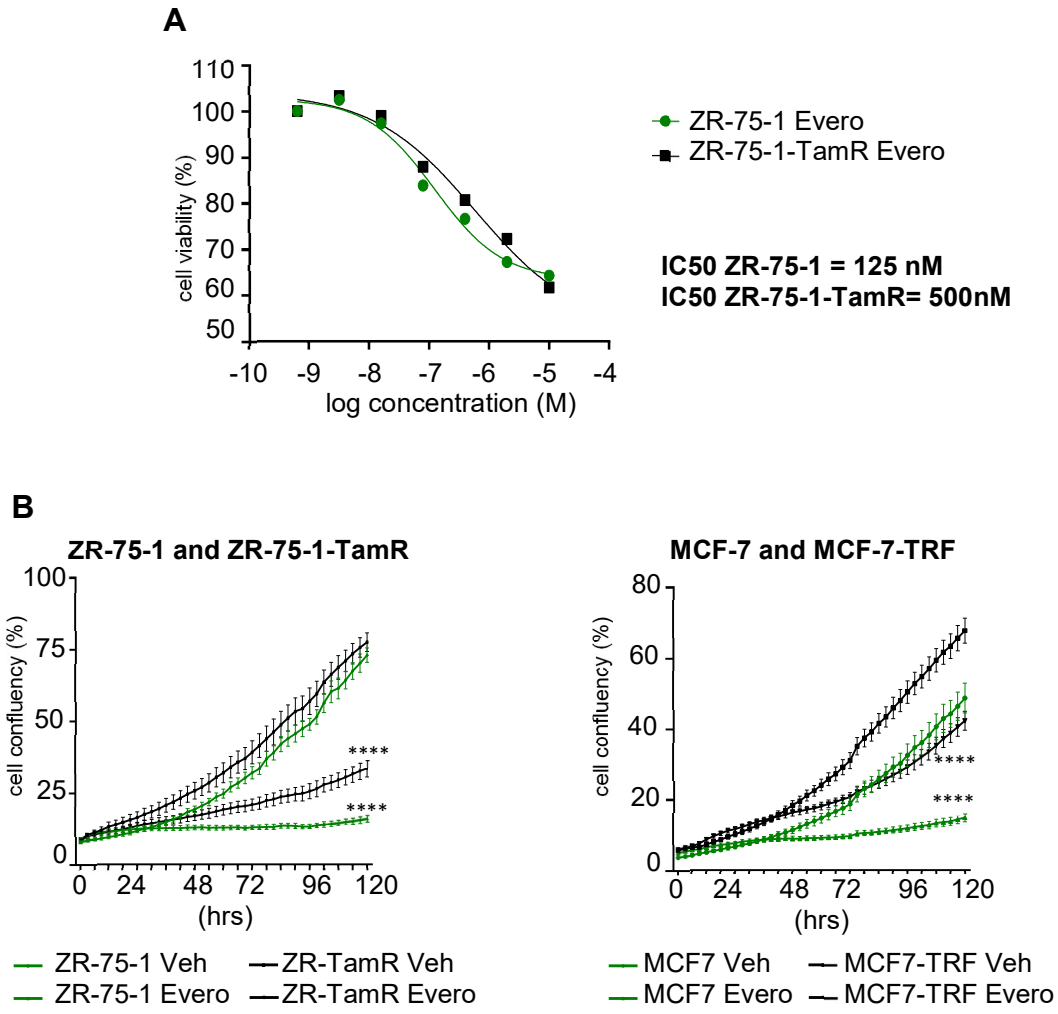

Figure 5.5. Everolimus effect on cell viability and cell growth: (A) generation of IC50 in ZR-75-1 and ZR-75-1-TamR. Cells were seeded in 6 technical replicates and treated 24 hours later with serial 1:3 dilutions of Everolimus ranging from 10μM to 4nM. Cell viability was assessed after 96 hours, using Cell Titre Glo. IC50 was calculated using GraphPad Prism Software and the non-linear regression model of log (inhibitor) vs response- variable slope settings. **(B)** Everolimus effect on MCF-7, ZR-75-1, MCF-7-TRF and ZR-75-1-TamR; cell growth is expressed as mean ±SD of % confluency, assessed using the Incucyte ZoomTM system. Cells were seeded in 6 technical replicates (wells) and treated with 500nM Everolimus 24 hours later. Two-way ANOVA multiple comparison was performed; p values ≤0.0001 are illustrated as (****).

In addition, other cancer therapeutics, including compounds that induce DNA damage, have emerged as top hits in the drug screen (Table 5.2). They are Irinotecan, Topotecan, Idarubicin and Camptothecin.

	%over control (DMSO)					
Compound	MCF-7	ZR-75-1	MCF-7-TRF	ZR-75-1-TamR	MDA-MB-231	MCF-10A
Camptothecin	13.986	16.150	11.889	27.998	31.772	16.545
Irinotecan	38.901	53.014	42.198	49.568	68.913	51.008
Topotecan	34.928	33.705	26.071	48.482	66.054	39.269
Idarubibin	16.107	19.433	12.935	19.414	26.605	20.250

Table 5.2. Effect of DNA damage inducing agents on cell viability; % cell viability compared to control is illustrated for the compounds on each cell line.

Camptothecin and its analogues - Irinotecan and Topotecan - induce DNA damage by inhibiting DNA topoisomerase II. They intercalate DNA, disrupt nucleic acid synthesis and induce DNA double strand breaks, ultimately resulting in cell death (Hollingshead and Faulds, 1991). Therefore, they are used as cancer chemotherapeutic agents in leukaemia, ovarian, small-cell lung, and refractory colorectal cancers (Liu et al., 2015). They have also been tested in clinical trials for metastatic breast cancer, but to date have not been introduced as standard of care. The clinical trials were small and showed variable response rates between 14-64%, indicating the need for an appropriate biomarker predictive of these drugs' response. Nonetheless, this class of compounds may benefit certain subgroups of metastatic breast cancer patients (Kümler et al., 2013).

Idarubicin is an anthracycline that also inhibits DNA topoisomerase II and has been successfully used is various cancer types, including breast cancer. They target proliferating cancer cells, although the exact mechanism for its cell killing ability is still not entirely understood (Zhong et al., 2019).

A potentially interesting cluster of drugs (Disulfiram, Fesoterodine, Valdecoxib) appear to specifically inhibit cancer cells and only marginally inhibit the normal epithelial breast cell line MCF10A. The percentage viability over control for these compounds is shown in Table 5.2. These compounds are promising, as their toxicity on normal tissues may be considerably lower compared to DNA damage inducers.

	%over control (DMSO)					
Compound	MCF-7	ZR-75-1	MCF-7-TRF	ZR-75-1-TamR	MDA-MB-231	MCF-10A
Disulfiram	16.919	42.385	47.191	40.863	53.366	85.897
Fesoterodine	16.928	42.439	47.110	40.825	53.384	85.878
Valdecoxib	16.898	42.409	47.189	40.908	53.313	85.485

Table 5.3. Effects of compounds that specifically inhibit breast cancer cell viability, but not normal epithelial cells: percentage cell viability compared to control is illustrated for each cell line.

Disulfiram is approved by the FDA for the treatment of alcohol dependence (Williams, 2019). In recent years, considerable evidence has emerged for the anti-cancer effects of this drug (Lun et al., 2016, Viola-Rhenals et al., 2018, Yang et al., 2015). In particular, it has been shown that treatment with Disulfiram/Copper complex results in cell proliferation inhibition *in vitro* and in ERBB2 transgenic mice. This effect was demonstrated to occur through inhibition of AKT and cyclin D1 signaling. In addition, Disulfiram promotes apoptosis by suppressing the nuclear factor kB signaling. These results suggest that treatment with Disulfiram/Copper complex may be a promising therapy for ERBB2 positive breast cancer (Yang et al., 2015). The preliminary results from our drug screen suggest that Disulfiram may also be beneficial for endocrine resistant ERα positive breast cancer.

Valdecoxib is a nonsteroidal anti-inflammatory drug from the same pharmacological class as Celecoxib. Their mechanism of action involves inhibition of Cyclooxygenase type-2 (COX-2) is the enzime that triggers Protaglandin synthesis. The use of COX-2 inhibitors was shown to modulate tumour growth in chemoresitant colorectal cancer (CRC) xenograft models (Rahman et al., 2012). In adition, it was observed that Celecoxib has a preventative effect againt progression of oral squamous cell carcinoma *in vitro* and in PDX models through inhibition of epithelial-to-mesenchial transition (Chiang et al., 2017). COX-2 therefore acts as biomarker for those cancer models that may benefit from inhibitors such as Valdecoxib or Celecoxib (Chiang et al., 2017, Rahman et al., 2012). Moreover, COX-2 expression was previously associated with an aggressive phenotype in ductal carcinoma in situ (Boland et al., 2004), implying that Cyclooxygenase type-2 inhibition with celecoxib or other coxibs

(Valdecoxib, Rofecoxib) may potentially prevent the development of both ERα-positive and ERα-negative breast cancers. Further investigations are required to clarify the benefits of COX-2 inhibition in breast cancer.

Fesoterodine is a compound that reduces spasms of the bladder muscles. It is therefore FDA-approved for the treatment of overactive bladder with symptoms of urinary frequency (2008). No studies of Fesoterodine's anti-cancer effects have been conducted to date. In contrast, this drug seems to increase the risk of lung and colon cancer (Löfling et al., 2019).

Another cluster of compounds from the screen is the one of Vincristine-sulfate, Betaxolol, Penciclovir and Sulbactam-sodium. They are clustered together because they specifically reduce cell viability in ERα positive breast cancer cell lines and, to a much lesser extent, in the triple negative MDA-MB-231 cells. In addition, the effect of these four agents on the normal epithelial MCF10A cells was moderate (Table 5.4).

	%over control (DMSO)					
Compound	MCF-7	ZR-75-1	MCF-7-TRF	ZR-75-1-TamR	MDA-MB-231	MCF-10A
Vincristine-sulfate	15.018	25.308	17.888	35.932	81.650	62.811
Betaxolol	15.039	25.342	17.857	35.912	81.621	62.808
Penciclovir	14.987	25.261	17.926	35.970	81.747	62.485
Sulbactam-sodium	15.009	25.331	17.885	36.008	81.592	62.529

Table 5.4. Effects of compounds that specifically inhibit ERα positive breast cancer cell viability and not ERα negative cells: the normal epithelial cells were moderately inhibited; percentage cell viability compared to control is illustrated for each cell line.

Vincristine is part of the alkaloid group of anti-cancer drugs. They stop mitosis by inhibiting polimerisation of microtubules, hece blocking cell growth (Zhou et al., 2019). It is already FDA-approved for the treatment of lymphomas.

Betaxolol hydrochloride is a beta-1-selective adrenergic receptor antagonist. It acts on the heart and circulatory system and decreases cardiac contractility and rate, thereby reducing cardiac output. It can be applied topically for the treatment of ocular

hypertension and glaucoma (Onishchenko et al., 2019). There are no studies to date about Betaxolol in cancer treatment.

Penciclovir is an antiviral drug for varicella-zoster virus and herpes simplex virus infections (Lazarus et al., 1999) with no previous connection to cancer. Sulbactam-sodium has antibacterial properties.

5.4 Discussion

To date, the estrogen receptor modulator Tamoxifen remains the most widely-used agent in pre-menopausal women and it is still one of the main options in post-menopausal context (Davies et al., 2011). However, subgroups of patients are resistant to this drug. The endocrine refractory phenotype can result though various mechanisms including, but not restricted to changes in ERα levels and activity, changes in its protein interactors, cross-talk with receptor tyrosine kinase signalling pathways or dysregulation of cellular proliferation.

Advances in our understanding of Tamoxifen resistance have paved the way for novel targeted therapies. Herceptin - a monoclonal antibody against HER2 (Namboodiri and Pandey 2011) – is currently used for ERα positive and ERBB2 positive patients. Another novel therapeutic approach is to target the PI3K/Akt/mTOR signalling pathways with compounds such as Everolimus and this has proved successful in postmenopausal patients with ERα positive breast cancer.

Nonetheless, certain patients are not responsive to any of the currently-available medicines, which is an indication of more yet unidentified pathways to resistance to therapies. Therefore, there is still a need to improve breast cancer treatment.

By conducting a screen of 1000 FDA-approved drugs, potential candidates that show efficacy in hormone-refractory breast cancer cell lines were identified. There are 62 compounds that reduce cell viability of MCF-7-TRF and ZR-75-1TamR with more than 50% compared to control DMSO.

Among these drugs, there are multiple mTOR inhibitors as well as DNA damage inducers that are already FDA-approved for breast cancer treatment (Kümler et al.,

2013, Lun et al., 2016, Yardley et al., 2013). Their presence as top inhibitors in this screen validates the quality of the data.

In contrast to mTOR inhibitors and DNA damage inducers that are associated with high toxicity (Junpaparp et al., 2013, Ryan et al., 1991), some of the compounds that emerged as top inhibitors in this drug screen seem to specifically inhibit ERα positive and negative cancer cells and only have a small impact on normal epithelial cells. This is particularly appealing as a therapeutic opportunity, as it implies reduced toxicity on normal cells. Among these compounds there are Disulfiram and Valdecoxib. The first agent is FDA-approved for the treatment of alcohol dependence, but recent studies have shown it inhibits cell proliferation in HER2 positive breast cancer cell lines and in ERBB2 transgenic mice (Yang et al., 2015).

Valdecoxib and its more potent analogue Celecoxib are FDA-approved as nonsteroidal anti-inflammatory drugs. They have also been identified as anti-tumour agents in chemo-resistant colorectal cancer xenograft models (Rahman et al., 2012) and oral squamous cell carcinoma *in vitro* and PDXs (Chiang et al., 2017).

The results from this screen indicate Disulfiram and Valdecoxib may also be beneficial in endocrine resistant breast cancer.

Moreover, Vincristine which is currently FDA-approved for the treatment of lymphomas (Zhou et al., 2019) seems to specifically reduce cell viability of endocrine sensitive and resistant ERα positive breast cancer cell lines.

In addition, all the other compounds identified as viability inhibitors for breast cancer cells are worth validating.

The next steps would be to titrate down the compound concentration and calculate the IC50 for these hits. The coumpounds would also be tested on a panel of other cell lines with common characteristics. Once *in vitro* steps are completed, the drugs would be validated *in vivo* (e.g. on tumour explants from PDX models and in mice).

Furthemore, assessing the effects of the compounds on ERα-chromatin interactions would shed light on subsequent gene regulation and would offer inhight into the drugs' mechanism of action in breast cancer models.

Taken together, this compound screen has identified potential candidates for the treatment of hormone-refractory breast cancer.

Chapter 6. General Discussion

ERα is the driving transcription factor in approximately three quarters of all breast cancer cases. This hormone receptor regulates genes involved in cell proliferation and survival (Musgrove and Sutherland, 2009) and its alterations result in oncogenesis.

ERα targeted therapies have been developed and have significantly improved patients' outcome. Notably, Tamoxifen was the first selective estrogen receptor modulator to be used widely in breast cancer treatment and it continues to be prescribed particularly to pre-menopausal women. However, certain subsets of patients are resistant to endocrine therapy.

A key protein in ERα positive breast cancer is FOXA1. Several studies have described FOXA1 as a pioneer transcription factor that opens up compacted chromatin for subsequent binding of the hormone receptor (Carroll et al., 2005, Carroll et al., 2006, Hurtado et al., 2011). Thus, FOXA1 acts upstream of ERα and dictates its transcriptional programme. As such, FOXA1 is an attractive therapeutic target that may benefit ERα breast cancer patients, including those with endocrine resistance.

One recent study has disputed the paradigm of FOXA1 pioneer activity in ERα positive breast cancer (Swinstead et al., 2016). *Swinstead et al.* suggested there is a subset of FOXA1 genomic binding sites induced by steroid activation. This conclusion challenges the importance of FOXA1 targeted therapy upstream of ERα.

6.1 FOXA1 functions independently of ERα signalling

In this context, the aim of chapter 3 from this dissertation was to investigate whether FOXA1 binding events are regulated by hormone stimuli (Glont et al, 2019). The data generated reinforced the concept of a transcription factor hierarchy with FOXA1 acting upstream of ERα. Only a very small number (less than 1%) of FOXA1-chromatin interactions appear to be E2-induced in the experiments conducted. These <1% of E2-induced FOXA1 binding sites were shown to be in fact "shadow" peaks created by pre-existing binding sites that form chromatin loops.

Thus, FOXA1 acts upstream of ERα, its chromatin binding capacity is not influenced by estrogen signalling, and it remains a relevant and important drug target in hormone-dependent cancers.

6.2 ETV6 is a newly identified interactor of FOXA1 and ERα that contributes to breast cancer progression and endocrine resistance

In recent years, several mechanisms of endocrine resistance in ERα positive breast cancer have been discovered, including changes in ERα levels and activity, changes in its protein interactors, cross-talk with growth factors and receptor tyrosine kinase signalling pathways or dysregulation of cellular proliferation. These insights have facilitated the development of several targeted therapies that have successfully prolonged disease-free survival in subsets of patients.

One novel successful therapeutic strategy for ERα positive, HER2 positive breast cancer patients is the inhibition of HER2-mediated aberrant cell growth using an antibody-drug conjugate. This treatment, T-DM1, combines the monoclonal antibody against HER2 Trastuzumab (T) with the potent cytotoxic maytansine derivative (DM1) (Okines, 2017).

In addition, inhibitors of cyclin D–CDK4/6-Retinoblastoma pathway such as Palbociclib (Finn et al., 2015) or inhibitors of the AKT/mTOR signalling pathway such as the mTOR inhibitor Everolimus (Yardley et al., 2013) have significantly improved disease-free survival in subsets of breast cancer patients.

Yet, certain patients do not respond to any of these therapies and therefore it is vital to identify alternative determinant factors in breast cancer progression and endocrine resistance. A better understanding of the events that contribute to disease progression would pave the way for the development of new therapeutic strategies for the overall improvement of breast cancer survival.

In chapter 4 of this thesis, the novel proteomics technique qPLEX-RIME was used to assess quantitative changes in FOXA1 and ERα interactome associated with the

development of the endocrine refractory phenotype. It was revealed that ERα and FOXA1 are enriched in Tamoxifen resistance, together with their newly identified interactor ETV6.

ETV6 is an ETS transcription factor, that can mediate cell cycle, differentiation and lineage specification in normal development (Findlay et al., 2013). Therefore, it was plausible to hypothesise that ETV6 enrichment in the ERα/FOXA1 interactome associated with Tamoxifen resistance may play a role in cancer progression.

Further validation of ETV6 relevance in endocrine resistance was provided by the growth inhibitory effect of ETV6 silencing in Tamoxifen resistant cell line models. This suggests that targeting ETV6 may be beneficial even for the endocrine refractory breast cancer patients.

Moreover, ETV6's direct contribution to breast cancer progression was shown by the growth promoting effects of ETV6 overexpression on MCF-7 colony formation ability.

More insights into the functional role of ETV6 in endocrine resistance would be achieved by assessing the influence of ETV6 silencing in Tamoxifen resistant models on FOXA1/ERα chromatin interactions and subsequent gene regulation.

In addition, assessing how would ETV6 overexpression in drug sensitive models affect ERα chromatin interactions and gene regulation would also reinforce the direct role of ETV6 in tumour progression.

Importantly, ChIP-seq analysis has revealed that ERα, FOXA1 and ETV6 cooperate to drive endocrine resistance both *in vitro* and *in vivo*. Diffbind analysis showed that ERα, FOXA1, ETV6-chromatin interactions are redistributed together to the same genomic regions in endocrine resistant, when compared to endocrine sensitive breast cancer models (Fig.6.1).

This redistribution is accompanied by an altered enhancer landscape. The genomic regions that lose ERα, FOXA1 and ETV6 binding also contain weak signal for the H3K27Ac marker of active chromatin, while the regions gained by the three transcription factors are also associated with stronger H3K27Ac peaks, proving they are more active for transcription.

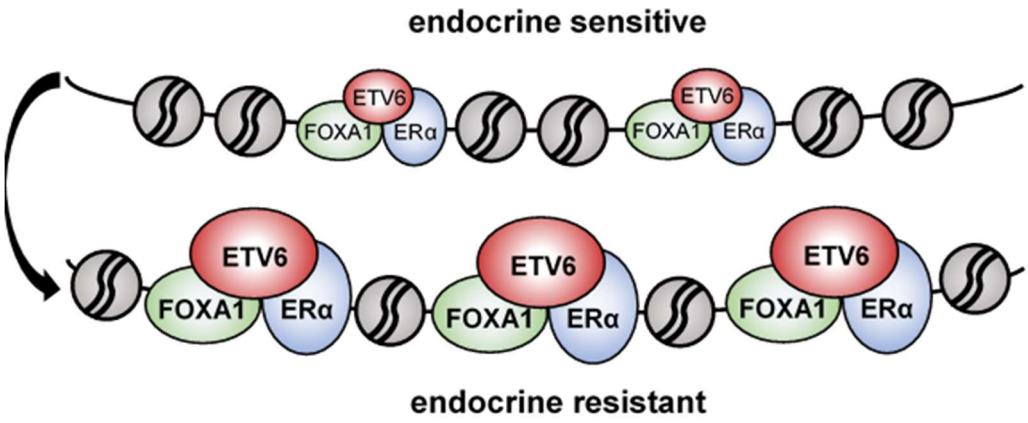

Figure 6.1. Model of ERα, FOXA1 and ETV6 cooperative redistribution in endocrine resistant compared to sensitive context.

Importantly, integration of ChIP-seq and RNA-seq data showed that ETV6-chromatin binding redistribution affects gene expression. A much higher percentage of ETV6 gained chromatin interactions in endocrine resistant compared to matched sensitive models were located closer to the transcription start site of upregulated genes rather than downregulated genes.

Furthermore, the ETV6 lost sites in endocrine resistant compared to matched sensitive models were located closer to the transcription start site of repressed genes rather than activated genes.

These data suggest that ETV6 differential chromatin interactions between endocrine resistant and sensitive breast cancer models affect the transcriptome and therefore may contribute to the more aggressive phenotype associated with drug resistance.

Further Genomic Regions Enrichment of Annotations Tool (GREAT) (McLean et al., 2010) analysis revealed that ETV6 differentially bound regions also correlate with Tamoxifen resistance signatures as assessed in previously published datasets (Massarweh et al., 2008, Creighton et al., 2008).

In addition, previous studies have described ETS transcription factors as being regulated by MAPK pathway (Chi et al., 2010). Therefore, the effects of MEK inhibitor Trametinib on endocrine sensitive and resistant models were assessed. It was found that inhibition of MAPK pathway reduced breast cancer progression and modulated ETV6-chromatin interactions. Further assessment of the enhancer landscape, as well

as gene expression analysis of Trametinib effects on Tamoxifen resistant models would shed more light on ETV6 regulation by MAPK pathway.

In order to gain confidence that the anti-proliferative effect of Trametinib in endocrine resistance occurs through ETV6 modulation, further experiments could be conducted to assess whether ETV6 overexpression minimises the effect of Trametinib.

Of importance, ETV6 copy number amplifications were assessed in the METABRIC cohort (Curtis et al., 2012). They were found to be associated with significantly reduced disease-free survival in ERα positive Luminal B breast cancer, which is the more aggressive subtype of cancer, more likely to metastasise.

Taken together, the work in chapter 4 describes ETV6 as a novel interactor of ERα and FOXA1 that contributes to breast cancer progression and endocrine refractory phenotype.

6.3 Repurposing of FDA-approved compounds identifies potential new therapeutic strategies for Tamoxifen resistant breast cancer

Another angle from which endocrine resistance was tackled in this dissertation was by aiming to repurpose FDA-approved drugs (chapter 5). Potential candidates that show efficacy in hormone-refractory breast cancer cell lines were identified using a 1000-compound screen. Due to time restrictions the follow-up work from this chapter could not be completed.

The next steps would be to titrate down the compound concentration and calculate the IC50 for these hits. The compounds IC50 would then be tested and validated on a panel of cell lines with common characteristics. Once *in vitro* steps are completed, the drugs would be validated *in vivo* (e.g. on tumour explants from PDX models and in mice-bearing PDX tumours).

Furthermore, assessing the effects of the compounds on ERα-chromatin interactions and gene regulation would offer insights into the drugs' mechanism of action in breast cancer models.

Taken together, this compound screen identified potential candidates for the treatment of hormone-refractory breast cancer.

6.4 Conclusions

In summary, this study has reinforced that FOXA1 functions independently of ERα signalling. In addition, it was revealed that FOXA1 and ERα are enriched in endocrine resistance, together with their newly identified interactor ETV6. The contribution of ETV6 to cancer progression and endocrine refractory phenotype was further validated by an independent siRNA screen. Furthermore, there is a global reprogramming of FOXA1, ERα and ETV6 – chromatin interactions that results in altered transcription activity in endocrine resistance. The clinical relevance of ETV6 copy number amplifications was assessed and it was found that they correlate with significantly worse prognosis in ERα positive, Luminal B breast cancer. Last but not least, potential candidates for the treatment of Tamoxifen resistant breast cancer models were identified.

Chapter 7. Bibliography

2008. New Drugs/Drug News. *P & T : a peer-reviewed journal for formulary management,* 33**,** 688-694.

ANZICK, S. L., KONONEN, J., WALKER, R. L., AZORSA, D. O., TANNER, M. M., GUAN, X. Y., SAUTER, G., KALLIONIEMI, O. P., TRENT, J. M. & MELTZER, P. S. 1997. AIB1, a steroid receptor coactivator amplified in breast and ovarian cancer. *Science (New York, N.Y.),* 277**,** 965-8.

ARPINO, G., WIECHMANN, L., OSBORNE, C. K. & SCHIFF, R. 2008. Crosstalk between the estrogen receptor and the HER tyrosine kinase receptor family: molecular mechanism and clinical implications for endocrine therapy resistance. *Endocr Rev,* 29**,** 217-33.

BAILEY, T. L., BODEN, M., BUSKE, F. A., FRITH, M., GRANT, C. E., CLEMENTI, L., REN, J., LI, W. W. & NOBLE, W. S. 2009. MEME SUITE: tools for motif discovery and searching. *Nucleic Acids Res,* 37**,** W202-8.

BAKER, K. M., WEI, G., SCHAFFNER, A. E. & OSTROWSKI, M. C. 2003. Ets-2 and components of mammalian SWI/SNF form a repressor complex that negatively regulates the BRCA1 promoter. *J Biol Chem,* 278**,** 17876-84.

BASUDAN, A., PRIEDIGKEIT, N., HARTMAIER, R. J., SOKOL, E. S., BAHREINI, A., WATTERS, R. J., BOISEN, M. M., BHARGAVA, R., WEISS, K. R., KARSTEN, M. M., DENKERT, C., BLOHMER, J. U., LEONE, J. P., HAMILTON, R. L., BRUFSKY, A. M., ELISHAEV, E., LUCAS, P. C., LEE, A. V. & OESTERREICH, S. 2019. Frequent ESR1 and CDK Pathway Copy-Number Alterations in Metastatic Breast Cancer. *Mol Cancer Res,* 17**,** 457-468.

BEATO, M., HERRLICH, P. & SCHÜTZ, G. 1995. Steroid hormone receptors: many actors in search of a plot. *Cell,* 83**,** 851-7.

BEHR, R., BRESTELLI, J., FULMER, J. T., MIYAWAKI, N., KLEYMAN, T. R. & KAESTNER, K. H. 2004. Mild nephrogenic diabetes insipidus caused by Foxa1 deficiency. *J Biol Chem,* 279**,** 41936-41.

BERLATO, C., CHAN, K. V., PRICE, A. M., CANOSA, M., SCIBETTA, A. G. & HURST, H. C. 2011. Alternative TFAP2A isoforms have distinct activities in breast cancer. *Breast Cancer Res,* 13**,** R23.

BERNARDO, G. M. & KERI, R. A. 2012. FOXA1: a transcription factor with parallel functions in development and cancer. *Biosci Rep,* 32**,** 113-30.

BERNARDO, G. M., LOZADA, K. L., MIEDLER, J. D., HARBURG, G., HEWITT, S. C., MOSLEY, J. D., GODWIN, A. K., KORACH, K. S., VISVADER, J. E., KAESTNER, K. H., ABDUL-KARIM, F. W., MONTANO, M. M. & KERI, R. A. 2010. FOXA1 is an essential determinant of ERalpha expression and mammary ductal morphogenesis. *Development,* 137**,** 2045-54.

BERRY, M., METZGER, D. & CHAMBON, P. 1990. Role of the two activating domains of the oestrogen receptor in the cell-type and promoter-context dependent agonistic activity of the anti-oestrogen 4-hydroxytamoxifen. *The EMBO journal,* 9**,** 2811-2818.

BI, M., ZHANG, Z., JIANG, Y.-Z., XUE, P., WANG, H., LAI, Z., FU, X., DE ANGELIS, C., GONG, Y., GAO, Z., RUAN, J., JIN, V. X., MARANGONI, E., MONTAUDON, E., GLASS, C. K., LI, W., HUANG, T. H.-M., SHAO, Z.-M., SCHIFF, R., CHEN, L. & LIU, Z. 2020. Enhancer reprogramming driven by high-order assemblies of transcription factors promotes phenotypic plasticity and breast cancer endocrine resistance. *Nature Cell Biology,* 22**,** 701-715.

BIDDIE, S. C., JOHN, S., SABO, P. J., THURMAN, R. E., JOHNSON, T. A., SCHILTZ, R. L., MIRANDA, T. B., SUNG, M. H., TRUMP, S., LIGHTMAN, S. L., VINSON, C., STAMATOYANNOPOULOS, J. A. & HAGER, G. L. 2011. Transcription factor AP1 potentiates chromatin accessibility and glucocorticoid receptor binding. *Mol Cell,* 43**,** 145-55.

BLACK, L. J., JONES, C. D. & FALCONE, J. F. 1983. Antagonism of estrogen action with a new benzothiophene derived antiestrogen. *Life Sci,* 32**,** 1031-6.

BOLAND, G. P., BUTT, I. S., PRASAD, R., KNOX, W. F. & BUNDRED, N. J. 2004. COX-2 expression is associated with an aggressive phenotype in ductal carcinoma in situ. *British Journal of Cancer,* 90**,** 423-429.

BONÉY-MONTOYA, J., ZIEGLER, Y. S., CURTIS, C. D., MONTOYA, J. A. & NARDULLI, A. M. 2010. Long-range transcriptional control of progesterone receptor gene expression. *Mol Endocrinol,* 24**,** 346-58.

BOSTNER, J., KARLSSON, E., PANDIYAN, M. J., WESTMAN, H., SKOOG, L., FORNANDER, T., NORDENSKJÖLD, B. & STÅL, O. 2013. Activation of Akt, mTOR, and the estrogen receptor as a signature to predict tamoxifen treatment benefit. *Breast Cancer Res Treat,* 137**,** 397-406.

BOYER, L. A., LEE, T. I., COLE, M. F., JOHNSTONE, S. E., LEVINE, S. S., ZUCKER, J. P., GUENTHER, M. G., KUMAR, R. M., MURRAY, H. L., JENNER, R. G., GIFFORD, D. K., MELTON, D. A., JAENISCH, R. & YOUNG, R. A. 2005. Core transcriptional regulatory circuitry in human embryonic stem cells. *Cell,* 122**,** 947-56.

BROWN, K. 2002. Breast cancer chemoprevention: risk-benefit effects of the antioestrogen tamoxifen. *Expert Opin Drug Saf,* 1**,** 253-67.

BROWN, L. A., HOOG, J., CHIN, S. F., TAO, Y., ZAYED, A. A., CHIN, K., TESCHENDORFF, A. E., QUACKENBUSH, J. F., MARIONI, J. C., LEUNG, S., PEROU, C. M., NEILSEN, T. O., ELLIS, M., GRAY, J. W., BERNARD, P. S., HUNTSMAN, D. G. & CALDAS, C. 2008. ESR1 gene amplification in breast cancer: a common phenomenon? *Nat Genet,* 40**,** 806-7; author reply 810-2.

BRUEGGEMEIER, R. W., HACKETT, J. C. & DIAZ-CRUZ, E. S. 2005. Aromatase Inhibitors in the Treatment of Breast Cancer. *Endocrine Reviews,* 26**,** 331-345.

CAIZZI, L., FERRERO, G., CUTRUPI, S., CORDERO, F., BALLARÉ, C., MIANO, V., REINERI, S., RICCI, L., FRIARD, O., TESTORI, A., CORÀ, D., CASELLE, M., DI CROCE, L. & DE BORTOLI, M. 2014. Genome-wide activity of unliganded estrogen receptor-α in breast cancer cells. *Proc Natl Acad Sci U S A,* 111**,** 4892-7.

CANCER RESEARCH UK. 2020. *Breast cancer statistics* [Online]. Available: https://www.cancerresearchuk.org/health-professional/cancer-statistics/statistics-by-cancer-type/breast-cancer [Accessed 2020, July].

CARIOU, S., DONOVAN, J. C., FLANAGAN, W. M., MILIC, A., BHATTACHARYA, N. & SLINGERLAND, J. M. 2000. Down-regulation of p21WAF1/CIP1 or p27Kip1

abrogates antiestrogen-mediated cell cycle arrest in human breast cancer cells. *PNAS,* 97**,** 9042-9046.

CARROLL, J. S. 2016. Mechanisms of oestrogen receptor (ER) gene regulation in breast cancer. *European Journal of Endocrinology,* 175**,** R41-R49.

CARROLL, J. S., LIU, X. S., BRODSKY, A. S., LI, W., MEYER, C. A., SZARY, A. J., EECKHOUTE, J., SHAO, W., HESTERMANN, E. V., GEISTLINGER, T. R., FOX, E. A., SILVER, P. A. & BROWN, M. 2005. Chromosome-Wide Mapping of Estrogen Receptor Binding Reveals Long-Range Regulation Requiring the Forkhead Protein FoxA1. *Cell,* 122**,** 33-43.

CARROLL, J. S., MEYER, C. A., SONG, J., LI, W., GEISTLINGER, T. R., EECKHOUTE, J., BRODSKY, A. S., KEETON, E. K., FERTUCK, K. C., HALL, G. F., WANG, Q., BEKIRANOV, S., SEMENTCHENKO, V., FOX, E. A., SILVER, P. A., GINGERAS, T. R., LIU, X. S. & BROWN, M. 2006. Genome-wide analysis of estrogen receptor binding sites. *Nature genetics,* 38**,** 1289-97.

CASTET, A., BOULAHTOUF, A., VERSINI, G., BONNET, S., AUGEREAU, P., VIGNON, F., KHOCHBIN, S., JALAGUIER, S. & CAVAILLÈS, V. 2004. Multiple domains of the Receptor-Interacting Protein 140 contribute to transcription inhibition. *Nucleic Acids Res,* 32**,** 1957-66.

CHARLOT, C., DUBOIS-POT, H., SERCHOV, T., TOURRETTE, Y. & WASYLYK, B. 2010. A review of post-translational modifications and subcellular localization of Ets transcription factors: possible connection with cancer and involvement in the hypoxic response. *Methods Mol Biol,* 647**,** 3-30.

CHEN, D., HUANG, S. M. & STALLCUP, M. R. 2000. Synergistic, p160 coactivator-dependent enhancement of estrogen receptor function by CARM1 and p300. *J Biol Chem,* 275**,** 40810-6.

CHI, P., CHEN, Y., ZHANG, L., GUO, X., WONGVIPAT, J., SHAMU, T., FLETCHER, J. A., DEWELL, S., MAKI, R. G., ZHENG, D., ANTONESCU, C. R., ALLIS, C. D. & SAWYERS, C. L. 2010. ETV1 is a lineage survival factor that cooperates with KIT in gastrointestinal stromal tumours. *Nature,* 467**,** 849-53.

CHIANG, S.-L., VELMURUGAN, B. K., CHUNG, C.-M., LIN, S.-H., WANG, Z.-H., HUA, C.-H., TSAI, M.-H., KUO, T.-M., YEH, K.-T., CHANG, P.-Y., YANG, Y.-H. & KO, Y.-C. 2017. Preventive effect of celecoxib use against cancer progression and occurrence of oral squamous cell carcinoma. *Scientific Reports,* 7**,** 6235.

CIRIELLO, G., GATZA, M. L., BECK, A. H., WILKERSON, M. D., RHIE, S. K., PASTORE, A., ZHANG, H., MCLELLAN, M., YAU, C., KANDOTH, C., BOWLBY, R., SHEN, H., HAYAT, S., FIELDHOUSE, R., LESTER, S. C., TSE, G. M., FACTOR, R. E., COLLINS, L. C., ALLISON, K. H., CHEN, Y. Y., JENSEN, K., JOHNSON, N. B., OESTERREICH, S., MILLS, G. B., CHERNIACK, A. D., ROBERTSON, G., BENZ, C., SANDER, C., LAIRD, P. W., HOADLEY, K. A., KING, T. A. & PEROU, C. M. 2015. Comprehensive Molecular Portraits of Invasive Lobular Breast Cancer. *Cell,* 163**,** 506-19.

CIRILLO, L. A., LIN, F. R., CUESTA, I., FRIEDMAN, D., JARNIK, M. & ZARET, K. S. 2002. Opening of Compacted Chromatin by Early Developmental Transcription Factors HNF3 (FoxA) and GATA-4. *Molecular Cell,* 9**,** 279-289.

CIRILLO, L. A., MCPHERSON, C. E., BOSSARD, P., STEVENS, K., CHERIAN, S., SHIM, E. Y., CLARK, K. L., BURLEY, S. K. & ZARET, K. S. 1998. Binding of the winged-helix transcription factor HNF3 to a linker histone site on the nucleosome. *Embo j,* 17**,** 244-54.

CIRILLO, L. A. & ZARET, K. S. 1999. An early developmental transcription factor complex that is more stable on nucleosome core particles than on free DNA. *Mol Cell,* 4**,** 961-9.

CLARK, K. L., HALAY, E. D., LAI, E. & BURLEY, S. K. 1993. Co-crystal structure of the HNF-3/fork head DNA-recognition motif resembles histone H5. *Nature,* 364**,** 412-20.

CLARKE, R., LIU, M. C., BOUKER, K. B., GU, Z., LEE, R. Y., ZHU, Y., SKAAR, T. C., GOMEZ, B., O'BRIEN, K., WANG, Y. & HILAKIVI-CLARKE, L. A. 2003. Antiestrogen resistance in breast cancer and the role of estrogen receptor signaling. *Oncogene,* 22**,** 7316-7339.

COATES, A. S., KESHAVIAH, A., THÜRLIMANN, B., MOURIDSEN, H., MAURIAC, L., FORBES, J. F., PARIDAENS, R., CASTIGLIONE-GERTSCH, M., GELBER, R. D., COLLEONI, M., LÁNG, I., DEL MASTRO, L., SMITH, I., CHIRGWIN, J., NOGARET, J.-M., PIENKOWSKI, T., WARDLEY, A., JAKOBSEN, E. H., PRICE, K. N. & GOLDHIRSCH, A. 2007. Five Years of Letrozole Compared With Tamoxifen As Initial Adjuvant Therapy for Postmenopausal Women With Endocrine-Responsive Early Breast Cancer: Update of Study BIG 1-98. *Journal of Clinical Oncology,* 25**,** 486-492.

COLE, M. P., JONES, C. T. & TODD, I. D. 1971. A new anti-oestrogenic agent in late breast cancer. An early clinical appraisal of ICI46474. *Br J Cancer,* 25**,** 270-5.

COLE, P. A. & ROBINSON, C. H. 1990. Mechanism and inhibition of cytochrome P-450 aromatase. *J Med Chem,* 33**,** 2933-42.

CORNELISSEN, L. M., DRENTH, A. P., VAN DER BURG, E., DE BRUIJN, R., PRITCHARD, C. E. J., HUIJBERS, I. J., ZWART, W. & JONKERS, J. 2020. TRPS1 acts as a context-dependent regulator of mammary epithelial cell growth/differentiation and breast cancer development. *Genes Dev,* 34**,** 179-193.

CREIGHTON, C. J., FU, X., HENNESSY, B. T., CASA, A. J., ZHANG, Y., GONZALEZ-ANGULO, A. M., LLUCH, A., GRAY, J. W., BROWN, P. H., HILSENBECK, S. G., OSBORNE, C. K., MILLS, G. B., LEE, A. V. & SCHIFF, R. 2010. Proteomic and transcriptomic profiling reveals a link between the PI3K pathway and lower estrogen-receptor (ER) levels and activity in ER+ breast cancer. *Breast Cancer Research,* 12**,** R40.

CREIGHTON, C. J., MASSARWEH, S., HUANG, S., TSIMELZON, A., HILSENBECK, S. G., OSBORNE, C. K., SHOU, J., MALORNI, L. & SCHIFF, R. 2008. Development of resistance to targeted therapies transforms the clinically associated molecular profile subtype of breast tumor xenografts. *Cancer Res,* 68**,** 7493-501.

CURTIS, C., SHAH, S. P., CHIN, S.-F., TURASHVILI, G., RUEDA, O. M., DUNNING, M. J., SPEED, D., LYNCH, A. G., SAMARAJIWA, S., YUAN, Y., GRÄF, S., HA, G., HAFFARI, G., BASHASHATI, A., RUSSELL, R., MCKINNEY, S., GROUP, M., LANGERØD, A., GREEN, A., PROVENZANO, E., WISHART, G., PINDER, S., WATSON, P., MARKOWETZ, F., MURPHY, L., ELLIS, I., PURUSHOTHAM, A., BØRRESEN-DALE, A.-L., BRENTON, J. D., TAVARÉ, S., CALDAS, C. & APARICIO,

S. 2012. The genomic and transcriptomic architecture of 2,000 breast tumours reveals novel subgroups. *Nature,* 486**,** 346-352.

DANIELIAN, P. S., WHITE, R., LEES, J. A. & PARKER, M. G. 1992. Identification of a conserved region required for hormone dependent transcriptional activation by steroid hormone receptors. *Embo j,* 11**,** 1025-33.

DAUVOIS, S., WHITE, R. & PARKER, M. G. 1993. The antiestrogen ICI 182780 disrupts estrogen receptor nucleocytoplasmic shuttling. *J Cell Sci,* 106 (Pt 4)**,** 1377-88.

DAVIES, C., GODWIN, J., GRAY, R., CLARKE, M., CUTTER, D., DARBY, S., MCGALE, P., PAN, H. C., TAYLOR, C., WANG, Y. C., DOWSETT, M., INGLE, J. & PETO, R. 2011. Relevance of breast cancer hormone receptors and other factors to the efficacy of adjuvant tamoxifen: patient-level meta-analysis of randomised trials. *Lancet,* 378**,** 771-84.

DE AZAMBUJA, E., HOLMES, A. P., PICCART-GEBHART, M., HOLMES, E., DI COSIMO, S., SWABY, R. F., UNTCH, M., JACKISCH, C., LANG, I., SMITH, I., BOYLE, F., XU, B., BARRIOS, C. H., PEREZ, E. A., AZIM, H. A., JR., KIM, S. B., KUEMMEL, S., HUANG, C. S., VUYLSTEKE, P., HSIEH, R. K., GORBUNOVA, V., ENIU, A., DREOSTI, L., TAVARTKILADZE, N., GELBER, R. D., EIDTMANN, H. & BASELGA, J. 2014. Lapatinib with trastuzumab for HER2-positive early breast cancer (NeoALTTO): survival outcomes of a randomised, open-label, multicentre, phase 3 trial and their association with pathological complete response. *Lancet Oncol,* 15**,** 1137-46.

DE BRAEKELEER, E., AUFFRET, R., GARCÍA, J. R., PADILLA, J. M., FLETES, C. C., MOREL, F., DOUET-GUILBERT, N. & DE BRAEKELEER, M. 2013. Identification of NIPBL, a new ETV6 partner gene in t(5;12) (p13;p13)-associated acute megakaryoblastic leukemia. *Leuk Lymphoma,* 54**,** 423-4.

DEEKS, E. D. 2018. Fulvestrant: A Review in Advanced Breast Cancer Not Previously Treated with Endocrine Therapy. *Drugs,* 78**,** 131-137.

DEGRAFFENRIED, L. A., FRIEDRICHS, W. E., RUSSELL, D. H., DONZIS, E. J., MIDDLETON, A. K., SILVA, J. M., ROTH, R. A. & HIDALGO, M. 2004. Inhibition of mTOR activity restores tamoxifen response in breast cancer cells with aberrant Akt Activity. *Clin Cancer Res,* 10**,** 8059-67.

DEKKER, J., RIPPE, K., DEKKER, M. & KLECKNER, N. 2002. Capturing Chromosome Conformation. *Science,* 295**,** 1306-1311.

DELAGE-MOURROUX, R., MARTINI, P. G., CHOI, I., KRAICHELY, D. M., HOEKSEMA, J. & KATZENELLENBOGEN, B. S. 2000. Analysis of estrogen receptor interaction with a repressor of estrogen receptor activity (REA) and the regulation of estrogen receptor transcriptional activity by REA. *J Biol Chem,* 275**,** 35848-56.

DINE, J. & DENG, C.-X. 2013. Mouse models of BRCA1 and their application to breast cancer research. *Cancer and Metastasis Reviews,* 32**,** 25-37.

DIRENZO, J., SHANG, Y., PHELAN, M., SIF, S., MYERS, M., KINGSTON, R. & BROWN, M. 2000. BRG-1 is recruited to estrogen-responsive promoters and cooperates with factors involved in histone acetylation. *Mol Cell Biol,* 20**,** 7541-9.

DOBIN, A. & GINGERAS, T. R. 2015. Mapping RNA-seq Reads with STAR. *Curr Protoc Bioinformatics,* 51**,** 11.14.1-11.14.19.

EECKHOUTE, J., KEETON, E. K., LUPIEN, M., KRUM, S. A., CARROLL, J. S. & BROWN, M. 2007. Positive cross-regulatory loop ties GATA-3 to estrogen receptor alpha expression in breast cancer. *Cancer Res,* 67**,** 6477-83.

FARIDI, J., WANG, L., ENDEMANN, G. & ROTH, R. A. 2003. Expression of constitutively active Akt-3 in MCF-7 breast cancer cells reverses the estrogen and tamoxifen responsivity of these cells in vivo. *Clin Cancer Res,* 9**,** 2933-9.

FAWELL, S. E., WHITE, R., HOARE, S., SYDENHAM, M., PAGE, M. & PARKER, M. G. 1990. Inhibition of estrogen receptor-DNA binding by the "pure" antiestrogen ICI 164,384 appears to be mediated by impaired receptor dimerization. *Proc Natl Acad Sci U S A,* 87**,** 6883-7.

FERLAY, J., SOERJOMATARAM, I., DIKSHIT, R., ESER, S., MATHERS, C., REBELO, M., PARKIN, D. M., FORMAN, D. & BRAY, F. 2015. Cancer incidence and mortality worldwide: Sources, methods and major patterns in GLOBOCAN 2012. *International Journal of Cancer,* 136**,** E359-E386.

FINDLAY, V. J., LARUE, A. C., TURNER, D. P., WATSON, P. M. & WATSON, D. K. 2013. Understanding the role of ETS-mediated gene regulation in complex biological processes. *Adv Cancer Res,* 119**,** 1-61.

FINN, R. S., CROWN, J. P., LANG, I., BOER, K., BONDARENKO, I. M., KULYK, S. O., ETTL, J., PATEL, R., PINTER, T., SCHMIDT, M., SHPARYK, Y., THUMMALA, A. R., VOYTKO, N. L., FOWST, C., HUANG, X., KIM, S. T., RANDOLPH, S. & SLAMON, D. J. 2015. The cyclin-dependent kinase 4/6 inhibitor palbociclib in combination with letrozole versus letrozole alone as first-line treatment of oestrogen receptor-positive, HER2-negative, advanced breast cancer (PALOMA-1/TRIO-18): a randomised phase 2 study. *Lancet Oncol,* 16**,** 25-35.

FISHER, B., COSTANTINO, J. P., REDMOND, C. K., FISHER, E. R., WICKERHAM, D. L. & CRONIN, W. M. 1994. Endometrial cancer in tamoxifen-treated breast cancer patients: findings from the National Surgical Adjuvant Breast and Bowel Project (NSABP) B-14. *J Natl Cancer Inst,* 86**,** 527-37.

FORD, D., EASTON, D. F., STRATTON, M., NAROD, S., GOLDGAR, D., DEVILEE, P., BISHOP, D. T., WEBER, B., LENOIR, G., CHANG-CLAUDE, J., SOBOL, H., TEARE, M. D., STRUEWING, J., ARASON, A., SCHERNECK, S., PETO, J., REBBECK, T. R., TONIN, P., NEUHAUSEN, S., BARKARDOTTIR, R., EYFJORD, J., LYNCH, H., PONDER, B. A., GAYTHER, S. A., ZELADA-HEDMAN, M. & ET AL. 1998. Genetic heterogeneity and penetrance analysis of the BRCA1 and BRCA2 genes in breast cancer families. The Breast Cancer Linkage Consortium. *Am J Hum Genet,* 62**,** 676-89.

FU, X., JESELSOHN, R., PEREIRA, R., HOLLINGSWORTH, E. F., CREIGHTON, C. J., LI, F., SHEA, M., NARDONE, A., DE ANGELIS, C., HEISER, L. M., ANUR, P., WANG, N., GRASSO, C. S., SPELLMAN, P. T., GRIFFITH, O. L., TSIMELZON, A., GUTIERREZ, C., HUANG, S., EDWARDS, D. P., TRIVEDI, M. V., RIMAWI, M. F., LOPEZ-TERRADA, D., HILSENBECK, S. G., GRAY, J. W., BROWN, M., OSBORNE, C. K. & SCHIFF, R. 2016. FOXA1 overexpression mediates endocrine resistance by altering the ER transcriptome and IL-8 expression in ER-positive breast cancer. *Proc Natl Acad Sci U S A,* 113**,** E6600-e6609.

FULLWOOD, M. J., LIU, M. H., PAN, Y. F., LIU, J., XU, H., MOHAMED, Y. B., ORLOV, Y. L., VELKOV, S., HO, A., MEI, P. H., CHEW, E. G. Y., HUANG, P. Y. H.,

WELBOREN, W.-J., HAN, Y., OOI, H. S., ARIYARATNE, P. N., VEGA, V. B., LUO, Y., TAN, P. Y., CHOY, P. Y., WANSA, K. D. S. A., ZHAO, B., LIM, K. S., LEOW, S. C., YOW, J. S., JOSEPH, R., LI, H., DESAI, K. V., THOMSEN, J. S., LEE, Y. K., KARUTURI, R. K. M., HERVE, T., BOURQUE, G., STUNNENBERG, H. G., RUAN, X., CACHEUX-RATABOUL, V., SUNG, W.-K., LIU, E. T., WEI, C.-L., CHEUNG, E. & RUAN, Y. 2009. An oestrogen-receptor-α-bound human chromatin interactome. *Nature,* 462**,** 58-64.

FUQUA, S. A., SCHIFF, R., PARRA, I., MOORE, J. T., MOHSIN, S. K., OSBORNE, C. K., CLARK, G. M. & ALLRED, D. C. 2003. Estrogen receptor beta protein in human breast cancer: correlation with clinical tumor parameters. *Cancer Res,* 63**,** 2434-9.

GAO, N., LELAY, J., VATAMANIUK, M. Z., RIECK, S., FRIEDMAN, J. R. & KAESTNER, K. H. 2008. Dynamic regulation of Pdx1 enhancers by Foxa1 and Foxa2 is essential for pancreas development. *Genes Dev,* 22**,** 3435-48.

GARCÍA-PEDRERO, J. M., KISKINIS, E., PARKER, M. G. & BELANDIA, B. 2006. The SWI/SNF chromatin remodeling subunit BAF57 is a critical regulator of estrogen receptor function in breast cancer cells. *J Biol Chem,* 281**,** 22656-64.

GBURCIK, V. & PICARD, D. 2006. The cell-specific activity of the estrogen receptor alpha may be fine-tuned by phosphorylation-induced structural gymnastics. *Nuclear Receptor Signaling,* 4**,** e005.

GIANNI, L., PIENKOWSKI, T., IM, Y. H., ROMAN, L., TSENG, L. M., LIU, M. C., LLUCH, A., STAROSLAWSKA, E., DE LA HABA-RODRIGUEZ, J., IM, S. A., PEDRINI, J. L., POIRIER, B., MORANDI, P., SEMIGLAZOV, V., SRIMUNINNIMIT, V., BIANCHI, G., SZADO, T., RATNAYAKE, J., ROSS, G. & VALAGUSSA, P. 2012. Efficacy and safety of neoadjuvant pertuzumab and trastuzumab in women with locally advanced, inflammatory, or early HER2-positive breast cancer (NeoSphere): a randomised multicentre, open-label, phase 2 trial. *Lancet Oncol,* 13**,** 25-32.

GLASS, C. K. & ROSENFELD, M. G. 2000. The coregulator exchange in transcriptional functions of nuclear receptors. *Genes Dev,* 14**,** 121-41.

GLONT, S. E., PAPACHRISTOU, E. K., SAWLE, A., HOLMES, K. A., CARROLL, J. S. & SIERSBAEK, R. 2019. Identification of ChIP-seq and RIME grade antibodies for Estrogen Receptor alpha. *PLoS One,* 14**,** e0215340.

GOLUB, T. R., BARKER, G. F., LOVETT, M. & GILLILAND, D. G. 1994. Fusion of PDGF receptor beta to a novel ets-like gene, tel, in chronic myelomonocytic leukemia with t(5;12) chromosomal translocation. *Cell,* 77**,** 307-16.

GRØNTVED, L., JOHN, S., BAEK, S., LIU, Y., BUCKLEY, J. R., VINSON, C., AGUILERA, G. & HAGER, G. L. 2013. C/EBP maintains chromatin accessibility in liver and facilitates glucocorticoid receptor recruitment to steroid response elements. *Embo j,* 32**,** 1568-83.

GUTIERREZ, M. C., DETRE, S., JOHNSTON, S., MOHSIN, S. K., SHOU, J., ALLRED, D. C., SCHIFF, R., OSBORNE, C. K. & DOWSETT, M. 2005. Molecular changes in tamoxifen-resistant breast cancer: relationship between estrogen receptor, HER-2, and p38 mitogen-activated protein kinase. *J Clin Oncol,* 23**,** 2469-76.

HASSON, S. P., RUBINEK, T., RYVO, L. & WOLF, I. 2013. Endocrine resistance in breast cancer: focus on the phosphatidylinositol 3-kinase/akt/mammalian target of rapamycin signaling pathway. *Breast Care (Basel),* 8**,** 248-55.

HEERY, D. M., KALKHOVEN, E., HOARE, S. & PARKER, M. G. 1997. A signature motif in transcriptional co-activators mediates binding to nuclear receptors. *Nature,* 387**,** 733-736.

HISAMATSU, Y., TOKUNAGA, E., YAMASHITA, N., AKIYOSHI, S., OKADA, S., NAKASHIMA, Y., AISHIMA, S., MORITA, M., KAKEJI, Y. & MAEHARA, Y. 2012. Impact of FOXA1 expression on the prognosis of patients with hormone receptor-positive breast cancer. *Ann Surg Oncol,* 19**,** 1145-52.

HOLLENHORST, P. C., MCINTOSH, L. P. & GRAVES, B. J. 2011. Genomic and biochemical insights into the specificity of ETS transcription factors. *Annu Rev Biochem,* 80**,** 437-71.

HOLLINGSHEAD, L. M. & FAULDS, D. 1991. Idarubicin. *Drugs,* 42**,** 690-719.

HOLST, F. & SINGER, C. F. 2016. ESR1-Amplification-Associated Estrogen Receptor α Activity in Breast Cancer. *Trends Endocrinol Metab,* 27**,** 751-752.

HOLST, F., STAHL, P. R., RUIZ, C., HELLWINKEL, O., JEHAN, Z., WENDLAND, M., LEBEAU, A., TERRACCIANO, L., AL-KURAYA, K., JÄNICKE, F., SAUTER, G. & SIMON, R. 2007. Estrogen receptor alpha (ESR1) gene amplification is frequent in breast cancer. *Nat Genet,* 39**,** 655-60.

HONG, H., KOHLI, K., GARABEDIAN, M. J. & STALLCUP, M. R. 1997. GRIP1, a transcriptional coactivator for the AF-2 transactivation domain of steroid, thyroid, retinoid, and vitamin D receptors. *Mol Cell Biol,* 17**,** 2735-44.

HOSKINS, J. M., CAREY, L. A. & MCLEOD, H. L. 2009. CYP2D6 and tamoxifen: DNA matters in breast cancer. *Nature Reviews Cancer,* 9**,** 576-586.

HURTADO, A., HOLMES, K. A., ROSS-INNES, C. S., SCHMIDT, D. & CARROLL, J. S. 2011. FOXA1 is a key determinant of estrogen receptor function and endocrine response. *Nature genetics,* 43**,** 27-33.

HUTCHESON, I. R., KNOWLDEN, J. M., MADDEN, T.-A., BARROW, D., GEE, J. M. W., WAKELING, A. E. & NICHOLSON, R. I. 2003. Oestrogen Receptor-Mediated Modulation of the EGFR/MAPK Pathway in Tamoxifen-Resistant MCF-7 Cells. *Breast Cancer Research and Treatment,* 81**,** 81-93.

IBRAHIM, Y. H., GARCÍA-GARCÍA, C., SERRA, V., HE, L., TORRES-LOCKHART, K., PRAT, A., ANTON, P., COZAR, P., GUZMÁN, M., GRUESO, J., RODRÍGUEZ, O., CALVO, M. T., AURA, C., DÍEZ, O., RUBIO, I. T., PÉREZ, J., RODÓN, J., CORTÉS, J., ELLISEN, L. W., SCALTRITI, M. & BASELGA, J. 2012. PI3K inhibition impairs BRCA1/2 expression and sensitizes BRCA-proficient triple-negative breast cancer to PARP inhibition. *Cancer Discov,* 2**,** 1036-47.

INTERNATIONAL AGENCY FOR RESEARCH ON CANCER. 2019. *Breast cancer fact sheet* [Online]. Available: https://gco.iarc.fr/today/data/factsheets/cancers/20-Breast-fact-sheet.pdf [Accessed May 2020].

JAKACKA, M., ITO, M., WEISS, J., CHIEN, P. Y., GEHM, B. D. & JAMESON, J. L. 2001. Estrogen Receptor Binding to DNA Is Not Required for Its Activity through the Nonclassical AP1 Pathway*. *The Journal of Biological Chemistry,* 276**,** 13615 - 13621.

JANGAL, M., COUTURE, J. P., BIANCO, S., MAGNANI, L., MOHAMMED, H. & GÉVRY, N. 2014. The transcriptional co-repressor TLE3 suppresses basal signaling on a subset of estrogen receptor α target genes. *Nucleic Acids Res,* 42**,** 11339-48.

JENSEN, E. V. & JORDAN, V. C. 2003. The estrogen receptor: a model for molecular medicine. *Clin Cancer Res,* 9**,** 1980-9.

JESELSOHN, R., BERGHOLZ, J. S., PUN, M., CORNWELL, M., LIU, W., NARDONE, A., XIAO, T., LI, W., QIU, X., BUCHWALTER, G., FEIGLIN, A., ABELL-HART, K., FEI, T., RAO, P., LONG, H., KWIATKOWSKI, N., ZHANG, T., GRAY, N., MELCHERS, D., HOUTMAN, R., LIU, X. S., COHEN, O., WAGLE, N., WINER, E. P., ZHAO, J. & BROWN, M. 2018. Allele-Specific Chromatin Recruitment and Therapeutic Vulnerabilities of ESR1 Activating Mutations. *Cancer cell,* 33**,** 173-186.e5.

JESELSOHN, R., YELENSKY, R., BUCHWALTER, G., FRAMPTON, G., MERIC-BERNSTAM, F., GONZALEZ-ANGULO, A. M., FERRER-LOZANO, J., PEREZ-FIDALGO, J. A., CRISTOFANILLI, M., GÓMEZ, H., ARTEAGA, C. L., GILTNANE, J., BALKO, J. M., CRONIN, M. T., JAROSZ, M., SUN, J., HAWRYLUK, M., LIPSON, D., OTTO, G., ROSS, J. S., DVIR, A., SOUSSAN-GUTMAN, L., WOLF, I., RUBINEK, T., GILMORE, L., SCHNITT, S., COME, S. E., PUSZTAI, L., STEPHENS, P., BROWN, M. & MILLER, V. A. 2014. Emergence of constitutively active estrogen receptor-α mutations in pretreated advanced estrogen receptor-positive breast cancer. *Clin Cancer Res,* 20**,** 1757-1767.

JIA, R., CHAI, P., ZHANG, H. & FAN, X. 2017. Novel insights into chromosomal conformations in cancer. *Mol Cancer,* 16**,** 173.

JORDAN, V. C. 1994. Molecular mechanisms of antiestrogen action in breast cancer. *Breast cancer research and treatment,* 31**,** 41-52.

JOZWIK, K. M. & CARROLL, J. S. 2012. Pioneer factors in hormone-dependent cancers. *Nat Rev Cancer,* 12**,** 381-5.

JUNPAPARP, P., SHARMA, B., SAMIAPPAN, A., RHEE, J. H. & YOUNG, K. R. 2013. Everolimus-induced severe pulmonary toxicity with diffuse alveolar hemorrhage. *Ann Am Thorac Soc,* 10**,** 727-9.

KARIM, F. D., URNESS, L. D., THUMMEL, C. S., KLEMSZ, M. J., MCKERCHER, S. R., CELADA, A., VAN BEVEREN, C., MAKI, R. A., GUNTHER, C. V., NYE, J. A. & ET AL. 1990. The ETS-domain: a new DNA-binding motif that recognizes a purine-rich core DNA sequence. *Genes Dev,* 4**,** 1451-3.

KASTRATI, I., SEMINA, S., GORDON, B. & SMART, E. 2019. Insights into how phosphorylation of estrogen receptor at serine 305 modulates tamoxifen activity in breast cancer. *Mol Cell Endocrinol,* 483**,** 97-101.

KAUFMAN, B., MACKEY, J. R., CLEMENS, M. R., BAPSY, P. P., VAID, A., WARDLEY, A., TJULANDIN, S., JAHN, M., LEHLE, M., FEYEREISLOVA, A., RÉVIL, C. & JONES, A. 2009. Trastuzumab plus anastrozole versus anastrozole alone for the treatment of postmenopausal women with human epidermal growth factor receptor 2-positive, hormone receptor-positive metastatic breast cancer: results from the randomized phase III TAnDEM study. *J Clin Oncol,* 27**,** 5529-37.

KEY, T. J., VERKASALO, P. K. & BANKS, E. 2001. Epidemiology of breast cancer. *Lancet Oncol,* 2**,** 133-40.

KLÄMBT, C. 1993. The Drosophila gene pointed encodes two ETS-like proteins which are involved in the development of the midline glial cells. *Development,* 117**,** 163-76.

KLEIN-HITPASS, L., TSAI, S. Y., GREENE, G. L., CLARK, J. H., TSAI, M. J. & O'MALLEY, B. W. 1989. Specific binding of estrogen receptor to the estrogen response element. *Mol Cell Biol,* 9**,** 43-9.

KLINGE, C. M. 2001. Estrogen receptor interaction with estrogen response elements. *Nucleic Acids Research,* 29**,** 2905-2919.

KNOWLDEN, J. M., HUTCHESON, I. R., BARROW, D., GEE, J. M. & NICHOLSON, R. I. 2005. Insulin-like growth factor-I receptor signaling in tamoxifen-resistant breast cancer: a supporting role to the epidermal growth factor receptor. *Endocrinology,* 146**,** 4609-18.

KOBOLDT, D. C., FULTON, R. S., MCLELLAN, M. D., SCHMIDT, H., KALICKI-VEIZER, J., MCMICHAEL, J. F., FULTON, L. L., DOOLING, D. J., DING, L., MARDIS, E. R., WILSON, R. K., ALLY, A., BALASUNDARAM, M., BUTTERFIELD, Y. S. N., CARLSEN, R., CARTER, C., CHU, A., CHUAH, E., CHUN, H.-J. E., COOPE, R. J. N., DHALLA, N., GUIN, R., HIRST, C., HIRST, M., HOLT, R. A., LEE, D., LI, H. I., MAYO, M., MOORE, R. A., MUNGALL, A. J., PLEASANCE, E., GORDON ROBERTSON, A., SCHEIN, J. E., SHAFIEI, A., SIPAHIMALANI, P., SLOBODAN, J. R., STOLL, D., TAM, A., THIESSEN, N., VARHOL, R. J., WYE, N., ZENG, T., ZHAO, Y., BIROL, I., JONES, S. J. M., MARRA, M. A., CHERNIACK, A. D., SAKSENA, G., ONOFRIO, R. C., PHO, N. H., CARTER, S. L., SCHUMACHER, S. E., TABAK, B., HERNANDEZ, B., GENTRY, J., NGUYEN, H., CRENSHAW, A., ARDLIE, K., BEROUKHIM, R., WINCKLER, W., GETZ, G., GABRIEL, S. B., MEYERSON, M., CHIN, L., PARK, P. J., KUCHERLAPATI, R., HOADLEY, K. A., TODD AUMAN, J., FAN, C., TURMAN, Y. J., SHI, Y., LI, L., TOPAL, M. D., HE, X., CHAO, H.-H., PRAT, A., SILVA, G. O., IGLESIA, M. D., ZHAO, W., USARY, J., BERG, J. S., ADAMS, M., BOOKER, J., WU, J., GULABANI, A., BODENHEIMER, T., HOYLE, A. P., SIMONS, J. V., SOLOWAY, M. G., MOSE, L. E., JEFFERYS, S. R., BALU, S., PARKER, J. S., NEIL HAYES, D., PEROU, C. M., MALIK, S., MAHURKAR, S., SHEN, H., WEISENBERGER, D. J., TRICHE JR, T., et al. 2012. Comprehensive molecular portraits of human breast tumours. *Nature,* 490**,** 61-70.

KOHLER, S. & CIRILLO, L. A. 2010. Stable chromatin binding prevents FoxA acetylation, preserving FoxA chromatin remodeling. *J Biol Chem,* 285**,** 464-72.

KOIDE, A., ZHAO, C., NAGANUMA, M., ABRAMS, J., DEIGHTON-COLLINS, S., SKAFAR, D. F. & KOIDE, S. 2007. Identification of regions within the F domain of the human estrogen receptor alpha that are important for modulating transactivation and protein-protein interactions. *Mol Endocrinol,* 21**,** 829-42.

KRALIK, J. M., KRANEWITTER, W., BOESMUELLER, H., MARSCHON, R., TSCHURTSCHENTHALER, G., RUMPOLD, H., WIESINGER, K., ERDEL, M., PETZER, A. L. & WEBERSINKE, G. 2011. Characterization of a newly identified ETV6-NTRK3 fusion transcript in acute myeloid leukemia. *Diagn Pathol,* 6**,** 19.

KRESSLER, D., HOCK, M. B. & KRALLI, A. 2007. Coactivators PGC-1beta and SRC-1 interact functionally to promote the agonist activity of the selective estrogen receptor modulator tamoxifen. *J Biol Chem,* 282**,** 26897-907.

KUIPER, G. G., ENMARK, E., PELTO-HUIKKO, M., NILSSON, S. & GUSTAFSSON, J. A. 1996. Cloning of a novel receptor expressed in rat prostate and ovary. *Proc Natl Acad Sci U S A,* 93**,** 5925-30.

KUMAR, R., ZAKHAROV, M. N., KHAN, S. H., MIKI, R., JANG, H., TORALDO, G., SINGH, R., BHASIN, S. & JASUJA, R. 2011. The Dynamic Structure of the Estrogen Receptor. *Journal of Amino Acids,* 2011**,** 812540.

KÜMLER, I., BRÜNNER, N., STENVANG, J., BALSLEV, E. & NIELSEN, D. L. 2013. A systematic review on topoisomerase 1 inhibition in the treatment of metastatic breast cancer. *Breast Cancer Res Treat,* 138**,** 347-58.

LACRONIQUE, V., BOUREUX, A., VALLE, V. D., POIREL, H., QUANG, C. T., MAUCHAUFFÉ, M., BERTHOU, C., LESSARD, M., BERGER, R., GHYSDAEL, J. & BERNARD, O. A. 1997. A TEL-JAK2 fusion protein with constitutive kinase activity in human leukemia. *Science,* 278**,** 1309-12.

LANGMEAD, B. & SALZBERG, S. L. 2012. Fast gapped-read alignment with Bowtie 2. *Nature Methods,* 9**,** 357-359.

LAVINSKY, R. M., JEPSEN, K., HEINZEL, T., TORCHIA, J., MULLEN, T. M., SCHIFF, R., DEL-RIO, A. L., RICOTE, M., NGO, S., GEMSCH, J., HILSENBECK, S. G., OSBORNE, C. K., GLASS, C. K., ROSENFELD, M. G. & ROSE, D. W. 1998. Diverse signaling pathways modulate nuclear receptor recruitment of N-CoR and SMRT complexes. *Proc Natl Acad Sci U S A,* 95**,** 2920-5.

LAZAR, M. A. 2003. Nuclear receptor corepressors. *Nucl Recept Signal,* 1**,** e001.

LAZARUS, H. M., BELANGER, R., CANDONI, A., AOUN, M., JUREWICZ, R. & MARKS, L. 1999. Intravenous penciclovir for treatment of herpes simplex infections in immunocompromised patients: results of a multicenter, acyclovir-controlled trial. The Penciclovir Immunocompromised Study Group. *Antimicrob Agents Chemother,* 43**,** 1192-7.

LE ROMANCER, M., POULARD, C., COHEN, P., SENTIS, S., RENOIR, J. M. & CORBO, L. 2011. Cracking the estrogen receptor's posttranslational code in breast tumors. *Endocr Rev,* 32**,** 597-622.

LEI, J. T., SHAO, J., ZHANG, J., IGLESIA, M., CHAN, D. W., CAO, J., ANURAG, M., SINGH, P., HE, X., KOSAKA, Y., MATSUNUMA, R., CROWDER, R., HOOG, J., PHOMMALY, C., GONCALVES, R., RAMALHO, S., PERES, R. M. R., PUNTURI, N., SCHMIDT, C., BARTRAM, A., JOU, E., DEVARAKONDA, V., HOLLOWAY, K. R., LAI, W. V., HAMPTON, O., ROGERS, A., TOBIAS, E., PARIKH, P. A., DAVIES, S. R., LI, S., MA, C. X., SUMAN, V. J., HUNT, K. K., WATSON, M. A., HOADLEY, K. A., THOMPSON, E. A., CHEN, X., KAVURI, S. M., CREIGHTON, C. J., MAHER, C. A., PEROU, C. M., HARICHARAN, S. & ELLIS, M. J. 2018. Functional Annotation of ESR1 Gene Fusions in Estrogen Receptor-Positive Breast Cancer. *Cell Rep,* 24**,** 1434-1444.e7.

LI, C. I., MALONE, K. E. & DALING, J. R. 2003. Differences in breast cancer stage, treatment, and survival by race and ethnicity. *Arch Intern Med,* 163**,** 49-56.

LIN, C. Y., VEGA, V. B., THOMSEN, J. S., ZHANG, T., KONG, S. L., XIE, M., CHIU, K. P., LIPOVICH, L., BARNETT, D. H., STOSSI, F., YEO, A., GEORGE, J., KUZNETSOV, V. A., LEE, Y. K., CHARN, T. H., PALANISAMY, N., MILLER, L. D., CHEUNG, E., KATZENELLENBOGEN, B. S., RUAN, Y., BOURQUE, G., WEI, C. L. & LIU, E. T. 2007. Whole-genome cartography of estrogen receptor alpha binding sites. *PLoS Genet,* 3**,** e87.

LIN, H. F., LIAO, K. F., CHANG, C. M., LIN, C. L., LAI, S. W. & HSU, C. Y. 2018. Correlation of the tamoxifen use with the increased risk of deep vein thrombosis and pulmonary embolism in elderly women with breast cancer: A case-control study. *Medicine (Baltimore),* 97**,** e12842.

LIU, J. K., DIPERSIO, C. M. & ZARET, K. S. 1991. Extracellular signals that regulate liver transcription factors during hepatic differentiation in vitro. *Mol Cell Biol,* 11**,** 773-84.

LIU, Y. Q., LI, W. Q., MORRIS-NATSCHKE, S. L., QIAN, K., YANG, L., ZHU, G. X., WU, X. B., CHEN, A. L., ZHANG, S. Y., NAN, X. & LEE, K. H. 2015. Perspectives on biologically active camptothecin derivatives. *Med Res Rev,* 35**,** 753-89.

LIVAK, K. J. & SCHMITTGEN, T. D. 2001. Analysis of relative gene expression data using real-time quantitative PCR and the 2(-Delta Delta C(T)) Method. *Methods,* 25**,** 402-8.

LÖFLING, L., SUNDSTRÖM, A., KIELER, H., BAHMANYAR, S. & LINDER, M. 2019. Exposure to antimuscarinic medications for treatment of overactive bladder and risk of lung cancer and colon cancer. *Clin Epidemiol,* 11**,** 133-143.

LOVE, M. I., HUBER, W. & ANDERS, S. 2014. Moderated estimation of fold change and dispersion for RNA-seq data with DESeq2. *Genome Biol,* 15**,** 550.

LUN, X., WELLS, J. C., GRINSHTEIN, N., KING, J. C., HAO, X., DANG, N. H., WANG, X., AMAN, A., UEHLING, D., DATTI, A., WRANA, J. L., EASAW, J. C., LUCHMAN, A., WEISS, S., CAIRNCROSS, J. G., KAPLAN, D. R., ROBBINS, S. M. & SENGER, D. L. 2016. Disulfiram when Combined with Copper Enhances the Therapeutic Effects of Temozolomide for the Treatment of Glioblastoma. *Clin Cancer Res,* 22**,** 3860-75.

LUPIEN, M., EECKHOUTE, J., MEYER, C. A., KRUM, S. A., RHODES, D. R., LIU, X. S. & BROWN, M. 2009. Coactivator Function Defines the Active Estrogen Receptor Alpha Cistrome. *Molecular and Cellular Biology,* 29**,** 3413 - 3423.

LUPIEN, M., EECKHOUTE, J., MEYER, C. A., WANG, Q., ZHANG, Y., LI, W., CARROLL, J. S., LIU, X. S. & BROWN, M. 2008. FoxA1 translates epigenetic signatures into enhancer-driven lineage-specific transcription. *Cell,* 132**,** 958-70.

MAGNANI, L., BALLANTYNE, E. B., ZHANG, X. & LUPIEN, M. 2011. PBX1 genomic pioneer function drives ERα signaling underlying progression in breast cancer. *PLoS Genet,* 7**,** e1002368.

MARTELOTTO, L. G., NG, C. K., PISCUOGLIO, S., WEIGELT, B. & REIS-FILHO, J. S. 2014. Breast cancer intra-tumor heterogeneity. *Breast Cancer Res,* 16**,** 210.

MASSARWEH, S., OSBORNE, C. K., CREIGHTON, C. J., QIN, L., TSIMELZON, A., HUANG, S., WEISS, H., RIMAWI, M. & SCHIFF, R. 2008. Tamoxifen resistance in breast tumors is driven by growth factor receptor signaling with repression of classic estrogen receptor genomic function. *Cancer Res,* 68**,** 826-33.

MCCLELLAND, R. A., BARROW, D., MADDEN, T.-A., DUTKOWSKI, C. M., PAMMENT, J., KNOWLDEN, J. M., GEE, J. M. W. & NICHOLSON, R. I. 2001. Enhanced Epidermal Growth Factor Receptor Signaling in MCF7 Breast Cancer Cells after Long-Term Culture in the Presence of the Pure Antiestrogen ICI 182,780 (Faslodex)*. *Endocrinology,* 142**,** 2776-2788.

MCLEAN, C. Y., BRISTOR, D., HILLER, M., CLARKE, S. L., SCHAAR, B. T., LOWE, C. B., WENGER, A. M. & BEJERANO, G. 2010. GREAT improves functional interpretation of cis-regulatory regions. *Nat Biotechnol,* 28**,** 495-501.

MEHRA, R., TOMLINS, S. A., SHEN, R., NADEEM, O., WANG, L., WEI, J. T., PIENTA, K. J., GHOSH, D., RUBIN, M. A., CHINNAIYAN, A. M. & SHAH, R. B. 2007. Comprehensive assessment of TMPRSS2 and ETS family gene aberrations in clinically localized prostate cancer. *Mod Pathol,* 20**,** 538-44.

MÉNDEZ, J. & STILLMAN, B. 2000. Chromatin association of human origin recognition complex, cdc6, and minichromosome maintenance proteins during the cell cycle: assembly of prereplication complexes in late mitosis. *Mol Cell Biol,* 20**,** 8602-12.

MESQUITA, B., LOPES, P., RODRIGUES, A., PEREIRA, D., AFONSO, M., LEAL, C., HENRIQUE, R., LIND, G. E., JERÓNIMO, C., LOTHE, R. A. & TEIXEIRA, M. R. 2013. Frequent copy number gains at 1q21 and 1q32 are associated with overexpression of the ETS transcription factors ETV3 and ELF3 in breast cancer irrespective of molecular subtypes. *Breast Cancer Res Treat,* 138**,** 37-45.

MIKI, Y., SWENSEN, J., SHATTUCK-EIDENS, D., FUTREAL, P., HARSHMAN, K., TAVTIGIAN, S., LIU, Q., COCHRAN, C., BENNETT, L., DING, W. & ET, A. 1994. A strong candidate for the breast and ovarian cancer susceptibility gene BRCA1. *Science,* 266**,** 66-71.

MILLER, W. R. 2003. Aromatase inhibitors: mechanism of action and role in the treatment of breast cancer. *Semin Oncol,* 30**,** 3-11.

MILLS, J. N., RUTKOVSKY, A. C. & GIORDANO, A. 2018. Mechanisms of resistance in estrogen receptor positive breast cancer: overcoming resistance to tamoxifen/aromatase inhibitors. *Curr Opin Pharmacol,* 41**,** 59-65.

MIRANDA, T. B., VOSS, T. C., SUNG, M. H., BAEK, S., JOHN, S., HAWKINS, M., GRØNTVED, L., SCHILTZ, R. L. & HAGER, G. L. 2013. Reprogramming the chromatin landscape: interplay of the estrogen and glucocorticoid receptors at the genomic level. *Cancer Res,* 73**,** 5130-9.

MOHAMMED, H., D'SANTOS, C., SERANDOUR, AURELIEN A., ALI, H. R., BROWN, GORDON D., ATKINS, A., RUEDA, OSCAR M., HOLMES, KELLY A., THEODOROU, V., ROBINSON, JESSICA L. L., ZWART, W., SAADI, A., ROSS-INNES, CARYN S., CHIN, S.-F., MENON, S., STINGL, J., PALMIERI, C., CALDAS, C. & CARROLL, JASON S. 2013. Endogenous Purification Reveals GREB1 as a Key Estrogen Receptor Regulatory Factor. *Cell Reports,* 3**,** 342-349.

MONTANO, M. M., MÜLLER, V., TROBAUGH, A. & KATZENELLENBOGEN, B. S. 1995. The carboxy-terminal F domain of the human estrogen receptor: role in the transcriptional activity of the receptor and the effectiveness of antiestrogens as estrogen antagonists. *Mol Endocrinol,* 9**,** 814-25.

MORIYAMA, T., METZGER, M. L., WU, G., NISHII, R., QIAN, M., DEVIDAS, M., YANG, W., CHENG, C., CAO, X., QUINN, E., RAIMONDI, S., GASTIER-FOSTER, J. M., RAETZ, E., LARSEN, E., MARTIN, P. L., BOWMAN, W. P., WINICK, N., KOMADA, Y., WANG, S., EDMONSON, M., XU, H., MARDIS, E., FULTON, R., PUI, C. H., MULLIGHAN, C., EVANS, W. E., ZHANG, J., HUNGER, S. P., RELLING, M. V., NICHOLS, K. E., LOH, M. L. & YANG, J. J. 2015. Germline genetic variation in

ETV6 and risk of childhood acute lymphoblastic leukaemia: a systematic genetic study. *Lancet Oncol,* 16**,** 1659-66.

MOURAD, R., HSU, P. Y., JUAN, L., SHEN, C., KONERU, P., LIN, H., LIU, Y., NEPHEW, K., HUANG, T. H. & LI, L. 2014. Estrogen induces global reorganization of chromatin structure in human breast cancer cells. *PLoS One,* 9**,** e113354.

MUSGROVE, E. A. & SUTHERLAND, R. L. 2009. Biological determinants of endocrine resistance in breast cancer. *Nature Reviews Cancer,* 9**,** 631-643.

NAKSHATRI, H. & BADVE, S. 2007. FOXA1 as a therapeutic target for breast cancer. *Expert Opin Ther Targets,* 11**,** 507-14.

NAKSHATRI, H. & BADVE, S. 2009. FOXA1 in breast cancer. *Expert Rev Mol Med,* 11**,** e8.

NAMBOODIRI, A. M. & PANDEY, J. P. 2011. Differential inhibition of trastuzumab- and cetuximab-induced cytotoxicity of cancer cells by immunoglobulin G1 expressing different GM allotypes. *Clin Exp Immunol,* 166**,** 361-5.

NAZARALI, S. A. & NAROD, S. A. 2014. Tamoxifen for women at high risk of breast cancer. *Breast Cancer (Dove Med Press),* 6**,** 29-36.

NEISH, A. S., ANDERSON, S. F., SCHLEGEL, B. P., WEI, W. & PARVIN, J. D. 1998. Factors associated with the mammalian RNA polymerase II holoenzyme. *Nucleic Acids Res,* 26**,** 847-53.

NEMBROT, M., QUINTANA, B. & MORDOH, J. 1990. Estrogen receptor gene amplification is found in some estrogen receptor-positive human breast tumors. *Biochem Biophys Res Commun,* 166**,** 601-7.

NICHOLSON, R. I., HUTCHESON, I. R., HISCOX, S. E., KNOWLDEN, J. M., GILES, M., BARROW, D. & GEE, J. M. 2005. Growth factor signalling and resistance to selective oestrogen receptor modulators and pure anti-oestrogens: the use of anti-growth factor therapies to treat or delay endocrine resistance in breast cancer. *Endocr Relat Cancer,* 12 Suppl 1**,** S29-36.

NOWAK-SLIWINSKA, P., SCAPOZZA, L. & RUIZ, I. A. A. 2019. Drug repurposing in oncology: Compounds, pathways, phenotypes and computational approaches for colorectal cancer. *Biochim Biophys Acta Rev Cancer,* 1871**,** 434-454.

ODERO, M. D., CARLSON, K., CALASANZ, M. J., LAHORTIGA, I., CHINWALLA, V. & ROWLEY, J. D. 2001. Identification of new translocations involving ETV6 in hematologic malignancies by fluorescence in situ hybridization and spectral karyotyping. *Genes Chromosomes Cancer,* 31**,** 134-42.

OKINES, A. F. 2017. T-DM1 in the Neo-Adjuvant Treatment of HER2-Positive Breast Cancer: Impact of the KRISTINE (TRIO-021) Trial. *Rev Recent Clin Trials,* 12**,** 216-222.

OÑATE, S. A., TSAI, S. Y., TSAI, M. J. & O'MALLEY, B. W. 1995. Sequence and characterization of a coactivator for the steroid hormone receptor superfamily. *Science,* 270**,** 1354-7.

ONISHCHENKO, A. L., ISAKOV, I. N., KOLBASKO, A. V. & MAKOGON, S. I. 2019. [Initial combination therapy for primary open-angle glaucoma]. *Vestn Oftalmol,* 135**,** 32-38.

OSBORNE, C. K. & SCHIFF, R. 2011. Mechanisms of endocrine resistance in breast cancer. *Annu Rev Med,* 62**,** 233-47.

OVERDIER, D. G., PORCELLA, A. & COSTA, R. H. 1994. The DNA-binding specificity of the hepatocyte nuclear factor 3/forkhead domain is influenced by amino-acid residues adjacent to the recognition helix. *Mol Cell Biol,* 14**,** 2755-66.

PANI, L., OVERDIER, D. G., PORCELLA, A., QIAN, X., LAI, E. & COSTA, R. H. 1992. Hepatocyte nuclear factor 3 beta contains two transcriptional activation domains, one of which is novel and conserved with the Drosophila fork head protein. *Mol Cell Biol,* 12**,** 3723-32.

PAPACHRISTOU, E. K., KISHORE, K., HOLDING, A. N., HARVEY, K., ROUMELIOTIS, T. I., CHILAMAKURI, C. S. R., OMARJEE, S., CHIA, K. M., SWARBRICK, A., LIM, E., MARKOWETZ, F., ELDRIDGE, M., SIERSBAEK, R., D'SANTOS, C. S. & CARROLL, J. S. 2018. A quantitative mass spectrometry-based approach to monitor the dynamics of endogenous chromatin-associated protein complexes. *Nature Communications,* 9**,** 2311.

PEREIRA, B., CHIN, S.-F., RUEDA, O. M., VOLLAN, H.-K. M., PROVENZANO, E., BARDWELL, H. A., PUGH, M., JONES, L., RUSSELL, R., SAMMUT, S.-J., TSUI, D. W. Y., LIU, B., DAWSON, S.-J., ABRAHAM, J., NORTHEN, H., PEDEN, J. F., MUKHERJEE, A., TURASHVILI, G., GREEN, A. R., MCKINNEY, S., OLOUMI, A., SHAH, S., ROSENFELD, N., MURPHY, L., BENTLEY, D. R., ELLIS, I. O., PURUSHOTHAM, A., PINDER, S. E., BØRRESEN-DALE, A.-L., EARL, H. M., PHAROAH, P. D., ROSS, M. T., APARICIO, S. & CALDAS, C. 2016. The somatic mutation profiles of 2,433 breast cancers refine their genomic and transcriptomic landscapes. *Nature Communications,* 7**,** 11479.

PEROU, C. M., SØRLIE, T., EISEN, M. B., VAN DE RIJN, M., JEFFREY, S. S., REES, C. A., POLLACK, J. R., ROSS, D. T., JOHNSEN, H., AKSLEN, L. A., FLUGE, Ø., PERGAMENSCHIKOV, A., WILLIAMS, C., ZHU, S. X., LØNNING, P. E., BØRRESEN-DALE, A.-L., BROWN, P. O. & BOTSTEIN, D. 2000. Molecular portraits of human breast tumours. *Nature,* 406**,** 747-752.

PORTER, W., SAVILLE, B., HOIVIK, D. & SAFE, S. 1997. Functional synergy between the transcription factor Sp1 and the estrogen receptor. *Mol Endocrinol,* 11**,** 1569-80.

RAE, J. M., JOHNSON, M. D., SCHEYS, J. O., CORDERO, K. E., LARIOS, J. M. & LIPPMAN, M. E. 2005. GREB1 is a critical regulator of hormone dependent breast cancer growth. *Breast Cancer Research and Treatment,* 92**,** 141-149.

RAHMAN, M., SELVARAJAN, K., HASAN, M. R., CHAN, A. P., JIN, C., KIM, J., CHAN, S. K., LE, N. D., KIM, Y. B. & TAI, I. T. 2012. Inhibition of COX-2 in colon cancer modulates tumor growth and MDR-1 expression to enhance tumor regression in therapy-refractory cancers in vivo. *Neoplasia,* 14**,** 624-33.

RASTINEJAD, F., HUANG, P., CHANDRA, V. & KHORASANIZADEH, S. 2013. Understanding nuclear receptor form and function using structural biology. *Journal of molecular endocrinology,* 51**,** T1-T21.

RIPPERGER, T., GADZICKI, D., MEINDL, A. & SCHLEGELBERGER, B. 2009. Breast cancer susceptibility: current knowledge and implications for genetic counselling. *Eur J Hum Genet,* 17**,** 722-31.

ROBINSON, D. R., WU, Y.-M., VATS, P., SU, F., LONIGRO, R. J., CAO, X., KALYANA-SUNDARAM, S., WANG, R., NING, Y., HODGES, L., GURSKY, A., SIDDIQUI, J., TOMLINS, S. A., ROYCHOWDHURY, S., PIENTA, K. J., KIM, S. Y., ROBERTS, J. S., RAE, J. M., VAN POZNAK, C. H., HAYES, D. F., CHUGH, R., KUNJU, L. P., TALPAZ, M., SCHOTT, A. F. & CHINNAIYAN, A. M. 2013. Activating ESR1 mutations in hormone-resistant metastatic breast cancer. *Nature genetics,* 45**,** 1446-51.

ROLLINS, D. A., COPPO, M. & ROGATSKY, I. 2015. Minireview: nuclear receptor coregulators of the p160 family: insights into inflammation and metabolism. *Molecular endocrinology,* 29**,** 502-517.

ROSS-INNES, C. S., STARK, R., TESCHENDORFF, A. E., HOLMES, K. A., ALI, H. R., DUNNING, M. J., BROWN, G. D., GOJIS, O., ELLIS, I. O., GREEN, A. R., ALI, S., CHIN, S.-F., PALMIERI, C., CALDAS, C. & CARROLL, J. S. 2012a. Differential oestrogen receptor binding is associated with clinical outcome in breast cancer. *Nature,* 481**,** 389-93.

ROSS-INNES, C. S., STARK, R., TESCHENDORFF, A. E., HOLMES, K. A., ALI, H. R., DUNNING, M. J., BROWN, G. D., GOJIS, O., ELLIS, I. O., GREEN, A. R., ALI, S., CHIN, S. F., PALMIERI, C., CALDAS, C. & CARROLL, J. S. 2012b. Differential oestrogen receptor binding is associated with clinical outcome in breast cancer. *Nature,* 481**,** 389-93.

RUEDA, O. M., SAMMUT, S.-J., SEOANE, J. A., CHIN, S.-F., CASWELL-JIN, J. L., CALLARI, M., BATRA, R., PEREIRA, B., BRUNA, A., ALI, H. R., PROVENZANO, E., LIU, B., PARISIEN, M., GILLETT, C., MCKINNEY, S., GREEN, A. R., MURPHY, L., PURUSHOTHAM, A., ELLIS, I. O., PHAROAH, P. D., RUEDA, C., APARICIO, S., CALDAS, C. & CURTIS, C. 2019. Dynamics of breast-cancer relapse reveal late-recurring ER-positive genomic subgroups. *Nature,* 567**,** 399-404.

RYAN, A. J., SQUIRES, S., STRUTT, H. L. & JOHNSON, R. T. 1991. Camptothecin cytotoxicity in mammalian cells is associated with the induction of persistent double strand breaks in replicating DNA. *Nucleic Acids Res,* 19**,** 3295-300.

SCHMIDT, D., WILSON, M. D., SPYROU, C., BROWN, G. D., HADFIELD, J. & ODOM, D. T. 2009. ChIP-seq: Using high-throughput sequencing to discover protein–DNA interactions. *Methods,* 48**,** 240-248.

SERANDOUR, A. A., MOHAMMED, H., MIREMADI, A., MULDER, K. W. & CARROLL, J. S. 2018. TRPS1 regulates oestrogen receptor binding and histone acetylation at enhancers. *Oncogene,* 37**,** 5281-5291.

SHANG, Y., HU, X., DIRENZO, J., LAZAR, M. A. & BROWN, M. 2000. Cofactor dynamics and sufficiency in estrogen receptor-regulated transcription. *Cell,* 103**,** 843-52.

SOOD, A. K., GERADTS, J. & YOUNG, J. 2017. Prostate-derived Ets factor, an oncogenic driver in breast cancer. *Tumour Biol,* 39**,** 1010428317691688.

SØRLIE, T., PEROU, C. M., TIBSHIRANI, R., AAS, T., GEISLER, S., JOHNSEN, H., HASTIE, T., EISEN, M. B., VAN DE RIJN, M., JEFFREY, S. S., THORSEN, T., QUIST, H., MATESE, J. C., BROWN, P. O., BOTSTEIN, D., LØNNING, P. E. & BØRRESEN-DALE, A.-L. 2001. Gene expression patterns of breast carcinomas distinguish tumor subclasses with clinical implications. *Proceedings of the National Academy of Sciences,* 98**,** 10869-10874.

SPORN, M. B. & LIPPMAN, S. M. 2003. Agents for Chemoprevention and Their Mechanism of Action.

SQUIRE, J. A. 2009. TMPRSS2-ERG and PTEN loss in prostate cancer. *Nature Genetics,* 41**,** 509-510.

STARK, R. & BROWN, G. D. DiffBind: differential binding analysis of ChIP-Seq peak data. *Bioconductor,* http://www.http://http://bioconductor.org/packages/release/bioc/html/DiffBind.html.

STENDER, J. D., KIM, K., CHARN, T. H., KOMM, B., CHANG, K. C. N., KRAUS, W. L., BENNER, C., GLASS, C. K. & KATZENELLENBOGEN, B. S. 2010. Genome-wide analysis of estrogen receptor alpha DNA binding and tethering mechanisms identifies Runx1 as a novel tethering factor in receptor-mediated transcriptional activation. *Molecular and cellular biology,* 30**,** 3943-55.

STRÖM, A., HARTMAN, J., FOSTER, J. S., KIETZ, S., WIMALASENA, J. & GUSTAFSSON, J.-A. 2004. Estrogen receptor beta inhibits 17beta-estradiol-stimulated proliferation of the breast cancer cell line T47D. *Proceedings of the National Academy of Sciences of the United States of America,* 101**,** 1566-71.

SUTINEN, P., RAHKAMA, V., RYTINKI, M. & PALVIMO, J. J. 2014. Nuclear mobility and activity of FOXA1 with androgen receptor are regulated by SUMOylation. *Mol Endocrinol,* 28**,** 1719-28.

SWINSTEAD, E. E., MIRANDA, T. B., PAAKINAHO, V., BAEK, S., GOLDSTEIN, I., HAWKINS, M., KARPOVA, T. S., BALL, D., MAZZA, D., LAVIS, L. D., GRIMM, J. B., MORISAKI, T., GRØNTVED, L., PRESMAN, D. M. & HAGER, G. L. 2016. Steroid Receptors Reprogram FoxA1 Occupancy through Dynamic Chromatin Transitions. *Cell,* 165**,** 593-605.

TAN, S. K., LIN, Z. H., CHANG, C. W., VARANG, V., CHNG, K. R., PAN, Y. F., YONG, E. L., SUNG, W. K. & CHEUNG, E. 2011. AP-2γ regulates oestrogen receptor-mediated long-range chromatin interaction and gene transcription. *Embo j,* 30**,** 2569-81.

TAUBE, J. H., ALLTON, K., DUNCAN, S. A., SHEN, L. & BARTON, M. C. 2010. Foxa1 functions as a pioneer transcription factor at transposable elements to activate Afp during differentiation of embryonic stem cells. *J Biol Chem,* 285**,** 16135-44.

THEODOROU, V., STARK, R., MENON, S. & CARROLL, J. S. 2013. GATA3 acts upstream of FOXA1 in mediating ESR1 binding by shaping enhancer accessibility. *Genome research,* 23**,** 12-22.

TOGNON, C., KNEZEVICH, S. R., HUNTSMAN, D., ROSKELLEY, C. D., MELNYK, N., MATHERS, J. A., BECKER, L., CARNEIRO, F., MACPHERSON, N., HORSMAN, D., POREMBA, C. & SORENSEN, P. H. 2002. Expression of the ETV6-NTRK3 gene fusion as a primary event in human secretory breast carcinoma. *Cancer Cell,* 2**,** 367-76.

TOMITA, S., ZHANG, Z., NAKANO, M., IBUSUKI, M., KAWAZOE, T., YAMAMOTO, Y. & IWASE, H. 2009. Estrogen receptor alpha gene ESR1 amplification may predict endocrine therapy responsiveness in breast cancer patients. *Cancer Sci,* 100**,** 1012-7.

TOY, W., SHEN, Y., WON, H., GREEN, B., SAKR, R. A., WILL, M., LI, Z., GALA, K., FANNING, S., KING, T. A., HUDIS, C., CHEN, D., TARAN, T., HORTOBAGYI, G.,

GREENE, G., BERGER, M., BASELGA, J. & CHANDARLAPATY, S. 2013. ESR1 ligand-binding domain mutations in hormone-resistant breast cancer. *Nat Genet,* 45**,** 1439-45.

TOY, W., WEIR, H., RAZAVI, P., LAWSON, M., GOEPPERT, A. U., MAZZOLA, A. M., SMITH, A., WILSON, J., MORROW, C., WONG, W. L., DE STANCHINA, E., CARLSON, K. E., MARTIN, T. S., UDDIN, S., LI, Z., FANNING, S., KATZENELLENBOGEN, J. A., GREENE, G., BASELGA, J. & CHANDARLAPATY, S. 2017. Activating ESR1 Mutations Differentially Affect the Efficacy of ER Antagonists. *Cancer Discov,* 7**,** 277-287.

VAN ROMPAEY, L., POTTER, M., ADAMS, C. & GROSVELD, G. 2000. Tel induces a G1 arrest and suppresses Ras-induced transformation. *Oncogene,* 19**,** 5244-5250.

VARLAKHANOVA, N., SNYDER, C., JOSE, S., HAHM, J. B. & PRIVALSKY, M. L. 2010. Estrogen receptors recruit SMRT and N-CoR corepressors through newly recognized contacts between the corepressor N terminus and the receptor DNA binding domain. *Mol Cell Biol,* 30**,** 1434-45.

VEERARAGHAVAN, J., TAN, Y., CAO, X. X., KIM, J. A., WANG, X., CHAMNESS, G. C., MAITI, S. N., COOPER, L. J., EDWARDS, D. P., CONTRERAS, A., HILSENBECK, S. G., CHANG, E. C., SCHIFF, R. & WANG, X. S. 2014. Recurrent ESR1-CCDC170 rearrangements in an aggressive subset of oestrogen receptor-positive breast cancers. *Nat Commun,* 5**,** 4577.

VIOLA-RHENALS, M., PATEL, K. R., JAIMES-SANTAMARIA, L., WU, G., LIU, J. & DOU, Q. P. 2018. Recent Advances in Antabuse (Disulfiram): The Importance of its Metal-binding Ability to its Anticancer Activity. *Curr Med Chem,* 25**,** 506-524.

VOGEL, V. G., COSTANTINO, J. P., WICKERHAM, D. L., CRONIN, W. M., CECCHINI, R. S., ATKINS, J. N., BEVERS, T. B., FEHRENBACHER, L., PAJON, E. R., WADE, J. L., 3RD, ROBIDOUX, A., MARGOLESE, R. G., JAMES, J., RUNOWICZ, C. D., GANZ, P. A., REIS, S. E., MCCASKILL-STEVENS, W., FORD, L. G., JORDAN, V. C. & WOLMARK, N. 2010. Update of the National Surgical Adjuvant Breast and Bowel Project Study of Tamoxifen and Raloxifene (STAR) P-2 Trial: Preventing breast cancer. *Cancer Prev Res (Phila),* 3**,** 696-706.

VOSS, T. C. & HAGER, G. L. 2014. Dynamic regulation of transcriptional states by chromatin and transcription factors. *Nat Rev Genet,* 15**,** 69-81.

WAGNER, S., WEBER, S., KLEINSCHMIDT, M. A., NAGATA, K. & BAUER, U. M. 2006. SET-mediated promoter hypoacetylation is a prerequisite for coactivation of the estrogen-responsive pS2 gene by PRMT1. *J Biol Chem,* 281**,** 27242-50.

WANG, G. G., ALLIS, C. D. & CHI, P. 2007. Chromatin remodeling and cancer, Part II: ATP-dependent chromatin remodeling. *Trends Mol Med,* 13**,** 373-80.

WANG, M., GU, D., DU, M., XU, Z., ZHANG, S., ZHU, L., LU, J., ZHANG, R., XING, J., MIAO, X., CHU, H., HU, Z., YANG, L., TANG, C., PAN, L., DU, H., ZHAO, J., DU, J., TONG, N., SUN, J., SHEN, H., XU, J., ZHANG, Z. & CHEN, J. 2016. Common genetic variation in ETV6 is associated with colorectal cancer susceptibility. *Nat Commun,* 7**,** 11478.

WATSON, P. J., FAIRALL, L. & SCHWABE, J. W. 2012. Nuclear hormone receptor co-repressors: structure and function. *Mol Cell Endocrinol,* 348**,** 440-9.

WEBB, P., NGUYEN, P., SHINSAKO, J., ANDERSON, C., FENG, W., NGUYEN, M. P., CHEN, D., HUANG, S. M., SUBRAMANIAN, S., MCKINERNEY, E., KATZENELLENBOGEN, B. S., STALLCUP, M. R. & KUSHNER, P. J. 1998. Estrogen receptor activation function 1 works by binding p160 coactivator proteins. *Mol Endocrinol,* 12**,** 1605-18.

WILLIAMS, J. B. 2019. Use of Disulfiram for Treatment of Alcohol Addiction in Patients With Psychotic Illness. *Am J Psychiatry,* 176**,** 80-81.

WOLFRUM, C., BESSER, D., LUCA, E. & STOFFEL, M. 2003. Insulin regulates the activity of forkhead transcription factor Hnf-3beta/Foxa-2 by Akt-mediated phosphorylation and nuclear/cytosolic localization. *Proc Natl Acad Sci U S A,* 100**,** 11624-9.

WOOSTER, R., BIGNELL, G., LANCASTER, J., SWIFT, S., SEAL, S., MANGION, J., COLLINS, N., GREGORY, S., GUMBS, C., MICKLEM, G., BARFOOT, R., HAMOUDI, R., PATEL, S., RICES, C., BIGGS, P., HASHIM, Y., SMITH, A., CONNOR, F., ARASON, A., GUDMUNDSSON, J., FICENEC, D., KELSELL, D., FORD, D., TONIN, P., TIMOTHY BISHOP, D., SPURR, N. K., PONDER, B. A. J., EELES, R., PETO, J., DEVILEE, P., CORNELISSE, C., LYNCH, H., NAROD, S., LENOIR, G., EGILSSON, V., BJORK BARKADOTTIR, R., EASTON, D. F., BENTLEY, D. R., FUTREAL, P. A., ASHWORTH, A. & STRATTON, M. R. 1995. Identification of the breast cancer susceptibility gene BRCA2. *Nature,* 378**,** 789-792.

YANG, J., SINGLETON, D. W., SHAUGHNESSY, E. A. & KHAN, S. A. 2008. The F-domain of estrogen receptor-alpha inhibits ligand induced receptor dimerization. *Mol Cell Endocrinol,* 295**,** 94-100.

YANG, Y., DENG, Q., FENG, X. & SUN, J. 2015. Use of the disulfiram/copper complex for breast cancer chemoprevention in MMTV-erbB2 transgenic mice. *Mol Med Rep,* 12**,** 746-52.

YARDLEY, D. A., NOGUCHI, S., PRITCHARD, K. I., BURRIS, H. A., 3RD, BASELGA, J., GNANT, M., HORTOBAGYI, G. N., CAMPONE, M., PISTILLI, B., PICCART, M., MELICHAR, B., PETRAKOVA, K., ARENA, F. P., ERDKAMP, F., HARB, W. A., FENG, W., CAHANA, A., TARAN, T., LEBWOHL, D. & RUGO, H. S. 2013. Everolimus plus exemestane in postmenopausal patients with HR(+) breast cancer: BOLERO-2 final progression-free survival analysis. *Adv Ther,* 30**,** 870-84.

ZARET, K. S. & CARROLL, J. S. 2011. Pioneer transcription factors: establishing competence for gene expression. *Genes Dev,* 25**,** 2227-41.

ZHANG, Y., LIU, T., MEYER, C. A., EECKHOUTE, J., JOHNSON, D. S., BERNSTEIN, B. E., NUSSBAUM, C., MYERS, R. M., BROWN, M., LI, W. & LIU, X. S. 2008. Model-based Analysis of ChIP-Seq (MACS). *Genome Biol,* 9**,** R137.

ZHAO, C., LAM, E. W. F., SUNTERS, A., ENMARK, E., DE BELLA, M. T., COOMBES, R. C., GUSTAFSSON, J.-Å. & DAHLMAN-WRIGHT, K. 2003. Expression of estrogen receptor β isoforms in normal breast epithelial cells and breast cancer: regulation by methylation. *Oncogene,* 22**,** 7600-7606.

ZHONG, S., LI, C., HAN, X., LI, X., YANG, Y. G. & WANG, H. 2019. Idarubicin Stimulates Cell Cycle- and TET2-Dependent Oxidation of DNA 5-Methylcytosine in Cancer Cells. *Chem Res Toxicol,* 32**,** 861-868.

ZHOU, V. W., GOREN, A. & BERNSTEIN, B. E. 2011. Charting histone modifications and the functional organization of mammalian genomes. *Nature Reviews Genetics,* 12**,** 7-18.

ZHOU, X., XU, Z., LI, A., ZHANG, Z. & XU, S. 2019. Double-sides sticking mechanism of vinblastine interacting with α,β-tubulin to get activity against cancer cells. *J Biomol Struct Dyn,* 37**,** 4080-4091.

ZUBAIRY, S. & OESTERREICH, S. 2005. Estrogen-repressed genes -- key mediators of estrogen action? *Breast Cancer Res,* 7**,** 163-4.

ZWART, W., THEODOROU, V. & CARROLL, J. S. 2011. Estrogen receptor-positive breast cancer: a multidisciplinary challenge. *Wiley Interdisciplinary Reviews: Systems Biology and Medicine,* 3**,** 216-230.

Annexes

Annexe 1: Information about all target genes and siRNA sequences from LP_34662 RNAi Cherry-pick Library (Dharmacon, Horizon Discovery, ref. G-CUSTOM-294730).

LP_34662 G-CUSTOM-294730								
Plate	Well	Pool Catalog Number	Duplex Catalog Number	Gene Symbol	GENE ID	Gene Accession	GI Number	Sequence
Plate 1	B02	M-011591-01	D-011591-02	BCL6	604	NM_001706	21040323	GAGAACAACCUGCCACUGA
Plate 1	B02	M-011591-01	D-011591-03	BCL6	604	NM_001706	21040323	GUACACAUCUCGGCUCAAU
Plate 1	B02	M-011591-01	D-011591-04	BCL6	604	NM_001706	21040323	GUCGAGACAUCUUGACUGA
Plate 1	B02	M-011591-01	D-011591-05	BCL6	604	NM_001706	21040323	UUACAGACCAGUUGAAAUG
Plate 1	B03	M-004584-01	D-004584-01	BCOR	54880	NM_020926	21071035	CCAAAUGGCUUCAGUGCUA
Plate 1	B03	M-004584-01	D-004584-04	BCOR	54880	NM_020926	21071035	CCAUAGAGAUUACUAAAGA
Plate 1	B03	M-004584-01	D-004584-17	BCOR	54880	NM_020926	21071035	GAAGUGAGAUUCCGAAAGA
Plate 1	B03	M-004584-01	D-004584-18	BCOR	54880	NM_020926	21071035	UCGCCAACUCAGCGGGUUA
Plate 1	B04	M-008456-01	D-008456-01	NFIB	4781	NM_005596	93004091	GGAGUCAACUUCCCAAUUG
Plate 1	B04	M-008456-01	D-008456-02	NFIB	4781	NM_005596	93004091	GCACCACCAUCCCGGAAUA
Plate 1	B04	M-008456-01	D-008456-03	NFIB	4781	NM_005596	93004091	AAAGAGCAGUCAAAGAUGA
Plate 1	B04	M-008456-01	D-008456-04	NFIB	4781	NM_005596	93004091	GCCAAACUGCGCAAAGAUA
Plate 1	B05	M-003422-00	D-003422-01	NR2F2	7026	NM_021005	31377723	GUACCUGUCCGGAUAUAUU
Plate 1	B05	M-003422-00	D-003422-02	NR2F2	7026	NM_021005	31377723	CCAACCAGCCGACGAGAUU
Plate 1	B05	M-003422-00	D-003422-03	NR2F2	7026	NM_021005	31377723	ACUCGUACCUGUCCGGAUA
Plate 1	B05	M-003422-00	D-003422-04	NR2F2	7026	NM_021005	31377723	GGCCGUAUAUGGCAAUUCA
Plate 1	B06	M-019085-00	D-019085-01	SNRPD3	6634	NM_004175	34328935	GAAGAACGCACCCAUGUUA
Plate 1	B06	M-019085-00	D-019085-02	SNRPD3	6634	NM_004175	34328935	GAACACCGGUGAGGUAUAU
Plate 1	B06	M-019085-00	D-019085-03	SNRPD3	6634	NM_004175	34328935	CGAUUAAAGUACUGCAUGA
Plate 1	B06	M-019085-00	D-019085-04	SNRPD3	6634	NM_004175	34328935	AUACAUCCGUGGCAGCAAA
Plate 1	B07	M-011984-02	D-011984-01	WDR1	9948	NM_005112	53729351	GGAAAGUGCGUCAUCCUAA
Plate 1	B07	M-011984-02	D-011984-02	WDR1	9948	NM_005112	53729351	GGUGGGAUUUACGCAAUUA
Plate 1	B07	M-011984-02	D-011984-03	WDR1	9948	NM_005112	53729351	GCGGCAAGUCCUACAUUUA
Plate 1	B07	M-011984-02	D-011984-18	WDR1	9948	NM_005112	53729351	UUGUCAACUGUGUGCGAUU
Plate 1	B08	M-004743-01	D-004743-01	SBNO2	22904	NM_001100122	154355003	GCUAAUAUAUGCAAUUCUC
Plate 1	B08	M-004743-01	D-004743-03	SBNO2	22904	NM_001100122	154355003	GAGAGUGGCUACGCUUUGU
Plate 1	B08	M-004743-01	D-004743-04	SBNO2	22904	NM_001100122	154355003	GGACCUUGCUCCCGGUAUC
Plate 1	B08	M-004743-01	D-004743-17	SBNO2	22904	NM_001100122	154355003	UGAUGGAUGCGGACGUGAA
Plate 1	B09	M-019929-01	D-019929-01	TLE3	7090	NM_020908	157384983	GCCAUUAUGUGAUGUACUA
Plate 1	B09	M-019929-01	D-019929-17	TLE3	7090	NM_020908	157384983	GGAUGUAGCAUAUCGAAGA
Plate 1	B09	M-019929-01	D-019929-18	TLE3	7090	NM_020908	157384983	GCCUCAAAGUGGAGUACGA
Plate 1	B09	M-019929-01	D-019929-19	TLE3	7090	NM_020908	157384983	AAGGACAGCUUGAGCCGAU
Plate 1	B10	M-006422-03	D-006422-02	CEBPA	1050	NM_004364	28872793	CAGAGAGCUCCUUGGUCAA
Plate 1	B10	M-006422-03	D-006422-04	CEBPA	1050	NM_004364	28872793	ACAAGAACAGCAACGAGUA
Plate 1	B10	M-006422-03	D-006422-05	CEBPA	1050	NM_004364	28872793	CGGUGGACAAGAACAGCAA
Plate 1	B10	M-006422-03	D-006422-19	CEBPA	1050	NM_004364	28872793	GGAACACGAAGCACGAUCA
Plate 1	B11	M-010510-03	D-010510-02	ETV6	2120	NM_001987	153267458	GGAGCUGGAUGAACAAAUA
Plate 1	B11	M-010510-03	D-010510-03	ETV6	2120	NM_001987	153267458	GUAGACUGCUUUGGGAUUA
Plate 1	B11	M-010510-03	D-010510-04	ETV6	2120	NM_001987	153267458	GAACGAAUUUCAUAUACAC
Plate 1	B11	M-010510-03	D-010510-05	ETV6	2120	NM_001987	153267458	GGGAUUACGUCUAUCAGUU
Plate 1	C02	M-010509-00	D-010509-01	ETV3	2117	NM_005240	20270187	ACAAGAGGAUCCUUCAUAA
Plate 1	C02	M-010509-00	D-010509-02	ETV3	2117	NM_005240	20270187	GGGAAAAGAUUUACCUAUA
Plate 1	C02	M-010509-00	D-010509-03	ETV3	2117	NM_005240	20270187	GGGAAUUUGUCAUCAAGGA
Plate 1	C02	M-010509-00	D-010509-04	ETV3	2117	NM_005240	20270187	AACAUUCGGUCAAGUGGUA
Plate 1	C03	M-015412-01	D-015412-01	ZFHX3	463	NM_006885	118498344	GAACAAGGUUUACGGACUA
Plate 1	C03	M-015412-01	D-015412-02	ZFHX3	463	NM_006885	118498344	CCACUAUGCUAGAAUGUGA
Plate 1	C03	M-015412-01	D-015412-04	ZFHX3	463	NM_006885	118498344	GUACAGAGACCACUACGAU
Plate 1	C03	M-015412-01	D-015412-17	ZFHX3	463	NM_006885	118498344	GUAUAAACCAAACGAGUUA
Plate 1	C04	M-009504-00	D-009504-01	TFAP4	7023	NM_003223	4507446	GGAUUCCAGUCCCUCAAGA
Plate 1	C04	M-009504-00	D-009504-02	TFAP4	7023	NM_003223	4507446	GAAGGUGCCCUCUUUGCAA
Plate 1	C04	M-009504-00	D-009504-03	TFAP4	7023	NM_003223	4507446	GCAGACAGCCGAGUACAUC
Plate 1	C04	M-009504-00	D-009504-04	TFAP4	7023	NM_003223	4507446	GCCCACAUGUACCCGGAAA
Plate 1	C05	M-006913-00	D-006913-01	RNF40	9810	NM_014771	37588854	GAGAUGCGCCACCUGAUUA
Plate 1	C05	M-006913-00	D-006913-02	RNF40	9810	NM_014771	37588854	GAUGCCAACUUUAAGCUAA
Plate 1	C05	M-006913-00	D-006913-03	RNF40	9810	NM_014771	37588854	GAUCAAGGCCAACCAGAUU
Plate 1	C05	M-006913-00	D-006913-04	RNF40	9810	NM_014771	37588854	CAACGAGUCUCUGCAAGUG
Plate 1	C06	M-006448-02	D-006448-02	HLTF	6596	NM_139048	117968479	UAAAGGAGAUAGUCCAUUA
Plate 1	C06	M-006448-02	D-006448-03	HLTF	6596	NM_139048	117968479	GAACAACACUGAUCAUCUG
Plate 1	C06	M-006448-02	D-006448-04	HLTF	6596	NM_139048	117968479	CCAGAUGACUUUCUAACUA
Plate 1	C06	M-006448-02	D-006448-05	HLTF	6596	NM_139048	117968479	GGACUACGCUAUUACACGG
Plate 1	C07	M-020007-01	D-020007-01	IRX5	10265	NM_005853	139394645	GUACAGCACCAGCGUCAUU
Plate 1	C07	M-020007-01	D-020007-02	IRX5	10265	NM_005853	139394645	GAACUAUGGCUCCUUCGGA
Plate 1	C07	M-020007-01	D-020007-03	IRX5	10265	NM_005853	139394645	GUGCAAAGACUCUCCCUAU
Plate 1	C07	M-020007-01	D-020007-04	IRX5	10265	NM_005853	139394645	GAAGAAAGGUAUGUCCGAC
Plate 1	C08	M-010738-00	D-010738-01	CREB3L4	148327	NM_130898	31542090	GGAGUGACUUCCAGAAAUA
Plate 1	C08	M-010738-00	D-010738-02	CREB3L4	148327	NM_130898	31542090	GAACCAAGAAUUACAGAAA
Plate 1	C08	M-010738-00	D-010738-03	CREB3L4	148327	NM_130898	31542090	UCAGUGAGCUGCCCUUUGA
Plate 1	C08	M-010738-00	D-010738-04	CREB3L4	148327	NM_130898	31542090	GCACAACAUCUCCUUGGUA
Plate 1	C09	M-008927-01	D-008927-02	PPP1CA	5499	NM_206873	45827797	CAAGAGACGCUACAACAUC
Plate 1	C09	M-008927-01	D-008927-03	PPP1CA	5499	NM_206873	45827797	GAACGACCGUGGCGUCUCU
Plate 1	C09	M-008927-01	D-008927-04	PPP1CA	5499	NM_206873	45827797	CCAAGUUCCUCCACAAGCA
Plate 1	C09	M-008927-01	D-008927-17	PPP1CA	5499	NM_206873	45827797	AAAGCUGGAUUCUCGCAAA
Plate 1	C10	M-012157-02	D-012157-01	AES	166	NM_198970	39812026	GCUCGAAUGUGACAAGUUG
Plate 1	C10	M-012157-02	D-012157-02	AES	166	NM_198970	39812026	CAAAGACGAAUUUCAGCUA
Plate 1	C10	M-012157-02	D-012157-03	AES	166	NM_198970	39812026	GCACAAACAGGCUGAGAUC
Plate 1	C10	M-012157-02	D-012157-18	AES	166	NM_198970	39812026	GGUACUGCAUGCACGCAAU
Plate 1	C11	M-010319-01	D-010319-01	FOXA1	3169	NM_004496	24497500	CCUCGGAGCAGCAGCAUAA
Plate 1	C11	M-010319-01	D-010319-03	FOXA1	3169	NM_004496	24497500	GCGCUGAGCCCGAGCGGCA
Plate 1	C11	M-010319-01	D-010319-04	FOXA1	3169	NM_004496	24497500	CGGGAAGACCGGCCAGCUA
Plate 1	C11	M-010319-01	D-010319-17	FOXA1	3169	NM_004496	24497500	GUGUAGACAUCCUCCGUAU

Annexe 2: The compound library L1300-Selleck-FDA-Approved-Drug-Library-978cpds (Stratech, Selleckchem). Full list of the 978 compounds, their descriptions and their effects on cell viability for the cell lines investigated: MCF10A, MDA-MB-231, MCF-7, MCF-7-TRF, ZR-75-1, ZR-75-1-TamR.

	Cell viability in response to 4-day treatment with 1μM of each drug; results are shown as % over control (DMSO)							
DRUG	**MCF-7**	**ZR-75-1**	**MCF-7-TRF**	**ZR-75-1-TamR**	**MCF10A**	**MDA-MB-231**	**Indication**	**Target**
10-dab-10-deacetylbaccatin	103.1	99.3	101.0	101.2	99.3	98.9		Others
1-hexadecanol	53.2	68.6	51.6	67.6	48.1	78.2		Others
2-Methoxyestradiol(2ME2)	75.9	103.8	65.3	76.9	50.3	75.1	Cancer	HIF
2-thiouracil	82.4	104.4	101.0	106.3	87.3	95.2	Endocrinology	Others
5-Aminolevulinic-acid-hydrochloride	94.5	101.0	101.9	104.1	88.8	99.0	Neurological Disease	Others
9-aminoacridine	86.5	89.9	94.7	95.3	80.6	99.0		Others
Abitrexate	45.0	62.0	37.1	48.6	17.6	47.0	Cancer	DHFR
Acadesine	15.1	26.1	11.7	34.0	20.6	37.1	Cardiovascular Disease	AMPK
Acarbose	107.1	97.6	109.1	108.1	97.9	102.3	Metabolic Disease	Others
acebutolol-hcl	102.7	100.0	98.1	98.2	100.6	97.6	Neurological Disease	Adrenergic Receptor
aceclidine-hcl	100.2	101.7	111.0	110.6	92.8	103.0		Others
acemetacin-emflex	73.4	75.6	70.8	83.5	70.8	98.6	Infection	Others
Acetanilide-Antifebrin	53.3	68.8	51.5	67.6	48.1	78.1	Neurological Disease	Others
acetarsone	88.0	93.6	85.2	110.1	63.7	77.0		Others
Acetylcholine-chloride	58.2	72.2	85.6	76.3	58.0	88.8	Neurological Disease	AChR
Acetylcysteine	103.8	100.3	94.2	101.1	109.1	98.1	Respiratory Disease	AChR
Acipimox	53.4	68.8	51.4	67.4	48.3	78.1	Cardiovascular Disease	Others
Acitretin	61.3	64.0	54.3	83.0	83.0	83.6	Infection	Others
aclidinium-bromide	105.9	99.1	97.7	96.8	101.3	101.3	Neurological Disease	AChR
Acyclovir(Aciclovir)	65.3	75.4	84.3	98.9	57.3	106.8	Infection	Others
Adapalene	63.0	68.5	61.1	84.7	25.9	99.6	Inflammation	Others
Adefovir-Dipivoxil(Preveon)	74.2	63.3	63.5	57.2	28.5	76.9	Infection	Others
adenine-hydrochloride	104.1	97.0	79.6	99.5	87.5	90.2	Cancer	DNA/RNA Synthesis
Adenosine(Adenocard)	106.0	101.0	97.0	106.0	97.8	101.2	Cardiovascular Disease	Others
adiphenine-hcl	103.2	99.9	99.1	100.0	109.0	105.3	Cardiovascular Disease	Others
adrenalone-hcl	97.7	99.4	103.3	96.8	95.6	96.2	Cardiovascular Disease	Adrenergic Receptor
Adriamycin	10.9	26.1	8.0	31.7	4.0	26.4	Cancer	Topoisomerase
Adrucil(Fluorouracil)	75.4	72.1	70.1	77.4	75.2	92.7	Cancer	DNA/RNA Synthesis
Agomelatine	97.6	102.5	106.4	108.2	90.6	101.6		5-HT Receptor
Albendazole(Albenza)	31.2	52.1	36.8	35.0	47.9	64.9	Vermifuge	Others
albendazole-oxide-ricobendazole	76.6	91.2	90.2	102.6	59.9	97.5	Infection	Others
Alfacalcidol	85.4	80.2	68.3	88.7	73.3	96.3	Endocrinology	Others
Alfuzosin-hydrochloride	87.0	92.2	89.0	102.5	81.8	97.5	Cardiovascular Disease	Adrenergic Receptor
alibendol	96.3	91.6	92.8	98.2	82.1	89.2	Neurological Disease	Others
Aliskiren-hemifumarate	100.2	102.3	97.8	98.3	100.6	98.9	Cardiovascular Disease	RAAS
Allopurinol(Zyloprim)	103.4	104.0	104.0	99.7	99.4	102.5	Neurological Disease	Others
allylthiourea	96.1	99.3	96.8	97.9	96.8	101.3	Metabolic Disease	Others
almotriptan-malate-axert	103.9	100.4	94.1	101.0	109.1	98.1	Cardiovascular Disease	5-HT Receptor
Alprostadil(Caverject)	91.7	93.1	99.5	102.8	101.8	101.4	Endocrinology	Others
altrenogest	107.3	101.3	106.2	116.1	97.6	101.3	Neurological Disease	Estrogen/progestogen Receptor
Altretamine	90.4	90.1	101.6	108.7	89.0	95.0	Cancer	Others
alverine-citrate	103.9	97.0	79.7	99.7	87.2	90.1	Digestive system disease	Others
Amantadine-hydrochloride(Symmetrel)	94.3	94.5	101.5	103.1	96.5	92.7	Cardiovascular Disease	Dopamine Receptor
ambrisentan	101.6	100.3	116.9	123.3	100.4	104.2	Neurological Disease	Others
Amfebutamone-hydrochloride(Bupropion)	100.6	101.1	109.3	102.5	95.8	101.0	Infection	Dopamine Receptor
amfenac-sodium-monohydrate	78.8	79.6	87.7	94.3	65.5	74.9	Inflammation	Others
amidopyrine	103.7	100.4	94.2	101.3	108.6	98.1	Neurological Disease	Others
amilorida	104.2	101.2	111.1	110.1	99.6	100.7	Cardiovascular Disease	Sodium Channel
Amiloride-hydrochloride(Midamor)	79.0	97.6	87.6	97.4	80.4	98.3	Metabolic Disease	Others

DRUG	MCF-7	ZR-75-1	MCF-7-TRF	ZR-75-1-TamR	MCF10A	MDA-MB-231	Indication	Target
Aminocaproic-acid(Amicar)	97.6	97.2	106.4	99.7	106.5	99.7	Cardiovascular Disease	Others
Aminoglutethimide(Cytadren)	97.8	98.5	100.0	104.9	98.2	102.9	Endocrinology	Aromatase
Aminophylline(Truphylline)	102.2	98.1	100.0	101.2	98.7	102.7	Respiratory Disease	PDE
aminosalicylate-sodium	102.7	100.3	104.0	102.5	101.9	93.3	Neurological Disease	NF-?B
aminothiazole	107.5	100.6	111.0	108.5	69.2	95.9	Infection	Others
amiodarone-hcl	102.7	101.1	84.5	100.3	81.2	104.8	Cardiovascular Disease	Potassium Channel
Amisulpride	98.5	99.0	107.2	110.2	98.9	96.8	Neurological Disease	Dopamine Receptor
amitriptyline-hydrochloride	99.6	101.0	104.5	94.7	81.3	104.1	Infection	5-HT Receptor
Amlodipine(Norvasc)	86.6	97.3	90.1	97.6	80.4	98.6	Cardiovascular Disease	Calcium Channel
Amlodipine-besylate(Norvasc)	35.0	33.7	26.0	48.4	39.2	66.1	Cardiovascular Disease	Others
Ammonium-Glycyrrhizinate(AMGZ)	103.7	90.9	103.4	84.7	96.5	125.9		Others
Amorolfine-Hydrochloride	97.9	98.1	99.8	96.8	79.2	99.7	Infection	Others
amoxicillin-(amox)	97.3	101.6	104.0	112.3	93.1	101.9	Infection	Others
amoxicillin-amoxycillin	61.2	64.0	54.3	83.2	82.7	83.5	Neurological Disease	Others
Amphotericin-B(Abelcet).	103.9	97.1	95.5	99.7	94.8	108.2		Others
ampicillin-sodium	67.3	71.4	54.0	80.0	89.0	85.9	Infection	Others
ampicillin-trihydrate	38.8	52.9	42.3	49.6	50.7	68.9	Infection	Others
ampiroxicam	100.1	97.2	101.6	102.0	105.4	98.5	Cardiovascular Disease	COX
Amprenavir-(Agenerase)	99.9	101.5	97.4	98.1	96.6	99.6	Infection	HIV Protease
amprolium-hcl	74.6	89.3	89.6	91.6	77.8	91.3	Metabolic Disease	Others
anagrelide-hydrochloride	91.1	95.8	95.9	96.2	98.2	98.9	Endocrinology	PDE
Anastrozole	82.6	92.8	87.7	96.8	85.8	95.7	Endocrinology	Aromatase
Aniracetam	100.1	100.1	112.1	109.4	92.2	99.0	Neurological Disease	AMPA Receptor-kainate Receptor-NMDA Receptor
anisotropine-methylbromide	68.6	92.9	96.1	100.7	81.3	98.9	Neurological Disease	Others
antazoline-hcl	106.8	97.3	109.3	108.1	97.5	102.4	Neurological Disease	Others
antipyrine	101.6	98.4	98.4	93.9	99.1	104.6	Infection	Others
AP24534	88.2	93.8	85.0	110.0	64.0	76.9	Cancer	Bcr-Abl, VEGFR, FGFR, PDGFR, Flt
Apatinib-YN968D1	102.2	98.2	99.8	101.2	98.7	102.7	Cancer	VEGFR
Apixaban(BMS-562247-01)	100.6	101.6	96.4	99.3	100.9	98.0	Cardiovascular Disease	Factor Xa
Aprepitant	85.3	91.8	97.7	100.2	77.3	95.4	Neurological Disease	Substance P
Arbidol-hcl	103.9	96.6	107.4	98.1	107.3	106.3	Cardiovascular Disease	Others
arecoline	85.3	92.4	96.2	96.4	81.6	96.0	Endocrinology	AChR
argatroban	99.2	98.4	96.5	100.3	99.2	103.6	Cardiovascular Disease	Others
aripiprazole-abilify	82.3	93.9	95.3	93.0	77.9	104.6	Neurological Disease	5-HT Receptor
Arranon	101.4	95.3	89.0	99.3	80.9	101.2	Cancer	DNA/RNA Synthesis
Artemether(SM-224)	101.0	102.4	103.8	99.6	105.1	96.2	Cancer	Others
Artemisinin	70.4	83.8	91.4	103.9	80.5	94.6	Infection	Others
articaine-hydrochloride	99.6	89.6	98.1	98.8	99.2	99.4	Neurological Disease	Others
Asenapine	95.7	90.0	105.2	108.1	89.7	93.8	Neurological Disease	Adrenergic Receptor, 5-HT Receptor
aspartame	104.0	97.4	106.5	108.9	97.8	102.4	Metabolic Disease	Others
aspirin-acetylsalicylic-acid	77.2	87.8	83.1	96.6	81.0	92.7	Cancer	Others
Atazanavir	93.6	93.8	101.0	113.3	87.8	101.2	Cancer	HIV Protease
atomoxetine-hydrochloride	100.4	101.7	96.4	99.5	100.5	97.9	Neurological Disease	5-HT Receptor
atorvastatin-calcium-lipitor	97.8	99.3	103.1	96.6	96.0	96.3	Cardiovascular Disease	HMG-CoA Reductase
atovaquone-atavaquone	97.5	94.0	107.7	108.8	99.1	92.1	Neurological Disease	Free Base
atracurium-besylate	102.3	98.6	101.0	109.2	91.8	97.6	Neurological Disease	Others
Atropine-sulfate-monohydrate	104.5	100.0	101.2	97.8	106.5	96.6	Respiratory Disease	Others
auflomedil-hcl	92.3	85.1	89.7	88.4	79.6	93.8	Neurological Disease	Others
avanafil	105.9	99.1	96.4	98.6	100.9	95.5	Cardiovascular Disease	PDE
Avobenzone(Parsol-1789)	85.5	92.4	96.0	96.2	81.9	96.0		Others
Axitinib	40.0	65.6	24.4	51.5	53.6	88.2	Cancer	VEGFR, PDGFR, c-Kit

DRUG	MCF-7	ZR-75-1	MCF-7-TRF	ZR-75-1-TamR	MCF10A	MDA-MB-231	Indication	Target
Azacitidine(Vidaza)	77.9	86.8	80.4	88.9	76.9	97.6	Cancer	DNA/RNA Synthesis
azacyclonol	97.8	97.2	99.9	103.2	95.1	101.2	Neurological Disease	Others
azaguanine-8	100.5	99.5	110.1	106.5	89.3	103.6	Cancer	Others
azaperone	80.8	79.3	70.8	78.0	73.6	95.4	Neurological Disease	Others
azatadine-dimaleate	106.4	100.5	100.5	95.3	100.1	99.9	Infection	Histamine Receptor
Azathioprine(Azasan)	71.7	74.1	60.7	75.0	72.7	82.0	Immunology	Others
Azelastine-hydrochloride-Astelin	97.5	102.6	106.4	108.4	90.2	101.6	Neurological Disease	Histamine Receptor
azelnidipine	102.5	101.1	84.6	100.5	80.9	104.7	Neurological Disease	Calcium Channel
azilsartan-medoxomil-tak-491	94.5	99.5	96.4	105.3	93.5	98.1	Cardiovascular Disease	RAAS
azilsartan-tak-536	88.0	98.2	91.9	96.6	79.8	101.0	Neurological Disease	RAAS
azithromycin-dihydrate	87.2	89.9	86.8	96.9	81.4	93.4	Infection	Others
azithromycin-zithromax.h	104.4	101.2	110.9	109.9	100.0	100.8	Cancer	autophagy
azlocillin-sodium-salt	102.9	100.0	99.3	100.3	108.6	105.3	Neurological Disease	Others
Aztreonam(Azactam)	102.7	98.5	102.3	107.7	100.3	97.1	Infection	Others
bacitracin	92.3	89.8	84.4	82.2	84.1	92.5	Infection	Others
balofloxacin	101.8	98.3	98.2	93.6	99.5	104.7	Metabolic Disease	Others
BAY-73-4506	88.3	96.3	90.3	80.0	40.1	53.6	Cancer	c-Kit, Raf, VEGFR
bazedoxifene-hcl	106.1	99.1	97.5	96.6	101.7	101.3	Metabolic Disease	Estrogen/progestin receptor
beclomethasone-dipropionate	106.1	98.4	97.7	110.7	93.7	94.5	Inflammation	Others
bemegride	97.7	97.4	103.7	110.4	91.8	96.6		Others
Benazepril-hydrochloride	106.3	100.3	114.7	109.2	95.1	98.7	Cardiovascular Disease	RAAS
Bendamustine-Hydrochloride	82.0	87.0	85.4	91.9	80.5	95.7	Cancer	Others
benidipine-hydrochloride	82.5	104.3	100.8	106.0	87.6	95.2	Cardiovascular Disease	calcium channel
Benserazide-hydrochloride(Serazide)	102.9	100.3	103.8	102.2	102.3	93.4	Neurological Disease	Dopamine Receptor
benzbromarone	73.4	75.4	71.0	83.4	70.7	98.8		Others
benzethonium-chloride	44.9	61.8	37.1	48.7	17.5	47.0	Neurological Disease	Others
benzocaine	13.9	16.1	11.9	28.0	16.4	31.8	Respiratory Disease	Others
benzoic-acid	75.1	71.9	70.3	77.5	74.8	92.8		Others
benzthiazide	52.2	58.6	61.8	61.1	70.5	95.4	Cardiovascular Disease	Others
benztropine-mesylate	94.0	90.8	96.1	95.0	96.4	94.5	Infection	Histamine Receptor
benzydamine-hcl	101.2	95.0	89.2	99.4	80.5	101.3	Inflammation	Others
benzylpenicillin-sodium	10.9	26.1	8.1	31.8	4.0	26.4	Infection	Others
bephenium-hydroxynaphthoate	96.6	96.0	107.7	110.6	94.1	96.1	Vermifuge	Others
bepotastine-besilate	97.6	88.4	84.3	86.9	76.6	95.0	Cancer	Histamine Receptor
bergapten	94.5	100.2	110.6	111.7	82.9	87.4	Cancer	Others
Beta-Carotene	74.8	89.7	89.2	91.5	78.2	91.3		Others
betahistine-dihydrochloride	104.8	93.3	103.3	96.4	98.9	97.1		Histamine Receptor
Betamethasone-(Celestone)	81.3	85.7	112.9	85.6	91.7	118.3	Inflammation	Others
Betamethasone-Dipropionate(Diprolene)	103.6	90.9	103.5	84.7	96.6	125.9		Others
Betamethasone-valerate(Betnovate)	88.0	92.0	103.3	78.5	92.7	117.4	Inflammation	Others
betamipron	104.0	100.8	111.3	110.0	99.5	100.9	Infection	Others
Betapar(Meprednisone)	105.3	104.9	103.6	103.6	96.5	106.1	Inflammation	Others
betaxolol-betoptic	104.9	101.8	96.3	95.9	103.0	95.0	Neurological Disease	Adrenergic Receptor
betaxolol-hydrochloride-betoptic	15.0	25.3	17.9	35.9	62.8	81.6	Cardiovascular Disease	Adrenergic Receptor
bexarotene	103.6	101.6	98.7	113.7	97.8	97.9	Cardiovascular Disease	Others
bezafibrate	77.7	86.5	80.7	89.1	76.5	97.6	Metabolic Disease	Others
BIBR-1048(Dabigatran-etexilate)	93.1	97.5	106.3	100.4	96.7	102.6	Infection	Others
BIBW2992	70.0	64.5	52.0	56.6	26.6	52.7	Cancer	EGFR
Bicalutamide(Casodex)	88.5	100.5	95.5	104.9	82.0	94.3	Endocrinology	Androgen Receptor, P450
bifonazole	90.5	90.2	101.4	108.6	88.9	95.0	Infection	others
Bimatoprost	104.0	96.9	79.7	99.6	87.5	90.2	Cardiovascular Disease	Others
bindarit	96.6	95.0	89.7	95.2	79.9	90.0	Cancer	Others
biotin-vitamin-b7	98.9	97.1	110.8	106.4	87.1	91.7	Infection	Others

DRUG	MCF-7	ZR-75-1	MCF-7-TRF	ZR-75-1-TamR	MCF10A	MDA-MB-231	Indication	Target
bisacodyl	84.0	104.4	105.2	102.7	95.1	98.4	Cardiovascular Disease	Others
Bisoprolol-Fumarate	77.9	86.7	80.5	89.0	76.9	97.6		Adrenergic Receptor
Bleomycin-sulfate	85.5	74.9	82.9	85.7	67.4	73.4	Cancer	DNA/RNA Synthesis
Bortezomib	6.1	10.8	4.1	8.4	3.4	4.0	Cancer	Proteasome
bosentan	93.5	80.7	78.4	84.1	78.1	91.0		Others
Bosutinib	50.3	71.3	47.3	59.9	41.1	77.6	Cancer	Src
brinzolamide	91.6	98.6	94.2	95.0	106.9	93.6	Neurological Disease	Carbonic Anhydrase
bromhexine-hydrochloride	107.5	101.2	106.0	115.8	98.0	101.4	Cardiovascular Disease	Others
brompheniramine	104.4	99.2	107.7	106.1	98.1	99.6	Infection	Histamine Receptor
broxyquinoline	97.2	101.2	104.2	112.1	92.9	102.0	Vermifuge	Others
brucine	44.4	61.0	46.9	52.9	17.4	76.2		Others
Budesonide	104.1	97.4	113.1	103.3	99.6	96.5	Endocrinology	Others
bufexamac	88.9	87.8	80.7	88.6	78.5	98.6	Metabolic Disease	HDAC
Bumetanide	104.5	99.1	107.7	105.9	98.5	99.6	Cardiovascular Disease	Others
Bupivacaine-hydrochloride(Marcain)	98.1	108.1	121.2	115.8	107.5	101.0	Neurological Disease	Others
Busulfan(Busulfex)	103.0	99.2	101.2	101.3	99.3	98.9	Cardiovascular Disease	NULL
butenafine-hydrochloride	88.6	92.4	98.6	95.3	102.1	103.2	Neurological Disease	Others
butoconazole-nitrate	104.1	95.2	98.0	110.9	102.5	95.1	Infection	Others
cabazitaxel-jevtana	52.3	58.8	61.7	61.1	70.6	95.2	Neurological Disease	Others
Calcitriol-(Rocaltrol)	55.3	68.4	54.7	75.3	65.1	95.8	Endocrinology	Others
calcium-gluceptate	88.8	87.5	80.9	88.6	78.3	98.8		Others
Camptothecine	14.0	16.2	11.9	28.0	16.5	31.8	Cancer	Topoisomerase
camylofin-chlorhydrate	81.2	85.5	113.2	85.6	91.1	118.4	Digestive system disease	Others
Candesartan(Atacand)	101.8	98.2	98.4	93.7	99.5	104.7	Cardiovascular Disease	RAAS
Candesartan-cilexetil-Atacand	88.2	93.9	84.9	110.0	64.0	76.9	Cardiovascular Disease	Others
Capecitabine(Xeloda)	68.8	101.6	100.0	103.9	79.9	101.2	Cancer	DNA/RNA Synthesis
captopril-capoten	99.8	89.6	98.0	98.5	99.6	99.4	Metabolic Disease	RAAS
carbachol	103.0	96.0	94.7	109.3	88.0	97.8		Others
carbadox	92.9	89.4	85.6	89.3	77.6	95.8	Infection	Others
Carbamazepine(Carbatrol)	101.7	97.7	101.8	99.1	100.8	93.3	Neurological Disease	Others
Carbamyl-beta-methylcholine-chloride(Bethanechol-chloride)	40.0	65.6	24.4	51.6	53.4	88.1	Neurological Disease	AChR
carbazochrome-sodium-sulfonate	88.0	95.6	97.3	96.3	64.8	101.1	Cancer	Others
carbenicillin-disodium	99.0	98.4	96.7	100.5	98.8	103.5	Infection	Others
carbenoxolone-sodium	82.3	104.0	101.3	106.2	87.2	95.3	Endocrinology	Others
Carbidopa	73.6	75.6	70.7	83.3	71.1	98.7	Neurological Disease	others
carbimazole	99.2	102.1	96.5	100.2	96.3	103.0	Infection	Others
carfilzomib-pr-171	90.7	100.9	94.8	100.4	87.8	90.7	Cardiovascular Disease	Proteasome
Carmofur	70.5	66.3	64.6	68.5	70.2	88.9	Cancer	Antimetabolites
carprofen	88.3	100.3	95.8	105.0	81.6	94.4	Inflammation	Others
carvedilol	90.1	95.6	105.8	113.4	87.6	98.3	Cardiovascular Disease	Adrenergic Receptor
caspofungin-acetate	89.0	102.7	100.1	109.6	90.7	96.5	Infection	Others
catharanthine	98.0	100.7	102.1	95.7	97.9	102.6		Others
Cefdinir(Omnicef)	99.7	98.7	96.6	105.9	100.6	101.6	Infection	Others
Cefditoren-pivoxil	92.6	90.2	84.1	82.0	84.6	92.4	Infection	5-alpha Reductase
cefoperazone-cefobid	103.1	99.8	99.3	100.1	109.0	105.3	Infection	Others
ceftazidime-pentahydrate	82.9	89.3	85.1	83.1	82.4	95.2	Infection	Others
Ceftiofur-hydrochloride	78.8	97.6	87.8	97.7	80.1	98.2		Others
Celecoxib	97.9	97.7	103.5	110.3	92.3	96.6	Inflammation	COX
Cephalexin-(Cefalexin)	100.2	99.7	115.2	107.9	97.2	96.8	Infection	Others
cephalomannine	101.8	99.2	101.0	102.4	97.1	99.6	Cancer	Others
cepharanthine	89.4	92.9	96.2	95.6	83.6	98.1	Metabolic Disease	Others
Cetirizine-di-hcl	72.8	79.1	72.9	78.6	73.4	88.7	Inflammation	Histamine Receptor
cetrimonium-bromide	72.6	93.6	77.6	84.1	41.9	95.6	Infection	Others
cetylpyridinium-chloride	58.0	72.0	85.9	76.5	57.7	88.9	Infection	Others
Chenodeoxycholic-acid	82.1	96.7	100.8	102.4	87.4	96.0	Infection	NULL
Chloramphenicol(Chloromycetin)	84.1	104.2	105.2	102.5	95.5	98.5	Infection	Others

DRUG	MCF-7	ZR-75-1	MCF-7-TRF	ZR-75-1-TamR	MCF10A	MDA-MB-231	Indication	Target
Chlormezanone(Trancopal)	105.3	95.9	107.3	111.4	92.9	93.3	Respiratory Disease	Others
chlorocresol	104.3	98.9	107.9	105.9	98.0	99.7		Others
Chlorothiazide(Diuril)	96.2	99.2	96.8	97.7	97.2	101.4	Cardiovascular Disease	Others
Chloroxine	100.8	99.8	109.6	106.4	89.8	103.5	Infection	Others
Chlorpheniramine-maleate	75.9	103.9	65.2	76.9	50.3	75.1	Neurological Disease	Histamine Receptor
Chlorpromazine-hydrochloride(Sonazine)	69.9	64.6	52.0	56.6	26.5	52.7	Neurological Disease	Dopamine Receptor, Potassium Channel
chlorpropamide	85.3	74.7	83.0	85.9	67.0	73.5	Infection	Others
Chlorprothixene	38.9	53.1	42.1	49.5	51.0	68.9	Neurological Disease	Others
chlorquinaldol	76.4	90.9	90.6	102.7	59.6	97.6	Infection	Others
chlorzoxazone	72.8	87.2	92.3	88.6	76.9	90.4	Metabolic Disease	Others
choline-chloride	15.0	26.0	11.8	34.0	20.5	37.1		Others
chromocarb	103.8	97.2	113.3	103.4	99.0	96.6	Cardiovascular Disease	Others
ciclopirox-ethanolamine	86.7	90.2	94.5	95.4	80.7	98.9	Infection	ATPase
Ciclopirox-Penlac	101.3	95.4	89.0	99.5	80.6	101.1	Neurological Disease	Others
Cilnidipine	61.4	76.8	67.2	74.9	52.9	86.7	Cardiovascular Disease	Calcium Channel
Cilostazol	74.0	82.9	78.9	79.2	74.2	85.5	Cardiovascular Disease	PDE
Cimetidine(Tagamet)	98.0	97.8	103.3	110.2	92.3	96.6	Inflammation	NULL
Cinacalcet-hydrochloride	82.1	96.6	101.0	102.4	87.5	96.0	Endocrinology	CaSR
cinchophen	103.8	94.9	98.4	111.0	102.0	95.1	Immunology	Others
cinepazide-maleate	105.2	95.9	89.4	99.4	78.7	96.0	Inflammation	Others
cisatracurium-besylate-nimbex	100.0	101.6	97.2	98.0	96.6	99.6	Neurological Disease	Adrenergic Receptor
Cisplatin	80.3	97.5	94.3	93.0	83.8	93.8		DNA/RNA Synthesis
Cladribine	79.0	79.8	87.5	94.2	65.9	74.8	Cancer	DNA/RNA Synthesis
clarithromycin	81.2	96.7	97.0	102.5	87.2	100.2	Neurological Disease	P450
Clemastine-Fumarate	107.9	100.9	110.5	108.4	69.4	95.8	Immunology	Histamine Receptor
cleviprex-clevidipine	105.9	101.3	94.5	94.5	103.5	95.0	Cardiovascular Disease	Calcium Channel
climbazole	34.9	33.6	26.1	48.6	39.0	66.1	Infection	Others
clindamycin	94.7	100.6	110.4	111.9	83.0	87.3	Infection	Others
Clindamycin-hydrochloride(Dalacin)	6.1	10.8	4.1	8.5	3.4	4.0	Neurological Disease	Others
clindamycin-palmitate-hcl	47.6	51.7	36.3	48.1	42.4	32.1	Infection	Others
clobetasol-propionate	104.0	97.5	113.1	103.5	99.2	96.5	Neurological Disease	Others
Clofarabine	40.8	57.0	40.0	40.9	42.1	60.9	Cancer	DNA/RNA Synthesis
clofazimine	24.7	37.7	25.9	53.5	28.4	40.2	Infection	Others
clofibric-acid	106.0	100.1	114.9	109.2	94.6	98.8	Metabolic Disease	Others
clofoctol	70.2	55.0	99.9	90.4	49.1	74.3	Infection	Others
Clomifene-citrate-Serophene	76.5	91.2	90.4	102.9	59.7	97.4	Cancer	Estrogen/progestogen Receptor
Clomipramine-hydrochloride-Anafranil	65.2	75.5	84.5	99.1	57.1	106.8		5-HT Receptor
Clonidine-hydrochloride(Catapres)	50.2	71.4	47.3	60.0	40.9	77.6	Infection	Adrenergic Receptor
Clopidogrel-bisulfate	99.6	102.1	104.5	103.6	86.2	101.3	Cardiovascular Disease	P2 Receptor
clorprenaline-hcl	85.1	91.6	97.9	100.2	76.9	95.4	Cardiovascular Disease	Others
clorsulon	83.2	89.5	80.3	87.1	74.5	86.2	Cancer	Others
closantel	84.3	92.8	78.5	89.1	55.0	93.8	Vermifuge	Others
closantel-sodium	91.5	97.2	89.3	98.9	84.0	96.8	Vermifuge	Others
Clotrimazole(Canesten)	99.8	100.8	104.5	94.6	81.6	104.2	Infection	Others
Cloxacillin-sodium-Cloxacap	100.6	99.8	109.9	106.6	89.5	103.5	Cardiovascular Disease	Others
Clozapine(Clozaril)	42.5	53.9	41.0	53.0	31.3	31.0	Cardiovascular Disease	5-HT Receptor
cobicistat-gs-9350	72.6	93.9	77.4	84.3	42.0	95.5	Cancer	P450 (e.g. CYP17)
conivaptan-hcl-vaprisol	96.3	99.3	96.6	97.7	97.2	101.4	Cardiovascular Disease	Others
Cortisone-acetate-Cortone	103.9	95.3	98.2	111.2	102.1	95.0	Cancer	Others
coumarin	94.2	94.2	77.6	93.1	80.1	95.6		Others
CP-690550	94.2	94.1	95.0	90.4	96.4	90.3	Cancer	JAK
Crystal-violet	68.5	94.5	101.5	106.8	81.0	94.4	Infection	Others
Curcumin	107.2	97.7	108.9	108.1	97.9	102.3		Others
cyclamic-acid	99.8	101.6	97.4	98.3	96.2	99.5	Inflammation	Others

DRUG	MCF-7	ZR-75-1	MCF-7-TRF	ZR-75-1-TamR	MCF10A	MDA-MB-231	Indication	Target
cyclandelate	101.9	98.3	101.5	109.3	91.3	97.7	Neurological Disease	Others
cyclophosphamide-monohydrate	98.7	98.7	101.0	101.0	99.7	103.4	Cancer	Others
Cyclosporine	90.0	91.9	88.1	97.9	94.1	96.4	Immunology	Others
cyproheptadine-hydrochloride-periactin	100.3	99.9	115.0	107.8	97.2	96.8	Neurological Disease	Histamine Receptor
cyromazine	40.7	56.9	40.1	41.0	41.8	61.0	Vermifuge	Others
cysteamine-hcl	95.6	89.8	105.4	108.1	89.2	93.9	Metabolic Disease	Others
cytidine	88.8	92.4	98.4	95.1	102.5	103.3	Cardiovascular Disease	Others
dabrafenib-gsk2118436a	89.5	93.3	96.0	95.7	83.7	97.9	Infection	Raf
Dacarbazine	85.8	90.9	89.9	92.8	78.5	102.3	Cancer	DNA/RNA Synthesis
Daidzein	63.1	68.5	61.0	84.6	25.9	99.6	Cardiovascular Disease	Others
Dapoxetine-hydrochloride(Priligy)	104.2	97.5	112.9	103.3	99.5	96.5	Neurological Disease	5-HT Receptor
DAPT-GSI-IX	97.7	97.3	106.2	99.7	106.5	99.7	Cancer	Gamma-secretase, Beta Amyloid
darifenacin-hydrobromide	100.1	99.9	115.2	108.1	96.9	96.8	Infection	AChR
Darunavir-Ethanolate(Prezista)	104.9	101.7	96.4	95.9	103.0	95.0	Infection	HIV Protease
Dasatinib	42.6	53.9	41.0	53.0	31.4	31.0	Cancer	Src, Bcr-Abl, c-Kit
daunorubicin-hcl-daunomycin-hcl	81.4	89.9	79.1	92.9	90.7	89.2	Cancer	Telomerase
decamethonium-bromide	100.4	101.1	109.5	102.8	95.5	100.9	Neurological Disease	AChR
Decitabine	68.7	85.7	65.7	97.0	59.3	87.6	Cardiovascular Disease	DNA/RNA Synthesis
Deferasirox(Exjade)	40.0	65.6	24.3	51.5	53.6	88.2	Endocrinology	Others
Deflazacor	81.1	79.6	70.5	77.8	74.0	95.3	Endocrinology	Others
Dehydroepiandrosterone(DHEA)	90.7	86.2	98.2	91.9	77.1	92.1	Endocrinology	Androgen Receptor
deoxyarbutin	82.4	92.6	87.9	96.8	85.4	95.8	Cardiovascular Disease	Others
deoxycorticosterone-acetate	87.9	95.3	97.5	96.2	64.7	101.2	Endocrinology	Others
desloratadine	103.7	97.2	95.5	99.9	94.4	108.2	Cardiovascular Disease	Histamine Receptor
Desonide	93.4	94.6	104.0	87.1	88.3	121.4	Inflammation	Others
detomidine-hcl	97.6	99.8	99.3	97.0	103.0	100.2	Cardiovascular Disease	Adrenergic Receptor
Dexamethasone	70.4	82.3	93.6	68.5	71.4	119.2	Inflammation	IL Receptor
dexamethasone-acetate	76.5	72.9	62.1	86.4	64.4	93.8	Inflammation	Others
dexlansoprazole	81.2	91.3	82.7	96.3	70.8	99.8	Cardiovascular Disease	Others
dexmedetomidine	103.1	96.3	94.4	109.4	88.1	97.7	Neurological Disease	Adrenergic Receptor
dexmedetomidine-hcl-precedex	98.2	100.7	101.8	95.5	98.2	102.6	Neurological Disease	Androgen Receptor
Dexrazoxane-Hydrochloride	94.5	94.4	77.4	92.9	80.5	95.5	Cardiovascular Disease	Others
Dextrose(D-glucose)	106.1	101.1	96.8	105.9	97.7	101.2	Infection	Others
dibenzothiophene	70.3	83.6	91.7	103.9	80.1	94.7		Others
dibucaine-cinchocaine-hcl	93.0	97.5	106.5	100.6	96.2	102.6	Endocrinology	Sodium Channel
diclazuril	100.9	99.8	108.7	114.6	93.7	102.8	Infection	Others
diclofenac-diethylamine	98.4	101.1	100.8	107.6	93.2	102.8	Neurological Disease	Others
diclofenac-potassium	99.5	102.2	104.5	103.8	85.8	101.3	Infection	Others
Diclofenac-sodium	83.3	89.5	80.1	86.9	74.8	86.3	Neurological Disease	COX
dicloxacillin-sodium	27.1	47.4	26.0	51.6	37.0	47.1	Infection	Others
dicyclomine-hcl	97.7	97.4	111.3	107.7	97.7	101.5	Neurological Disease	Others
Didanosine(Videx)	101.1	101.5	102.9	108.6	99.9	95.9	Infection	NULL
Dienogest	90.1	95.5	106.0	113.5	87.6	98.3	Endocrinology	Estrogen/progestogen Receptor
Diethylstilbestrol(Stilbestrol)	70.5	83.9	91.3	103.8	80.5	94.6	Cancer	Others
difloxacin-hcl	98.7	96.7	111.0	106.2	86.9	91.8	Infection	Others
difluprednate	31.9	40.2	39.6	46.0	47.4	71.8	Endocrinology	Others
Diltiazem-HCl(Tiazac)	95.8	90.1	105.0	108.0	89.7	93.8	Cardiovascular Disease	Others
dimethyl-Fumarate	14.0	16.2	11.9	28.0	16.5	31.7	Inflammation	Others
diminazene-aceturate	36.9	44.7	45.5	46.2	54.7	68.4	Vermifuge	Others
diperodon-hcl	99.9	99.5	115.5	107.9	96.8	96.9	Neurological Disease	Others
diphemanil-methylsulfate	104.3	100.0	101.4	98.1	106.1	96.5	Neurological Disease	AChR
Diphenhydramine-hydrochloride(Benadryl)	106.4	100.4	114.4	109.1	95.0	98.7	Immunology	Others

DRUG	MCF-7	ZR-75-1	MCF-7-TRF	ZR-75-1-TamR	MCF10A	MDA-MB-231	Indication	Target
diphenylpyraline-hcl	78.2	78.1	84.8	91.8	75.8	89.3	Neurological Disease	Others
Dipyridamole(Permole,-Persantine)	90.8	86.2	98.0	91.7	77.3	92.1	Cardiovascular Disease	Others
dirithromycin	72.6	78.9	73.1	78.8	73.0	88.8	Infection	Others
disopyramide-phosphate	96.5	92.6	89.0	100.3	82.7	104.3	Cardiovascular Disease	Others
Disulfiram(Antabuse)	16.9	42.4	47.2	40.9	85.9	53.4	Neurological Disease	Others
Divalproex-sodium	87.2	101.0	108.9	105.1	96.7	104.4	Neurological Disease	Others
DL-Carnitine-hydrochloride	100.9	100.8	105.9	100.8	104.9	97.1	Cardiovascular Disease	Others
D-Mannitol(Osmitrol)	105.3	105.0	103.4	103.5	96.5	106.1	Cardiovascular Disease	Others
Docetaxel(Taxotere)	24.8	37.8	25.9	53.4	28.5	40.2	Cancer	Microtubule Associated
Dofetilide(Tikosyn)	105.4	101.5	95.0	101.4	95.4	103.8	Cardiovascular Disease	Others
domiphen-bromide	94.3	100.6	102.1	104.0	88.7	99.2	Infection	Others
Domperidone(Motilium)	73.6	72.0	57.1	60.3	27.2	89.3	Neurological Disease	Dopamine Receptor
Dopamine-hydrochloride-Inotropin	85.4	74.9	82.9	85.9	67.2	73.3	Infection	Dopamine Receptor
Doripenem-Hydrate	77.3	87.7	83.1	96.3	81.3	92.7	Infection	Others
doxapram-hcl	105.2	101.6	95.0	101.6	95.0	103.7	Neurological Disease	Others
Doxazosin-mesylate	82.5	88.4	85.2	87.2	69.7	95.5	Cardiovascular Disease	Adrenergic Receptor
Doxercalciferol(Hectorol)	76.6	72.8	62.1	86.3	64.7	93.9	Endocrinology	Others
doxifluridine	99.2	91.2	111.0	101.4	98.4	90.6	Immunology	Others
doxofylline	81.8	86.8	85.6	92.0	80.0	95.8	Metabolic Disease	Others
doxylamine-succinate	90.6	100.6	95.0	100.3	87.8	90.8	Neurological Disease	Others
dronedarone-hcl-multaq	31.2	52.1	36.7	35.0	47.9	64.9	Neurological Disease	Others
droperidol	61.2	76.4	65.5	72.4	38.1	82.5	Neurological Disease	Others
dropropizine	39.1	70.7	58.2	88.1	77.8	84.8	Respiratory Disease	Others
Drospirenone	86.8	90.1	94.5	95.2	81.0	99.0	Endocrinology	Estrogen/progestogen Receptor
duloxetine-hcl-cymbalta	98.0	97.2	99.8	102.9	95.4	101.2	Neurological Disease	5-HT Receptor
Dutasteride	86.6	93.1	84.4	98.6	74.8	93.4	Endocrinology	5-alpha Reductase
dyclonine-hydrochloride	81.4	85.8	112.7	85.5	91.6	118.3	Inflammation	Others
dydrogesterone	51.0	83.0	78.3	56.3	50.2	43.1	Endocrinology	Others
Dyphylline(Dilor)	99.1	91.1	111.2	101.4	98.4	90.7	Respiratory Disease	PDE
Econazole-nitrate-Spectazole	94.4	94.5	77.4	93.1	80.2	95.5	Neurological Disease	Others
Edaravone	92.4	85.0	89.7	88.2	79.9	93.9	Cardiovascular Disease	Others
Ellence	15.1	26.1	11.7	34.0	20.6	37.1		Topoisomerase
Eloxatin	58.2	72.2	85.8	76.4	58.0	88.8	Cancer	DNA/RNA Synthesis
Eltrombopag-SB-497115-GR	84.1	104.3	105.0	102.4	95.5	98.5	Cancer	Others
Elvitegravir	86.3	100.1	97.5	103.1	89.6	99.8	Immunology	Integrase
Emtricitabine	87.5	100.0	106.3	106.9	94.3	92.4	Infection	Reverse Transcriptase
Enalaprilat	92.5	95.9	98.0	97.4	97.0	99.8	Cardiovascular Disease	RAAS
Enalapril-maleate(Vasotec)	52.4	58.8	61.6	61.0	70.9	95.3	Cardiovascular Disease	Opioid Receptor
Enoxacin(Penetrex)	87.4	95.6	92.1	99.0	83.3	91.0	Infection	Others
entacapone	102.5	98.6	102.3	107.9	99.9	97.0	Neurological Disease	Others
Entecavir	102.2	98.5	101.2	109.3	91.8	97.6	Infection	Others
epalrestat	99.0	97.1	110.5	106.1	87.4	91.7	Inflammation	Others
Epinephrine-bitartrate-Adrenalinium	77.8	86.8	80.5	89.1	76.6	97.5	Cancer	Adrenergic Receptor
eprosartan-mesylate	91.0	93.1	84.1	86.8	68.0	87.1	Cardiovascular Disease	Others
erdosteine	100.3	96.7	101.0	106.6	93.7	97.1	Respiratory Disease	Others
Erlotinib-Hydrochloride.	74.2	63.2	63.6	57.2	28.5	76.9	Cancer	EGFR
Erythromycin(E-Mycin).ht	100.2	97.1	101.6	101.8	105.8	98.5	Infection	Others
erythromycin-ethylsuccinate	101.5	97.8	101.8	99.3	100.4	93.2	Infection	Others
escitalopram-oxalate	100.9	101.6	102.9	108.9	99.5	95.8	Infection	5-HT Receptor
esmolol-hcl	34.1	79.4	53.0	66.8	42.8	79.7	Cardiovascular Disease	Others
Esomeprazole-magnesium(Nexium)	84.5	93.1	78.2	89.0	55.3	93.8	Digestive system disease	5-alpha Reductase
Esomeprazole-sodium-Nexium-I.V.	99.4	102.1	96.3	100.0	96.6	103.1	Cancer	ATPase
Estradiol	98.0	108.0	121.4	115.8	107.6	101.1	Endocrinology	Others

DRUG	MCF-7	ZR-75-1	MCF-7-TRF	ZR-75-1-TamR	MCF10A	MDA-MB-231	Indication	Target
estradiol-cypionate	97.8	98.2	99.8	97.0	78.9	99.6		Estrogen/progestogen Receptor
estradiol-valerate	91.6	93.2	99.5	103.0	101.3	101.3	Endocrinology	Estrogen/progestogen Receptor
Estriol(Oestriol)	71.6	74.1	60.8	75.2	72.5	82.0	Neurological Disease	Estrogen/progestogen Receptor
Estrone	90.3	107.5	112.8	115.5	94.0	99.8	Endocrinology	Others
ethacridine-lactate-monohydrate	82.0	96.4	101.2	102.5	87.0	96.0	Infection	Others
ethambutol-hcl	87.4	93.7	100.1	76.3	95.8	128.1	Neurological Disease	Others
ethamsylate	86.4	92.9	84.6	98.7	74.3	93.5	Cardiovascular Disease	Others
Ethinyl-Estradiol	101.5	100.2	117.1	123.3	100.4	104.2	Endocrinology	Others
Ethionamide	86.7	93.2	84.3	98.6	74.8	93.4	Infection	Others
ethoxzolamide	96.5	94.6	89.9	95.2	79.8	90.1	Neurological Disease	Others
ethynodiol-diacetate	98.0	98.5	98.7	98.7	102.9	101.3	Endocrinology	Estrogen/progestogen Receptor
Etodolac	84.9	89.3	90.4	87.1	78.2	88.0	Inflammation	COX
Etomidate	95.8	88.8	84.3	95.0	79.4	87.4	Neurological Disease	GABA Receptor
Etopophos	53.3	68.7	51.5	67.5	48.3	78.1	Cancer	Topoisomerase
etravirine-tmc125	91.2	96.9	103.5	108.4	87.6	99.6	Neurological Disease	Reverse Transcriptase
Everolimus(RAD001)	36.9	44.8	45.4	46.2	55.1	68.3	Cancer	mTOR
Evista	65.3	75.4	84.5	99.0	57.3	106.9	Endocrinology	Estrogen/progestogen Receptor
Exemestane	92.6	90.1	84.2	82.1	84.6	92.4	Endocrinology	Aromatase
Ezetimibe(Zetia)	104.4	99.9	101.4	97.9	106.5	96.6	Cardiovascular Disease	Others
Famciclovir(Famvir)	64.1	67.5	57.8	71.7	26.6	85.3	Cancer	Others
famotidine-pepcid	106.6	100.4	100.3	95.1	100.5	100.0	Cardiovascular Disease	Histamine Receptor
famprofazone	76.4	90.4	94.6	88.1	75.4	100.7	Inflammation	Others
Febuxostat(Uloric)	98.7	98.6	101.2	101.0	99.7	103.4	Inflammation	Others
Felbamate	83.3	89.4	80.3	87.0	74.8	86.3	Neurological Disease	Others
Felodipine(Plendil)	47.7	51.7	36.3	48.0	42.6	32.2	Cardiovascular Disease	NULL
Fenbendazole(Panacur)	87.9	84.8	85.8	90.6	75.3	91.5		Others
Fenofibrate(Tricor)	40.8	57.1	40.0	40.8	42.1	61.0	Cardiovascular Disease	NULL
fenoprofen-calcium	100.4	100.1	88.8	108.6	91.0	99.3	Inflammation	Others
fenoprofen-calcium-hydrate	78.3	78.3	84.6	91.9	75.9	89.2	Immunology	Others
Fenspiride-hcl	85.6	75.9	79.9	77.9	46.5	63.7	Inflammation	Others
fenticonazole-nitrate	76.7	72.9	62.0	86.2	64.7	93.9	Neurological Disease	Others
Fesoterodine-fumarate-Toviaz	16.9	42.4	47.1	40.8	85.9	53.4	Immunology	AChR
fexofenadine-hcl	97.4	99.8	99.4	97.2	102.6	100.1	Neurological Disease	Histamine Receptor
fidaxomicin	82.4	88.2	85.4	87.3	69.4	95.5	Infection	Others
Finasteride	87.4	90.1	86.6	96.8	81.8	93.3	Endocrinology	5-alpha Reductase
FK-506-(Tacrolimus)	93.9	90.5	96.3	94.9	96.3	94.6	Cancer	Others
flavoxate-hcl	63.8	60.1	49.8	60.7	88.1	84.1	Neurological Disease	AChR
florfenicol	90.2	89.9	101.8	108.8	88.5	95.1	Infection	Others
Floxuridine	47.7	51.6	36.3	48.0	42.6	32.1	Cancer	DNA/RNA Synthesis
Fluconazole	85.4	92.3	96.2	96.2	81.9	96.0	Infection	Others
Flucytosine(Ancobon)	100.1	104.0	96.0	97.0	94.5	101.7	Infection	Others
Fludara	78.9	97.5	87.8	97.5	80.4	98.3	Cancer	DNA/RNA Synthesis
Fludarabine(Fludara)	96.9	96.2	107.5	110.5	94.6	96.1	Cancer	STAT, DNA/RNA Synthesis
Flumazenil	86.5	97.2	90.2	97.7	80.4	98.6	Neurological Disease	GABA Receptor
flumequine	99.5	98.9	96.6	106.1	100.1	101.5	Metabolic Disease	Others
flumethasone	73.4	79.9	73.8	76.9	59.8	86.5	Endocrinology	Others
flunarizine-dihydrochloride	55.4	68.5	54.6	75.3	65.1	95.8	Cancer	Calcium Channel
flunixin-meglumin	100.3	97.2	101.4	101.7	105.8	98.5	Immunology	COX
Fluocinolone-acetonide(Flucort-N)	78.1	77.7	80.5	80.4	69.7	68.7	Infection	Others
Fluocinonide(Vanos)	84.8	89.4	90.4	87.3	77.9	87.9	Endocrinology	Others
fluorometholone-acetate	92.2	84.8	89.9	88.3	79.5	94.0	Inflammation	Others
Fluoxetine-hydrochloride	65.1	95.4	95.8	99.0	80.4	101.1	Neurological Disease	5-HT Receptor
Flurbiprofen(Ansaid)	99.3	102.0	96.5	100.0	96.7	103.1	Inflammation	Others
Flutamide(Eulexin)	78.2	91.1	98.5	88.1	81.5	89.7	Cancer	P450
fluticasone-propionate-Flonase-Veramyst	99.7	102.2	104.3	103.6	86.1	101.3	Inflammation	Others

DRUG	MCF-7	ZR-75-1	MCF-7-TRF	ZR-75-1-TamR	MCF10A	MDA-MB-231	Indication	Target
Fluvastatin-Sodium(Lescol).htm	89.7	93.2	95.9	95.5	84.0	98.0	Cardiovascular Disease	HMG-CoA Reductase
Fluvoxamine-maleate	78.2	91.0	98.7	88.1	81.5	89.7	Neurological Disease	5-HT Receptor
formoterol-hemifumarate	93.2	93.0	96.8	111.7	85.0	96.6	Neurological Disease	Adrenergic Receptor
fosaprepitant	97.9	91.4	85.6	88.9	88.6	95.0	Cardiovascular Disease	Others
fosfomycin-tromethamine	103.6	97.1	106.9	109.1	97.3	102.5		Others
Ftorafur	81.0	79.5	70.7	77.8	74.0	95.3	Cancer	DNA/RNA Synthesis
Fulvestrant	39.2	70.8	58.1	88.1	78.3	84.7	Cancer	Estrogen/progestogen Receptor
furaltadone-hcl	98.2	98.7	107.4	110.3	98.6	96.8	Infection	Others
Furosemide(Lasix)	91.8	98.5	94.1	94.8	107.4	93.7	Cardiovascular Disease	Others
gabexate-mesylate	87.5	93.7	99.9	76.1	96.2	128.2	Cardiovascular Disease	Proteasome
Gallamine-triethiodide(Flaxedil)	73.5	80.2	73.7	76.9	59.9	86.3	Inflammation	AChR
ganciclovir	14.0	16.2	11.9	28.0	16.5	31.8	Infection	Others
Gatifloxacin	89.7	93.1	96.0	95.5	84.0	98.0		Others
GDC-0449	76.9	87.7	88.1	85.9	75.6	92.9	Cancer	Hedgehog, P-gp
Gefitinib	73.7	71.9	57.1	60.2	27.3	89.4	Cancer	EGFR
Gemcitabine(Gemzar)	6.1	10.8	4.1	8.4	3.4	4.0	Metabolic Disease	Others
Gemfibrozil(Lopid)	73.6	80.1	73.5	76.8	60.2	86.4	Cardiovascular Disease	Others
genipin	93.5	94.7	103.8	87.0	88.3	121.3		Others
geniposide	95.9	97.7	108.7	86.6	104.0	116.1		Others
geniposidic-acid	101.1	101.6	102.7	108.6	99.9	95.9		Others
Genistein	94.8	100.5	110.4	111.6	83.2	87.4	Cancer	Topoisomerase
Gestodene	87.6	87.2	90.5	92.9	78.1	93.6	Endocrinology	Estrogen/progestogen Receptor
gimeracil	98.2	98.5	98.5	98.4	103.3	101.4	Neurological Disease	Dehydrogenase
ginkgolide-a	93.7	93.9	100.8	113.3	87.8	101.2	Cardiovascular Disease	GABA Receptor
glafenine-hcl	97.3	93.7	108.0	108.7	99.1	92.2	Inflammation	Others
gliclazide-diamicron	93.6	81.0	78.2	84.1	78.2	90.9	Neurological Disease	Others
Glimepiride	90.8	100.8	94.8	100.2	88.1	90.8	Metabolic Disease	DPP-4
Glipizide(Glucotrol)	50.3	71.4	47.2	59.8	41.1	77.6	Endocrinology	Others
gliquidone	89.8	92.0	88.1	98.1	93.7	96.3	Metabolic Disease	Others
Glyburide(Diabeta)	42.6	54.0	41.0	52.9	31.4	31.0	Endocrinology	Others
Guaifenesin(Guaiphenesin)	91.2	93.4	83.7	86.7	68.3	87.0	Respiratory Disease	Others
guanabenz-wy-8678-acetate	87.0	101.1	108.9	105.3	96.4	104.4	Endocrinology	Adrenergic Receptor
guanidine-aminoformamidine-hcl	94.1	94.5	101.7	103.3	96.1	92.7	Vermifuge	Others
halobetasol-propionate	27.1	36.2	36.2	44.3	45.7	75.5	Inflammation	Others
Haloperidol(Haldol)	79.5	93.6	93.8	91.2	83.6	93.4	Neurological Disease	Others
homatropine-bromide	93.2	102.9	94.1	99.6	96.2	97.4	Infection	AChR
homatropine-methylbromide	104.3	103.1	90.9	103.2	96.2	101.5		AChR
Hydrochlorothiazide	102.9	100.2	104.0	102.3	102.3	93.4	Cardiovascular Disease	Others
Hydrocortisone	95.8	97.6	108.9	86.6	104.0	116.1	Infection	Others
Hydroxyurea(Cytodrox)	70.5	82.4	93.4	68.5	71.4	119.2	Cancer	Others
hydroxyzine-2hcl	100.4	101.8	96.6	96.6	92.0	100.4	Neurological Disease	Histamine Receptor
hyoscyamine-daturine	103.8	104.7	94.3	108.9	100.1	102.2	Neurological Disease	AChR
Ibuprofen(Advil)	104.0	104.5	94.3	108.6	100.5	102.2	Inflammation	COX
ibutilide-fumarate	106.1	99.1	96.2	98.4	101.3	95.6	Cardiovascular Disease	Sodium Channel
Idarubicin	16.1	19.4	12.9	19.4	20.2	26.6	Cancer	Topoisomerase
idebenone	70.4	82.4	93.6	68.6	71.1	119.1	Inflammation	Others
idoxuridine	61.5	76.8	67.1	74.9	52.9	86.7	Infection	Others
Ifosfamide	93.7	80.9	78.2	84.0	78.5	90.9	Cancer	DNA/RNA Synthesis
Iloperidone(Fanapt)	99.0	96.9	110.7	106.2	87.4	91.7	Neurological Disease	Others
Imatinib(STI571)	27.1	36.3	36.2	44.3	45.8	75.4	Neurological Disease	PDGFR,c-Kit, v-Abl
Imatinib-Mesylate	71.7	74.0	60.8	75.1	72.7	82.0	Cancer	PDGFR, c-Kit, Bcr-Abl
imidapril-tanatril	104.0	97.2	95.3	99.7	94.7	108.2	Cardiovascular Disease	RAAS
imipramine-hcl	55.3	68.3	54.8	75.4	64.7	95.9	Neurological Disease	Others
INCB18424	68.7	93.1	95.9	100.6	81.7	98.8	Cancer	JAK
indacaterol-maleate	95.7	103.8	104.6	115.6	93.4	98.1	Infection	Adrenergic Receptor
Indapamide(Lozol)	27.2	36.3	36.1	44.2	46.0	75.4	Cardiovascular Disease	Others

DRUG	MCF-7	ZR-75-1	MCF-7-TRF	ZR-75-1-TamR	MCF10A	MDA-MB-231	Indication	Target
Indomethacin(Indocid)	64.2	67.5	57.7	71.5	26.6	85.3	Inflammation	Others
Ipratropium-bromide	100.8	100.7	106.1	100.9	104.9	97.1	Respiratory Disease	Others
Irinotecan	38.9	53.0	42.2	49.6	51.0	68.9	Cancer	Topoisomerase
Irinotecan-Hcl-Trihydrate-Campto	97.8	98.6	99.8	104.8	98.1	102.9	Neurological Disease	Topoisomerase
Irsogladine-maleate	61.4	64.1	54.2	83.0	83.0	83.5	Neurological Disease	Others
Isoconazole-nitrate-Travogen	85.7	91.0	89.9	93.0	78.2	102.2	Infection	Others
isoetharine-mesylate	81.3	89.5	79.3	92.9	90.7	89.3	Cardiovascular Disease	Others
Isoniazid(Tubizid)	86.8	90.2	94.3	95.2	81.0	99.0	Infection	Angiogenesis
Isoprenaline-hydrochloride	82.0	96.8	101.0	102.7	87.1	95.9	Infection	Adrenergic Receptor
isosorbide	99.9	99.9	112.3	109.5	91.7	99.1		Others
Isotretinoin	52.3	58.8	61.7	61.1	70.9	95.3	Metabolic Disease	Hydroxylase
isovaleramide	80.2	97.3	94.6	93.0	83.4	93.9	Neurological Disease	Others
isoxicam	98.8	90.9	111.4	101.5	97.9	90.7	Inflammation	Others
Isradipine(Dynacirc)	93.1	97.4	106.5	100.5	96.6	102.7	Neurological Disease	Others
Itraconazole(Sporanox)	85.7	76.2	79.7	77.9	46.5	63.6	Cancer	Others
ivabradine-hcl-procoralan	105.1	103.2	95.0	103.3	97.4	103.0	Neurological Disease	Adrenergic Receptor
Ivermectin	72.7	93.8	77.4	84.1	42.1	95.5	Vermifuge	Others
Ketoconazole	88.1	95.5	97.3	96.1	65.1	101.1	Infection	P450
Ketoprofen(Actron)	103.9	96.5	107.6	98.2	107.3	106.3	Inflammation	COX
Ketorolac-Tromethamine(Toradol)	91.7	95.3	97.7	99.1	94.7	98.9	Neurological Disease	COX
ketotifen-fumarate-zaditor	96.5	90.4	102.7	106.8	84.5	87.7	Neurological Disease	Histamine Receptor
lacidipine-lacipil-motens	98.5	101.1	100.6	107.4	93.6	102.9	Cardiovascular Disease	Calcium Channel
L-Adrenaline-Epinephrine	10.9	26.2	8.0	31.7	4.0	26.4	Cardiovascular Disease	Others
lafutidine	100.6	101.7	96.2	99.2	100.9	98.0	Infection	Histamine Receptor
Lamivudine(Epivir)	100.5	101.0	109.5	102.6	95.8	101.0	Infection	Others
lamotrigine	93.0	89.7	85.4	89.3	77.7	95.7	Cancer	Sodium Channel
Lansoprazole	84.3	95.2	94.1	92.1	79.5	95.4	Infection	Proton Pump
lapatinib	104.0	104.6	94.1	108.6	100.5	102.2	Neurological Disease	EGFR, HER2
Lapatinib-Ditosylate	64.1	67.4	57.8	71.5	26.7	85.3	Cancer	EGFR, HER2
Leflunomide	94.6	100.8	101.9	103.9	89.2	99.1	Inflammation	Others
Lenalidomide	88.0	84.7	85.8	90.4	75.6	91.6	Cardiovascular Disease	TNF-alpha
Letrozole	100.4	100.0	89.0	108.7	91.0	99.3	Endocrinology	Aromatase
Levetiracetam	68.5	94.4	101.7	106.9	81.1	94.4	Neurological Disease	Others
levobetaxolol-hcl	87.8	84.5	85.9	90.5	75.2	91.6	Cardiovascular Disease	Others
Levofloxacin(Levaquin)	68.8	93.2	95.7	100.5	81.7	98.8	Infection	Others
Levonorgestrel(Levonelle)	78.2	77.7	80.3	80.2	69.9	68.8	Endocrinology	Others
levosimendan	87.5	100.1	106.1	106.8	94.2	92.4	Metabolic Disease	Others
levosulpiride-levogastrol	102.9	100.0	98.0	98.0	101.0	97.6	Neurological Disease	Dopamine Receptor
licofelone	91.8	95.4	97.5	99.1	94.7	98.8		COX
Lidocaine	79.4	93.5	93.9	91.2	83.6	93.4	Neurological Disease	Histamine Receptor
linagliptin-bi-1356	96.7	93.0	88.8	100.4	82.8	104.1	Cancer	DPP-4
Lincomycin-hydrochloride(Lincocin)	82.2	85.7	67.6	79.8	70.2	94.2	Cancer	Others
Linezolid(Zyvox)	94.6	99.4	96.3	105.1	93.9	98.1	Infection	Others
liothyronine-sodium	47.5	51.5	36.4	48.1	42.4	32.2	Endocrinology	Others
lithocholic-acid	104.5	102.5	98.6	102.8	96.7	104.3	Neurological Disease	Others
lomerizine-hcl	64.0	67.2	57.9	71.7	26.5	85.4	Cardiovascular Disease	Others
Lomustine(CeeNU)	97.5	101.6	103.8	112.0	93.4	101.9	Cancer	Others
lonidamine	95.6	88.9	84.3	95.2	79.1	87.3	Cardiovascular Disease	Others
Loperamide-hydrochloride	31.9	40.3	39.5	46.0	47.5	71.7	Infection	Opioid Receptor
Lopinavir	89.1	87.7	80.7	88.5	78.8	98.7	Infection	HIV Protease
Loratadine	88.5	94.3	89.2	97.5	80.8	93.7	Inflammation	Histamine Receptor
lornoxicam-xefo	91.8	93.1	99.3	102.7	101.7	101.3	Inflammation	Others
losartan-potassium	96.2	91.5	93.0	98.3	82.1	89.1	Cardiovascular Disease	RAAS
Loteprednol-etabonate	94.5	90.9	101.3	90.0	101.1	111.7		Others
lovastatin-mevacor	67.5	71.4	53.9	79.8	89.4	86.0	Respiratory Disease	HMG-CoA Reductase
loxapine-succinate	78.0	77.4	80.6	80.4	69.6	68.8	Neurological Disease	Others
l-thyroxine	80.9	79.6	70.7	78.0	73.8	95.3	Neurological Disease	Others
Malotilate	91.8	97.4	89.1	98.9	84.3	96.7	Metabolic Disease	Others

DRUG	MCF-7	ZR-75-1	MCF-7-TRF	ZR-75-1-TamR	MCF10A	MDA-MB-231	Indication	Target
Manidipine(Manyper)	61.3	76.6	65.3	72.4	38.2	82.4	Metabolic Disease	Calcium Channel
Maprotiline-hydrochloride	86.5	93.2	84.4	98.8	74.5	93.3	Neurological Disease	Reuptake inhibitor
Maraviroc	89.1	102.6	99.9	109.3	91.0	96.6	Inflammation	CCR5
Marbofloxacin	100.8	99.7	108.9	114.7	93.7	102.8		Others
Masitinib-(AB1010)	81.4	91.5	82.5	96.2	71.2	99.7	Respiratory Disease	c-Kit, PDGFR, FGFR, FAK
MDV3100	81.3	96.6	97.0	102.3	87.6	100.3	Cancer	Androgen Receptor, P450
mecarbinate	99.7	98.8	96.4	105.9	100.5	101.6	Metabolic Disease	Others
meclofenamate-sodium	77.1	87.5	83.2	96.4	80.9	92.8		COX
medetomidine-hcl	86.9	92.3	89.0	102.7	81.5	97.5	Infection	Adrenergic Receptor
Medroxyprogesterone-acetate	97.8	97.8	103.5	110.5	92.0	96.5	Infection	Estrogen/progestogen Receptor
mefenamic-acid	50.2	71.1	47.4	60.0	40.9	77.7	Cardiovascular Disease	COX
Megestrol-Acetate	73.5	75.6	70.8	83.3	71.1	98.7	Infection	Androgen Receptor
meglumine	88.2	98.2	91.7	96.4	80.0	101.1		Others
Melatonin	72.9	87.4	92.1	88.5	77.3	90.3	Endocrinology	Others
Meloxicam(Mobic)	32.0	40.4	39.4	45.9	47.7	71.7	Inflammation	Others
memantine-hydrochloride-namenda	70.4	55.2	99.5	90.3	49.3	74.3	Neurological Disease	AMPA Receptor-kainate Receptor-NMDA Receptor
Menadione	89.1	87.8	80.5	88.4	78.8	98.7	Endocrinology	Others
mepenzolate-bromide	100.6	99.5	109.2	114.8	93.2	102.9		Others
mepiroxol	93.3	92.8	73.9	85.0	74.8	94.7		Others
mepivacaine-hydrochloride	90.6	96.1	100.2	96.2	105.1	94.4	Metabolic Disease	Others
meptazinol-hydrochloride	104.7	101.8	96.4	96.1	102.5	94.9		Others
mequinol	6.1	10.8	4.1	8.4	3.4	4.0	Infection	Others
Mercaptopurine	60.5	77.4	52.2	83.2	57.5	91.6	Cancer	DNA/RNA Synthesis
Meropenem	93.1	89.6	85.4	89.2	78.0	95.7	Infection	Others
Mesalamine(Lialda)	100.9	102.3	104.0	99.6	105.2	96.2	Inflammation	Others
Mesna(Uromitexan)	61.4	76.6	65.2	72.2	38.3	82.4	Cancer	Others
mesoridazine-besylate	97.5	88.1	84.5	86.8	76.5	95.2	Neurological Disease	Others
Mestranol	93.3	102.9	93.9	99.3	96.6	97.4	Endocrinology	NULL
metaproterenol-sulfate	97.7	91.1	85.8	88.8	88.4	95.2	Respiratory Disease	Others
metaraminol-bitartrate	90.3	90.2	87.5	99.0	81.1	101.2		Others
Methacycline-hydrochloride-Physiomycine	81.9	87.1	85.4	92.1	80.2	95.6	Cancer	Others
methazolamide	90.2	107.6	112.8	115.7	93.6	99.7	Neurological Disease	Carbonic Anhydrase
Methazolastone	100.2	96.5	101.2	106.7	93.7	97.1	Cancer	Others
methenamine-mandelamine	81.3	85.8	112.9	85.7	91.3	118.2	Inflammation	Others
Methimazole(Tapazole)	102.7	97.6	90.6	93.5	102.2	98.2	Endocrinology	Others
Methocarbamol(Robaxin)	51.2	83.3	77.9	56.2	50.4	43.1	Neurological Disease	Others
Methoxsalen(Oxsoralen)	93.2	89.7	85.2	89.1	78.0	95.7	Inflammation	Others
Methscopolamine-bromide(Pamine)	87.9	90.0	83.5	91.1	79.8	103.1	Neurological Disease	AChR
methyclothiazide	87.9	92.1	103.3	78.6	92.3	117.3	Cardiovascular Disease	Others
Methylprednisolone	82.4	85.7	67.5	79.6	70.5	94.2	Immunology	Others
methylthiouracil	44.4	61.2	46.8	52.9	17.4	76.1	Infection	Others
meticrane	105.1	95.6	89.6	99.3	78.6	96.1	Cardiovascular Disease	Others
Metolazone(Zaroxolyn)	105.8	101.2	94.7	94.6	103.5	95.0	Cardiovascular Disease	Others
metoprolol-tartrate	100.2	100.2	111.9	109.4	92.2	99.0	Cardiovascular Disease	Adrenergic Receptor
Metronidazole(Flagyl)	65.2	95.5	95.6	99.0	80.4	101.1	Infection	Others
mevastatin	90.6	85.9	98.4	91.9	76.9	92.2	Cardiovascular Disease	Others
mexiletine-hcl	70.3	82.1	93.8	68.6	71.1	119.4	Cardiovascular Disease	Others
mezlocillin-sodium	75.7	103.6	65.5	77.0	50.0	75.2	Infection	Others
Mianserin-hydrochloride	83.1	89.5	84.9	83.0	82.9	95.1	Neurological Disease	Others
Miconazole-Monistat	15.0	26.1	11.7	34.0	20.5	37.0	Neurological Disease	Others
Miconazole-nitrate	83.2	89.6	84.7	82.9	82.9	95.1	Infection	Others
Mifepristone(Mifeprex)	82.4	88.5	85.2	87.4	69.5	95.4	Metabolic Disease	Estrogen/progestogen Receptor
miglitol-glyset	70.4	66.4	64.6	68.6	69.9	88.8	Neurological Disease	Others
milnacipran-hydrochloride	70.3	55.2	99.7	90.5	49.1	74.2	Endocrinology	Others

DRUG	MCF-7	ZR-75-1	MCF-7-TRF	ZR-75-1-TamR	MCF10A	MDA-MB-231	Indication	Target
Milrinone(Primacor)	51.1	83.3	78.1	56.3	50.3	43.1	Cardiovascular Disease	ATPase
mirabegron-ym178	103.3	104.2	104.1	99.9	99.1	102.4	Cancer	Adrenergic Receptor
mirtazapine-remeron-avanza	95.9	103.7	104.3	115.3	93.7	98.2	Immunology	Others
Mitotane(Lysodren)	85.9	76.2	79.6	77.7	46.7	63.6	Cancer	Others
Mitoxantrone	81.3	91.6	82.5	96.4	70.9	99.6	Cardiovascular Disease	Others
moclobemide	101.4	100.3	117.1	123.6	100.0	104.1	Neurological Disease	MAO
moexipril-hydrochloride	102.8	97.7	90.5	93.5	102.2	98.2	Digestive system disease	RAAS
moguisteine	93.1	93.0	97.0	112.0	84.7	96.5	Respiratory Disease	Others
mometasone-furoate	94.7	99.5	96.2	105.1	93.8	98.1	Inflammation	Others
Monobenzone(Benoquin)	100.5	101.7	96.6	96.4	92.4	100.5	Metabolic Disease	Others
montelukast-sodium	70.3	66.1	64.7	68.6	69.8	88.9	Respiratory Disease	Others
Moroxydine-hydrochloride	34.2	79.6	52.9	66.9	42.9	79.5	Cancer	Others
Mosapride-citrate	78.4	78.3	84.6	91.7	76.2	89.2	Neurological Disease	5-HT Receptor
moxalactam-disodium	87.9	97.9	92.1	96.5	79.6	101.1	Infection	Others
Moxifloxacin	100.4	101.9	110.8	110.5	93.3	102.9	Infection	Topoisomerase
moxonidine	105.0	93.3	103.1	96.1	99.2	97.2	Digestive system disease	Others
mupirocin	87.3	87.0	90.7	92.9	77.7	93.7		DNA/RNA Synthesis
Mycophenolate-mofetil-(CellCept)	70.4	55.2	99.7	90.3	49.3	74.3	Immunology	Others
Mycophenolic-acid(Mycophenolate)	76.9	87.8	88.1	86.1	75.4	92.8	Infection	Others
nabumetone	100.7	100.8	106.1	101.1	104.4	97.0	Inflammation	COX
nadifloxacin	105.1	95.8	107.5	111.7	92.6	93.2	Neurological Disease	Others
Nafamostat-mesylate	96.8	92.9	88.8	100.2	83.1	104.2	Cardiovascular Disease	Proteasome
nafcillin-sodium	94.3	91.0	101.3	90.2	100.7	111.6	Endocrinology	Others
Naftopidil(Flivas)	100.6	101.8	96.4	96.3	92.4	100.5	Endocrinology	Adrenergic Receptor
Nalidixic-acid(NegGram)	104.5	100.6	105.7	102.0	96.6	101.7	Infection	Others
nalmefene-hcl	82.2	93.6	95.7	93.2	77.5	104.7	Neurological Disease	Others
naloxone-hcl	86.1	100.2	97.7	103.3	89.3	99.7	Cancer	Opioid Receptor
naltrexone-hcl	103.5	104.2	103.8	99.7	99.4	102.5	Neurological Disease	Opioid Receptor
Naphazoline-hydrochloride-Naphcon	72.9	87.5	92.1	88.7	77.0	90.3	Neurological Disease	Adrenergic Receptor
Naproxen-Sodium(Aleve)	103.5	101.5	98.9	113.8	97.8	97.9	Inflammation	COX
Naratriptan(Amerge)	103.9	97.3	106.7	109.0	97.8	102.4	Neurological Disease	5-HT Receptor
Natamycin(Pimaricin).htm	88.7	92.3	98.6	95.1	102.5	103.3	Infection	Others
Nateglinide(Starlix)	91.1	93.4	83.9	86.9	68.0	87.0	Immunology	Potassium Channel
Nebivolol(Bystolic)	94.5	94.3	94.8	90.3	97.0	90.2	Cardiovascular Disease	Adrenergic Receptor
Nefiracetam(Translon)	98.1	91.4	85.4	88.6	88.9	95.1	Neurological Disease	GABA Receptor
nelfinavir-mesylate	96.0	91.2	93.2	98.4	81.7	89.2		HIV Protease
Nepafenac	104.1	95.1	98.2	110.9	102.5	95.1	Inflammation	Others
Nevirapine(Viramune)	91.8	97.5	89.0	98.8	84.3	96.7	Infection	Others
Niacin(Nicotinic-acid)	24.8	37.9	25.8	53.4	28.5	40.2	Metabolic Disease	Others
nialamide	87.7	89.7	83.9	91.3	79.4	103.1	Neurological Disease	Others
nicardipine-hcl	100.1	99.8	89.2	108.7	90.5	99.4	Neurological Disease	Others
Nicorandil(Ikorel)	90.5	90.5	87.1	98.8	81.6	101.1	Cardiovascular Disease	Others
Nicotinamide(Niacinamide)	84.9	89.4	90.3	87.1	78.2	88.0	Neurological Disease	NULL
nicotine-ditartrate	93.0	92.7	97.2	111.8	84.6	96.6	Neurological Disease	Others
Nifedipine(Adalat)	16.1	19.4	12.9	19.4	20.2	26.6	Cardiovascular Disease	Others
nifenazone	102.4	98.2	102.6	107.8	99.8	97.1	Inflammation	Others
niflumic-acid	87.4	87.3	90.5	93.1	77.8	93.5	Infection	GABA Receptor
nifuroxazide	100.0	96.3	101.5	106.7	93.2	97.2	Infection	Others
Nilotinib	78.2	77.6	80.5	80.2	69.9	68.8	Cancer	Bcr-Abl
nilvadipine-arc029	78.1	91.1	98.7	88.3	81.2	89.7	Cancer	Calcium Channel
nimesulide	44.6	61.2	46.7	52.8	17.5	76.2	Cardiovascular Disease	Others
Nimodipine(Nimotop)	27.2	47.5	25.9	51.6	37.3	47.1	Cardiovascular Disease	Others
Nisoldipine(Sular)	68.9	101.7	99.8	103.8	79.8	101.2	Cardiovascular Disease	Others
Nitazoxanide(Alinia)	104.6	102.4	98.6	102.6	97.1	104.4	Vermifuge	Others
nithiamide	85.2	92.1	96.4	96.3	81.5	96.1		Others
Nitrendipine	36.9	44.8	45.4	46.3	54.8	68.2	Neurological Disease	Calcium Channel

DRUG	MCF-7	ZR-75-1	MCF-7-TRF	ZR-75-1-TamR	MCF10A	MDA-MB-231	Indication	Target
Nitrofurazone(ACTIN-N)	99.2	100.7	93.5	97.2	100.8	98.3	Infection	Others
Nizatidine(Axid)	93.8	81.0	78.1	83.9	78.5	90.9	Metabolic Disease	Others
noradrenaline-bitartrate-monohydrate-levophed	86.4	97.3	90.2	97.9	80.1	98.5	Metabolic Disease	Others
norethindrone-norethisterone	100.0	104.1	96.1	97.2	94.1	101.6	Neurological Disease	Others
noscapine-hcl	91.1	96.6	103.7	108.3	87.5	99.8	Cancer	Others
Nystatin(Mycostatin).htm	87.6	87.3	90.3	92.8	78.1	93.6	Infection	Others
octopamine-hcl	102.6	97.7	90.6	93.7	101.7	98.2	Immunology	Others
Olanzapine(Zyprexa)	84.4	93.1	78.3	89.2	55.1	93.7	Infection	5-HT Receptor, Dopamine Receptor
olmesartan-medoxomil-Benicar	99.1	98.3	96.7	100.3	99.3	103.6	Cardiovascular Disease	RAAS
Olopatadine-hydrochloride(Opatanol)	24.8	37.8	25.9	53.5	28.4	40.2	Neurological Disease	Histamine Receptor
olsalazine-sodium	100.0	102.3	98.0	98.5	100.2	98.8	Inflammation	Others
Omeprazole	96.7	94.9	89.7	95.0	80.2	90.1	Metabolic Disease	Proton Pump, ATPase
Ondansetron-hydrochloride	76.4	90.6	94.3	87.9	75.8	100.6	Infection	5-HT Receptor
Orlistat(Alli)	99.3	97.9	98.1	96.6	89.3	95.7	Metabolic Disease	Others
ornidazole	55.3	68.5	54.7	75.4	64.8	95.7	Endocrinology	Others
orphenadrine-citrate-norflex	90.7	96.1	100.0	95.9	105.5	94.4	Infection	AChR
OSI-420-Desmethyl-Erlotinib,CP-473420	94.5	91.0	101.1	90.0	101.1	111.7	Cancer	EGFR
ospemifene	61.1	63.8	54.4	83.1	82.7	83.6		Estrogen/progestogen Receptor
otilonium-bromide	82.2	93.9	95.5	93.3	77.7	104.5	Cardiovascular Disease	AChR
ouabain	31.1	52.1	36.8	35.0	47.7	64.8	Neurological Disease	Sodium Channel
oxaprozin	95.5	88.5	84.5	95.1	78.9	87.4	Inflammation	Others
Oxcarbazepine	81.5	89.7	79.1	92.8	91.0	89.3	Neurological Disease	Sodium Channel
oxeladin-citrate	91.4	92.9	99.7	102.9	101.2	101.5	Respiratory Disease	Others
oxethazaine	102.4	100.7	84.8	100.4	80.8	104.8	Neurological Disease	Others
oxfendazole	81.3	96.7	96.8	102.2	87.5	100.3	Vermifuge	Others
oxybuprocaine-hcl	84.7	89.1	90.6	87.2	77.8	88.0	Neurological Disease	Others
Oxybutynin(Ditropan)	80.4	97.6	94.2	93.0	83.8	93.8	Neurological Disease	Others
oxybutynin-chloride	100.3	102.0	110.8	110.8	92.9	102.8	Neurological Disease	AChR
Oxymetazoline-hydrochloride	27.1	47.5	25.9	51.7	37.1	47.0	Immunology	Adrenergic Receptor
Oxytetracycline(Terramycin)	79.1	79.9	87.4	94.1	65.8	74.8	Infection	NULL
oxytetracycline-dihydrate	90.0	92.0	88.0	97.8	94.1	96.4	Infection	Others
Ozagrel	68.8	101.7	100.0	104.1	79.6	101.2	Cardiovascular Disease	Factor Xa
ozagrel-hydrochloride	91.8	98.6	94.0	94.8	107.3	93.7	Cardiovascular Disease	Others
Paclitaxel(Taxol)	27.2	47.5	25.9	51.6	37.3	47.1	Cancer	Microtubule Associated
paeoniflorin	101.8	97.8	101.6	99.0	100.8	93.3		Others
Pancuronium-bromide(Pavulon)	80.2	97.6	94.4	93.2	83.5	93.7	Cardiovascular Disease	AChR
paromomycin-sulfate	65.1	95.2	96.0	99.1	79.9	101.2	Cardiovascular Disease	Others
paroxetine-hcl	68.4	94.5	101.7	107.1	80.8	94.3	Infection	5-HT Receptor
pasiniazid	99.4	89.3	98.3	98.7	99.2	99.5	Infection	Others
pazopanib	96.1	91.6	93.0	98.5	81.8	89.1	Cardiovascular Disease	VEGFR
Pazopanib-Hydrochloride	73.5	80.1	73.7	76.8	60.2	86.4	Cancer	VEGFR, PDGFR, c-Kit
pci-32765	65.1	95.5	95.8	99.2	80.1	101.0	Neurological Disease	Src
pefloxacin-mesylate	98.5	99.1	107.0	110.2	98.9	96.8	Infection	Others
penciclovir	15.0	25.3	17.9	36.0	62.5	81.7	Infection	Others
penfluridol	68.5	85.5	65.8	97.1	59.0	87.7	Neurological Disease	Others
pentamidine	99.1	98.0	98.1	96.8	88.9	95.7	Infection	Others
pentoxifylline	103.7	96.7	79.9	99.7	87.1	90.3		Others
Pergolide-mesylate	103.4	101.7	98.9	114.0	97.4	97.9	Neurological Disease	Dopamine Receptor
PF-2341066	34.2	79.5	52.9	66.7	43.0	79.6	Cancer	c-Met, ALK
phenacetin	100.0	100.2	112.1	109.7	91.9	98.9	Infection	COX
Phenformin-hydrochloride	16.1	19.4	12.9	19.4	20.2	26.6	Metabolic Disease	AMPK
Phenindione(Rectadione)	88.5	94.4	89.1	97.4	80.8	93.7	Cardiovascular Disease	Others
pheniramine-maleate	102.0	98.2	100.0	101.4	98.3	102.6	Neurological Disease	Others
phenothrin	101.2	101.7	110.7	106.8	91.2	92.8		Others

DRUG	MCF-7	ZR-75-1	MCF-7-TRF	ZR-75-1-TamR	MCF10A	MDA-MB-231	Indication	Target
Phenoxybenzamine-hydrochloride	87.2	95.6	92.2	99.3	83.0	90.9	Endocrinology	Androgen Receptor
phentolamine-mesilate	97.0	96.3	107.3	110.5	94.6	96.1	Cardiovascular Disease	adrenergic receptor
Phenylbutazone(Butazolidin)	106.1	99.0	97.7	96.6	101.8	101.3	Cancer	Others
Phenylephrine-hydrochloride	107.7	100.9	110.7	108.7	69.2	95.8	Endocrinology	Adrenergic Receptor
Phenytoin-Lepitoin	45.0	62.1	37.1	48.7	17.5	47.0	Endocrinology	Sodium Channel
Phenytoin-sodium-Dilantin	75.2	72.2	70.2	77.5	74.9	92.6	Metabolic Disease	Sodium Channel
phthalylsulfacetamide	95.6	103.4	104.8	115.5	93.2	98.2		Others
pidotimod	96.3	90.4	102.9	107.1	84.2	87.6	Immunology	Others
pilocarpine-hcl	83.1	89.3	80.4	87.1	74.4	86.4	Neurological Disease	Others
Pimecrolimus	107.1	100.9	106.4	115.9	97.5	101.4	Cancer	Others
Pimobendan(Vetmedin)	94.2	90.7	96.1	94.8	96.8	94.5	Cardiovascular Disease	PDE
pimozide	88.9	102.3	100.3	109.5	90.5	96.6	Neurological Disease	Others
pioglitazone-actos	72.7	79.2	72.9	78.8	73.1	88.6	Cancer	Others
pioglitazone-hydrochloride-actos	102.7	98.6	102.1	107.6	100.2	97.1	Metabolic Disease	Others
piperacillin-sodium	60.3	77.3	52.3	83.3	57.2	91.7	Infection	Others
piromidic-acid	94.4	99.2	96.6	105.2	93.4	98.2	Infection	Others
Piroxicam(Feldene)	70.0	64.6	52.0	56.5	26.6	52.7	Inflammation	COX
Pitavastatin-calcium(Livalo)	88.4	96.4	90.1	80.0	40.1	53.6	Cardiovascular Disease	Others
Pizotifen-malate	93.6	93.0	73.7	84.9	75.2	94.6	Inflammation	Others
PLX-4032	107.8	100.8	110.7	108.5	69.5	95.8	Cancer	Raf
pmsf-phenylmethylsulfonyl-fluoride	83.0	89.6	84.9	83.1	82.6	95.0	Inflammation	Others
Pomalidomide(CC-4047)	107.4	101.1	106.2	115.8	98.0	101.4	Cancer	TNF-alpha, COX
Posaconazole	76.6	91.1	90.4	102.6	59.9	97.5	Infection	Others
Potassium-iodide	82.6	88.5	85.0	87.2	69.7	95.5	Endocrinology	Others
Pralatrexate(Folotyn)	44.5	61.1	46.8	52.8	17.5	76.2	Metabolic Disease	DHFR
Pramipexole-dihydrochloride-monohydrate	91.4	96.9	103.3	108.2	87.9	99.7	Neurological Disease	Others
Pramipexole-Mirapex	74.0	63.3	63.6	57.3	28.4	76.9	Neurological Disease	Dopamine Receptor
pramiracetam	73.9	83.0	78.9	79.4	73.9	85.5	Endocrinology	Others
pramoxine-hcl	82.1	85.4	67.8	79.7	70.1	94.3	Neurological Disease	Others
pranlukast	94.6	101.0	101.6	103.8	89.2	99.1	Immunology	Others
pranoprofen	76.5	90.7	94.2	87.9	75.8	100.6	Inflammation	Others
Prasugrel	100.7	99.7	109.9	106.4	89.8	103.5	Cardiovascular Disease	P2 Receptor
pravastatin-pravachol	93.5	93.1	73.7	85.1	74.9	94.6	Metabolic Disease	HMG-CoA Reductase
Praziquantel(Biltricide)	101.7	99.1	101.2	102.5	97.1	99.6	Vermifuge	Others
Prednisolone(Hydroretrocortine)	81.4	91.6	82.4	96.1	71.2	99.7	Infection	Others
Prednisolone-acetate-Omnipred	107.0	97.7	109.1	108.3	97.6	102.2	Immunology	Others
Prednisone	97.5	99.7	99.4	97.0	103.0	100.2	Immunology	Others
pregnenolone	72.8	93.9	77.3	84.1	42.1	95.5	Neurological Disease	Estrogen/progestogen Receptor
pridinol-methanesulfonate	104.9	95.5	107.7	111.6	92.4	93.3		Others
Prilocaine	98.2	100.6	102.0	95.5	98.3	102.6	Neurological Disease	Others
primaquine-diphosphate	78.0	90.8	98.9	88.2	81.1	89.8		Others
Primidone(Mysoline)	97.8	88.4	84.1	86.7	76.9	95.0	Neurological Disease	Others
proadifen-hcl	76.4	72.6	62.2	86.4	64.4	94.0		Others
probenecid-benemid	91.6	95.4	97.7	99.3	94.4	98.8	Metabolic Disease	Others
probucol	99.3	100.8	93.4	97.1	100.8	98.3	Cardiovascular Disease	Others
procaine-novocaine-hcl	105.9	101.1	97.0	106.2	97.4	101.1	Neurological Disease	Sodium Channel
prochlorperazine-dimaleate	89.7	91.7	88.3	98.0	93.6	96.5	Neurological Disease	Others
procodazole	88.5	92.1	98.8	95.2	102.0	103.4		Others
procyclidine-hcl	86.8	92.0	89.2	102.6	81.4	97.6	Neurological Disease	Others
Progesterone(Prometrium)	94.2	94.4	101.7	103.1	96.5	92.7	Endocrinology	Others
Propafenone(Rytmonorm)	88.2	96.4	90.3	80.2	40.0	53.6	Cardiovascular Disease	Sodium Channel
proparacaine-hcl	97.7	102.6	106.2	108.1	90.6	101.6	Neurological Disease	Sodium Channel

DRUG	MCF-7	ZR-75-1	MCF-7-TRF	ZR-75-1-TamR	MCF10A	MDA-MB-231	Indication	Target
propranolol-hcl	69.8	64.3	52.1	56.7	26.4	52.7	Cardiovascular Disease	Adrenergic Receptor
Propylthiouracil	87.1	92.3	88.8	102.4	81.8	97.5	Endocrinology	Others
protionamide-prothionamide	72.8	79.2	72.8	78.6	73.4	88.7	Infection	Others
Pyrazinamide(Pyrazinoic-acid-amide)	85.4	91.9	97.5	100.1	77.3	95.4	Infection	Others
Pyridostigmine-Bromide(Mestinon)	106.6	100.4	100.5	95.1	100.5	100.0	Cardiovascular Disease	Others
pyridoxine-hydrochloride	97.8	97.7	111.0	107.9	97.8	101.3	Endocrinology	Others
pyrila	85.2	80.0	68.5	88.8	72.8	96.4	Neurological Disease	Others
Pyrimethamine	106.4	98.4	97.5	110.5	94.0	94.6	Immunology	NULL
Quetiapine-fumarate(Seroquel)	88.5	100.6	95.4	104.8	82.0	94.3	Neurological Disease	Dopamine Receptor
quinapril-hydrochloride-accupril	95.7	90.1	105.2	108.3	89.4	93.7	Inflammation	RAAS
Quinine-hydrochloride-dihydrate	84.2	95.9	89.7	95.6	84.3	94.0	Cardiovascular Disease	Others
Racecadotril(Acetorphan)	82.5	92.9	87.8	97.0	85.5	95.6	Infection	Opioid Receptor
ractopamine-hcl	99.4	101.9	104.8	103.7	85.7	101.4	Neurological Disease	Others
Raltegravir-(MK-0518)	103.3	96.3	94.3	109.1	88.5	97.7	Immunology	Integrase
Ramelteon	97.4	101.4	104.0	112.0	93.4	101.9	Neurological Disease	Others
Ramipril(Altace)	85.6	75.0	82.7	85.7	67.4	73.4	Cardiovascular Disease	RAAS
Ranitidine-hydrochloride(Zantac)	94.6	94.5	77.2	92.9	80.5	95.5	Metabolic Disease	NULL
Ranolazine(Ranexa)	85.9	91.0	89.7	92.8	78.5	102.3	Cardiovascular Disease	Others
Ranolazine-dihydrochloride	98.4	100.9	100.8	107.4	93.6	102.9	Cardiovascular Disease	Calcium Channel
Rapamycin	27.2	36.2	36.1	44.3	46.0	75.4	Immunology	mTOR
rasagiline-mesylate	99.3	98.0	98.0	96.5	89.2	95.7	Cardiovascular Disease	MAO
rebamipide	85.5	80.3	68.2	88.7	73.2	96.3	Infection	Others
reboxetine-mesylate	102.0	103.5	96.9	106.1	101.3	98.3	Neurological Disease	Others
Repaglinide	86.2	100.0	97.7	103.1	89.6	99.7	Endocrinology	Potassium Channel
Reserpine	105.0	93.2	103.3	96.2	99.3	97.2	Cardiovascular Disease	Others
Resveratrol	97.7	88.3	84.3	86.7	76.9	95.1	Infection	Sirtuin
retapamulin	105.1	105.0	103.6	103.8	96.1	106.0	Neurological Disease	Others
Ribavirin(Copegus)	85.2	91.9	97.7	100.4	77.0	95.3	Metabolic Disease	Others
Rifabutin(Mycobutin)	37.0	44.8	45.3	46.2	55.0	68.3	Infection	Others
Rifampin(Rifadin)	39.2	70.9	58.0	88.0	78.2	84.7	Infection	Others
Rifapentine(Priftin)	84.4	95.9	89.5	95.4	84.6	94.0	Infection	Others
Rifaximin(Xifaxan)	82.0	87.1	85.3	91.8	80.4	95.7	Infection	Others
Riluzole(Rilutek)	102.1	103.4	96.9	105.9	101.7	98.3	Neurological Disease	Sodium Channel
rimantadine-flumadine	93.6	93.1	73.6	84.8	75.2	94.6	Infection	Others
rimonabant-sr141716	68.7	93.3	95.9	100.8	81.4	98.7	Inflammation	Cannabinoid Receptor
Risperidone(Risperdal)	105.0	103.1	95.1	103.4	97.4	103.0	Neurological Disease	5-HT Receptor
Ritonavir	84.4	95.8	89.7	95.4	84.5	94.0	Infection	HIV Protease
Rivaroxaban	84.3	95.3	94.1	92.3	79.2	95.3	Metabolic Disease	Factor Xa
rivastigmine-tartrate-exelon	97.0	102.7	101.6	102.2	100.0	111.7	Cardiovascular Disease	AChR
Rizatriptan-Benzoate(Maxalt)	97.8	99.2	103.3	96.6	96.0	96.3		NULL
Rocuronium-bromide	98.0	91.3	85.6	88.7	88.9	95.1	Neurological Disease	AChR
rofecoxib-vioxx	90.4	90.5	87.3	99.0	81.3	101.0	Digestive system disease	COX
Roflumilast(Daxas)	92.6	96.0	97.8	97.4	97.0	99.8	Neurological Disease	PDE
Rolipram	89.1	102.5	100.1	109.4	91.0	96.6	Inflammation	PDE
ronidazole	95.7	97.7	108.9	86.8	103.6	116.1	Neurological Disease	Others
ropinirole-hydrochloride	105.6	101.3	94.7	94.8	103.1	95.0	Neurological Disease	Others
ropivacaine-hcl	101.6	99.3	101.2	102.7	96.7	99.5	Infection	Others
Rosiglitazone-Avandia	90.0	95.6	106.0	113.7	87.2	98.2	Cancer	PPAR
rosiglitazone-hydrochloride	99.9	100.9	104.3	94.5	81.6	104.2	Cardiovascular Disease	PPAR
Rosiglitazone-maleate	88.4	100.6	95.6	105.1	81.7	94.3	Infection	PPAR
Rosuvastatin-calcium(Crestor)	100.2	104.1	95.9	97.0	94.5	101.7	Infection	HMG-CoA Reductase
rotigotine	88.2	94.0	89.4	97.5	80.3	93.8		Dopamine Receptor
roxatidine-acetate-hcl	70.6	66.4	64.5	68.5	70.2	88.9	Digestive system disease	Histamine Receptor
Roxithromycin(Roxl-150)	39.1	70.9	58.1	88.2	77.9	84.6	Metabolic Disease	Others

DRUG	MCF-7	ZR-75-1	MCF-7-TRF	ZR-75-1-TamR	MCF10A	MDA-MB-231	Indication	Target
Rufinamide	104.3	101.0	111.1	109.9	100.0	100.8	Neurological Disease	Sodium Channel
salicylanilide	81.2	96.4	97.2	102.4	87.1	100.4	Infection	Others
sasapyrine	89.9	95.2	106.2	113.6	87.1	98.4	Inflammation	Others
Saxagliptin(Onglyza)	98.1	98.4	98.7	98.5	103.3	101.4	Infection	DPP-4
scopine	34.9	33.7	26.1	48.6	39.1	66.0	Metabolic Disease	Others
Scopolamine-hydrobromide	74.6	89.7	89.4	91.7	77.9	91.2	Respiratory Disease	Others
Secnidazole-Flagentyl	58.1	72.2	85.8	76.5	57.8	88.7	Infection	Others
serotonin-hcl	84.1	95.0	94.3	92.2	79.1	95.5	Neurological Disease	Others
sertaconazole-nitrate	98.5	98.7	101.2	101.2	99.3	103.3	Infection	Others
sertraline-hcl	104.3	100.6	105.9	102.2	96.2	101.7	Inflammation	5-HT Receptor
Sildenafil-citrate	103.2	96.2	94.4	109.2	88.5	97.7	Cardiovascular Disease	PDE
Silodosin(Rapaflo)	98.0	97.1	99.9	103.0	95.5	101.2	Cardiovascular Disease	Adrenergic Recepto
Simvastatin(Zocor)	101.5	95.4	88.8	99.2	80.9	101.2	Cardiovascular Disease	Others
Sitafloxacin(DU-6859A)	105.4	101.6	94.8	101.3	95.4	103.8		Others
sodium-4-aminohippurate-hydrate	90.4	95.8	100.4	96.0	105.0	94.5		Others
sodium-ascorbate	68.4	94.2	102.0	106.9	80.6	94.5	Endocrinology	Others
sodium-nitrite	97.9	108.2	121.4	116.1	107.2	101.0	Neurological Disease	Others
sodium-nitroprusside	102.8	99.4	101.2	101.5	98.9	98.9	Cardiovascular Disease	Others
sodium-picosulfate	99.1	100.8	93.5	97.4	100.4	98.3	Metabolic Disease	Others
sodium-salicylate	96.8	96.3	107.5	110.8	94.2	96.0	Infection	Others
Sodium-valproate	87.3	95.5	92.2	99.1	83.4	91.0	Cardiovascular Disease	GABA Receptor, HDAC
solifenacin-succinate	87.8	90.1	83.7	91.4	79.5	103.0	Cardiovascular Disease	AChR
Sorafenib-Tosylate	85.8	76.1	79.7	77.8	46.7	63.6	Cancer	VEGFR, PDGFR, Raf
Sorbitol(Glucitol)	88.1	92.1	103.1	78.4	92.7	117.4	Digestive system disease	Others
Sotalol-hydrochloride(Betapace)	92.5	90.2	84.2	82.3	84.3	92.4	Neurological Disease	Adrenergic Receptor
sparfloxacin	74.1	83.0	78.7	79.2	74.2	85.5	Infection	Others
spiramycin	71.5	73.8	60.9	75.2	72.4	82.1	Infection	Others
spironolactone	103.5	91.0	103.5	84.9	96.2	125.8	Infection	Androgen Receptor
sRolipram	63.9	60.1	49.7	60.5	88.4	84.1	Cardiovascular Disease	PDE
Stavudine	90.5	90.4	87.3	98.9	81.6	101.1	Infection	Reverse Transcriptase
Streptozotocin	90.8	86.1	98.2	91.8	77.4	92.1	Cancer	Others
sucralose	61.4	76.6	67.3	75.0	52.6	86.8		Others
sulbactam	96.8	93.0	88.6	100.1	83.1	104.2	Infection	Others
sulbactam-sodium-unasyn	15.0	25.3	17.9	36.0	62.5	81.6	Infection	Others
sulconazole-nitrate	87.1	95.3	92.4	99.1	82.9	91.1	Infection	Others
sulfacetamide-sodium	73.5	71.7	57.3	60.3	27.2	89.4	Cardiovascular Disease	Autophagy
Sulfadiazine	87.5	90.3	86.5	96.8	81.8	93.3	Infection	Others
sulfaguanidine	65.1	75.2	84.7	99.1	57.0	107.0	Infection	Others
sulfamerazine	103.8	97.4	106.7	109.2	97.4	102.3	Infection	Others
Sulfameter(Bayrena)	97.0	102.6	101.8	102.2	100.0	111.7	Infection	Others
sulfamethazine	88.1	93.9	85.0	110.3	63.8	76.9	Endocrinology	Others
Sulfamethizole(Proklar)	78.5	78.3	84.5	91.6	76.2	89.3	Infection	Others
Sulfamethoxazole	88.1	95.6	97.1	96.1	65.1	101.1	Infection	Others
Sulfanilamide	104.5	100.5	105.9	102.0	96.6	101.7	Infection	Others
Sulfasalazine(Azulfidine)	91.2	95.7	95.9	96.0	98.6	99.0	Inflammation	Others
sulfathiazole	100.7	99.8	108.9	114.9	93.3	102.8	Infection	Others
Sulfisoxazole	84.4	95.3	93.9	92.1	79.5	95.4	Infection	Others
Sulindac(Clinoril)	97.7	94.0	107.5	108.5	99.5	92.1	Cancer	NULL
sulphadimethoxine	81.5	89.9	79.0	92.7	91.0	89.3	Infection	Others
Sumatriptan-succinate	106.3	98.3	97.6	110.5	94.0	94.6	Neurological Disease	5-HT Receptor
Sunitinib-Malate-(Sutent)	82.3	85.6	67.6	79.6	70.5	94.2	Cancer	VEGFR, PDGFR, c-Kit, Flt
suplatast-tosilate	101.5	102.0	110.2	106.6	91.6	92.8	Cardiovascular Disease	Others
Suprofen(Profenal)	82.7	92.9	87.6	96.7	85.8	95.7	Inflammation	Others
tacrine-hcl	86.1	99.8	97.9	103.2	89.1	99.8	Neurological Disease	Others
Tadalafil(Cialis)	99.7	89.5	98.1	98.6	99.6	99.4	Cardiovascular Disease	PDE
TAME	98.0	98.2	99.6	96.8	79.2	99.7	Cancer	APC
Tamoxifen-Citrate(Nolvadex)	105.4	95.9	89.2	99.2	79.0	96.0	Endocrinology	Estrogen/progestogen Receptor

DRUG	MCF-7	ZR-75-1	MCF-7-TRF	ZR-75-1-TamR	MCF10A	MDA-MB-231	Indication	Target
Tazarotene(Avage)	67.5	71.3	54.0	79.8	89.4	86.0	Inflammation	Others
Tebipenem-pivoxil(L-084)	90.4	107.6	112.6	115.5	94.0	99.8	Cardiovascular Disease	Others
Telaprevir(VX-950)	90.7	96.0	100.2	96.0	105.5	94.4	Infection	HCV Protease
Telbivudine(Sebivo)	93.3	102.8	94.1	99.4	96.6	97.4	Infection	Others
Telmisartan(Micardis)	34.2	79.6	52.8	66.7	43.0	79.6	Cardiovascular Disease	Others
temocapril-hcl	104.7	102.5	98.4	102.5	97.1	104.4	Cancer	RAAS
Temsirolimus	32.0	40.3	39.5	45.9	47.7	71.7	Cancer	mTOR
Teniposide(Vumon)	45.1	62.0	37.0	48.6	17.6	47.0	Cancer	Others
Tenofovir	88.1	98.1	91.9	96.4	80.0	101.1		Reverse Transcriptase
Tenofovir-Disoproxil-Fumarate	105.4	95.8	89.3	99.2	79.0	96.0		Reverse Transcriptase
Tenoxicam(Mobiflex)	38.8	53.1	42.2	49.7	50.8	68.8	Infection	Others
terazosin-hydrochloride-hytrin	94.2	90.8	95.9	94.8	96.7	94.5	Infection	Adrenergic Receptor
Terbinafine(Lamisil)	88.1	84.8	85.6	90.3	75.6	91.5	Infection	Others
terfenadine	98.2	100.7	101.0	107.5	93.1	103.0	Neurological Disease	Others
teriflunomide	85.6	90.6	90.2	93.0	78.0	102.4	Immunology	Others
tetracaine-hydrochloride-pontocaine	63.0	68.5	61.1	84.9	25.8	99.5	Endocrinology	Calcium Channel
tetracycline-hydrochloride	90.3	90.2	101.6	108.9	88.6	94.9	Infection	Others
tetrahydrozoline-hcl	97.5	97.3	106.4	99.9	106.1	99.7	Inflammation	Adrenergic Receptor
Thalidomide	74.7	89.6	89.4	91.6	78.2	91.3	Immunology	Others
Thiabendazole	77.0	87.8	88.0	85.9	75.6	92.9	Vermifuge	Others
thiamphenicol-thiophenicol	106.2	100.4	114.7	109.4	94.7	98.7	Cardiovascular Disease	Others
thioridazine-hcl	93.4	93.6	101.3	113.4	87.3	101.3	Neurological Disease	Others
Tianeptine-sodium-salt	97.6	93.9	107.7	108.6	99.5	92.1	Neurological Disease	5-HT Receptor
ticagrelor	42.5	53.7	41.1	53.1	31.2	31.0	Cardiovascular Disease	P2 Receptor
Tigecycline	82.3	93.8	95.5	93.1	77.9	104.6	Infection	Others
tilmicosin	88.1	96.1	90.5	80.1	39.9	53.6	Infection	Others
tinidazole	87.4	100.1	106.4	107.1	93.9	92.3	Infection	S4068
tioconazole	94.8	100.6	110.2	111.6	83.2	87.4	Infection	Others
tiopronin-thiola	91.2	95.8	95.7	95.9	98.6	99.0	Cardiovascular Disease	Others
Tiotropium-Bromide-hydrate	75.8	103.9	65.3	77.1	50.1	75.0	Infection	AChR
tioxolone	60.4	77.5	52.2	83.3	57.3	91.6	Endocrinology	Carbonic Anhydrase
tiratricol	97.4	102.3	106.7	108.3	90.1	101.7	Endocrinology	Others
Tizanidine-hydrochloride	91.3	96.8	103.5	108.2	87.9	99.7	Neurological Disease	Adrenergic Receptor
tolbutamide	87.2	101.1	108.7	105.1	96.7	104.4	Cancer	Potassium Channel
tolcapone	103.7	96.6	107.6	98.3	106.8	106.3	Metabolic Disease	Transferase
tolfenamic-acid	96.8	95.0	89.5	95.0	80.2	90.1	Inflammation	Others
tolmetin-sodium	106.0	98.1	97.9	110.6	93.6	94.6	Inflammation	Others
tolnaftate	94.6	94.4	94.7	90.3	96.9	90.2	Cancer	Others
tolperisone-hcl	62.9	68.3	61.2	84.7	25.8	99.7	Neurological Disease	Others
Tolterodine-tartrate-Detrol-LA	100.1	96.7	101.2	106.9	93.3	97.1	Neurological Disease	AChR
toltrazuril	97.6	98.7	100.0	105.1	97.8	102.8	Infection	Others
tolvaptan-opc-41061	61.4	76.8	67.2	75.1	52.7	86.6	Metabolic Disease	Estrogen/progestogen Receptor
Topiramate	101.5	101.9	110.4	106.7	91.6	92.8	Neurological Disease	Carbonic Anhydrase
Topotecan-Hydrochloride	34.9	33.7	26.1	48.5	39.3	66.1	Cancer	Topoisomerase
Tranilast	95.8	103.6	104.5	115.4	93.8	98.2	Respiratory Disease	Others
Tretinoin(Aberela)	63.9	60.0	49.8	60.6	88.4	84.1	Cancer	Others
Triamcinolone(Aristocort)	77.3	87.8	82.9	96.3	81.3	92.8	Inflammation	Others
Triamcinolone-Acetonide	87.5	93.6	100.1	76.1	96.3	128.2	Inflammation	Others
triamterene	74.0	63.1	63.7	57.4	28.3	77.0	Inflammation	Sodium Channel
Trichlormethiazide(Achletin)	100.1	102.2	98.0	98.3	100.6	98.9	Cardiovascular Disease	Others
triclabendazole	68.7	101.3	100.2	103.9	79.4	101.3	Vermifuge	Others
trifluoperazine-dihydrochloride	96.9	102.8	101.8	102.4	99.6	111.6	Neurological Disease	Others
triflupromazine-hcl	96.1	90.1	103.1	106.9	84.1	87.7	Neurological Disease	Others
Trifluridine(Viroptic)	73.0	87.5	91.9	88.4	77.3	90.3	Infection	NULL
triflusal	104.9	103.2	95.1	103.6	97.0	103.0	Infection	COX
Trilostane	87.9	90.0	83.7	91.2	79.8	103.0	Endocrinology	Dehydrogenase
trimebutine	102.2	103.5	96.7	105.9	101.7	98.3	Neurological Disease	Opioid Receptor
trimethoprim	85.4	80.3	68.3	88.9	73.0	96.2	Infection	Others
trimipramine-maleate	97.8	98.2	98.9	98.5	102.8	101.5	Neurological Disease	Others

DRUG	MCF-7	ZR-75-1	MCF-7-TRF	ZR-75-1-TamR	MCF10A	MDA-MB-231	Indication	Target
tripelennamine-hydrochloride	99.0	91.1	111.2	101.7	98.1	90.6	Neurological Disease	Histamine Receptor
trometamol	16.1	19.4	13.0	19.4	20.1	26.6		Others
tropicamide	90.9	100.9	94.6	100.2	88.1	90.8	Neurological Disease	AChR
Tropisetron-hydrochloride	92.5	85.1	89.5	88.2	79.9	93.9	Neurological Disease	Others
Trospium-chloride-Sanctura	100.3	100.1	89.0	108.9	90.7	99.3	Cardiovascular Disease	AChR
troxipide	84.1	95.6	89.9	95.4	84.2	94.1	Digestive system disease	Others
tylosin-tartrate	94.4	94.4	94.8	90.5	96.6	90.1	Neurological Disease	Others
ulipristal	101.3	102.0	110.4	106.9	91.3	92.7	Infection	Estrogen/progestogen Receptor
uracil	78.8	97.3	88.0	97.6	80.0	98.3		Others
urapidil-hydrochloride	98.0	97.7	110.8	107.6	98.1	101.4	Respiratory Disease	5-HT Receptor
uridine	100.5	102.0	110.6	110.5	93.2	102.9	Vermifuge	DNA/RNA Synthesis
Ursodiol(Actigal)	106.0	99.0	96.3	98.4	101.3	95.6	Metabolic Disease	Others
valaciclovir-hcl	104.6	99.2	107.5	105.8	98.5	99.6	Infection	Others
valdecoxib	16.9	42.4	47.2	40.9	85.5	53.3	Neurological Disease	COX
valganciclovir-hcl	100.8	102.5	104.0	99.8	104.7	96.2	Endocrinology	Others
valnemulin-hcl	73.9	82.7	79.0	79.3	73.8	85.6	Infection	Others
Valsartan(Diovan)	60.5	77.5	52.1	83.1	57.5	91.6	Cardiovascular Disease	RAAS
Vandetanib	61.4	76.5	65.3	72.3	38.3	82.4	Cancer	VEGFR
Vardenafil(Vivanza)	78.9	79.9	87.5	94.4	65.6	74.8	Infection	PDE
Vecuronium-Bromide#	102.6	101.0	84.6	100.3	81.2	104.8	Neurological Disease	Others
Venlafaxine-hydrochloride	82.4	104.2	101.0	106.1	87.7	95.2	Neurological Disease	5-HT Receptor
Verteporfin(Visudyne)	75.4	72.2	70.0	77.3	75.2	92.7	Endocrinology	5-alpha Reductase
Vidarabine(Vira-A)	10.9	26.2	8.0	31.7	4.0	26.4	Infection	5-alpha Reductase
vildagliptin-laf-237	76.4	90.7	94.3	88.1	75.5	100.6	Metabolic Disease	DPP-4
vinblastine-sulfate	98.4	98.4	101.4	101.1	99.1	103.5	Neurological Disease	Microtubule Associated
Vincristine-Sulfate	15.0	25.3	17.9	35.9	62.8	81.7	Cancer	Autophagy,Microtubule Associated
vinorelbine-tartrate	79.3	93.2	94.1	91.3	83.2	93.5		Microtubule Associated
Vitamin-B12	95.8	88.9	84.2	95.0	79.4	87.4	Metabolic Disease	Others
vitamin-c-ascorbic-acid	93.5	93.9	101.1	113.6	87.5	101.1	Respiratory Disease	Others
vitamin-d2-ergocalciferol	92.4	96.0	98.0	97.6	96.6	99.8	Endocrinology	Others
vitamin-d3-cholecalciferol	93.3	94.7	104.0	87.3	88.0	121.3	Cardiovascular Disease	Others
voglibose	76.8	87.5	88.3	86.0	75.2	92.9	Metabolic Disease	Others
Voriconazole	93.2	92.9	97.0	111.7	85.0	96.6	Infection	P450
Vorinostat-(SAHA)	51.1	83.2	78.1	56.2	50.5	43.1	Cancer	HDAC
VX-770	84.4	93.0	78.3	89.0	55.3	93.8	Respiratory disease	CFTR
www.Novobiocin-sodium(Albamycin)	91.7	97.5	89.1	99.1	84.1	96.7	Cardiovascular Disease	Others
www.Ritodrine-hydrochloride-Yutopar	40.8	57.1	40.0	40.9	41.9	60.9	Infection	Adrenergic Receptor
www.Spectinomycin--hydrochloride	87.3	90.3	86.6	97.0	81.5	93.2	Cardiovascular Disease	Others
www.Terbinafine-hydrochloride(Zabel)	102.1	98.6	101.2	109.5	91.5	97.6	Infection	Others
www.Toremifene-Citrate(Fareston)	68.7	85.8	65.6	96.9	59.3	87.6	Endocrinology	Others
XL184	91.2	93.3	83.9	86.8	68.3	87.0	Cancer	VEGFR, c-Met, Flt, Tie-2, c-Kit
Xylazine(Rompun)	68.6	85.8	65.7	97.2	59.0	87.5	Cardiovascular Disease	Adrenergic Receptor
xylometazoline-hcl	98.4	99.1	107.2	110.4	98.6	96.7	Infection	Others
Xylose	104.5	103.1	90.7	102.9	96.6	101.6	Metabolic Disease	Others
Zafirlukast(Accolate)	102.9	99.9	98.1	98.0	101.0	97.6	Inflammation	Others
Zalcitabine	73.8	72.0	57.0	60.1	27.3	89.4	Infection	Others
zaltoprofen	88.4	94.4	89.2	97.7	80.5	93.6	Inflammation	COX
zanamivir-relenza	79.4	93.6	94.0	91.4	83.3	93.3		Others
zidovudine-retrovir	70.4	83.9	91.4	104.1	80.2	94.5	Cardiovascular Disease	Others
Zileuton	105.2	95.7	107.5	111.5	92.9	93.3	Respiratory Disease	Others
zinc-pyrithione	39.9	65.4	24.4	51.6	53.4	88.3	Infection	Proton Pump
Ziprasidone-hydrochloride	96.4	90.3	102.9	106.9	84.5	87.7	Neurological Disease	Others
Zolmitriptan(Zomig)	104.5	103.0	90.9	103.0	96.6	101.6	Neurological Disease	Others
Zonisamide	97.9	97.6	111.0	107.7	98.2	101.4	Neurological Disease	Others

DRUG	MCF-7	ZR-75-1	MCF-7-TRF	ZR-75-1-TamR	MCF10A	MDA-MB-231	Indication	Target
zoxazolamine	86.3	97.0	90.4	97.8	80.0	98.6	Neurological Disease	Others

Papers published during PhD

1. **Silvia-E. Glont**, Igor Chernukhin and Jason S. Carroll*: *Comprehensive Genomic Analysis Reveals that the Pioneering Function of FOXA1 Is Independent of Hormonal Signaling,* ***Cell Reports,*** *2019; 26(10): 2558–2565.e3,* DOI: 10.1016/j.celrep.2019.02.036

2. **Silvia-E. Glont#**, Evangelia K. Papachristou#, Ashley Sawle, Kelly A. Holmes, Jason S. Carroll*, Rasmus Siersbaek*: *Identification of ChIP-seq and RIME grade antibodies for Estrogen Receptor alpha,* ***PLOS ONE,*** *2019; 14(4): e0215340*, DOI: https://doi.org/10.1371/journal.pone.0215340

3. Rasmus Siersbæk, Valentina Scabia […], **Silvia Glont**, Sarah J Aitken, Kamal Kishore, Danya Cheeseman, Emad A Rakha, Clive D'Santos, Wilbert Zwart, Alasdair Russell, Cathrin Brisken, Jason S Carroll: *IL6/STAT3 Signaling Hijacks Estrogen Receptor α Enhancers to Drive Breast Cancer Metastasis,* **Cancer Cell,** 2020; S1535-6108(20)30311-1, DOI: 10.1016/j.ccell.2020.06.007

4. Nagarajan S, Rao SV#, Sutton J#, Cheeseman D, Dunn S, Papachristou EK, Prada J-EG, Couturier D-L, Kumar S, Kishore K, Chilamakuri CSR, **Glont S-E**, Archer Goode E, Brodie C, Guppy N, Natrajan R, Bruna A, Caldas C, Russell A, Siersbæk R, Yusa K, Chernukhin I, Carroll JS: *ARID1A influences HDAC1/BRD4 activity, intrinsic proliferative capacity and breast cancer treatment response,* ***Nature Genetics****, 2020; 52: 187–197,* DOI: 10.1038/s41588-019-0541-5

Cell Reports

Comprehensive Genomic Analysis Reveals that the Pioneering Function of FOXA1 Is Independent of Hormonal Signaling

Graphical Abstract

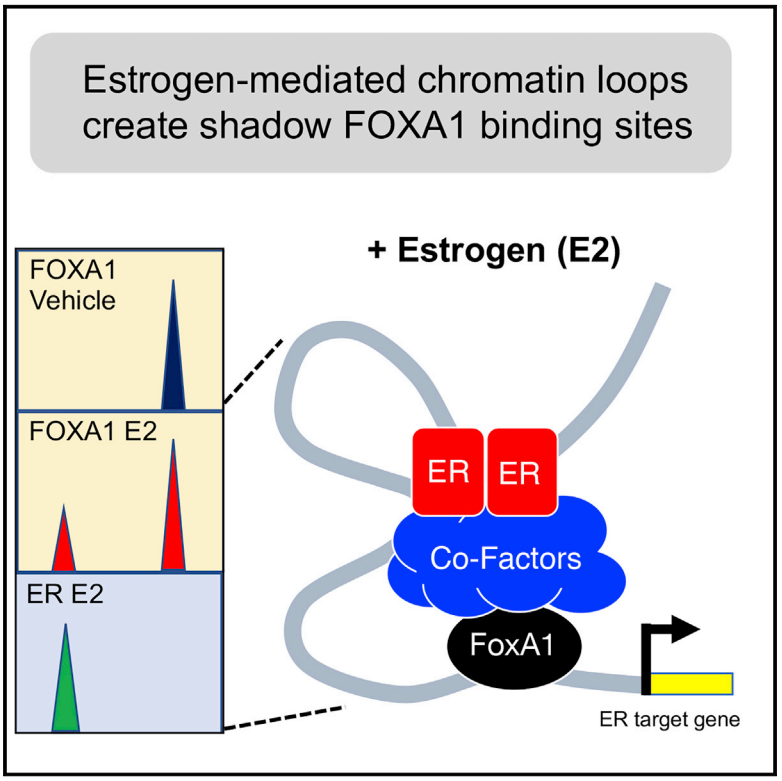

Highlights

- FOXA1 binding events are not regulated by hormones
- Chromatin loops create shadow FOXA1 binding sites
- FOXA1 is a bone fide pioneer factor independent of hormone stimuli

Authors

Silvia-E. Glont, Igor Chernukhin, Jason S. Carroll

Correspondence

jason.carroll@cruk.cam.ac.uk

In Brief

Glont et al. show that FOXA1 binding sites are not regulated by hormones. A small number (<1%) of FOXA1 binding events appear to be estrogen regulated, but these are shadow peaks that are created via pre-existing binding sites that form chromatin loops.

Glont et al., 2019, Cell Reports *26*, 2558–2565
March 5, 2019
https://doi.org/10.1016/j.celrep.2019.02.036

CellPress

OPEN ACCESS
CellPress

Cell Reports
Report

Comprehensive Genomic Analysis Reveals that the Pioneering Function of FOXA1 Is Independent of Hormonal Signaling

Silvia-E. Glont,[1] Igor Chernukhin,[1] and Jason S. Carroll[1,2,*]
[1]Cancer Research UK Cambridge Institute, University of Cambridge, Robinson Way, Cambridge, CB2 ORE, UK
[2]Lead Contact
*Correspondence: jason.carroll@cruk.cam.ac.uk
https://doi.org/10.1016/j.celrep.2019.02.036

SUMMARY

Considerable work has linked hormone receptors, such as estrogen receptor-alpha (ER), with the pioneer factor FOXA1. Altered FOXA1 levels contribute to endocrine-resistant breast cancer, where it maintains ER-chromatin interactions, even in contexts in which cells are refractory to ER-targeted drugs. A recent study controversially suggests that FOXA1 binding can be induced by hormonal pathways, including the estrogen-ER complex. We now show that the vast majority (>99%) of FOXA1 binding events are unaffected by steroid activation. A small number (<1%) of FOXA1 binding sites appear to be induced by estrogen, but these are created from chromatin interactions between ER binding sites and adjacent FOXA1 binding sites and do not represent genuine new FOXA1-pioneering elements. FOXA1 is therefore not regulated by estrogen and remains a bone fide pioneer factor that is entirely upstream of the ER complex.

INTRODUCTION

Although the term ''pioneer factor'' has been used recently for any transcription factor that can mediate binding of another transcription factor to chromatin, a bone fide pioneer can associate with condensed chromatin, independently of other factors, to initiate chromatin opening and creation of a *cis*-regulatory element (Zaret and Carroll, 2011). FOXA1 is the archetypal pioneer factor, capable of binding to compact chromatin independently of other proteins and creating a localized euchromatic environment (Cirillo et al., 1998, 2002). It can mediate estrogen receptor (ER) binding events in breast cancer cell lines (Carroll et al., 2005; Hurtado et al., 2011; Laganière et al., 2005), it is required for growth of drug-resistant cancer models (Hurtado et al., 2011), and it has been shown to directly contribute to endocrine resistance (Fu et al., 2016).

FOXA1 has been shown to be important for other nuclear receptors (NRs), such as androgen receptor (AR) in prostate cancer (Lupien et al., 2008), in which elevated levels can contribute to disease outcome (Jain et al., 2011; Robinson et al., 2014). A role for FOXA1 in castrate-resistant prostate cancer (CRPC) is exemplified by the fact that models of CRPC, driven by AR splice variants, are still dependent on FOXA1 for cell growth (He et al., 2018; Jones et al., 2015).

FOXA1 binding has been consistently implicated as an event that happens upstream of NR association with *cis*-regulatory elements, and experimental data to date show no change in FOXA1 binding when ER is modulated (Hurtado et al., 2011), and FOXA1 chromatin interaction does not require ER when exogenously expressed (Sérandour et al., 2011). The dependence on a single catalytic transcription factor for hormone receptor signaling represents an attractive therapeutic target (Jozwik and Carroll, 2012; Nakshatri and Badve, 2007). Importantly, an inhibitor targeting FOXA1 would circumvent many of the known mechanisms of resistance, including changes in NR fidelity, growth factor activation, changes in the occupancy of co-factors, and additional mechanisms that alter the binding potential or ligand dependency of the NR.

The aforementioned paradigms have recently been challenged, with a study suggesting that FOXA1 binding can be influenced by steroid activation of the cognate NR (Swinstead et al., 2016). This suggests that FOXA1 binding potential can be dictated partly by hormones, including estrogen and glucocorticoids. This questions the concept of transcription factor hierarchies, in which specialized transcription factors can function as biological pathway-determining catalysts. We have repeated the key genomic transcription factor mapping experiments that lead to the paradigm-challenging conclusions. We find that the estrogen-induced FOXA1 binding sites, which were described before (Swinstead et al., 2016), result from a lack of robust replicates and are not observable when additional, technically similar, chromatin immunoprecipitation sequencing (ChIP-seq) biological replicates are conducted. Any altered FOXA1 binding sites represent a tiny fraction of the overall FOXA1 binding sites (less than 1%) that result from chromatin loops that occur between *cis*-regulatory elements at estrogen-regulated gene regions, creating shadow binding events that do not represent new *cis*-regulatory elements.

RESULTS

By mapping FOXA1 binding using ChIP-seq in ER+ breast cancer cells, Swinstead et al. (2016) concluded that FOXA1 binding could be substantially altered by hormonal steroid treatment. The primary conclusion that FOXA1 binding was hormonally regulated was based largely on the results from their ChIP-seq

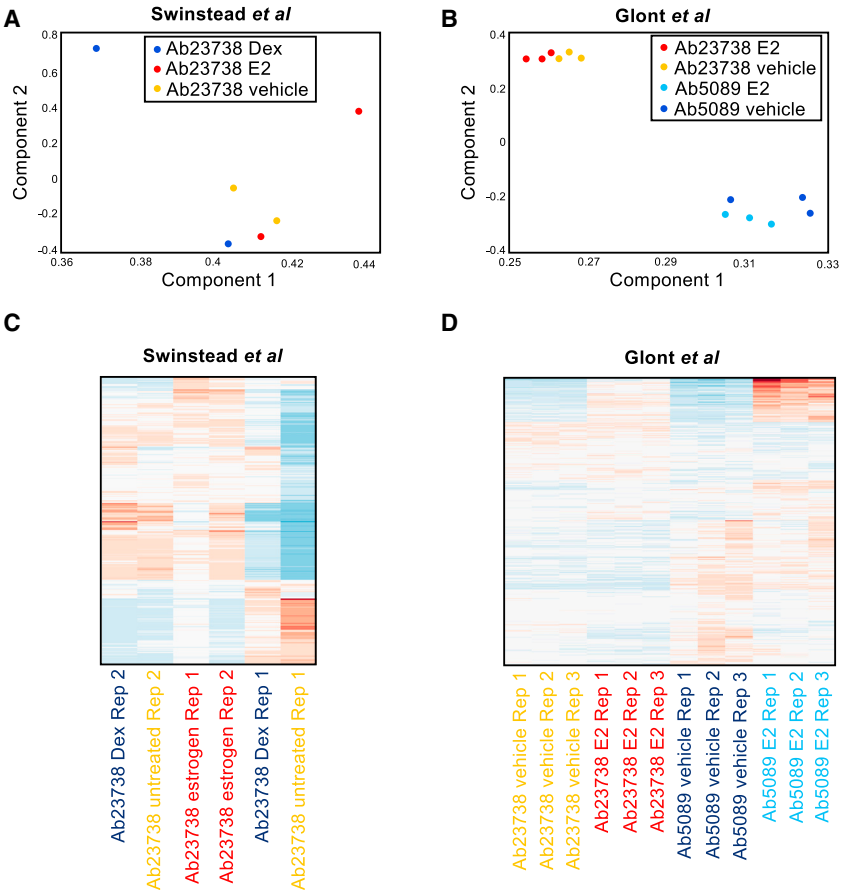

Figure 1. PCA and Unbiased Clustering of the Different ChIP-Seq Datasets

Read densities from aligned libraries of equal size of 20 million reads were measured on corresponding FOXA1 binding sites from Swinstead et al. (2016) (GEO: GSE72249).

(A) The peaks for all treatments were merged in a single set prior to the measurement for each study, and obtained data were subjected to PCA. The PCA plots illustrate degree of similarity between the replicates. Spearman rank correlation between ER-mediated chromatin interactions (ChIA-PET) and the 357 estrogen-induced FOXA1 binding sites (ab5089).

(B) Hierarchical clustering of the Swinstead et al. (2016) binding sites. For hierarchical clustering of the Swinstead et al. (2016) binding sites, the yielded read densities were normalized using median absolute deviation and clustered in MATLAB framework using the "ward" method with the linkage function. The duplicate samples from Swinstead et al. (2016) did not cluster on the basis of treatment condition.

(C) PCA of our FOXA1 ChIP-seq generated with two different FOXA1 antibodies (ab23738 and ab5089).

(D) Hierarchical clustering of our FOXA1 binding sites, showing clustering on the basis of replicates.

experiments. We downloaded their FOXA1 ChIP-seq data, obtained in breast cancer cell lines, but could not reproduce the binding numbers described in the publication, because of insufficient information about peak calling and how input DNA was integrated into the analyses. We used the peak coordinates described by Swinstead et al. (2016) and compared read densities of their duplicate libraries mapped to those coordinates using both principal-component analysis (PCA) and hierarchical clustering. Their samples did not cluster by treatment condition when assessed using PCA, and samples from the same treatment condition showed substantial variability (Figure 1A), suggesting that the replicate samples were not similar. This lack of consistency between duplicates is a potential source of false-positive "differential" binding sites. As expected, differential peak patterns showed little consistency between replicates (Figure 1B), implying that any differential binding sites might be due to technical variability between replicates. Given this replicate-to-replicate variability (even between samples of the same treatment conditions), the lack of any ChIP-qPCR validation, and the significant implication of the conclusions, we sought to repeat the key ChIP-seq experiments to determine if FOXA1 binding was in fact modulated by hormonal stimulation, as claimed (Swinstead et al., 2016).

We hormone deprived MCF-7 and ZR-75-1 breast cancer cells and treated with vehicle or estrogen for 45 min, a duration shown to result in maximal ER binding and enhancer activity (Shang et al., 2000). ER ChIP-qPCR was conducted at known binding loci (Figure S1; Table S1) in order to confirm the estrogen response. We subsequently conducted FOXA1 ChIP-seq experiments using two different antibodies in both cell line models with three biological replicates from independent passages. Importantly, these were collected from matched experiments used to confirm estrogen responsiveness (Figure S1). One of the antibodies used in our study was the same antibody (ab23738) used by Swinstead et al. (2016). Matched input samples were included for each experiment. Peaks were called using MACS2 (Ross-Innes et al., 2012; Stark and Brown, 2011). In MCF-7 cells, this resulted in 64,823 FOXA1 peaks in vehicle-treated and 62,000 peaks in estrogen-treated conditions using the same antibody as Swinstead et al. (2016) and 37,318 vehicle and 35,925 estrogen FOXA1 peaks with the second independent antibody ab5089 (Table S2). PCA of our samples showed that the samples clustered tightly on the basis of replicates (Figure 1C), providing confidence when comparing peaks (Figure 1D). The samples clustered on the basis of the antibody used for ChIP-seq and showed minimal difference between vehicle or estrogen conditions. In ZR-75-1 cells, the ab23738 antibody generated 70,602 FOXA1 peaks in vehicle conditions and 66,604 peaks in estrogen conditions. The second antibody (ab5089) generated 35,763 FOXA1 peaks in vehicle conditions and 31,361 peaks in estrogen conditions (Table S2). As such, estrogen treatment did not result in a global increase in FOXA1 binding events, with either antibody or in either cell line assessed.

One possibility is that FOXA1 binding could be redistributed, resulting in similar binding numbers, but at different locations

in the genome. We therefore performed DiffBind analyses (Ross-Innes et al., 2012) (Table S3) and observed no FOXA1 redistribution. In MCF-7 cells, there were 14 estrogen-induced peaks with the ab23738 antibody and 2 peaks enriched in vehicle conditions, representing 0.02% of all FOXA1 peaks that are estrogen induced (Figures 2A and 2C). This is in contrast to the results obtained using the exact same antibody and cell line in Swinstead et al. (2016), attesting to the potential problems that result from lack of sufficient replicates. The biggest change observed in any of the ChIP-seq experiments we undertook was in MCF-7 cells using the ab5089 FOXA1 antibody (which was not used by Swinstead et al., 2016) (Figures 2A–2C), which revealed a total of 357 FOXA1 peaks enriched in estrogen conditions (representing less than 1% of all peaks called) and 5 peaks enriched in vehicle conditions (Figure 2B).

To establish the degree of variability in this ChIP-seq experiment conducted with sufficient biological replicates, we purposely mixed up the samples from the ab23738 antibody-based ChIP-seq in different combinations and subsequently called peaks. Following DiffBind analysis, we found between 121 and 180 peaks that were considered differential, even in samples that were randomly mixed up with the incorrect treatment samples, representing ~0.5% of all peaks.

In the ZR-75-1 cell line, we observed 23 estrogen-enriched and 2 vehicle-enriched FOXA1 binding sites using the same FOXA1 antibody used by Swinstead et al. (2016) (Figures 2D and 2F). This small number of estrogen-induced FOXA1 binding sites represents less than 0.03% of all peaks. When using the second FOXA1 antibody (ab5089) in ZR-75-1 cells, we found 109 estrogen-induced FOXA1 binding sites (0.03% of total FOXA1 binding sites) and 1 vehicle-enriched site (Figure 2E).

Our ChIP-seq data with two different FOXA1 antibodies, conducted in two independent cell line models, revealed that 0.02%–1% of the FOXA1 binding sites were induced by estrogen. This is in contrast to Swinstead et al. (2016), who claimed that there is an appreciable number of FOXA1 binding events that can be hormonally regulated. Importantly, the same antibody that was used by Swinstead et al. (2016) revealed no significant changes in FOXA1 binding in either cell line model in our ChIP-seq analysis.

The second FOXA1 antibody (ab5089) that we used produced a small number of estrogen-induced FOXA1 binding sites (357 sites), although it is important to note that these differential binding events constitute less than 1% of total FOXA1 binding events in the ChIP-seq dataset. Only 28 common FOXA1 binding events were identified in both MCF-7 and ZR-75-1 cell lines, implying that these differential sites are not reproducible between different cancer models (Figure 2G).

Further analysis of the estrogen-induced FOXA1 binding sites in MCF-7 and ZR-75-1 revealed the estrogen responsive element (ERE) motif ($p = 1 \times 10^{-42}$), but no forkhead motifs (Figure 2H), suggesting that FOXA1 is not directly interacting with the chromatin at these regions. On the basis of the motif analysis, we hypothesized that the small number of estrogen-induced FOXA1 binding sites might be indirect FOXA1 binding events, potentially mediated via chromatin loops connecting estrogen-induced genes and their enhancers.

Given the wealth of genomic, transcriptomic, and chromatin looping data in the MCF-7 cell line model, we investigated the underlying properties of the 357 estrogen-induced FOXA1 binding sites. We used published RNA-seq data following estrogen treatment of MCF-7 cells (Figure 3A) and observed that the 357 estrogen-induced FOXA1 binding sites were significantly biased toward the most estrogen-regulated genes (Figure 3B) with almost all of the binding sites within *cis*-regulatory domains adjacent to ER target genes.

It is well established that lineage-specific genes tend to be regulated by clusters of transcription factor binding sites (Hnisz et al., 2013; Whyte et al., 2013). This is true for estrogen-regulated genes, in which the classic estrogen-induced genes (i.e., those with the greatest estrogen response) are regulated by clusters of closely associated *cis*-regulatory domains (Carroll et al., 2006). Several well-characterized ER target genes are shown in Figure 3C as examples. As typified by the examples shown, there are FOXA1 and ER co-bound regions, but importantly, there are sites at which one transcription factor binds but the other one does not. The 357 estrogen-induced FOXA1 binding sites are all adjacent to an independent ER binding event and other FOXA1 binding sites (Figures 3D and 3E), indicating their presence in regions of enriched transcription factor binding.

Following estrogen-mediated stimulation, physical associations between *cis*-regulatory elements occur (Fullwood et al., 2009; Pan et al., 2008), and we postulated that FOXA1 could associate with adjacent ER binding sites through chromatin looping. Because of the cross-linking in the ChIP-seq protocol, these indirect chromatin loops create FOXA1 binding sites that are not direct *cis*-regulatory elements and therefore represent "shadow peaks." At these regions, FOXA1 does not function as a pioneer factor, and new regulatory elements are not created. Our hypothesis is that the small fraction (<1%) of FOXA1 binding events that appear to be induced by estrogen are in fact simply indirect peaks mediated via ER at those genomic regions. To assess this possibility, we used the ChIA-PET (chromatin interaction analysis by paired-end tag sequencing) data that provide an unbiased map of the ER-mediated chromatin interactions that occur, in the presence of estrogen, in MCF-7 cells (Fullwood et al., 2009). Of the 357 estrogen-induced FOXA1 peaks in MCF-7 cells, 89% were detected in experimentally identified ER ChIA-PET chromatin loops (Figure 4A). Examples of estrogen-induced FOXA1 binding sites existing within ChIA-PET chromatin loops are shown in Figure 4B. This finding confirms that the limited number of estrogen-induced FOXA1 binding events are in fact created by clusters of *cis*-regulatory elements brought into proximity during gene expression. Therefore, FOXA1 is a bone fide pioneer factor that binds upstream of NRs, and direct FOXA1-chromatin binding is not influenced by steroid hormones.

DISCUSSION

It is well established that many NRs and other transcription factors regulate genes from significant distances (Carroll et al., 2005; Lin et al., 2007). However, additional factors are required for NR to work (Glass and Rosenfeld, 2000; Shang et al., 2000). Recent observations have revealed that cells containing

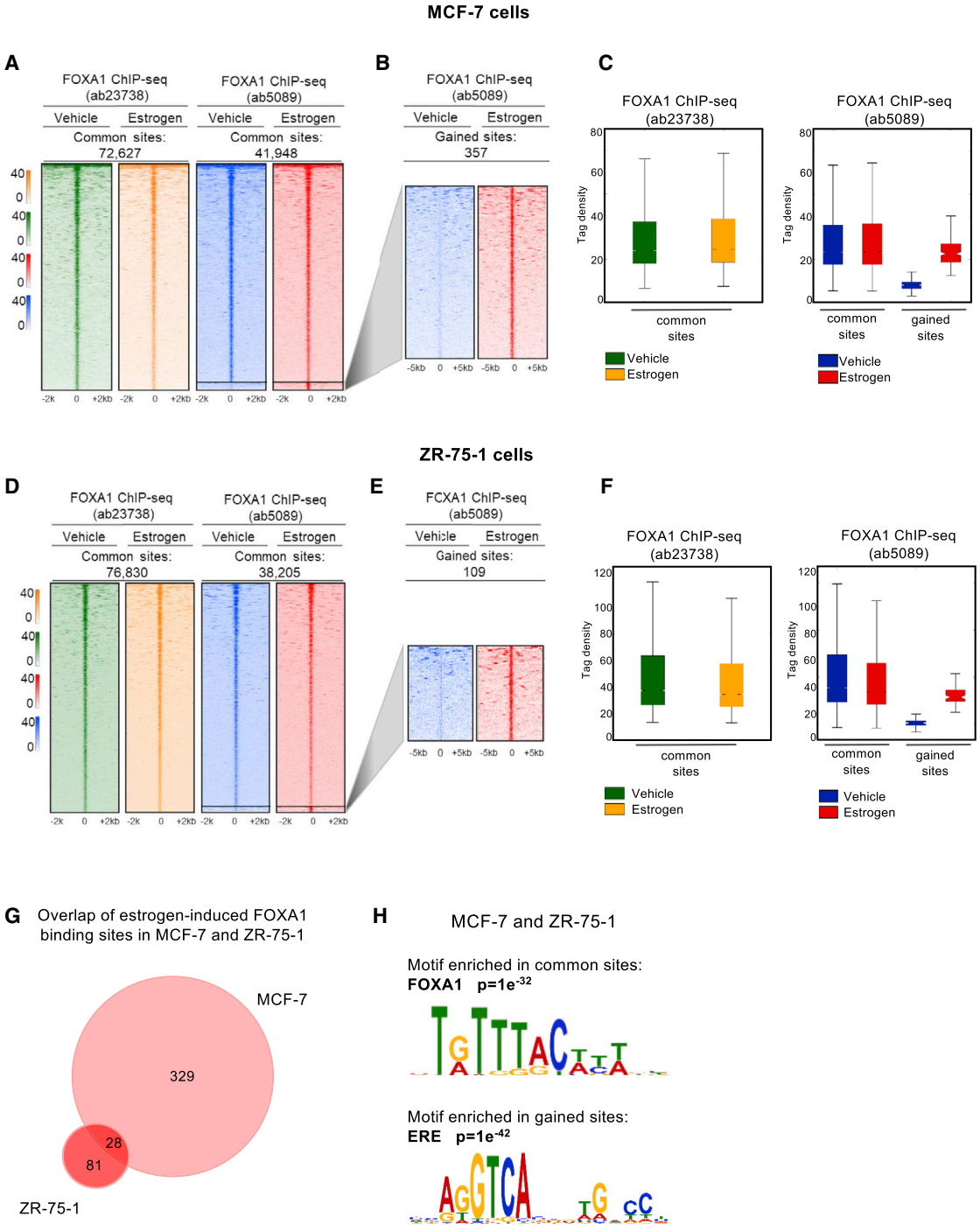

Figure 2. Analysis of FOXA1 ChIP-Seq Binding with Two Separate Antibodies in Response to Estrogen Treatment in MCF-7 and ZR-75-1 Cells

(A, C, D, and F) ChIP-seq tag densities visualized at FOXA1-occupied genomic locations in control and estrogen-treated MCF-7 (A and C) and ZR-75-1 (D and F) cells, using antibodies ab23738 and ab5089.

(B and E) Zoomed heatmap shows differential binding of FOXA1 specific to ab5089 in MCF-7 cells (B) and ZR-75-1 (E), respectively.

(G) Overlap of estrogen-enriched FOXA1 binding sites between MCF-7 and ZR-75-1 cells.

(H) Transcription factor motifs found overrepresented in the common and estrogen-induced FOXA1 sites.

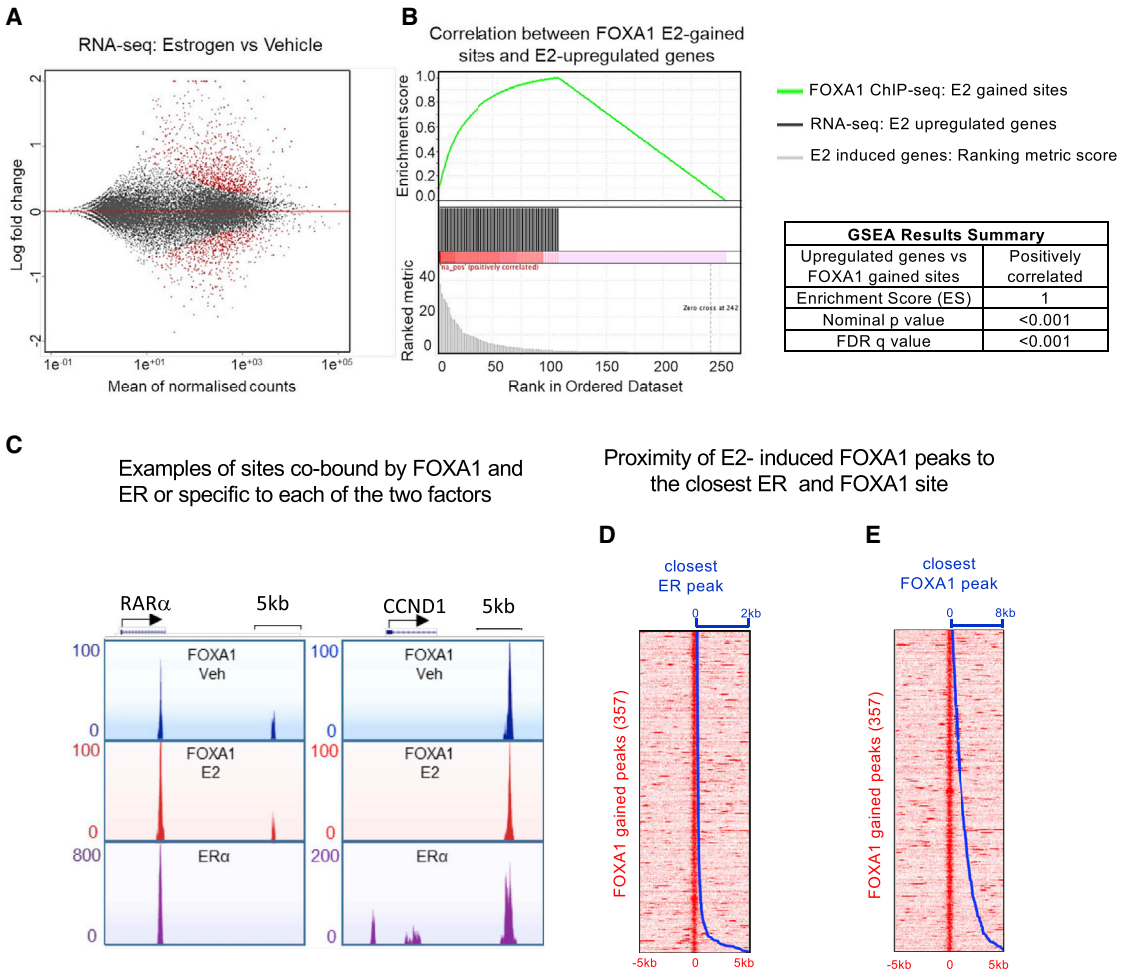

Figure 3. Integration of the Estrogen-Enriched FOXA1 Binding Events with Estrogen-Mediated Gene Expression Events

(A) RNA sequencing (RNA-seq) expression profile following short-term (3 h) estrogen treatment of MCF-7, shown as a dispersion plot.

(B) Gene set enrichment analysis (GSEA) pre-ranked test correlating estrogen-induced genes with the 357 estrogen-induced FOXA1 binding sites.

(C) Examples of sites co-bound by FOXA1 and ER, as well as sites unique to each of the two transcription factors.

(D and E) Proximity of estrogen-induced FOXA1 peaks and the closest ER (D) or FOXA1 (E) site. Heatmap represents FOXA1-gained sites in red.

mutations in ER (ESR1) can be enriched because of selective pressure imposed by specific ER-targeted drugs (Merenbakh-Lamin et al., 2013; Robinson et al., 2013; Toy et al., 2013), resulting in ligand-independent ER activity. As such, there is a significant interest in defining critical components of the ER complex that might constitute potential drug targets. One such protein is FOXA1, a pioneer factor, shown to facilitate chromatin "opening" independently of additional proteins, enabling binding and activity of other transcription factors. Importantly, this includes ER in breast cancer and AR in prostate cancer. Although additional modes of NR binding can occur, such as assisted loading, involving complexes of multiple ATP-dependent chromatin factors (Voss et al., 2011), an absolute dependence on a single functionally catalytic protein, such as FOXA1, holds promise for therapeutic exploitation.

FOXA1 has been shown to be required for growth of resistant cancers (Hurtado et al., 2011), it contributes to endocrine resistance (Fu et al., 2016), and, importantly, it is essential for ER binding and activity, even in endocrine-resistant contexts (Hurtado et al., 2011). This places FOXA1 as a key driver of resistance and reveals a vulnerability in the ER pathway, where absolute dependence on a single upstream pioneer factor creates an opportunity for therapeutic intervention, potentially overcoming known mechanisms of resistance. Interest in FOXA1 as a therapeutic target for ER+ breast cancer (Jozwik and Carroll, 2012; Nakshatri and Badve, 2007, 2009) was compromised by recent claims that FOXA1 binding is estrogen regulated (Swinstead et al., 2016). The significance of this conclusion means that ER-targeted agents should, in theory, show effectiveness in inhibiting FOXA1 binding and transcriptional potential, reducing the need to develop direct FOXA1 inhibitors. Our comprehensive analysis of FOXA1 binding following estrogen stimulation reveals no appreciable estrogen regulation of FOXA1 binding. Different antibodies and different

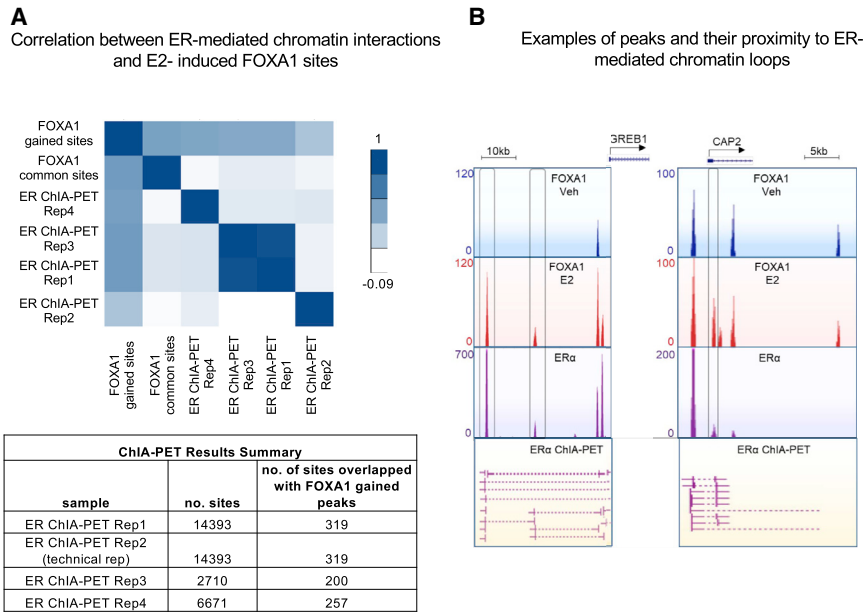

ChIA-PET Results Summary		
sample	no. sites	no. of sites overlapped with FOXA1 gained peaks
ER ChIA-PET Rep1	14393	319
ER ChIA-PET Rep2 (technical rep)	14393	319
ER ChIA-PET Rep3	2710	200
ER ChIA-PET Rep4	6671	257

Figure 4. ER Binding Mediates Indirect FOXA1 Binding via Chromatin Looping at *cis*-Regulatory Elements

(A) Correlation between ER-mediated chromatin interactions (ChIA-PET) and the 357 estrogen-induced FOXA1 binding sites (ab5089). The table shows the correlation values between ChIA-PET interactions and the 357 estrogen-induced FOXA1 binding sites.

(B) Examples of ER and FOXA1 peaks at regions that are involved in chromatin loops, as detected by ChIA-PET. The images of the ChIA-PET loops are taken from Fullwood et al. (2009).

ER+ breast cancer cell line models show that >99% of FOXA1 binding sites are impervious to hormonal context. The residual FOXA1 changes represent less than 1% of FOXA1 binding events and result from peaks formed within clusters of ER/FOXA1 binding sites at genes that are estrogen regulated. As such, these lack the hallmarks of genuine FOXA1 binding sites, they do not result in the creation of new regulatory elements, and they do not result in new gene expression events. The lack of robust, reproducible FOXA1 binding sites confirms that FOXA1 binding is not estrogen regulated and functions upstream of ER activity. In support of this conclusion, previous experimental data showed that the breast cancer treatment fulvestrant (ICI 182780), an ER degrader, does not alter FOXA1 binding (Hurtado et al., 2011).

The major distinction in conclusions between the work of Swinstead et al. (2016) and the present dataset results from technical differences that can be attributed to insufficient replicates in the previous study (Figure 1). A lack of biological and/or technical replicates is a source of problems in the reproducibility of ChIP-seq datasets, particularly when claiming treatment or condition-specific binding events. We conclude that recent claims of estrogen-mediated FOXA1 binding events are influenced, in large part, by a lack of independent biological ChIP-seq replicates and duplicate samples that show unacceptable variability between purportedly replicate samples (Figures 1A and 1B).

Swinstead et al. (2016) identified similar steroid hormone changes in FOXA1 binding in two distinct systems, namely, estrogen responsiveness and dexamethasone (dex) activation of glucocorticoid receptor (GR) (Swinstead et al., 2016). Although we have only focused on the estrogen-treated conditions, it is reasonable to assume that the majority of dex-mediated changes in FOXA1 are also false positives that result from a lack of independent biological replicates. This is based on the fact that the experimental approach was comparable, and the same degree of differential FOXA1 binding was observed in both hormonal systems. The conclusion that steroids could change FOXA1 binding was suggested in large part by ChIP-seq analyses. In addition to these assays, Swinstead et al. (2016) also assessed FOXA1 chromatin dwell time using an exogenous, tagged FOXA1-based approach. Despite the caveat that exogenous FOXA1 alters levels and potentially the function of endogenous FOXA1, and the tagged protein might not faithfully recapitulate endogenous FOXA1, there was a minimal change in FOXA1 dwell time comparing the presence or absence of estrogen, suggesting that this non-ChIP-based method supports the conclusion that FOXA1 binding is not altered in an appreciable way by hormone status.

Understanding what enables FOXA1 binding is of importance, and recent suggestions that steroid hormones could function in this capacity to modulate FOXA1-DNA binding potential (Swinstead et al., 2016) present an attractive hypothesis. We show that the vast majority (>99%) of FOXA1 binding is not regulated by estrogen, and the small fraction of altered FOXA1 binding events are created via chromatin interactions during the course of ER-mediated gene expression. FOXA1 therefore exists entirely upstream of the NR, its chromatin binding capacity is not influenced by estrogen signaling, and it remains a relevant and important drug target in hormone-dependent cancers.

STAR★METHODS

Detailed methods are provided in the online version of this paper and include the following:

- KEY RESOURCES TABLE
- CONTACT FOR REAGENT AND RESOURCE SHARING
- EXPERIMENTAL MODEL AND SUBJECT DETAILS
  - Cell culture
- METHOD DETAILS
  - Chromatin Immunoprecipitation
  - Integration of RNA-seq and ChIP-seq data
- QUANTIFICATION AND STATISTICAL ANALYSIS
  - ChIP Sequencing Analysis
- DATA AND SOFTWARE AVAILABILITY

SUPPLEMENTAL INFORMATION

Supplemental Information includes one figure and three tables and can be found with this article online at https://doi.org/10.1016/j.celrep.2019.02.036.

ACKNOWLEDGMENTS

We would like to thank the genomics core and the Bioinformatics Core at Cancer Research UK (CRUK) Cambridge Institute. We thank Dr. Sankari Nagarajan and Dr. Rasmus Siersbæk from CRUK Cambridge Institute for critical reading of the manuscript. We thank Danya Cheeseman and Emily Archer Goode for help compiling information about the methods. We acknowledge the support of the University of Cambridge and Cancer Research UK. J.S.C. is supported by an ERC Consolidator award (project number 646876), CRUK funding, and a Susan G. Komen Breast Cancer Foundation scholarship.

AUTHOR CONTRIBUTIONS

Experiments were designed by S.-E.G. and J.S.C., and all work was conducted by S.-E.G. All bioinformatic work was conducted by I.C. All authors wrote the paper.

DECLARATION OF INTERESTS

J.C. is the founder and CSO of Azeria Therapeutics.

Received: April 12, 2018
Revised: October 17, 2018
Accepted: February 11, 2019
Published: March 5, 2019

REFERENCES

Bailey, T.L., Boden, M., Buske, F.A., Frith, M., Grant, C.E., Clementi, L., Ren, J., Li, W.W., and Noble, W.S. (2009). MEME SUITE: tools for motif discovery and searching. Nucleic Acids Res. *37*, W202–W208.

Carroll, J.S., Liu, X.S., Brodsky, A.S., Li, W., Meyer, C.A., Szary, A.J., Eeckhoute, J., Shao, W., Hestermann, E.V., Geistlinger, T.R., et al. (2005). Chromosome-wide mapping of estrogen receptor binding reveals long-range regulation requiring the forkhead protein FoxA1. Cell *122*, 33–43.

Carroll, J.S., Meyer, C.A., Song, J., Li, W., Geistlinger, T.R., Eeckhoute, J., Brodsky, A.S., Keeton, E.K., Fertuck, K.C., Hall, G.F., et al. (2006). Genome-wide analysis of estrogen receptor binding sites. Nat. Genet. *38*, 1289–1297.

Cirillo, L.A., McPherson, C.E., Bossard, P., Stevens, K., Cherian, S., Shim, E.Y., Clark, K.L., Burley, S.K., and Zaret, K.S. (1998). Binding of the winged-helix transcription factor HNF3 to a linker histone site on the nucleosome. EMBO J. *17*, 244–254.

Cirillo, L.A., Lin, F.R., Cuesta, I., Friedman, D., Jarnik, M., and Zaret, K.S. (2002). Opening of compacted chromatin by early developmental transcription factors HNF3 (FoxA) and GATA-4. Mol. Cell *9*, 279–289.

Fu, X., Jeselsohn, R., Pereira, R., Hollingsworth, E.F., Creighton, C.J., Li, F., Shea, M., Nardone, A., De Angelis, C., Heiser, L.M., et al. (2016). FOXA1 overexpression mediates endocrine resistance by altering the ER transcriptome and IL-8 expression in ER-positive breast cancer. Proc. Natl. Acad. Sci. U S A *113*, E6600–E6609.

Fullwood, M.J., Liu, M.H., Pan, Y.F., Liu, J., Xu, H., Mohamed, Y.B., Orlov, Y.L., Velkov, S., Ho, A., Mei, P.H., et al. (2009). An oestrogen-receptor-alpha-bound human chromatin interactome. Nature *462*, 58–64.

Glass, C.K., and Rosenfeld, M.G. (2000). The coregulator exchange in transcriptional functions of nuclear receptors. Genes Dev. *14*, 121–141.

He, Y., Lu, J., Ye, Z., Hao, S., Wang, L., Kohli, M., Tindall, D.J., Li, B., Zhu, R., Wang, L., and Huang, H. (2018). Androgen receptor splice variants bind to constitutively open chromatin and promote abiraterone-resistant growth of prostate cancer. Nucleic Acids Res. *46*, 1895–1911.

Hnisz, D., Abraham, B.J., Lee, T.I., Lau, A., Saint-André, V., Sigova, A.A., Hoke, H.A., and Young, R.A. (2013). Super-enhancers in the control of cell identity and disease. Cell *155*, 934–947.

Hurtado, A., Holmes, K.A., Ross-Innes, C.S., Schmidt, D., and Carroll, J.S. (2011). FOXA1 is a key determinant of estrogen receptor function and endocrine response. Nat. Genet. *43*, 27–33.

Jain, R.K., Mehta, R.J., Nakshatri, H., Idrees, M.T., and Badve, S.S. (2011). High-level expression of forkhead-box protein A1 in metastatic prostate cancer. Histopathology *58*, 766–772.

Jones, D., Wade, M., Nakjang, S., Chaytor, L., Grey, J., Robson, C.N., and Gaughan, L. (2015). FOXA1 regulates androgen receptor variant activity in models of castrate-resistant prostate cancer. Oncotarget *6*, 29782–29794.

Jozwik, K.M., and Carroll, J.S. (2012). Pioneer factors in hormone-dependent cancers. Nat. Rev. *12*, 381–385.

Laganière, J., Deblois, G., Lefebvre, C., Bataille, A.R., Robert, F., and Giguère, V. (2005). From the Cover: Location analysis of estrogen receptor alpha target promoters reveals that FOXA1 defines a domain of the estrogen response. Proc. Natl. Acad. Sci. U S A *102*, 11651–11656.

Langmead, B., and Salzberg, S.L. (2012). Fast gapped-read alignment with Bowtie 2. Nat. Methods *9*, 357–359.

Lin, C.Y., Vega, V.B., Thomsen, J.S., Zhang, T., Kong, S.L., Xie, M., Chiu, K.P., Lipovich, L., Barnett, D.H., Stossi, F., et al. (2007). Whole-genome cartography of estrogen receptor alpha binding sites. PLoS Genet. *3*, e87.

Love, M.I., Huber, W., and Anders, S. (2014). Moderated estimation of fold change and dispersion for RNA-seq data with DESeq2. Genome Biol. *15*, 550.

Lupien, M., Eeckhoute, J., Meyer, C.A., Wang, Q., Zhang, Y., Li, W., Carroll, J.S., Liu, X.S., and Brown, M. (2008). FoxA1 translates epigenetic signatures into enhancer-driven lineage-specific transcription. Cell *132*, 958–970.

Merenbakh-Lamin, K., Ben-Baruch, N., Yeheskel, A., Dvir, A., Soussan-Gutman, L., Jeselsohn, R., Yelensky, R., Brown, M., Miller, V.A., Sarid, D., et al. (2013). D538G mutation in estrogen receptor-α: A novel mechanism for acquired endocrine resistance in breast cancer. Cancer Res. *73*, 6856–6864.

Nakshatri, H., and Badve, S. (2007). FOXA1 as a therapeutic target for breast cancer. Expert Opin. Ther. Targets *11*, 507–514.

Nakshatri, H., and Badve, S. (2009). FOXA1 in breast cancer. Expert Rev. Mol. Med. *11*, e8.

Pan, Y.F., Wansa, K.D., Liu, M.H., Zhao, B., Hong, S.Z., Tan, P.Y., Lim, K.S., Bourque, G., Liu, E.T., and Cheung, E. (2008). Regulation of estrogen receptor-mediated long range transcription via evolutionarily conserved distal response elements. J. Biol. Chem. *283*, 32977–32988.

Robinson, D.R., Wu, Y.M., Vats, P., Su, F., Lonigro, R.J., Cao, X., Kalyana-Sundaram, S., Wang, R., Ning, Y., Hodges, L., et al. (2013). Activating ESR1 mutations in hormone-resistant metastatic breast cancer. Nat. Genet. *45*, 1446–1451.

Robinson, J.L., Hickey, T.E., Warren, A.Y., Vowler, S.L., Carroll, T., Lamb, A.D., Papoutsoglou, N., Neal, D.E., Tilley, W.D., and Carroll, J.S. (2014). Elevated levels of FOXA1 facilitate A chromatin binding resulting in a CRPC-like phenotype. Oncogene *33*, 5666–5674.

Ross-Innes, C.S., Stark, R., Teschendorff, A.E., Holmes, K.A., Ali, H.R., Dunning, M.J., Brown, G.D., Gojis, O., Ellis, I.O., Green, A.R., et al. (2012). Differential oestrogen receptor binding is associated with clinical outcome in breast cancer. Nature *481*, 389–393.

Schmidt, D., Wilson, M.D., Spyrou, C., Brown, G.D., Hadfield, J., and Odom, D.T. (2009). ChIP-seq: using high-throughput sequencing to discover protein-DNA interactions. Methods *48*, 240–248.

Sérandour, A.A., Avner, S., Percevault, F., Demay, F., Bizot, M., Lucchetti-Miganeh, C., Barloy-Hubler, F., Brown, M., Lupien, M., Métivier, R., et al. (2011). Epigenetic switch involved in activation of pioneer factor FOXA1-dependent enhancers. Genome Res. *21*, 555–565.

Shang, Y., Hu, X., DiRenzo, J., Lazar, M.A., and Brown, M. (2000). Cofactor dynamics and sufficiency in estrogen receptor-regulated transcription. Cell *103*, 843–852.

Stark, R., and Brown, G.D. (2011). DiffBind: differential binding analysis of ChIP-Seq peak data. http://bioconductor.org/packages/release/bioc/html/DiffBind.html.

Swinstead, E.E., Miranda, T.B., Paakinaho, V., Baek, S., Goldstein, I., Hawkins, M., Karpova, T.S., Ball, D., Mazza, D., Lavis, L.D., et al. (2016). Steroid receptors reprogram FoxA1 occupancy through dynamic chromatin transitions. Cell *165*, 593–605.

Toy, W., Shen, Y., Won, H., Green, B., Sakr, R.A., Will, M., Li, Z., Gala, K., Fanning, S., King, T.A., et al. (2013). ESR1 ligand-binding domain mutations in hormone-resistant breast cancer. Nat. Genet. *45*, 1439–1445.

Voss, T.C., Schiltz, R.L., Sung, M.H., Yen, P.M., Stamatoyannopoulos, J.A., Biddie, S.C., Johnson, T.A., Miranda, T.B., John, S., and Hager, G.L. (2011). Dynamic exchange at regulatory elements during chromatin remodeling underlies assisted loading mechanism. Cell *146*, 544–554.

Whyte, W.A., Orlando, D.A., Hnisz, D., Abraham, B.J., Lin, C.Y., Kagey, M.H., Rahl, P.B., Lee, T.I., and Young, R.A. (2013). Master transcription factors and mediator establish super-enhancers at key cell identity genes. Cell *153*, 307–319.

Zaret, K.S., and Carroll, J.S. (2011). Pioneer transcription factors: establishing competence for gene expression. Genes Dev. *25*, 2227–2241.

Zhang, Y., Liu, T., Meyer, C.A., Eeckhoute, J., Johnson, D.S., Bernstein, B.E., Nusbaum, C., Myers, R.M., Brown, M., Li, W., and Liu, X.S. (2008). Model-based analysis of ChIP-Seq (MACS). Genome Biol. *9*, R137.

STAR★METHODS

KEY RESOURCES TABLE

REAGENT or RESOURCE	SOURCE	IDENTIFIER
Antibodies		
Rabbit Anti- ERα (HC-20) polyclonal antibody	Santa Cruz	Cat# sc-543, RRID; AB_631471
Goat Anti-FOXA1 polyclonal antibody – ChIP grade	Abcam	Cat# ab5089, RRID; AB_304744
Rabbit Anti-FOXA1 polyclonal antibody – ChIP grade	Abcam	Cat# ab23738, RRID; AB_2104842
Chemicals, Peptides, and Recombinant Proteins		
Dynabeads Protein A	Invitrogen	Cat#10001D
Dynabeads Protein G	Invitrogen	Cat#10003D
Pierce 16% Formaldehyde (w/v), Methanol-free	Thermo Scientific	Cat# 28908
β-Estradiol	Sigma-Aldrich	Cat# E8875
Dulbecco's Modified Eagle Medium (DMEM)	GIBCO	Cat# 41966029
RPMI 1640 Medium	GIBCO	Cat# 21875034
Fetal Bovine Serum, qualified, heat inactivated	GIBCO	Cat# 16140071
Fetal Bovine Serum, charcoal stripped	GIBCO	Cat# 12676029
Penicillin-Streptomycin	GIBCO	Cat#15070063
L-Glutamine (200 mM)	GIBCO	Cat# 25030081
Trypsin-EDTA (0.5%), no phenol red	GIBCO	Cat# 15400054
cOmplete EDTA-free Protease inhibitor cocktail	Sigma-Aldrich	Cat# 05056489 001
Phosphatase Inhibitor cocktail	Thermo Scientific	Cat#78427
Critical Commercial Assays		
ThruPlex DNA-seq kit	Rubicon Genomics	Cat# R400407
Deposited Data		
Gene Expression Omnibus (GEO)	https://www.ncbi.nlm.nih.gov/geo/	GSE112969; RRID:SCR_005012
Experimental Models: Cell Lines		
MCF-7	ATCC	Cat# HTB-22, RRID:CVCL_0031; ATCC HTB-22
ZR-75-1	ATCC	Cat# CRL-1500, RRID:CVCL_0588; ATCC CRL-1500
Oligonucleotides		
Primer for ChIP Forward: ER3 negative site (5′- GCCACCAGCCTGCTTTCTGT-3′)	This study	n/a
Primer for ChIP Reverse: ER3 negative site (5′- CGTGGATGGGTCCGAGAAAC-3′)	This study	n/a
Primer for ChIP Forward: XBP1 negative site (5′- ACCCTCCAAAATTCTTCTGC-3′)	This study	n/a
Primer for ChIP Reverse: XBP1 negative site (5′- ATGAGCATCTGAGAGCAAGC-3′)	This study	n/a
Primer for ChIP Forward: XBP1 target site (5′- ATACTTGGCAGCCTGTGACC-3′)	This study	n/a
Primer for ChIP Reverse: XBP1 target site (5′- GGTCCACAAAGCAGGAAAAA-3′)	This study	n/a

(*Continued on next page*)

Continued

REAGENT or RESOURCE	SOURCE	IDENTIFIER
Primer for ChIP Forward: GREB1 target site (5′- GAAGGGCAGAGCTGATAACG-3′)	This study	n/a
Primer for ChIP Reverse: GREB1 target site (5′- GACCCAGTTGCCACACTTTT-3′)	This study	n/a
Primer for ChIP Forward: MYC target site (5′- GCTCTGGGCACACACATTGG-3′)	This study	n/a
Primer for ChIP Reverse: MYC target site (5′- GGCTCACCCTTGCTGATGCT-3′)	This study	n/a
Software and Algorithms		
Bowtie 2 v2.2.6	Langmead and Salzberg, 2012	https://sourceforge.net/projects/bowtie-bio/files/bowtie2/2.2.6/ ; RRID:SCR_016368
MEME tool FIMO v4.9.1	Bailey et al., 2009	http://meme-suite.org/doc/install.html?man_type=web ; RRID:SCR_001783
JASPAR CORE 2016 vertebrates	JASPAR	http://jaspar.genereg.net/matrix-clusters/vertebrates/ ; RRID:SCR_003030
MACS2 version 2.0.10.20131216	Zhang et al., 2008	https://pypi.org/project/MACS2/2.0.10.20131216/ ; RRID:SCR_013291
GSEAPreranked (18) analysis tool Gene Set Enrichment Analysis (GSEA) v2.2.3	Broad Institute, Massachusetts Institute of Technology	http://www.broadinstitute.org/gsea/ ; RRID:SCR_003199
Diffbind	Stark and Brown, 2011	https://bioconductor.org/packages/release/bioc/html/DiffBind.html ; RRID:SCR_012918
DESeq2	Love et al., 2014	https://bioconductor.org/packages/release/bioc/html/DESeq2.html ; RRID:SCR_015687
Other		
Bioruptor Plus sonicator	Diagenode	n/a

CONTACT FOR REAGENT AND RESOURCE SHARING

Further information and requests for resources and reagents should be directed to and will be fulfilled by the lead contact, Jason Carroll (Jason.carroll@cruk.cam.ac.uk).

EXPERIMENTAL MODEL AND SUBJECT DETAILS

Cell culture

MCF-7 and ZR-75-1 cell lines were obtained from ATCC (Middlesex, UK) and represent female breast cancer cell line models. MCF-7 cells were cultured in Dulbecco's Modified Eagle Medium DMEM (GIBCO, Thermo Scientific, Leicestershire, UK, ref. 41966). ZR-75-1 cells were grown in RPMI-1640 medium (GIBCO, Thermo Scientific, Leicestershire, UK, ref. 21875-034). Both media were supplemented with fetal bovine serum (FBS), 50 U/ml penicillin, 50 μg/ml streptomycin and 2 mM L-glutamine.

MCF-7 and ZR-75-1 cells were seeded and treated either with ethanol or with 10nM Estrogen (Sigma) for 45 minutes previously described (Schmidt et al., 2009). All cell lines were regularly genotyped to ensure they were the correct cell lines.

METHOD DETAILS

Chromatin Immunoprecipitation

To validate the Estrogen induction, ER ChIP-qPCR was performed using the rabbit polyclonal sc-543 (Santa Cruz) antibody. FOXA1 ChIP-seq was performed using the goat polyclonal ab5089 (Abcam), and rabbit polyclonal ab23738 (Abcam) antibodies. Chromatin was prepared as previously described (Schmidt et al., 2009). DNA was isolated and purified using the phenol-chloroform-isoamyl DNA extraction method. ChIP-seq and the input libraries were prepared using the ThruPlex® DNA-seq kit (Rubicon Genomics, ref. R400407).

Integration of RNA-seq and ChIP-seq data

Genes located around ± 50kb from the peak regions were selected. –log10 transformed p values from DESeq2 analyses of the RNA-Seq data were subsequently used for ranking and weighting of genes. GSEAPreranked (18) analysis tool from Gene Set Enrichment Analysis (GSEA) software, version 2.2.3, was used for the evaluation of statistically significant genes.

QUANTIFICATION AND STATISTICAL ANALYSIS

ChIP Sequencing Analysis

ER ChIP-qPCR and FOXA1 ChIP-seq were performed in biological triplicates, using cells from independent passages.

ChIP-seq reads were mapped to hg38 genome using bowtie2 2.2.6 (Langmead and Salzberg, 2012). Aligned reads with the mapping quality less than 5 were filtered out. The read alignments from three replicates were combined into a single library and peaks were called using MACS2 version 2.0.10.20131216 (Zhang et al., 2008) with sequences from MCF7 chromatin extracts as a background input control. The peaks yielded with MACS2 q value $\leq$ 1e-3 were selected for downstream analysis. MEME tool FIMO version 4.9.1 (Bailey et al., 2009) was used for searching all known TF motifs from JASPAR database (JASPAR CORE 2016 vertebrates) in the tag-enriched sequences. As a background control, peak size - matching sequences corresponding to known open chromatin regions in MCF7 cells were randomly selected from hg38. Motif frequency for both tag-enriched and control sequences calculated as sum of motif occurrences adjusted with MEM q-value. Motif enrichment analysis was performed by calculating odds of finding an overrepresented motif among MACS2-defined peaks by fitting Student's t-cumulative distribution to the ratios of motif frequencies between tag-enriched and background sequences. Yielded p values were further adjusted using Benjamini-Hochberg correction.

For visualizing tag density and signal distribution, heatmaps were generated with the read coverage in a window of ± 2.5 or 5 kb region flanking the tag midpoint using the bin size of 1/100 of the window length. Differential binding analysis (Diffbind) was performed as described previously (Stark and Brown, 2011).

DATA AND SOFTWARE AVAILABILITY

All ChIP-seq data is deposited in GEO under the accession number: GSE112969. Data can be accessed using the password: gzmtegactlqtxwp

PLOS ONE

RESEARCH ARTICLE

Identification of ChIP-seq and RIME grade antibodies for Estrogen Receptor alpha

Silvia-E. Glont☯, Evangelia K. Papachristou☯, Ashley Sawle, Kelly A. Holmes, Jason S. Carroll*, Rasmus Siersbaek*

Cancer Research UK Cambridge Institute, University of Cambridge, Robinson Way, Cambridge, United Kingdom

☯ These authors contributed equally to this work.
* Rasmus.Siersbaek@cruk.cam.ac.uk (RS); Jason.Carroll@cruk.cam.ac.uk (JC)

Citation: Glont S-E, Papachristou EK, Sawle A, Holmes KA, Carroll JS, Siersbaek R (2019) Identification of ChIP-seq and RIME grade antibodies for Estrogen Receptor alpha. PLoS ONE 14(4): e0215340. https://doi.org/10.1371/journal.pone.0215340

Editor: Alessandro Weisz, Universita degli Studi di Salerno, ITALY

Received: February 13, 2019

Accepted: March 29, 2019

Published: April 10, 2019

Data Availability Statement: All data is be available from GEO (Accession number GSE128208) or PRIDE (Accession number PXD012930).

Funding: All work was funded by Cancer Research UK. RS is supported by a fellowship from the Novo Nordisk Foundation (NNF15OC0014136). JSC is supported by an ERC Consolidator award. The funders had no role in study design, data collection and analysis, decision to publish, or preparation of the manuscript.

Abstract

Estrogen Receptor alpha (ERα) plays a major role in most breast cancers, and it is the target of endocrine therapies used in the clinic as standard of care for women with breast cancer expressing this receptor. The two methods ChIP-seq (chromatin immunoprecipitation coupled with deep sequencing) and RIME (Rapid Immunoprecipitation of Endogenous Proteins) have greatly improved our understanding of ERα function during breast cancer progression and in response to anti-estrogens. A critical component of both ChIP-seq and RIME protocols is the antibody that is used against the bait protein. To date, most of the ChIP-seq and RIME experiments for the study of ERα have been performed using the sc-543 antibody from Santa Cruz Biotechnology. However, this antibody has been discontinued, thereby severely impacting the study of ERα in normal physiology as well as diseases such as breast cancer and ovarian cancer. Here, we compare the sc-543 antibody with other commercially available antibodies, and we show that 06–935 (EMD Millipore) and ab3575 (Abcam) antibodies can successfully replace the sc-543 antibody for ChIP-seq and RIME experiments.

Introduction

In the last decades, there has been significant interest in studying Estrogen Receptor alpha (ERα) due to its causal role in more than three quarters of breast cancers[1]. Its key role in breast cancer progression makes ERα the major target for endocrine therapies, which have substantially improved patient survival. However, resistance to these therapies occurs in many patients[2], which leads to incurable metastatic disease. Therefore, it is important to understand the mechanisms underlying ERα action in cancer initiation as well as progression of the disease. In addition, ERα plays an important role in development[3] and other diseases such as ovarian cancer[4].

Our understanding of ERα-mediated gene transcription has evolved in recent years, due to delineation of ERα-chromatin binding mechanisms through ChIP-seq (chromatin immunoprecipitation followed by next generation sequencing) experiments[5–15]. It is now clear that

Competing interests: Jason Carroll is founder and CSO of Azeria Therapeutics. None of the work in this manuscript is related to the work in Azeria Therapeutics. The authors declare no additional competing interests and the declared funding does not alter our adherence to PLOS ONE policies on sharing data and materials.

differential binding of ERα to chromatin is associated with clinical outcome in primary ERα-positive breast tumours[5], suggesting that changes in ERα binding mediates the altered gene expression program that dictates endocrine responsiveness and clinical outcome. In addition to changes in binding to chromatin, ERα transcriptional activity can be modulated by its association with different co-regulators and other associated transcription factors. Our lab has previously developed a method termed RIME (Rapid Immunoprecipitation of Endogenous Proteins) for the study of protein complexes using mass spectrometry[16, 17]. A key component of ERα ChIP-seq and RIME assays is the antibody that specifically and with high sensitivity targets ERα. Most ChIP-seq and RIME experiments have been performed using the ERα antibody sc-543 from Santa Cruz Biotechnology[5, 9, 17–21]. This antibody has recently been discontinued, impacting the ability to study ERα function in breast cancer as well as in other diseases and physiological conditions. Here, we compare the sc-543 (Santa Cruz Biotechnology) with other commercially available antibodies using breast cancer cells as a model and demonstrate that 06–935 (EMD Millipore) and ab3575 (Abcam) antibodies can replace sc-543 in ChIP-seq and RIME assays.

Materials and methods

Cell culture

MCF7 cells were cultured in Dulbecco's Modified Eagle Medium DMEM (Gibco, Thermo Scientific) and MDA-MB-231 cells were grown in RPMI-1640 medium (Gibco, Thermo Scientific). Both media conditions were supplemented with 10% foetal bovine serum (FBS), 50 U/ml penicillin, 50 μg/ml streptomycin and 2 mM L-glutamine. Cell lines were obtained from ATCC (Middlesex). For both ChIP-seq and RIME experiments, $2x10^6$ cells were seeded in 15 cm^2 plates and collected at 80–90% confluency.

ChIP-Seq and RIME assays

The sc-543 (Santa Cruz), ab80922 (Abcam), ab3575 (Abcam), sc-514857 (C-3) (Santa Cruz Biotechnology), C15100066 (Diagenode) and 06–935 (EMD Millipore) antibodies were used for ChIP-qPCR. The sc-543, ab3575 and 06–935 antibodies were then used for ChIP-seq and RIME. For each ChIP, 10μg of each of the antibodies sc-543, 06–935 and ab3575 or the rabbit IgG ab37415 (Abcam) were used together with 100μl of Dynabeads Protein A (Invitrogen). The antibody and the beads were incubated overnight at 4˚C with rotation. MCF7 cells were fixed for 10 minutes using 1% formaldehyde (Thermo, #28908) and quenched with 0.1M glycine. Cells were then washed and harvested in ice-cold PBS containing protease inhibitors (Roche). In order to enrich for the nuclear fraction, pellets were resuspended in Lysis Buffer 1 (50mM Hepes–KOH, pH 7.5, 140mM NaCl, 1mM EDTA, 10% Glycerol, 0.5% NP-40/Igepal CA-630, 0.25% Triton X-100) and rotated for 10 minutes, at 4˚C. Cells were then pelleted, resuspended in Lysis buffer 2 (10mM Tris–HCL, pH8.0, 200mM NaCl, 1mM EDTA, 0.5mM EGTA) and incubated for 5 minutes, at 4˚C with rotation. For both ChIP-seq and RIME experiments, cells were pelleted, resuspended in 300 μl Lysis buffer 3 (10mM Tris–HCl, pH 8, 100mM NaCl, 1mM EDTA, 0.5mM EGTA, 0.1% Na–Deoxycholate) and sonicated using the Bioruptor Pico sonicator (Diagenode, Liege, Belgium) for 10 cycles (30 seconds on, 30 seconds off). After sonication the samples were centrifuged at maximum speed for 10 minutes at 4˚C and a small aliquot of supernatant was kept as input for ChIP-seq. The rest of the supernatant was added to the Protein A Dynabeads, which were incubated overnight with antibody. The next day, the beads for ChIP-seq were washed six times with RIPA buffer (150mM NaCl, 10mM Tris, pH 7.2, 0.1% SDS, 1% Triton X-100, 1% NaDeoxycholate), followed by one wash with TE (pH 7.4). Both ChIP samples and inputs were then de-crosslinked by adding 200 μl

elution buffer (1% SDS, 0.1 M $NaHCO_3$) overnight at 65˚C. After reverse crosslinking, DNA was purified using the phenol-chloroform-isoamyl DNA extraction method. ChIP-seq and the input libraries were prepared using the ThruPlex Sample Prep Kit (Illumina). ERα ChIP-seq was performed in at least duplicates for each condition. For RIME, the antibody-bound beads incubated with the chromatin samples were washed 10 times with RIPA buffer and twice with 100mM AMBIC (ammonium bicarbonate) prior to mass spectrometry analysis.

Sample preparation, LC-MS/MS analysis and data processing

A 10μL trypsin solution (15ng/ul) (Pierce) prepared in 100mM AMBIC was added to the beads followed by overnight incubation at 37˚C. The next day, trypsin solution was added for a second digestion step followed by incubation for 4h at 37˚C. At the end of the second step digestion, the tubes were placed on a magnet and the supernatant solution was collected and acidified by the addition of 2μl 5% formic acid. The peptides were cleaned with the Ultra-Micro C18 Spin Columns (Harvard Apparatus) and were analysed in the Dionex Ultimate 3000 UHPLC system coupled with the Q-Exactive HF (Thermo Scientific) mass spectrometer. Samples were loaded on the Acclaim PepMap 100, 100μm × 2cm C18, 5μm, 100Å trapping column with the ulPickUp injection method at loading flow rate 5μL/min for 10 min. For the peptide separation the EASY-Spray analytical column 75μm × 25cm, C18, 2μm, 100 Å was used for multi-step gradient elution. Mobile phase (A) was composed of 2% acetonitrile, 0.1% formic acid, 5% dimethyl sulfoxide (DMSO) and mobile phase (B) was composed of 80% acetonitrile, 0.1% formic acid, 5% DMSO. The full scan was performed in the Orbitrap in the range of 400-1600m/z at 60K resolution. For MS2, the 10 most intense fragments were selected at resolution 30K. A 2.0Th isolation window was used and the HCD collision energy was set up at 28%. The HCD tandem mass spectra were processed with the SequestHT search engine on Proteome Discoverer 2.2 software. The node for SequestHT included the following parameters: Precursor Mass Tolerance 20ppm, Maximum Missed Cleavages sites 2, Fragment Mass Tolerance 0.02Da and Dynamic Modifications were Oxidation of M (+15.995Da) and Deamidation of N, Q (+0.984Da). The Minora Feature Detector node was used for label-free quantification and the consensus workflow included the Feature Mapper and the Precursor Ion Quantifier nodes using intensity for the precursor quantification. The protein intensities were normalized by the summed intensity separately for the IgG and ERα pull downs (within group normalization). The plots for ERα coverage were created using the qPLEXanalyzer tool[22]. Heatmaps and PCA plot were done with the Phantasus Web tool (https://artyomovlab.wustl.edu/phantasus/). The mass spectrometry proteomics data have been deposited to the ProteomeXchange Consortium via the PRIDE[23] partner repository with the dataset identifier PXD012930.

ChIP-seq data analysis

Reads were mapped to the GRCh38 genome using bwa version 0.7.12[24]. Prior to peak calling, reads were filtered according to four criteria: (1) only reads aligning to canonical chromosomes (1–22, X, Y, MT) were considered for further analysis; (2) read aligning in blacklisted regions were excluded[25]; (3) grey lists were generated using the R package GreyListChIP and reads aligned in these regions were excluded; (4) reads with a mapping quality of less than 15 were excluded. Peak calling was carried out on each ChIP sample with MACS2 version 2.1.1.20160309 using the relevant input sample[26]. Peaks with a q-value < 0.01 were accepted for further analysis. To create tag heatmaps, a consensus peak set was generated using the R package DiffBind[5, 16]. The consensus peak set was composed of any peak that was called in at least two samples. Motif analysis was carried out using AME[27] from the MEME suite

version 4.12.0[28] and the HOCOMOCO Human (v10) motif database[29]. Sequences for motif analysis for each sample were derived by selecting the top 1000 peaks by q-value from the MACS2 peak set and then extracting the genomic sequence 500 bases either side of the peak summits. A detailed description of the pipeline can be found in **S1 File.** ChIP-seq data have been deposited in NCBI's Gene Expression Omnibus[30] and are accessible through GEO Series accession number GSE128208.

Results and discussion

ChIP-sequencing validates 06–935 and ab3575 as specific ERα antibodies

Given the discontinuation of anti-ERα antibody sc-543, we sought to validate alternatives for immunoprecipitation experiments. We first compared the established sc-543 (Santa Cruz Biotechnology) antibody with ab80922 (Abcam), ab3575 (Abcam), sc-514857 (C-3) (Santa Cruz Biotechnology), C15100066 (Diagenode) and 06–935 (Millipore). For this purpose, we used the ERα positive cell line MCF7 and performed ChIP-qPCR in biological duplicates (**S1 Fig**) to assess ERα binding at known target regions (**S1 Table**).

The ChIP-qPCR comparison suggested that 06–935 (Millipore) and ab3575 (Abcam) could successfully enrich ERα-bound chromatin at these selected loci and could therefore substitute for sc-543. We performed ChIP-seq to compare these three antibodies in MCF7 cells using IgG as a negative control. ERα ChIP-seq was performed in at least duplicates for each condition, using the same batch of chromatin, to ensure that antibodies could be directly compared. In addition, we included the ERα negative MDA-MB-231 cell line in order to assess non-specific binding by these antibodies. For MDA-MB-231, ChIP-seq was performed in biological triplicates.

We observed 6,031 ERα binding sites for sc-543 (Santa Cruz) antibody, 6,192 peaks for ab3575 (Abcam) and 6,552 for 06–935 (Millipore). Importantly, none of these binding sites were observed in the IgG negative control. The vast majority of sites identified in MCF7 cells by sc-543 overlapped with those detected by ab3575 and 06–935 (**Fig 1A**). Consistently, we found a strong correlation between the binding intensities for the three antibodies, which was similar to the correlation between replicates for the same antibody (**Fig 1B**). All three antibodies showed robust enrichment at binding sites compared to background and motif analysis identified the ERα response element (ERE) as highly significantly enriched at these sites (**Fig 1C**). Importantly, neither of the ab3575 and 06–935 antibodies showed any significant enrichment in the ERα negative cell line MDA-MB-231 (**Fig 1C**). In total, one peak was detected in ER-negative cells using ab3575, two peaks for 06–935 and 124 binding sites for sc-543, confirming the specificity of the antibodies. Examples of ERα binding to previously described ERα binding sites[16, 31] are illustrated in **Fig 1D**. Taken together, this indicates that the ab3575 (Abcam) and 06–935 (Millipore) antibodies perform similarly to the sc-543 (Santa Cruz) antibody in ChIP-seq experiments, both in terms of sensitivity and specificity.

Validation of 06–935 and ab3575 antibodies using RIME

We next sought to evaluate the performance of ab3575 (Abcam) and 06–935 (Millipore) in RIME experiments to directly compare with the sc-543 (Santa Cruz) antibody, which has previously been successfully used in RIME experiments to explore the ERα interactome[9, 16, 22]. To this end, we tested the 06–935, ab3575 and sc-543 antibodies in two technical replicates each using MCF7 cells. IgG controls were also analysed to discriminate specific associations from non-specific interaction events.

To evaluate the pull-down efficiencies, we compared the sequence coverage of the bait protein obtained by the different antibodies. ERα was identified with a similar number of peptides (**Fig 2A**) across the three different pull-downs, confirming that all three antibodies achieve

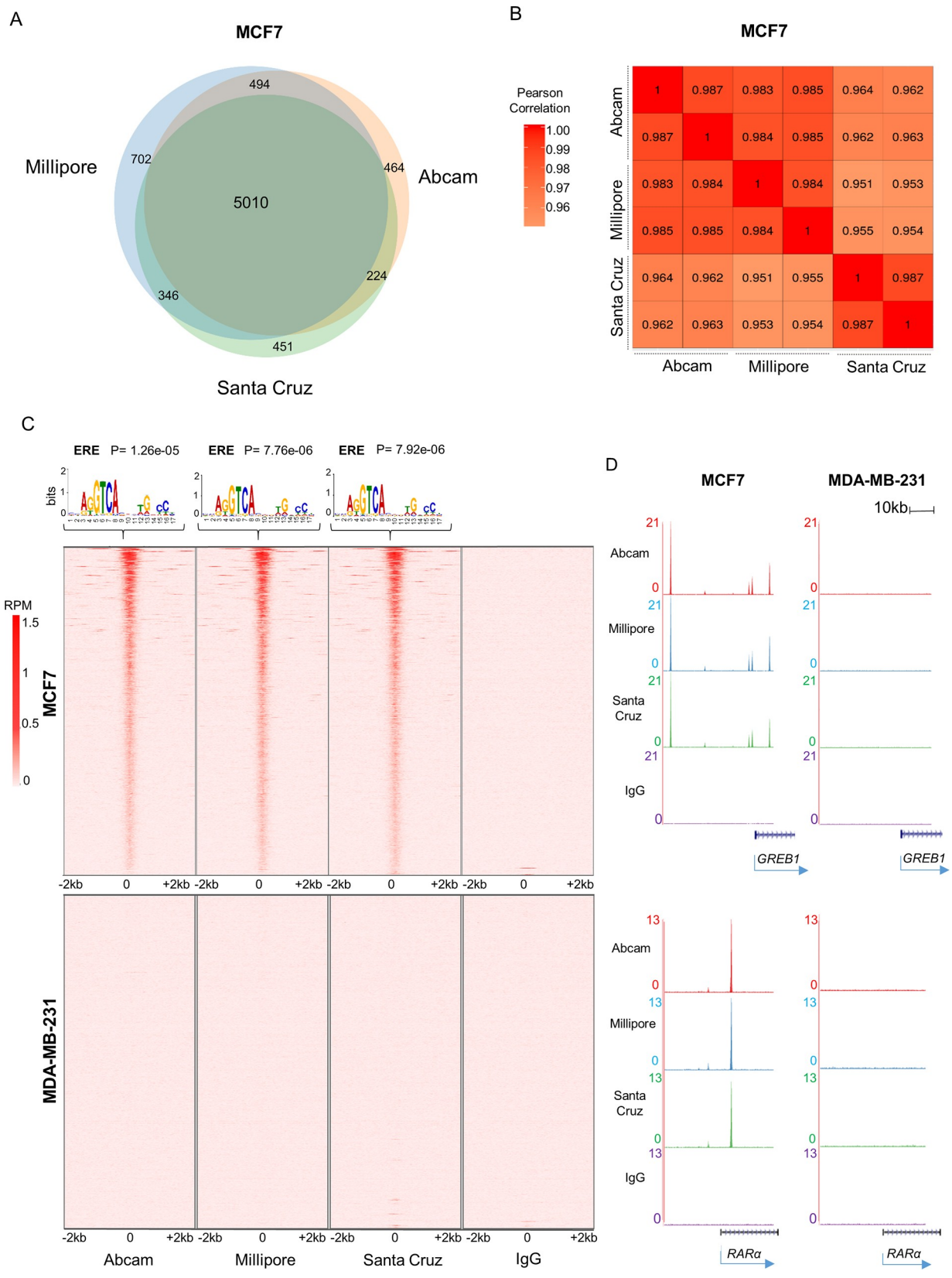
A
MCF7
494
Millipore
702
464
Abcam
5010
224
346
451
Santa Cruz
B
MCF7
Pearson Correlation
1.00
0.99
0.98
0.97
0.96
Abcam
Millipore
Santa Cruz
1 0.987 0.983 0.985 0.964 0.962
0.987 1 0.984 0.985 0.962 0.963
0.983 0.984 1 0.984 0.951 0.953
0.985 0.985 0.984 1 0.955 0.954
0.964 0.962 0.951 0.955 1 0.987
0.962 0.963 0.953 0.954 0.987 1
C
ERE P= 1.26e-05
ERE P= 7.76e-06
ERE P= 7.92e-06
bits
RPM
1.5
1
0.5
0
MCF7
MDA-MB-231
-2kb 0 +2kb
Abcam
Millipore
Santa Cruz
IgG
D
MCF7
MDA-MB-231
10kb
Abcam
Millipore
Santa Cruz
IgG
GREB1
RARα

Fig 1. ChIP-seq comparison between Santa Cruz (sc-543), Millipore (06–935) and Abcam (ab3575) antibodies. A) Venn diagram showing the overlap between ERα binding sites for Santa Cruz (sc-543), Millipore (06–935) and Abcam (ab3575) antibodies in MCF7 cells. B) Pearson's correlation between each replicate of all three antibodies in MCF7 cells. C) Top: De novo motif analysis of ERα binding sites using MEME. Bottom: Heatmap of total number of ERα binding sites identified in both technical replicates of MCF7, and in all three biological replicates for MDA-MB-231, respectively. D) Examples of ERα- bound regions. Tag densities are shown as reads per million.

https://doi.org/10.1371/journal.pone.0215340.g001

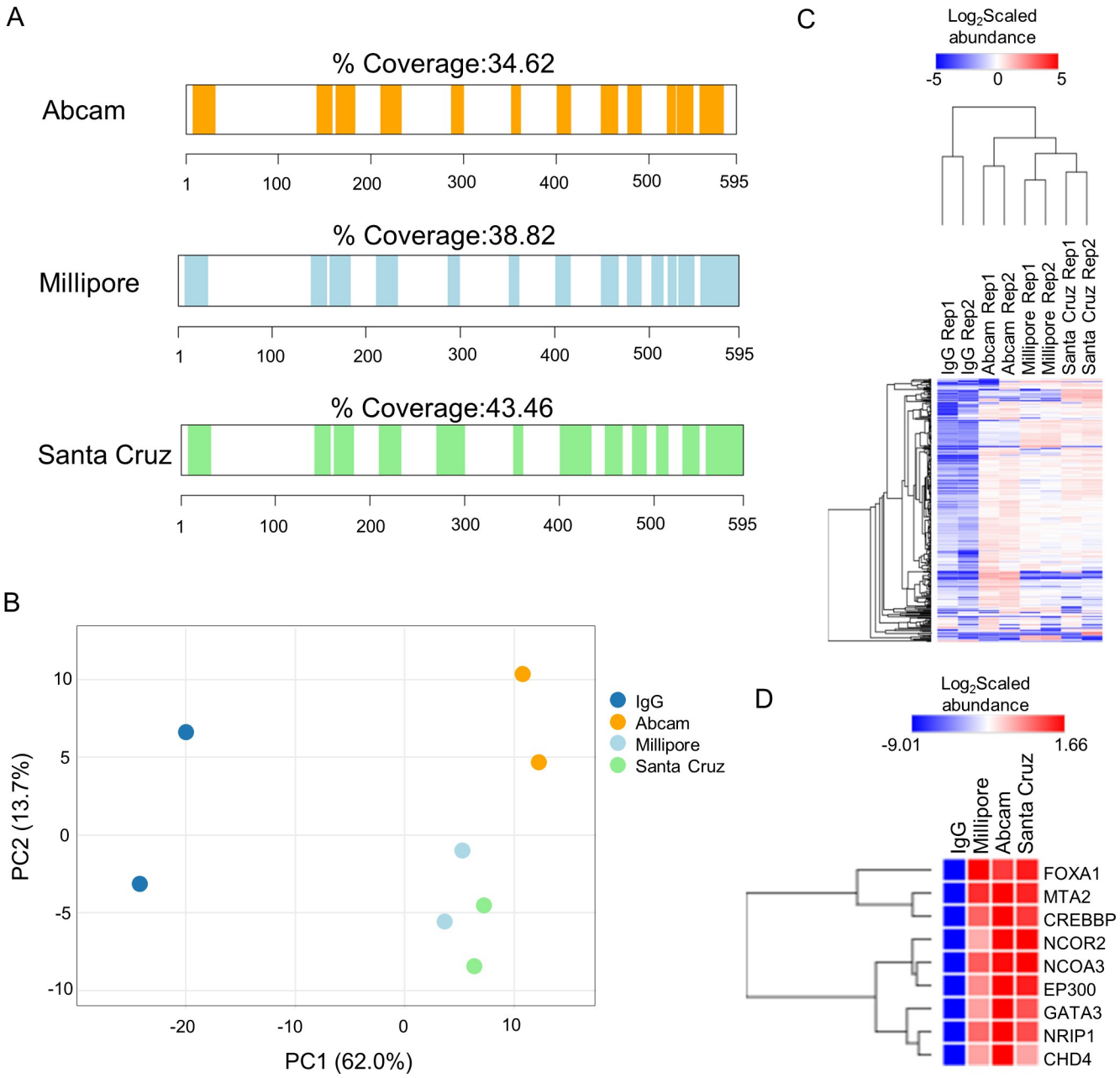

Fig 2. Comparison of RIME data between Santa Cruz (sc-543), Millipore (06–935) and Abcam (ab3575) antibodies. A) Protein sequence coverage of ERα achieved by the use of Abcam (ab3575), Millipore (06–935) and Santa Cruz (sc-543) antibodies in RIME. B) PCA plot of known ERα interactors (n = 319, BIOGRID and STRING databases) for the four different RIME pull-downs. C) Hierarchical clustering of the scaled intensities of known ERα interactors from BIOGRID and STRING databases (n = 319). D) Hierarchical clustering of well-characterized ERα interactors.

https://doi.org/10.1371/journal.pone.0215340.g002

efficient immunoprecipitation of the bait protein. Next, to compare the efficiency of the different antibodies to detect known ERα interactors, we used a label-free quantification method based on the Minora algorithm implemented in Proteome Discoverer 2.2 software (**S2 File**). The PCA plot using intensities of known ERα-associated proteins (n = 319, BIOGRID and STRING databases) across all four samples revealed a good separation between the ERα RIME samples and the IgG controls, indicative of high specificity of all antibodies (**Fig 2B**). Importantly, we identify only minor differences between the three antibodies, suggesting that they all efficiently pull down known ERα-associated proteins (**Fig 2B and 2C**). Specifically, amongst the known ERα interactors we identified FOXA1, GATA3 and members of the p160 family that were all highly enriched by all three antibodies (**Fig 2D**). Taken together, the three ERα antibodies perform similarly in RIME experiments, enriching for well-known key ERα interactors.

Conclusions

Genome-wide analyses of ERα-chromatin binding sites using ChIP-based methods have exponentially increased our knowledge of the role of ERα in breast cancer. Most of the published ChIP-seq and RIME studies for ERα have been performed using the sc-543 antibody from Santa Cruz Biotechnology[13, 16, 17, 19–21, 32] and the quality and specificity of sc-543 has made it the 'golden standard' for immunoprecipitation experiments. However, this antibody has recently been discontinued, which has significantly impacted our ability to study ERα biology. Here, we have assessed commercially available alternative antibodies. We demonstrate using ChIP-seq and RIME that the two antibodies 06–935 (Millipore) and ab3575 (Abcam) perform similarly to sc-543, in terms of sensitivity and specificity. We therefore propose that these antibodies can replace the sc-543 antibody for immunoprecipitation-based experiments such as ChIP-seq and RIME to explore ERα function.

Supporting information

S1 Fig. ERα antibody comparison by ChIP-qPCR. ChIP-qPCR analysis for ERα known binding sites was performed in MCF7 cells in biological duplicates. Results are shown as arbitrary units. Antibodies used: sc-543 (Santa Cruz Biotechnology), ab80922 (Abcam), ab3575 (Abcam), sc-514857 (C-3) (Santa Cruz Biotechnology), C15100066 (Diagenode) and 6–935 (EMD Millipore).
(TIF)

S1 File. Main steps of the ChIP-seq analysis. The file provides details for the main steps of the Bioinformatic analysis of the ChIP-seq data.
(PDF)

S2 File. Quantitative proteomics analysis results. The file contains the protein intensities across all the different RIME samples based on a label free quantification method using the Minora algorithm in Proteome Discoverer 2.2.
(XLSX)

S1 Table. ChIP-qPCR primers. Table listing the primers used for the ChIP-qPCR experiment.
(DOCX)

Acknowledgments

The authors would like to thank the Genomics core, the head of the Proteomics Core Clive D'Santos and the Bioinformatics Core especially Kamal Kishore.

Author Contributions

Conceptualization: Silvia-E. Glont, Evangelia K. Papachristou, Jason S. Carroll, Rasmus Siersbaek.

Data curation: Ashley Sawle.

Formal analysis: Silvia-E. Glont, Evangelia K. Papachristou, Ashley Sawle.

Funding acquisition: Jason S. Carroll.

Investigation: Silvia-E. Glont, Evangelia K. Papachristou, Kelly A. Holmes, Rasmus Siersbaek.

Project administration: Jason S. Carroll, Rasmus Siersbaek.

Supervision: Jason S. Carroll, Rasmus Siersbaek.

Visualization: Silvia-E. Glont, Evangelia K. Papachristou, Ashley Sawle, Rasmus Siersbaek.

Writing – original draft: Silvia-E. Glont, Evangelia K. Papachristou, Jason S. Carroll, Rasmus Siersbaek.

Writing – review & editing: Silvia-E. Glont, Evangelia K. Papachristou, Ashley Sawle, Kelly A. Holmes, Jason S. Carroll, Rasmus Siersbaek.

References

1. Ali S, Coombes RC. Estrogen receptor alpha in human breast cancer: occurrence and significance. J Mammary Gland Biol Neoplasia. 2000; 5(3):271–81. Epub 2004/02/20. PMID: 14973389.
2. Ali S, Coombes RC. Endocrine-responsive breast cancer and strategies for combating resistance. Nat Rev Cancer. 2002; 2(2):101–12. Epub 2003/03/15. https://doi.org/10.1038/nrc721 PMID: 12635173.
3. Brisken C, O'Malley B. Hormone action in the mammary gland. Cold Spring Harb Perspect Biol. 2010; 2 (12):a003178. Epub 2010/08/27. https://doi.org/10.1101/cshperspect.a003178 PMID: 20739412; PubMed Central PMCID: PMCPMC2982168.
4. Voutsadakis IA. Hormone Receptors in Serous Ovarian Carcinoma: Prognosis, Pathogenesis, and Treatment Considerations. Clin Med Insights Oncol. 2016; 10:17–25. Epub 2016/04/08. https://doi.org/10.4137/CMO.S32813 PMID: 27053923; PubMed Central PMCID: PMCPMC4814131.
5. Ross-Innes CS, Stark R, Teschendorff AE, Holmes KA, Ali HR, Dunning MJ, et al. Differential oestrogen receptor binding is associated with clinical outcome in breast cancer. Nature. 2012; 481(7381):389–93. Epub 2012/01/06. https://doi.org/10.1038/nature10730 PMID: 22217937; PubMed Central PMCID: PMCPMC3272464.
6. Harrod A, Fulton J, Nguyen VTM, Periyasamy M, Ramos-Garcia L, Lai CF, et al. Genomic modelling of the ESR1 Y537S mutation for evaluating function and new therapeutic approaches for metastatic breast cancer. Oncogene. 2017; 36(16):2286–96. Epub 2016/10/18. https://doi.org/10.1038/onc.2016.382 PMID: 27748765; PubMed Central PMCID: PMCPMC5245767.
7. Lupien M, Meyer CA, Bailey ST, Eeckhoute J, Cook J, Westerling T, et al. Growth factor stimulation induces a distinct ER(alpha) cistrome underlying breast cancer endocrine resistance. Genes Dev. 2010; 24(19):2219–27. Epub 2010/10/05. https://doi.org/10.1101/gad.1944810 PMID: 20889718; PubMed Central PMCID: PMCPMC2947773.
8. Jeselsohn R, Cornwell M, Pun M, Buchwalter G, Nguyen M, Bango C, et al. Embryonic transcription factor SOX9 drives breast cancer endocrine resistance. Proc Natl Acad Sci U S A. 2017; 114(22):E4482–E91. Epub 2017/05/17. https://doi.org/10.1073/pnas.1620993114 PMID: 28507152; PubMed Central PMCID: PMCPMC5465894.
9. Mohammed H, Russell IA, Stark R, Rueda OM, Hickey TE, Tarulli GA, et al. Progesterone receptor modulates ERalpha action in breast cancer. Nature. 2015; 523(7560):313–7. Epub 2015/07/15. https://doi.org/10.1038/nature14583 PMID: 26153859; PubMed Central PMCID: PMCPMC4650274.
10. Kong SL, Li G, Loh SL, Sung WK, Liu ET. Cellular reprogramming by the conjoint action of ERalpha, FOXA1, and GATA3 to a ligand-inducible growth state. Mol Syst Biol. 2011; 7:526. Epub 2011/09/01. https://doi.org/10.1038/msb.2011.59 PMID: 21878914; PubMed Central PMCID: PMCPMC3202798.
11. Hurtado A, Holmes KA, Ross-Innes CS, Schmidt D, Carroll JS. FOXA1 is a key determinant of estrogen receptor function and endocrine response. Nat Genet. 2011; 43(1):27–33. Epub 2010/12/15. https://doi.org/10.1038/ng.730 PMID: 21151129; PubMed Central PMCID: PMCPMC3024537.

12. Theodorou V, Stark R, Menon S, Carroll JS. GATA3 acts upstream of FOXA1 in mediating ESR1 binding by shaping enhancer accessibility. Genome Res. 2013; 23(1):12–22. Epub 2012/11/23. https://doi.org/10.1101/gr.139469.112 PMID: 23172872; PubMed Central PMCID: PMCPMC3530671.

13. Stender JD, Kim K, Charn TH, Komm B, Chang KC, Kraus WL, et al. Genome-wide analysis of estrogen receptor alpha DNA binding and tethering mechanisms identifies Runx1 as a novel tethering factor in receptor-mediated transcriptional activation. Mol Cell Biol. 2010; 30(16):3943–55. Epub 2010/06/16. https://doi.org/10.1128/MCB.00118-10 PMID: 20547749; PubMed Central PMCID: PMCPMC2916448.

14. Tan SK, Lin ZH, Chang CW, Varang V, Chng KR, Pan YF, et al. AP-2gamma regulates oestrogen receptor-mediated long-range chromatin interaction and gene transcription. EMBO J. 2011; 30(13):2569–81. Epub 2011/05/17. https://doi.org/10.1038/emboj.2011.151 PMID: 21572391; PubMed Central PMCID: PMCPMC3155293.

15. Schmidt D, Wilson MD, Spyrou C, Brown GD, Hadfield J, Odom DT. ChIP-seq: using high-throughput sequencing to discover protein-DNA interactions. Methods. 2009; 48(3):240–8. Epub 2009/03/12. https://doi.org/10.1016/j.ymeth.2009.03.001 PMID: 19275939; PubMed Central PMCID: PMCPMC4052679.

16. Mohammed H, D'Santos C, Serandour AA, Ali HR, Brown GD, Atkins A, et al. Endogenous purification reveals GREB1 as a key estrogen receptor regulatory factor. Cell Rep. 2013; 3(2):342–9. Epub 2013/02/14. https://doi.org/10.1016/j.celrep.2013.01.010 PMID: 23403292.

17. Mohammed H, Taylor C, Brown GD, Papachristou EK, Carroll JS, D'Santos CS. Rapid immunoprecipitation mass spectrometry of endogenous proteins (RIME) for analysis of chromatin complexes. Nat Protoc. 2016; 11(2):316–26. Epub 2016/01/23. https://doi.org/10.1038/nprot.2016.020 PMID: 26797456.

18. Carroll JS, Liu XS, Brodsky AS, Li W, Meyer CA, Szary AJ, et al. Chromosome-wide mapping of estrogen receptor binding reveals long-range regulation requiring the forkhead protein FoxA1. Cell. 2005; 122(1):33–43. Epub 2005/07/13. https://doi.org/10.1016/j.cell.2005.05.008 PMID: 16009131.

19. Fournier M, Bourriquen G, Lamaze FC, Cote MC, Fournier E, Joly-Beauparlant C, et al. FOXA and master transcription factors recruit Mediator and Cohesin to the core transcriptional regulatory circuitry of cancer cells. Sci Rep. 2016; 6:34962. Epub 2016/10/16. https://doi.org/10.1038/srep34962 PMID: 27739523; PubMed Central PMCID: PMCPMC5064413.

20. Jeselsohn R, Bergholz JS, Pun M, Cornwell M, Liu W, Nardone A, et al. Allele-Specific Chromatin Recruitment and Therapeutic Vulnerabilities of ESR1 Activating Mutations. Cancer Cell. 2018; 33(2):173–86 e5. Epub 2018/02/14. https://doi.org/10.1016/j.ccell.2018.01.004 PMID: 29438694; PubMed Central PMCID: PMCPMC5813700.

21. Zwart W, Flach KD, Rudraraju B, Abdel-Fatah TM, Gojis O, Canisius S, et al. SRC3 Phosphorylation at Serine 543 Is a Positive Independent Prognostic Factor in ER-Positive Breast Cancer. Clin Cancer Res. 2016; 22(2):479–91. Epub 2015/09/16. https://doi.org/10.1158/1078-0432.CCR-14-3277 PMID: 26369632.

22. Papachristou EK, Kishore K, Holding AN, Harvey K, Roumeliotis TI, Chilamakuri CSR, et al. A quantitative mass spectrometry-based approach to monitor the dynamics of endogenous chromatin-associated protein complexes. Nat Commun. 2018; 9(1):2311. Epub 2018/06/15. https://doi.org/10.1038/s41467-018-04619-5 PMID: 29899353; PubMed Central PMCID: PMCPMC5998130.

23. Perez-Riverol Y, Csordas A, Bai J, Bernal-Llinares M, Hewapathirana S, Kundu DJ, et al. The PRIDE database and related tools and resources in 2019: improving support for quantification data. Nucleic Acids Res. 2019; 47(D1):D442–D50. Epub 2018/11/06. https://doi.org/10.1093/nar/gky1106 PMID: 30395289; PubMed Central PMCID: PMCPMC6323896.

24. Li H, Durbin R. Fast and accurate short read alignment with Burrows-Wheeler transform. Bioinformatics. 2009; 25(14):1754–60. Epub 2009/05/20. https://doi.org/10.1093/bioinformatics/btp324 PMID: 19451168; PubMed Central PMCID: PMCPMC2705234.

25. Consortium EP. An integrated encyclopedia of DNA elements in the human genome. Nature. 2012; 489(7414):57–74. Epub 2012/09/08. https://doi.org/10.1038/nature11247 PMID: 22955616; PubMed Central PMCID: PMCPMC3439153.

26. Zhang Y, Liu T, Meyer CA, Eeckhoute J, Johnson DS, Bernstein BE, et al. Model-based analysis of ChIP-Seq (MACS). Genome Biol. 2008; 9(9):R137. Epub 2008/09/19. https://doi.org/10.1186/gb-2008-9-9-r137 PMID: 18798982; PubMed Central PMCID: PMCPMC2592715.

27. McLeay RC, Bailey TL. Motif Enrichment Analysis: a unified framework and an evaluation on ChIP data. BMC Bioinformatics. 2010; 11:165. Epub 2010/04/02. https://doi.org/10.1186/1471-2105-11-165 PMID: 20356413; PubMed Central PMCID: PMCPMC2868005.

28. Bailey TL, Boden M, Buske FA, Frith M, Grant CE, Clementi L, et al. MEME SUITE: tools for motif discovery and searching. Nucleic Acids Res. 2009; 37(Web Server issue):W202–8. Epub 2009/05/22. https://doi.org/10.1093/nar/gkp335 PMID: 19458158; PubMed Central PMCID: PMCPMC2703892.

29. Kulakovskiy IV, Vorontsov IE, Yevshin IS, Soboleva AV, Kasianov AS, Ashoor H, et al. HOCOMOCO: expansion and enhancement of the collection of transcription factor binding sites models. Nucleic Acids Res. 2016; 44(D1):D116–25. Epub 2015/11/21. https://doi.org/10.1093/nar/gkv1249 PMID: 26586801; PubMed Central PMCID: PMCPMC4702883.

30. Barrett T, Wilhite SE, Ledoux P, Evangelista C, Kim IF, Tomashevsky M, et al. NCBI GEO: archive for functional genomics data sets—update. Nucleic Acids Res. 2013; 41(Database issue):D991–5. Epub 2012/11/30. https://doi.org/10.1093/nar/gks1193 PMID: 23193258; PubMed Central PMCID: PMCPMC3531084.

31. Ross-Innes CS, Stark R, Holmes KA, Schmidt D, Spyrou C, Russell R, et al. Cooperative interaction between retinoic acid receptor-alpha and estrogen receptor in breast cancer. Genes Dev. 2010; 24 (2):171–82. Epub 2010/01/19. https://doi.org/10.1101/gad.552910 PMID: 20080953; PubMed Central PMCID: PMCPMC2807352.

32. Carroll JS, Meyer CA, Song J, Li W, Geistlinger TR, Eeckhoute J, et al. Genome-wide analysis of estrogen receptor binding sites. Nat Genet. 2006; 38(11):1289–97. Epub 2006/10/03. https://doi.org/10.1038/ng1901 PMID: 17013392.